PB81-179368

U.S. Department
of Transportation
Federal Railroad Administration

Nondestructive Techniques for Measuring the Longitudinal Force in Rails

Office of Research
and Development

Washington, D.C. 20590

Proceedings of a Joint Government-Industry Conference

Held in Washington D.C.,
February 26-27, 1979

FRA/ORD-80/50

DECEMBER 1980

Paul Elliot
(Proceedings Editor)

Document is available to the U.S. public through the National Technical Information Service, Springfield, Virginia 22161

NOTICE

Technical Report Documentation Page

1. Report No. FRA/ORD-80/50	2. Government Accession No.	3. Recipient's Catalog No.
4. Title and Subtitle NONDESTRUCTIVE TECHNIQUES FOR MEASURING THE LONGITUDINAL FORCE IN RAILS: Proceedings of a Joint Government-Industry Conference held in Washington, D. C., February 26–27, 1979		5. Report Date December 1979 6. Performing Organization Code
7. Author(s) Paul Elliott (Proceedings editor)		8. Performing Organization Report No. FRA/ORD-80/50
9. Performing Organization Name and Address Unified Industries Incorporated 5400 Cherokee Avenue Alexandria, Virginia 22312		10. Work Unit No. (TRAIS) 11. Contract or Grant No. DOT-FR-8046/DOT-FR-9044
12. Sponsoring Agency Name and Address U.S. Department of Transportation Federal Railroad Administration Office of Research and Development Washington, D.C. 20590		13. Type of Report and Period Covered Final Report February 26–27, 1979 14. Sponsoring Agency Code RRD-32

15. Supplementary Notes

Conference was sponsored by the Federal Railroad Administration and the Association of American Railroads in support of Track Train Dynamics (an international government-industry research program)

16. Abstract

The Conference on Nondestructive Techniques for Measuring the Longitudinal Force in Rails consisted of an introductory session followed by three major sessions on ultrasonic techniques, Barkhausen and sonic techniques, and X-ray diffraction techniques. This report is made up of the technical papers presented at the conference, together with the edited transcripts of the panel discussions and question-and-answer periods held at the end of each major session.

17. Key Words Railroad research, track-train dynamics, track and structures, materials science, nondestructive testing, track buckling stresses, longitudinal rail force	18. Distribution Statement Document is available through the National Technical Information Service, Springfield, Virginia 22161

19. Security Classif. (of this report)	20. Security Classif. (of this page)	21. No. of Pages	22. Price
Unclassified	Unclassified	191	

Form DOT F 1700.7 (8-72) Reproduction of completed page authorized

METRIC CONVERSION FACTORS

Approximate Conversions to Metric Measures

Symbol	When You Know	Multiply by	To Find	Symbol
	LENGTH			
in	inches	*2.5	centimeters	cm
ft	feet	30	centimeters	cm
yd	yards	0.9	meters	m
mi	miles	1.6	kilometers	km
	AREA			
in^2	square inches	6.5	square centimeters	cm^2
ft^2	square feet	0.09	square meters	m^2
yd^2	square yards	0.8	square meters	m^2
mi^2	square miles	2.6	square kilometers	km^2
	acres	0.4	hectares	ha
	MASS (weight)			
oz	ounces	28	grams	g
lb	pounds	0.45	kilograms	kg
	short tons (2000 lb)	0.9	tonnes	t
	VOLUME			
tsp	teaspoons	5	milliliters	ml
Tbsp	tablespoons	15	milliliters	ml
fl oz	fluid ounces	30	milliliters	ml
c	cups	0.24	liters	l
pt	pints	0.47	liters	l
qt	quarts	0.95	liters	l
gal	gallons	3.8	liters	l
ft^3	cubic feet	0.03	cubic meters	m^3
yd^3	cubic yards	0.76	cubic meters	m^3
	TEMPERATURE (exact)			
°F	Fahrenheit temperature	5/9 (after subtracting 32)	Celsius temperature	°C

*1 in. = 2.54 cm (exactly). For other exact conversions and more detail tables see NBS Misc. Publ. 286. Units of Weight and Measures. Price $2.25 SD Catalog No. C13 10 286.

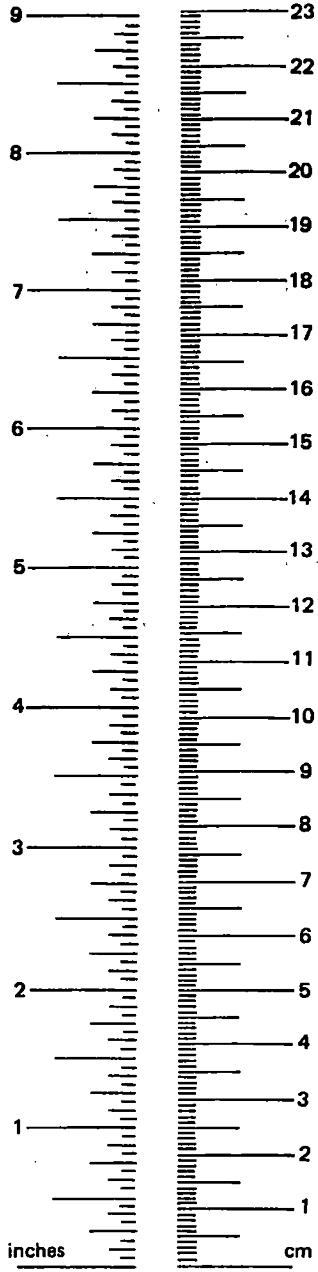

Approximate Conversions from Metric Measures

Symbol	When You Know	Multiply by	To Find	Symbol
	LENGTH			
mm	millimeters	0.04	inches	in
cm	centimeters	0.4	inches	in
m	meters	3.3	feet	ft
m	meters	1.1	yards	yd
km	kilometers	0.6	miles	mi
	AREA			
cm^2	square centimeters	0.16	square inches	in^2
m^2	square meters	1.2	square yards	yd^2
km^2	square kilometers	0.4	square miles	mi^2
ha	hectares (10,000 m^2)	2.5	acres	
	MASS (weight)			
g	grams	0.035	ounces	oz
kg	kilograms	2.2	pounds	lb
t	tonnes (1000 kg)	1.1	short tons	
	VOLUME			
ml	milliliters	0.03	fluid ounces	fl oz
l	liters	2.1	pints	pt
l	liters	1.06	quarts	qt
l	liters	0.26	gallons	gal
m^3	cubic meters	36	cubic feet	ft^3
m^3	cubic meters	1.3	cubic yards	yd^3
	TEMPERATURE (exact)			
°C	Celsius temperature	9/5 (then add 32)	Fahrenheit temperature	°F

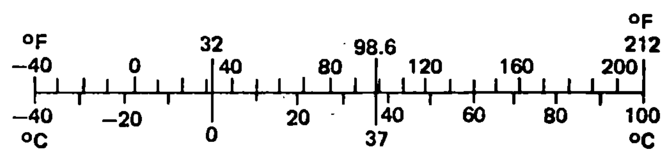

TABLE OF CONTENTS

TABLE OF CONTENTS (Continued)

INTRODUCTION

GENERAL INTRODUCTION

R. E. Parsons
Federal Railroad Administration

The Federal Railroad Administration and the Association of American Railroads are pleased to cosponsor this conference to consider nondestructive techniques for measuring internal longitudinal force or stress in rails.

We have invited representatives of the railroad research, operating, and supply communities, along with several government agencies and universities, to participate.

Track research is one of the highest priority R&D programs in the FRA. Accordingly, a large percentage of the Office of Research and Development's budget supports this program. This emphasis is dictated by the fact that over 40 percent of the train accidents are due to track-related causes.

The number of accidents unfortunately continues to rise each year, even though the railroad industry spends ever-increasing amounts for maintenance of way. In 1977, for example, over $3.4 billion was spent in track maintenance.

The FRA has been involved in track research for several years, with a major portion of this effort being dedicated to and directed at improving the safety of train operations through development of more effective track safety standards in support of our Office of Safety.

Establishment of the existing track safety standards was based on requirements of the Safety Act of 1970 and, essentially, they are design-based standards reflecting minimum maintenance requirements.

As track accidents continue to rise, a first thought is to tighten the existing standards. However, tightening the requirements of the design standards to reduce track-caused derailments only further restricts the industry's options for compliance.

Since the FRA's goal is to provide the rail industry with design options and maximum flexibility consistent with equitable safety or acceptable safety, a search commenced for a more flexible framework on which to define "acceptable levels of safety."

Accordingly, within the past year and a half, the FRA's research management shifted emphasis toward the development of technically sound safety standards based on performance requirements. This approach, it is believed, should give industry the flexibility to select the most economic design or repair practices to suit their individual needs while still providing an acceptable level of safety.

One of the performance requirements would be an acceptable level of track strength capable of withstanding the dynamic forces applied to the rail.

Studies and test results to date show that the lateral and vertical forces are the prime contributors to rail rollover, rail spreading, and wheel lift-type accidents, and the FRA is conducting considerable research and development activities in that area. The FRA also supports joint programs with the Association of American Railroads in this area as well, hopefully to define acceptable track-loading levels.

Nonetheless, we are also very concerned with the impact of longitudinal loading of the track structure, particularly as it contributes to internal stress buildup leading to buckling. As is widely known, track buckling alone caused over 100 accidents last year.

This conference is directed at providing an exchange of state-of-the-art information on, and determining the feasibility of, measurement of internal longitudinal rail stress. As this is to be a working conference, each attendee is urged to participate by addressing any comments (critical or otherwise) or questions to the conference panel and the speakers. In addition, I personally solicit any written comments you may have on any area of the conference or on the purpose of having such conferences in general.

Hopefully, the outcome of this gathering will result in a clearer understanding of procedures that may be applicable to the measurement of internal longitudinal stresses in rail, and as a result we may be able to make better decisions in the direction of future research.

One goal of such research may be the development of portable instrumentation for field measurement of these stresses or forces.

TECHNICAL INTRODUCTION

"On the Nondestructive In-Track Measurement of Longitudinal Rail Force"

Allan M. Zarembski
Association of American Railroads

Introduction

A conventional railroad track consists of two long steel rails resting on and fastened to discretely spaced crossties, which in turn are embedded in a layer of crushed stone ballast. The ends of the rails either are connected by joint bars to form an expandable joint or are welded together to form long lengths of continuously welded rail (CWR).

The track structure, when subjected to sufficiently high longitudinal compressive forces in the rail, can exhibit sudden and rapid lateral or vertical movement over a relatively short length. This lateral movement, or buckling of the track,* results in a severe misalignment condition that may not permit the safe negotiation of train traffic (figure 1).

*Railroad track maintenance personnel often call it a "sun-kink."

FIGURE 1. BUCKLED TRACK

If buckling occurs under the train, a derailment is likely to occur. If it occurs between trains, traffic must either be stopped or slowed down until the buckled track condition is corrected.

The magnitude of this problem can be seen in the fact that, during 1977, there were 109 train derailments attributed to buckling of the track. The reported damage for these derailments amounted to over $5.5 million [1]. Furthermore, for every track buckle that resulted in a derailment, there were three to four instances of buckled track where the railroad maintenance forces were able to correct the problem before a derailment occurred. Consequently, countless hours of maintenance time are devoted to inspecting for and correcting buckled track.

When the track structure is subjected to longitudinal tensile forces, pull-apart of the rail can occur. In CWR track, these pull-aparts, which generally occur at the welded joints, result in the appearance of a gap or separation in the rails. Such a gap, which can result in derailment or at the very least rail batter, requires the slowing down or halting of traffic until appropriate corrective action is taken. Although the detection of pull-aparts in signaled territory is facilitated by the interruption of the traffic signals, the maintenance cost of pull-aparts is appreciable.

One of the greatest difficulties associated with the detection and prevention of track buckling or rail pull-apart is that it often occurs without real warning. This is because the buildup of longitudinal forces in track that is in good condition, particularly continuously welded rail track, will not be evident until it reaches the point where the track will fail. That can be too late. Yet, there is presently no practical method available for measuring the longitudinal force in the track without disturbing the track structure itself. Railroads currently rely on the subjective judgment of the maintenance-of-way man on the scene.

It is the purpose of this paper to explore the various techniques used to date to measure longitudinal rail force and to lay the groundwork for the continuing research effort aimed at developing a practical technique for the nondestructive in-track measurement of longitudinal force in rail.

Longitudinal Rail Forces

The track structure is subject to both mechanically and thermally induced longitudinal rail forces. When the magnitude of these forces, either individually or in combination, exceeds the restraint capacity of the track structure, track buckling or rail pull-apart occurs. It is not the purpose of this paper to attempt to explain the mechanisms of track buckling or rail pull-apart (extensive surveys and summary papers are already available [2], [3], [4]). However, a brief description of the loading mechanisms and corresponding rail behavior will help to define the measurement problem.

Mechanically induced longitudinal rail force is developed under the acceleration or deceleration of a train. In order for a locomotive to overcome the train resistance and move the train, a force or tractive effort must be exerted by the locomotive and reacted by the track structure. Similarly, when deceleration or braking, the necessary train forces are reacted against the track. When the train is on a grade, particularly during a severe braking action, the net longitudinal force can be as high as 60,000 pounds per rail [5].

By itself, this mechanical loading usually is not sufficient to buckle the track. In fact, according to A. D. Kerr [6], track subjected to mechanical compressive loading should buckle vertically, a phenomenon almost never experienced in the field. However, the mechanical force can result in longitudinal creep or movement of the rails. Additional rail creep is also generated by the action of passing trains. When this creep is restrained, as occurs with well-anchored track or at turnouts and grade crossings, longitudinal compressive forces are built up in the rail. For a more complete description of the development of rail creepage forces, see the work of J. P. Hiltz, Jr. [7].

Thermally induced longitudinal rail force occurs when the rail is no longer free to expand; i.e., when the joints are either closed as in a tight or frozen joint situation or altogether eliminated as in the case with CWR track. When a constrained rail of length L is subject to a uniform temperature rise (or drop) ΔT, the longitudinal compressive (tensile) force experienced by the track is $N_t = EA\ \alpha\ \Delta T$; where E is the Young's modulus of the rail steel, A is the cross-sectional area of the two rails, and α is the coefficient of linear thermal expansion. Figure 2 illustrates graphically the magnitude of the thermal force that can be experienced by the rails. The distribution of thermal stresses in a long length of welded rail is shown in figure 3; these data were taken from field measurements on the Bessemer and Lake Erie Railroad [8]. It should be noted however, that, although the longitudinal stress in the rail changes with temperature, the constrained portion of the rail does not move. Thus, the strain in the center portion of the rail section, away from the end regions (where "breathing" occurs [4]), is zero, although the stress and force in the rail is not. This can readily be seen in the field measurement data given in figure 4 [8]. It is this absence of strain that results in many of the difficulties encountered in the measurement of thermally induced longitudinal rail forces.

Since it is the change in rail temperature from its initial or laying temperature that determines the magnitude of the thermally induced rail force, proper selection and control of the CWR installation temperature is of great importance [4]. Consequently, many railroads have defined installation temperatures for different geographic locations. When the ambient temperature at the time of installation is below the recommended installation temperature, the rail is artificially brought to the proper "temperature" through either heating the rail or mechanically stretching it to the appropriate length. In the latter case, mechanical strains and consequently stresses (tensile) are introduced. Furthermore, rail installed in and near curves often undergoes contraction and expansion cycles that result in a shifting of the track, usually noted by a change in the curvature. This behavior often changes the actual installation temperature so that it no longer is the same as the initial laying temperature. In fact, in many cases, this stress-free temperature is no longer known.

Finally, it must be noted that, in addition to the stresses introduced into the rails by temperature change, installation, and train action, residual stresses in the rail section can be present. These residual stresses are introduced by the rail manufacturing process, by various heat treatment techniques, by the work hardening and softening of the rail head under wheel-rail interaction, and by the welding process (in the vicinity of the welds). However, these residual stresses generally are distributed so that the net force across the rail section is zero. This stress distribution is similar to that encountered by the rail in bending, where at any given point in the rail section a stress can be present. However, the net force in the rail section, obtained by summing all the stresses in the cross section, is zero. In that case, the effect of these residual stresses on track buckling is negligible, since it is the net longitudinal force in the rails that contributes to this track failure mode.

Consequently, it is necessary to be able to distinguish between those stresses in the rail that produce net longitudinal force, such as those introduced by temperature change, installation, train acceleration or braking, and rail creep and

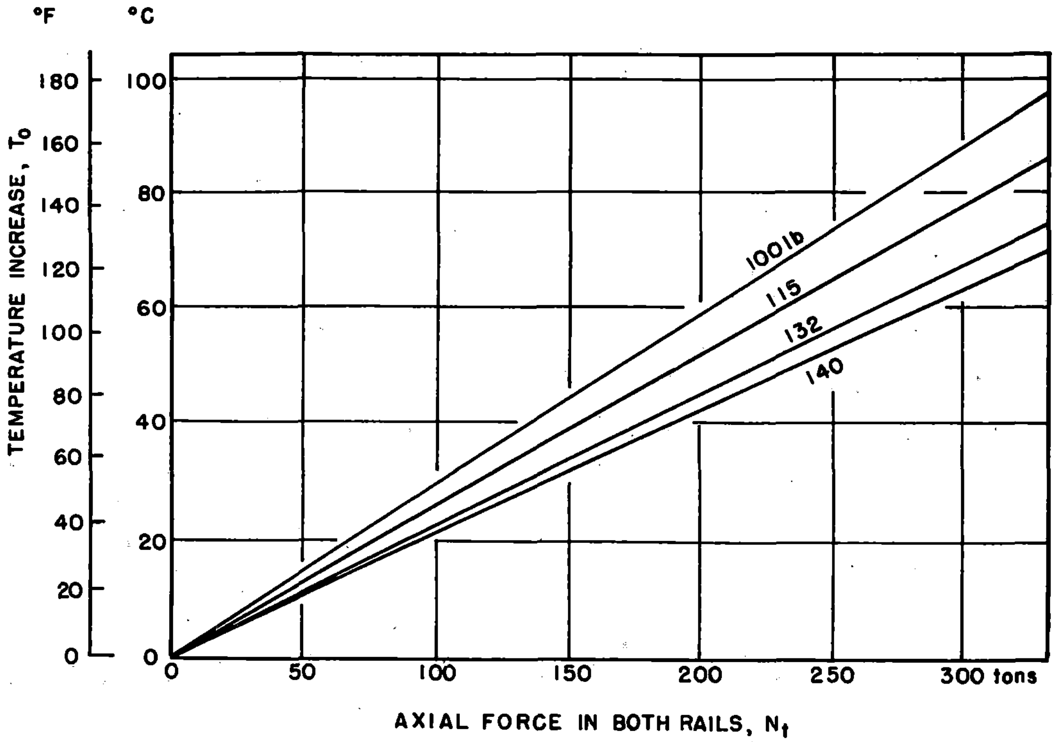

FIGURE 2. RAIL TEMPERATURE INCREASE VERSUS AXIAL FORCE IN RAILS

those stresses that produce little or no net longitudinal force, such as rail bending stresses and residual stresses introduced by manufacturing, heat treatment, wheel-rail interaction, and welding. It is for this reason that the measurement of the resultant forces, rather than rail stresses, must be the objective of any track measurement device.

Current Measurement Techniques

There are several techniques currently available for measuring longitudinal rail stress (or strain). However, they all require some degree of disturbance of the track structure in order to properly measure the longitudinal rail force. Furthermore, some techniques, while suitable for measurement of stress in jointed rail track, are not suitable for measurement of thermally induced stresses in continuously welded rail.

As noted earlier, jointed rail track consists of rail connected at the ends by joint bars and track bolts. The design of the joint bar and bolt system is such that the holes drilled in the rail are generally 1/8 inch larger (in diameter) than the bolt. Thus, when the track is laid with the bolts centered in the hole and a gap of 1/8 inch between ends [9], the 39-foot length of rail is capable of expanding 1/8 inch without additional restraint. This freedom to expand or strain, which also is instrumental in reducing the thermal stress buildup in jointed track, permits the utilization of strain measuring techniques to directly determine the strain and consequently the stress. Continuously welded rail track, however, constrains the rail, away from the rail ends, and consequently does not permit the development of thermally induced strain, as was noted earlier (figure 4). Thus, strain measuring techniques require significant modification for use in CWR track.

At the present time, none of these techniques is used by the railroads in the United States and Canada to measure longitudinal rail force in track, with the possible exception of isolated test locations. Instead, the railroads rely on the judgment of the local maintenance-of-way personnel to evaluate the condition of the track. Although these personnel do not have any specific equipment to measure and quantify rail force, they can note, through general observation and study of the rail movement, certain trends that can be used to anticipate failure. In particular, significant rail creep can be observed by noting anchor movement away from ties, together with movement of the ties themselves. In jointed track, loss of rail-end gaps can be monitored. In CWR track, observation of joints connecting the CWR strings for closing of gaps and bending of track bolts can give a good indication of the buildup of compressive forces in the center of the string. Finally, by observing changes in small track misalignments, as well as any increase in or development of waves or kinks in the track, compressive forces can be noted. When coupled with a knowledge of the laying temperature of the rail and the temperature at the time of inspection, these observations all provide subjective indications to the maintenance personnel that the track is experiencing significant longitudinal forces. However, their magnitude and consequently the likelihood of track failure, either by buckling or pull-apart, is still largely unknown.

Strain Gage Techniques. The use of strain gages to measure strain and consequently stress in structure members is a commonly employed

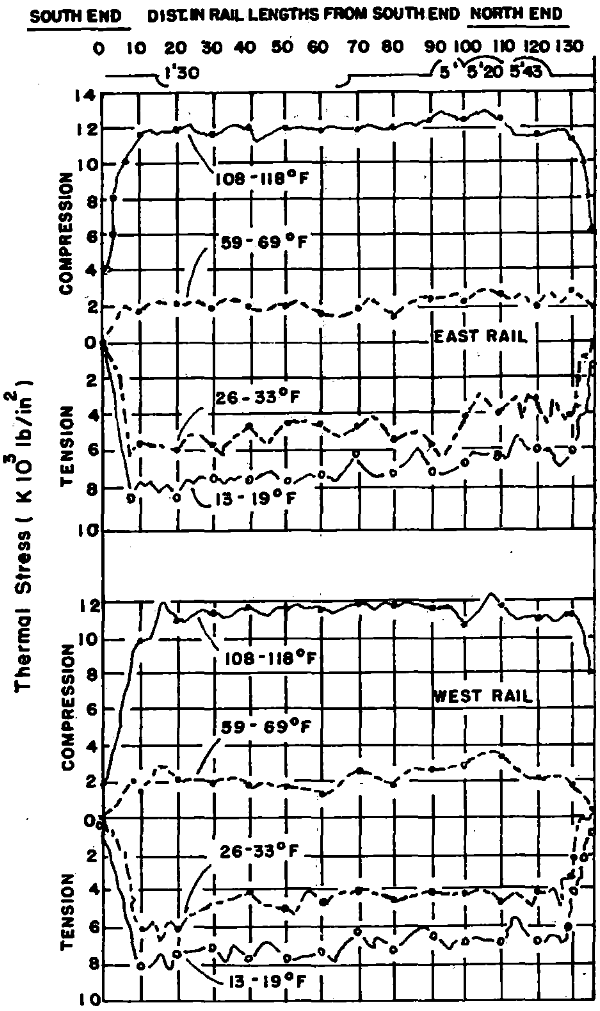

FIGURE 3. THERMAL STRESSES IN RAIL (BASE 53 DEGREES F). WELDED LENGTH 1 MILE. BESSEMER AND LAKE ERIE RAILROAD.

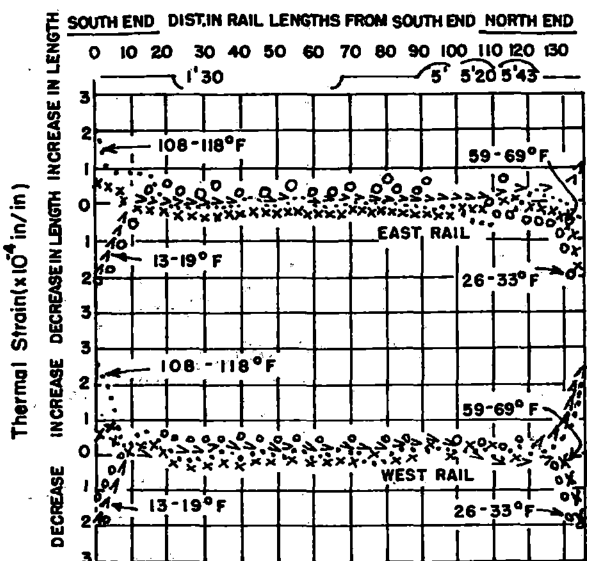

FIGURE 4. THERMAL STRAIN IN RAIL (BASE 53 DEGREES F). WELDED LENGTH 1 MILE. BESSEMER AND LAKE ERIE RAILROAD.

measurement technique. Both mechanical and electrical resistance strain gages are available and have been employed. The strain gage measures the strain or change in length per unit of the member under load. For loadings that induce strains in the rail, such as mechanical and creep forces, strain gages can be directly employed. For loadings that do not induce strains, such as stresses induced by temperature changes in CWRs, the strain gage must be used in conjunction with a known standard. In all cases, for the strain gages to be able to measure the absolute force in the rail, they must be initially installed when the rail is in a strain-free state.

Historically, the first known application of a rail force measurement technique in the United States occurred in 1936, when the joint A.R.E.A.-A.S.C.E. Special Committee on Stresses in the Railroad Track, under the direction of A. N. Talbot, used a Berry mechanical strain gage to measure stresses in a stretch of welded rail track on the Delaware and Hudson Railroad [10]. This was soon followed by additional measurements on the Bessemer and Lake Erie Railroad [8] and the Central of Georgia Railway [11], both using Berry strain gages.

The Berry strain gage is a mechanical gage used to measure the change in length of a member over a 10- or 20-inch span (figure 5). The gage, which is capable of measuring displacements of 0.0002 inch, was originally designed for use in a member subjected to mechanical strain. To use the gage, two indentations, 10 or 20 inches apart depending on the size of the gage, are punched in the member at the neutral axis when the member is unloaded. Changes in length are then measured when the member is strained. For long CWRs which experience no strain, a standard, usually a short segment of the rail under consideration, is used. At the stress-free temperature, a set of indentations is made in both the rail in track and in the standard. The standard is then left in the field near the rail being measured, and at the desired temperature, the standard is measured for strain (figure 6). The net strain in the standard then corresponds to the stress experienced by the rail constrained in the track. Figures 3 and 4 illustrate corresponding rail stresses and strains taken using this technique.

With the advent of electric resistance strain gages, the utilization of strain gage measurement techniques was simplified. These gages, which may be either bonded or welded to the neutral axis of the rail, are then combined electrically to give the strain values (figure 7). While these gages are quite practical for measuring mechanically induced strains, they again require the use of a standard to measure thermally induced stresses. The standard can be either a short segment of rail, as used for the Berry gage, or a short piece of steel with similar thermal expansion properties. This latter approach appears to be the one utilized by the U.S.S.R., as shown in figure 8 [12].

In general, strain gage techniques have not been widely adopted for measurement of stresses in rail because of the difficulties encountered

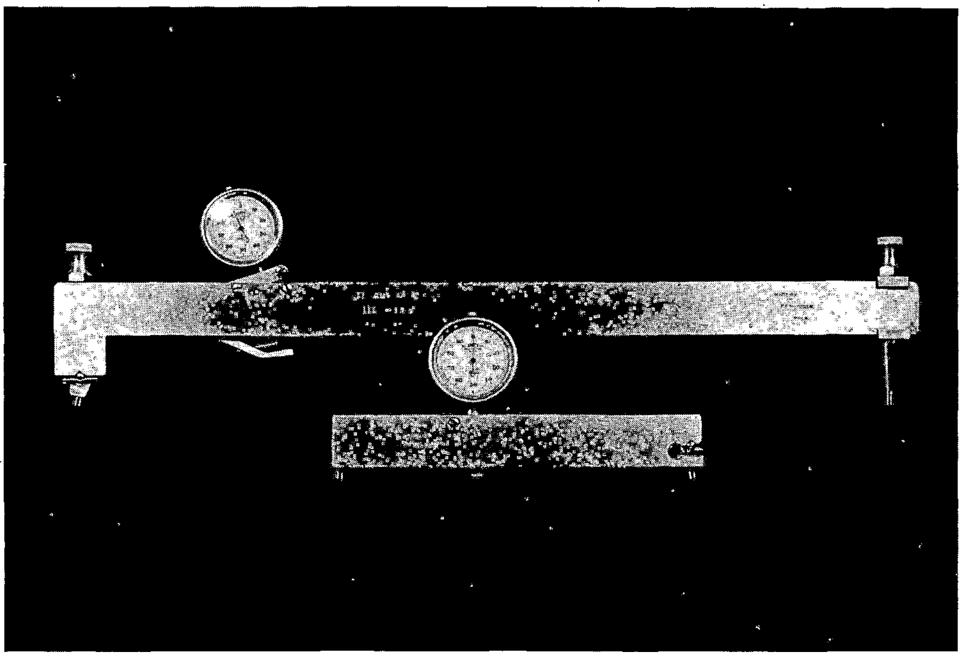

FIGURE 5. BERRY STRAIN GAGES

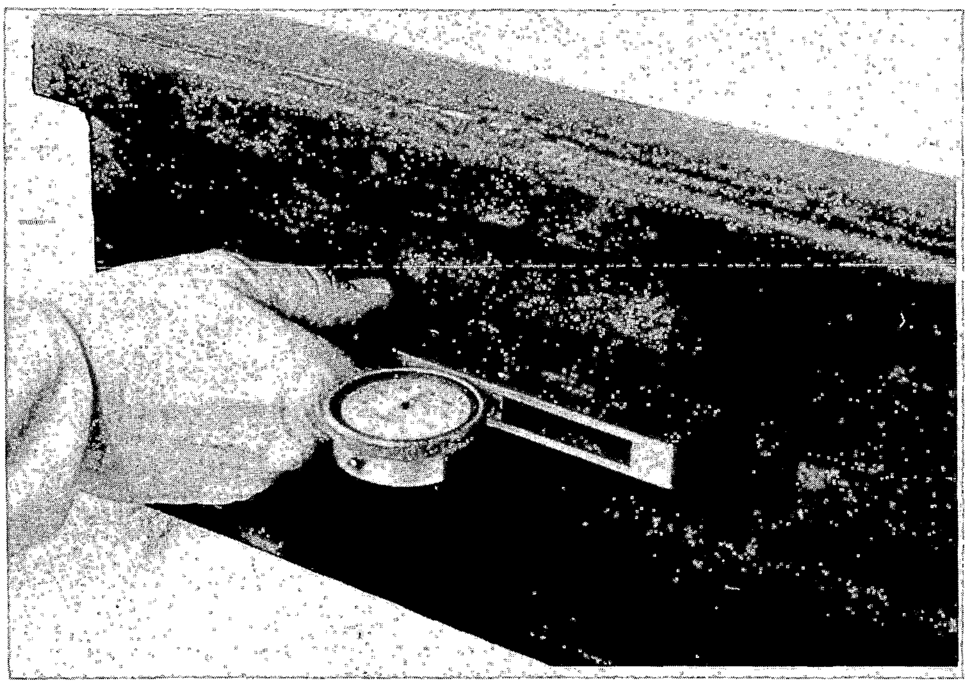

FIGURE 6. BERRY STRAIN GAGE MEASUREMENTS ON RAIL STANDARD

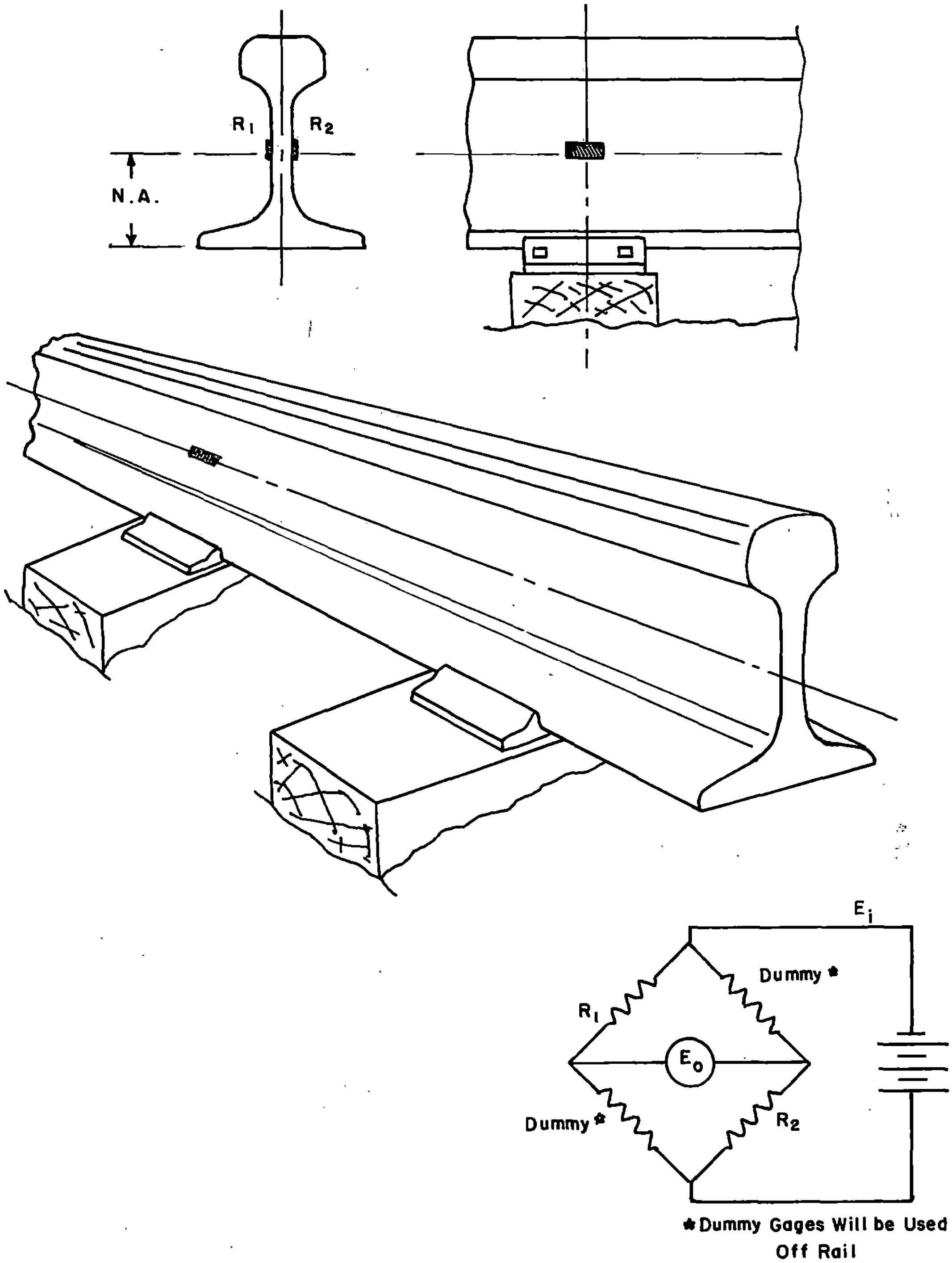

FIGURE 7. STRAIN GAGE PLACEMENT

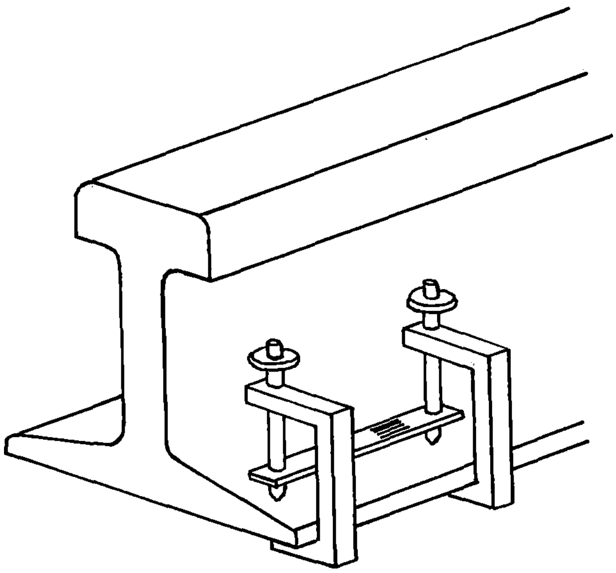

FIGURE 8. STRAIN GAGE DEVICE FOR THE MEASUREMENT OF STRESS IN RAILS, AS USED IN THE U.S.S.R.

in measuring thermally induced rail stresses, together with the requirement that the gages be applied while in a stress-free state. This latter requirement poses significant practical difficulties for track that has already been laid with CWR since it entails the removal of all rail anchors and fasteners for the entire length, together with mechanical destressing of the rail.

BR Rail Force Measuring Transducer. An alternate technique for measuring rail force has been recently developed by British Rail's Railway Technical Centre at Derby, England [13]. This technique utilizes the principle of vibrating wire strain gages in which the natural frequency of vibration of a taut wire is related to its tension. The BR transducer consists of a steel annulus of approximately 1-inch outside diameter with two wires fixed to it. The annulus is inserted into a hole drilled on the neutral axis of the rail (figure 9). When changes occur in the longitudinal rail force, the shape of the hole changes slightly, resulting in a change in wire tension and consequently in the wire's natural frequency. Using calibration data, the changes in frequency can be related to the force in the rail.

This technique does not require the use of an external standard. However, it does require the drilling of a hole in the rail web and an onsite calibration using a rail web loading device similar to a hydraulic rail puller. It also requires that a zero datum reading be taken with the rail in a stress-free state. This reading can be taken at installation or when the rail is stress free.

Recent Research

In view of the restrictions and difficulties associated with the measurement systems discussed in the preceding section, several research programs have been undertaken recently in a attempt to develop an effective longitudinal force measurement system. None of these programs has yet progressed to the point of having developed and tested a practical measurement system, but several of them appear to offer potential solutions to this measurement problem. Although it is beyond the scope of this paper to present the theory behind these techniques, it is appropriate to include a brief discussion of the respective methodologies, together with any relevant tests that have been conducted to date.

Rail Vibration. It is known from beam theory that the dynamic response of a beam subject to an impulse loading is dependent on the axial force in the beam. In fact, before the advent of more sophisticated measurement techniques, bridge engineers were known to judge the force in a prestressed member from the pitch emitted by the member when struck a light blow. This concept can be extended to rails in track. By proper monitoring of the rail vibration responses most sensitive to longitudinal force, this longitudinal force can be identified and measured.

One possibility is suggested by examination of the rail section where the rail head can be considered to be a beam resting on and continuously supported by the web acting as an elastic foundation in the lateral plane. The corresponding equation for the rail head subject to a lateral impulse load is:

$$EI_h \frac{\partial^4 w}{\partial x^4} + N \frac{\partial^2 w}{\partial x^2} + m \frac{\partial^2 w}{\partial t^2} + k\, w = P\, \delta\ (x,t),$$

where

w is the lateral deflection of the rail head,

x is the longitudinal distance along the rail,

t is the time,

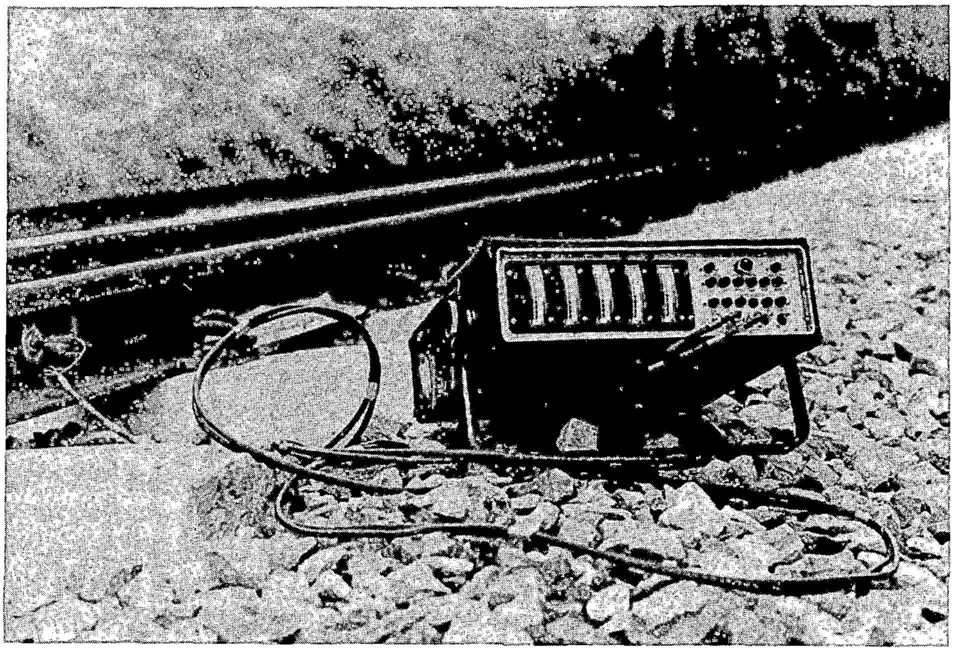

FIGURE 9. BRITISH RAIL RAIL FORCE TRANSDUCER

EI_h is the flexural rigidity of the rail head in the lateral plane,

m is the mass of the head per unit length,

k is the foundation parameter representing the rail web and remaining track structure,

N is the longitudinal force in the rail head, and,

P is the applied lateral force.

Solution of this equation shows that the rail response is dependent on the longitudinal force.

Preliminary testing at Princeton University in the spring of 1976 and at the Association of American Railroad's Track Structures Dynamic Test Facility in January 1979 appears to confirm this concept. In the Princeton test, a length of rail, mounted longitudinally on a wood tie to simulate track damping, was placed in a hydraulic compression machine. In the AAR test, a hydraulic rail puller was used to introduce a longitudinal compressive force onto a test track, over a 20-foot length (figure 10). In both cases an accelerometer was mounted on the side of the rail head and the rail was excited by hitting the head laterally with either a cut spike or a bolt. Examination of the rail head acceleration data indicated that, for both the Princeton test [14] and the AAR test (figure 11), the dynamic response was affected by the applied longitudinal load. Additionally, the AAR tests, which are still in progress, indicated that this response is sensitive to the magnitude of the exciting force. Thus, smaller exciting forces appear to generate the rail response most sensitive to the longitudinal force, while the larger forces appear to mask these responses.

Although both tests give indications that this technique is applicable to the track problem, further testing and refinement of the measurement system is required. In addition, the effect of temperature variation, rail head wear, and calibration requirements must be carefully examined and studied.

X-Ray Diffraction. A second approach that has been examined recently for measurement of rail stresses is X-ray diffraction. In this technique an X-ray beam is used to measure the interplanar spacing on the surface of the specimen under examination. Since the spacing of the atomic planes is altered by an applied stress, the change in atomic spacing can be measured and then related back to the applied stress [15].

In the past, a major constraint of the X-ray diffraction method was the size of the X-ray tube and accessory equipment. However, the development of a portable X-ray diffraction unit (figure 12) has increased the potential for practical application. In addition, recent examination of samples taken from the webs of both old and new rail has indicated that it is feasible to use this technique on standard carbon rail steel [16].

Although preliminary indications seem to show that this technique can be applicable to the rail force measurement problem, further investigation of the technique, together with field testing, is still required. Still to be answered are such

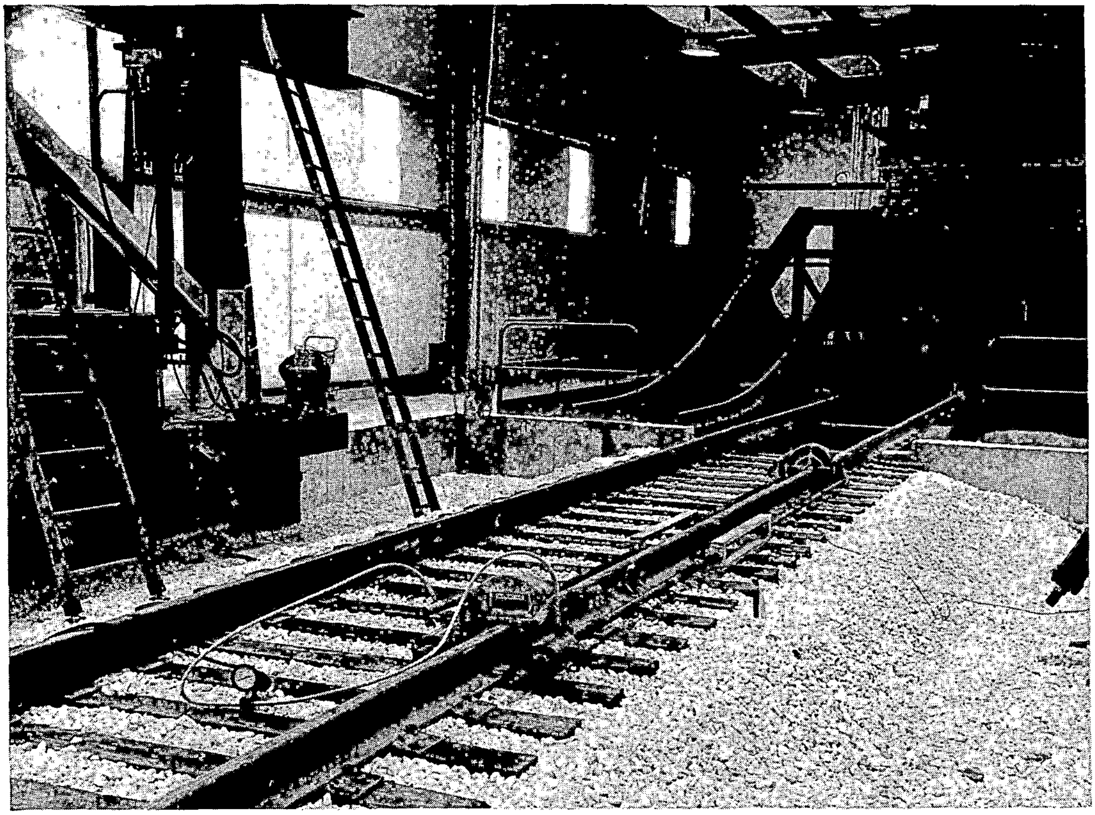

FIGURE 10. MEASUREMENT OF LONGITUDINAL RAIL FORCE IN AAR TRACK LABORATORY: LATERAL VIBRATION OF RAIL HEAD. NOTE ACCELEROMETER MOUNTED ON FIELD SIDE OF THE RAIL HEAD (CENTER OF RAIL SECTION IN PULLER).

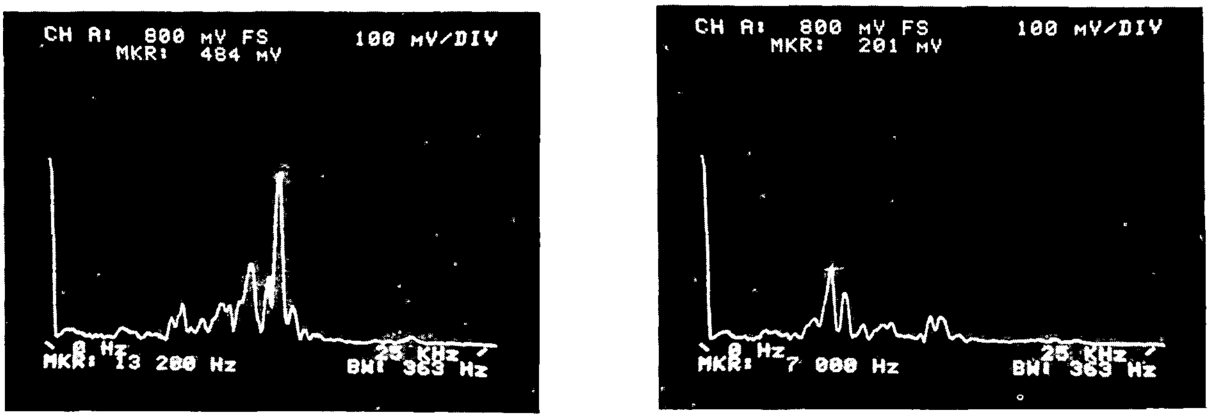

AXIAL FORCE: 0 KIPS

AXIAL FORCE: 200 KIPS

FIGURE 11. RAIL HEAD RESPONSE (FREQUENCY DOMAIN) FOR DIFFERENT LONGITUDINAL LOAD LEVELS (AAR TEST)

questions as the ability of this technique to measure stresses produced by constrained thermal expansion, differentiation between rail forces and stresses (specifically, surface residual stresses), calibration and setup requirements, and effect of the railroad operating environment.

Ultrasonic Wave Propagation. A research investigation of the feasibility of utilizing ultrasonic pulse propagation in rails to measure longitudinal stresses was recently completed [17]. The technique involved in this investigation included the measurement of the speed of elastic waves propagating longitudinally, parallel to the axis of the rail. Since the elastic wave speed is affected by the presence of stresses in the rail, the change in the wave speed could be measured and then used to determine the longitudinal stress in the rail.

In order to evaluate this concept, an ultrasonic probe that attaches to the web of the rail was developed. This probe was then tested in track on the Santa Fe Railway and at the Transportation Test Center track to determine its feasibility for measurement of thermally induced rail stresses.

It was found that when a stress-free reference measurement was provided, the probe was capable of measuring stress changes with an accuracy of ± 1 ksi. However, it was further concluded that, because of the "variations in longitudinal wave travel times apparently due to residual stresses and difficulties encountered with shear wave measurements (used for a reference measurement) in the field, absolute stress measurement is not feasible at this time" [7]. In addition, further investigation into the effects of material properties, wave speed, and prior deformation histories on the wave propagation speed variations is needed to establish the usefulness of this measurement technique even when a stress-free reference or "zero" is provided.

Measurements System Requirements

There is a well-defined need in the railroad industry for a system that can nondestructively measure the longitudinal rail force. This need was dramatically emphasized by the National Transportation Safety Board in its investigation of a derailment attributed to track buckling, where it stated that "the railroad industry needs badly a portable stress measuring device which could give instant readings of compression or tension in a rail without disturbing it" [18].

In keeping with the purpose of this paper, which is the presentation and definition of the problem of longitudinal rail force measurement in the railroad environment, the following requirements for a practical measurement system are presented:

1. It should be ruggedly constructed and capable of surviving in the field.

2. It should be easy to handle and require only limited interpretation of data.

3. It should be nondestructive to the rail and track structure.

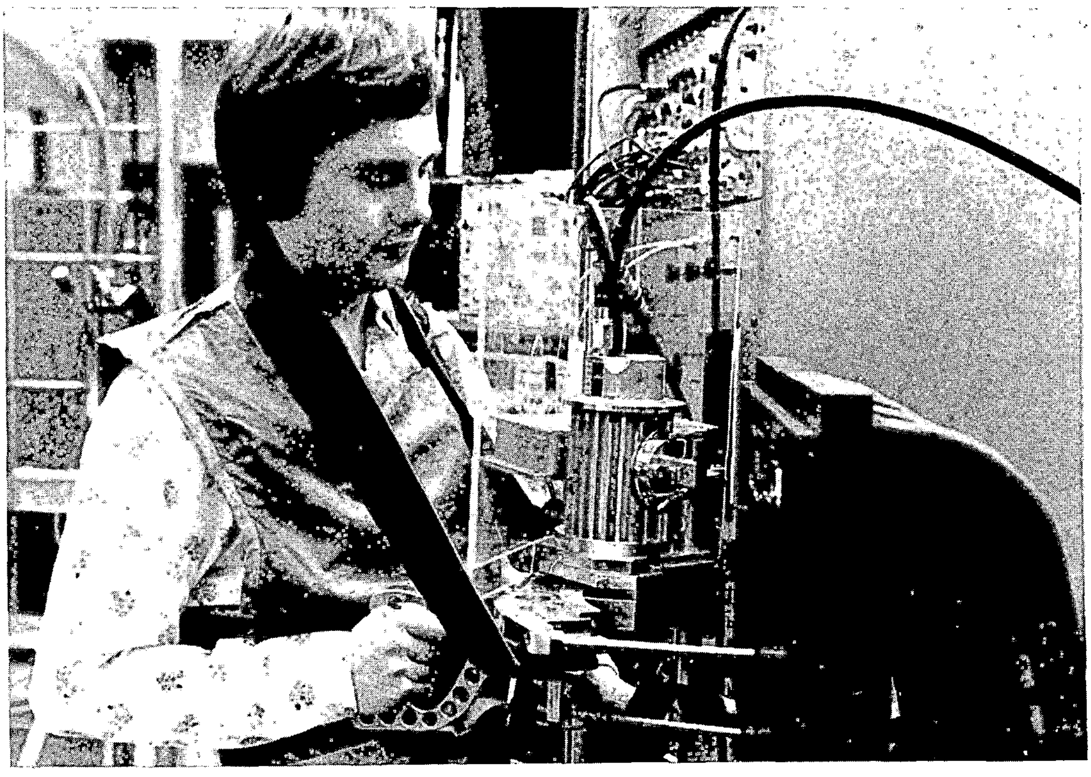

FIGURE 12. PORTABLE X-RAY DIFFRACTION UNIT

4. It should not require the disturbance of the track structure either during application or during "zeroing," if the latter is at all necessary.

5. It should require minimum or no calibration. If calibration is needed, it should not require heavy equipment or significant track time.

6. It should be independent of or readily compensated for:

a. rail size

b. rail metallurgy

c. heat treatment

d. rail head wear

e. work hardening or softening of the rail head

7. It should require minimum or no surface preparation of the rail.

8. It should provide for direct measurement of net longitudinal force (absolute).

9. It should not have to be permanently affixed to the rail or track structure.

10. It should permit "continuous" or at a minimum very frequent measurement of rail force from a moving vehicle.

It is hoped that this set of requirements adequately presents the scope of the problem and the practical difficulties that must be surmounted in order for a viable measurement system to be developed and utilized by the railroad industry. The problem is a significant one for railroad track maintenance forces and its solution is urgently needed.

References

[1] Federal Railroad Administration, Department of Transportation, summary of track buckling accidents (cause code 115) reported for 1977, Private correspondence.

[2] Kerr, A. D. "Lateral Buckling of Railroad Tracks Due to Constrained Thermal Expansion--A Critical Survey." In Railroad Track Mechanics and Technology, ed. A. D. Kerr. Proceedings of symposium held at Princeton University, April 21-23, 1975. Elmsford, New York: Pergamon Press, 1978.

[3] Kerr, A. D. "A Bibliography on the Determination of Stresses in Rails and Ties and Thermal Track Buckling." Report prepared for Department of Transportation, Transportation Systems Center, February 1976.

[4] Kerr, A. D. "Thermal Buckling of Straight Tracks, Fundamentals, Analyses, and Preventive Measures." Bulletin of the American Railway Engineering Association, bulletin 669, vol. 80 (September 1978).

[5] Private communication with AAR/TTD Track Strength Characterization Program, subcommittee 3.

[6] Kerr, A. D. "The Stress and Stability Analysis of Railroad Tracks." Journal of Applied Mechanics, vol. 41, no. 4 (December 1974).

[7] Hiltz, J. P., Jr., et al. "Measurement under Traffic of the Dynamic Rail Creepage Forces...." Bulletin of the American Railway Engineering Association, vol. 56 (1955) p. 283.

[8] Talbot, A. N., et al. "Discussion of Stresses in Railroad Track." Bulletin of the American Railway Engineering Association, vol. 38 (1937), p. 674.

[9] American Railway Engineering Association, Manual for Railway Engineering (Fixed Properties), section 5.5 (1962).

[10] Talbot, A. N., et al. "Discussion on Stresses in Railroad Track." Bulletin of the American Railway Engineering Association, vol. 37 (1936), p. 954.

[11] Magee, G. M., et al. "Fastenings for Continuous Welding of Rail." Bulletin of the American Railway Engineering Association, vol. 40 (1938), p. 549.

[12] Becker, F. L. "US - USSR Rail Inspection Information Exchange." Federal Railroad Administration, report no. FRA/ORD-77/35 (June 1977).

[13] "British Rail's Rail Force Measuring Transducer." Bulletin BRT 475. Trowbridge, Wiltshire, England: Gage Techniques, Ltd.

[14] Unpublished test data, A. D. Kerr and A. M. Zarembski, Department of Civil Engineering, Princeton University, Princeton, N.J., spring 1976.

[15] Barrett, C. S. Structure of Metals. New York: McGraw Hill, 1952.

[16] Private correspondence with C. J. Lambright, American Analytical Corporation, Grafton, Ohio, November 1978.

[17] Egle, D. M., and D. E. Bray. "Nondestructive Measurement of Longitudinal Rail Stresses: Application of the Acoustoelastic Effect on Rail Stress Measurement." Federal Railroad Administration, report no. FRA/ORD-77/09.1 (January 1978).

[18] National Transportation Safety Board. "Railroad Accident Report, Penn Central Company Train Second 115 (Silver Star) Derailment at Glenn Dale Maryland, June 23, 1969." Report no. NTSB-RAR-70-1 (June 1970), p. 20.

TECHNICAL PAPERS

"Field Tests on the Use of Ultrasonic Wave Velocity Changes to Detect Longitudinal Stress Variations in Railroad Rail"*

D. E. Bray
Texas A&M University

and

D. M. Egle
The University of Oklahoma

Introduction

This paper represents a summary of the work conducted at The University of Oklahoma on the use of acoustoelastic effect to detect thermally induced stress changes in continuously welded rail (CWR). Some of the details relating to the program either have been or will be reported in the technical literature and are incorporated herein by reference.

Initial studies began at The University of Oklahoma in June 1974 and ran through June 1975 [1], [2]. This phase was concentrated on a laboratory evaluation of the acoustoelastic effect in rail steel and a detailed study of the ultrasonic wave of propagation properties on the rail material. One principal finding from this phase showed that, when stressed in a loading machine, rail steel demonstrated velocity changes that are consistent with those that may be expected from any steel material. Investigations of wave propagation velocities at different locations on several rails showed the variations to be considerable. As a result of this phase, the initial intent to perform nondestructive stress measurements on the rolling surface of the rail was abandoned, primarily because of the severe velocity effect in the cold-worked zone. Laboratory tests showed that the rail web produced much more reliable results.

The follow-on phase (June 1975 to January 1977) concentrated on ultrasonic probe development -- some additional studies of the anisotropy of the cold-worked zone and a single field test of the system at the Department of Transportation's Transportation Test Center (TTC) at Pueblo, Colorado [3], [4], [5], [6]. These tests at the TTC showed that the ultrasonic system was, in fact, capable of detecting stress changes in rail installed in track. The remainder of this paper reviews the design of the probe assembly and ultrasonic system and the results the TTC tests. The published literature should be consulted for more details.

Ultrasonic Probe for Longitudinal Stress Measurement

The measurement of the acoustoelastic properties of rail steel showed that the effect is greatest for longitudinal waves propagating in the direction of the applied stress [2]. The probe was designed to generate a critically refracted longitudinal wave (P-wave) along the rail length. Travel time data were obtained from the two receiving probes located in the wave path. A reference shear wave was included in the design.

The data also showed that the relative change in speed for longitudinal waves propagating along the direction of the applied stress is

$$\frac{dV_L/V_L^o}{d_\varepsilon} = -2.45, \qquad (1)$$

where V_L = speed of longitudinal waves,

V_L^o = speed of longitudinal waves in absence of stress, and

ε = longitudinal strain corresponding to stress σ.

The relative change in travel time may be shown to be

$$\frac{d(t_L/t_L^o)}{d_\varepsilon} = +2.45 \qquad (2)$$

or, in terms of the change of applied stress $d\sigma$

$$dt_L = \frac{2.45\ t_L^o}{E}\, d\sigma, \qquad (3)$$

where E is the Young's modulus and t_L, t_L^o are longitudinal wave travel times.

The probe was designed to measure the wave travel times over a nominal distance of 216 millimeters (8.5 inches). Typical wave speeds in rail steel are 5,900 meters per second (2.32 x 10^5 inches per second) and 3,230 meters per second (1.27 x 10^5 inches per second) for longitudinal and transverse waves, respectively. Hence, the changes in travel times are expected to be near 0.44 nanosecond per meganewton per square meter (ns/[MN/m^2]) (3 nanoseconds per 1,000 pound-force per square inch [ns/ksi]) and 0.09 ns(MN/m^2) (0.6 ns/ksi), respectively.

The probe design, which evolved through four steps, is shown in figure 1. It consists of two transmitters and four receivers held in position by a steel frame. The transmitters and receivers use the conventional technique of diffraction through a plastic-steel interface for generating and detecting waves parallel to the rail surface. Incident angles in the plastic wedges are 28 and 55 degrees, respectively, for the longitudinal and transverse waves. The transducers are PZT-5 piezoelectric plates 25.4 milimeters (1 inch square and 1.27 millimeters (0.05 inch) thick, with a nominal resonant frequency of 1.6 megahertz. A pulse-overlay technique was used for travel time measurements. The accuracy of the system was felt to be about 3 nanoseconds.

*Presented at conference by D. E. Bray.

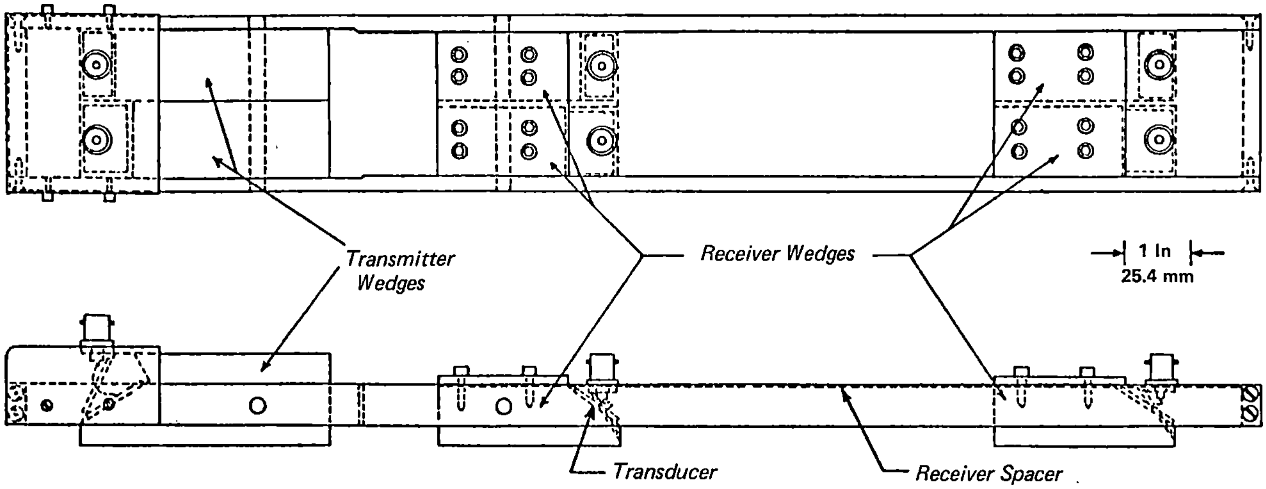

FIGURE 1. ULTRASONIC PROBE FOR MEASURING RAIL STRESSES

Figure 2 illustrates the electronic instrumentation for travel time measurements and figure 3 provides a diagram of the frequency divider.

Field Evaluation of Probe

Field Tests at the TTC. The principal field tests were conducted at the Department of Transportation's Transportation Test Center (TTC), Pueblo, Colorado, from approximately 1500 hours on 10 December 1976 to 1600 hours on 11 December 1976. Weather through this period was generally favorable for conducting the tests. Skies were clear and the ambient temperature reached a low of -12°C (11°F) at 0500 hours on 11 December. The high ambient reading was 8.3°C (47°F), at 1600 hours on 11 December. Rail temperatures peaked near 15.5°C (60°F) at noon the same day. There was very little wind.

Four stations were instrumented by TTC personnel for strain and temperature data. These locations were 91.4 meters (100 yards) apart toward the middle of a 609-meter (2,000-foot) tangent section of the access track to the test section used for operating the linear induction motor (LIM) rail vehicle. Stations 26 and 35 were located near a weld. Station 26 was 1.2 meters (4 feet) and station 35 was 0.51 meter (2 feet) from the nearest weld. Stations 29 and 32 were located near the center of a rail. Station 29 was 4.6 meters (15 feet) and station 32 was 3.6 meters (12 feet) from the nearest weld. The track is oriented east-northeast and is constructed of 119-pound rail with 23-inch tie spacings. Each station was instrumented to read longitudinal strain at the neutral axis on each side of the rail, vertical strain at the same location, and lateral strain at the top of the rail. Rail temperature also was recorded.

The ultrasonic probe was alternately placed on each side of the rail at each station and a full set of travel time data was recorded for both the shear wave and the longitudinal wave. The ultrasonic instrumentation was housed in a van located on the road adjacent to the track. The probe was held in place by C clamps. The rail surface was prepared by wire brushing and wiping the web area. Precautions were taken to insure that both the rail and the probe surface were free from grit and other loose particles since their presence would yield erratic readings. Low viscosity oil was used as the ultrasonic couplant.

A 0.91-meter (3-foot) length of 110-pound AREA rail located near each measuring station was used as a reference. Travel time measurements on the reference rail were used to assess temperature effects and to detect abnormalities in the probe.

Results of the TTC Field Test. The strain histories recorded at the two rail stations are shown in figure 4. Similar, although less complete, data were obtained at stations 32 and 35. This strain is that associated with the thermal stress in the rail since the strain due to thermal expansion is compensated for by the gages on the unstressed rail. The strains plotted are not absolute strains but are relative to the strain present in the rail when the bridges were initially balanced. The strains are plotted as functions of time beginning at about 2200 hours on 10 December (shown as -2 hours) and continuing to about 2100 hours on 11 December. The dotted lines shown in the figure are interpolations during periods when either the data recorded were obviously in error or the data were not recorded.

The strain histories are reasonably consistent with expectations. The maximum longitudinal tensile strain occurs at all four stations at approximately 0700 hours, which was shortly after sunrise. The histories show rapid changes from 0700 to 1200 hours due to solar heating, and a rapid increase in tensile strain due to cooling from 1500 hours to 1800-1900 hours. Most of the vertical transverse strain histories show trends consistent with the longitudinal strains.

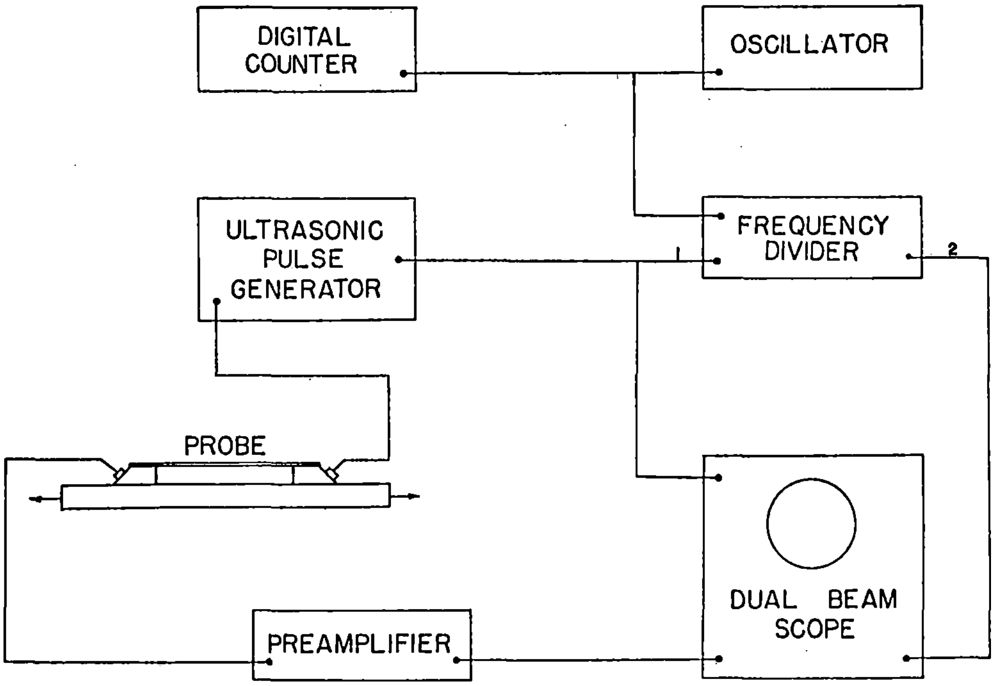

FIGURE 2. ELECTRONIC INSTRUMENTATION FOR TRAVEL TIME MEASUREMENTS

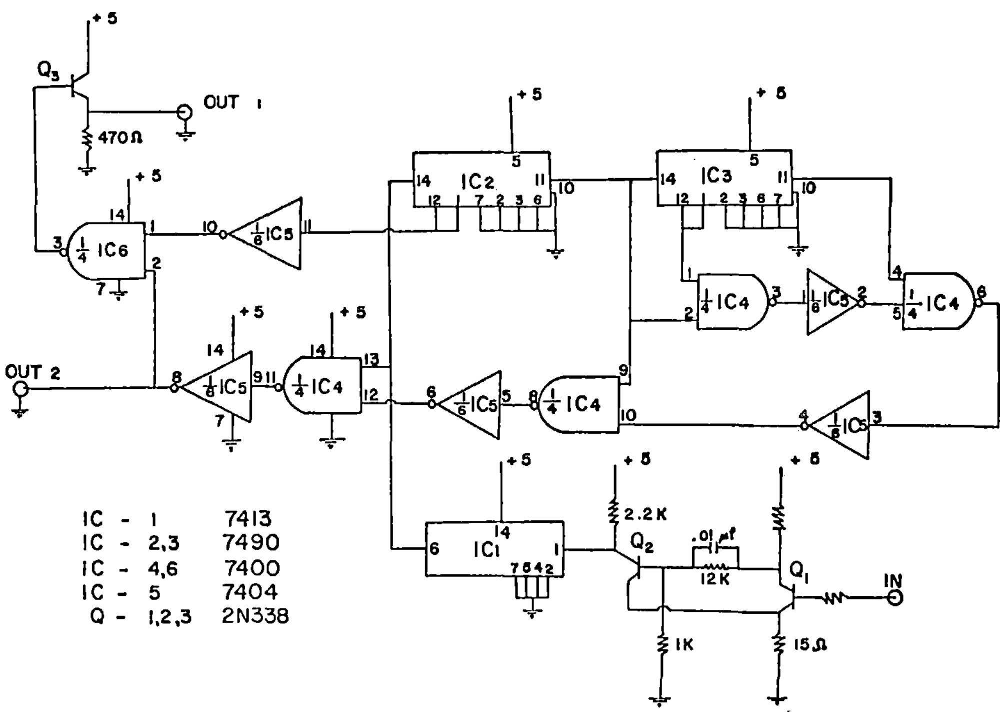

FIGURE 3. SCHEMATIC DIAGRAM OF FREQUENCY DIVIDER

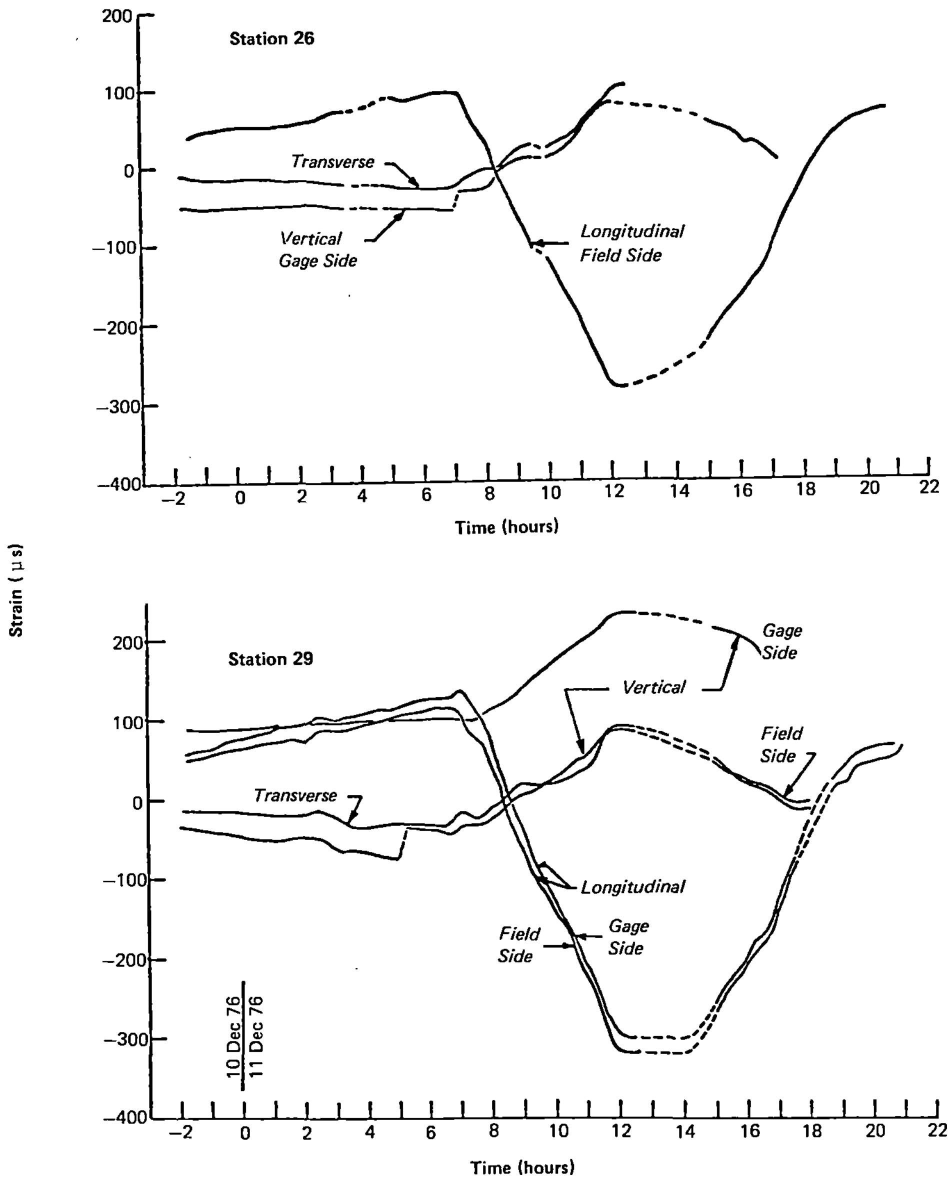

FIGURE 4. STRAIN HISTORIES AT STATIONS 26 AND 29 (TTC FIELD TEST)

The longitudinal wave travel time measurements at the four stations on the rail are shown in figure 5. Each data point shown is the average of measurements made on the field and gage sides of the rail web and has been temperature corrected.

The experimental data at station 26 shows more inconsistency than the data at the other three stations. However, the data for stations 29, 32, and 35 agree within ± 6.9 MN/m^2 (± 1 ksi) with the expected relationship between stress changes and longitudinal wave travel time. That is they have a common slope of 0.44 $\mu s/(MN/m^2)$ (3 ns/ksi) shown by the straight lines in figure 5.

The absolute travel time data at stations 29 and 32 are less than the travel time data at stations 26 and 35. That difference could be due to different longitudinal stresses or to different material properties. Note that stations 29 and 32 are both located near the center of a rail, and stations 26 and 35 are both near welds. That fact implies that the difference in absolute travel times may be associated with different rail-web stresses caused by either the manufacturing process or the rail welding process. The difference in the absolute travel times for the two data sets is seen to be about 0.02 microsecond. This is within the range of the longitudinal travel times observed in the laboratory along the length of a new unstressed 119-pound rail [3], [5].

The shear wave travel times for stations 26, 32, and 35 were relatively independent of stress level, but the data for station 29 show larger variations than had been expected. Further, the shear wave data for stations 26, 29, and 32 show

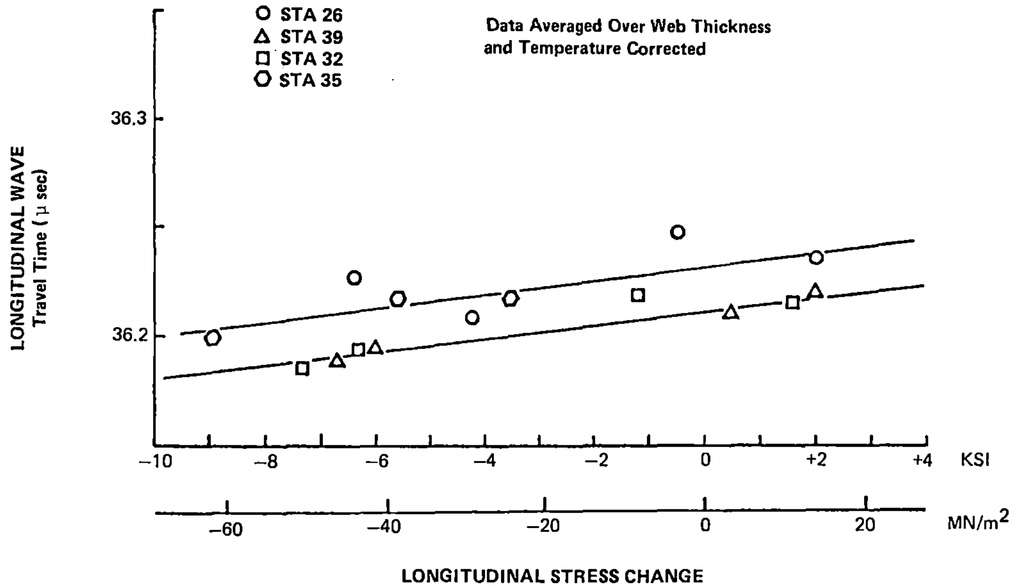

FIGURE 5. LONGITUDINAL WAVE TRAVEL TIME MEASUREMENTS ON FOUR RAIL STATIONS (TTC FIELD TEST)

reasonable agreement, but that for station 35 is considerably lower. This indicates that the elastic properties at station 35 are significantly different from those at the other locations.

Stress Relieving Tests at Station 32. After all of the ultrasonic and strain gage data had been compiled for the 24-hour period of the test, a decision was made to cut the rail at station 32 to establish the true stress levels throughout the 24-hour test. Full strain gage data were recorded for the stress relieving test but no ultrasonic measurements were made.

The tests were conducted in five stages at a time in the afternoon when rail temperature was reasonably uniform at approximately 26.1°C (79°F). First, strain data were recorded with the rail fully constrained. The strain data were recorded after each of the following steps. The rail clips were removed from seven ties on the side of the planned cut containing the strain gage. Then, the tie plates were removed from the same seven ties. Following that, the rail was saw cut. Finally, the loose rail was hit with a hammer along its length in order to insure that it was lying free on its ties.

The strain data behaved as expected. The longitudinal strains on either side of the rail were not severely affected until after the saw cut. However, greater longitudinal strain was recorded on the gage side of the rail compared to the field side, indicating that the rail was not entirely straight. With these data, the true rail stress can be estimated. The mean stress-free temperature is approximately 24.5°C (76.1°F). For the temperature encountered during the ultrasonic tests, the true longitudinal rail stresses ranged from approximately 6.9 MN/m^2 (1 ksi) to 74.5 MN/m^2 (10.8 ksi) in tension.

Conclusion

Based on the results of the field evaluation, it is concluded that the ultrasonic probe is capable of measuring longitudinal stress changes at specific locations in rail with an accuracy of ± 6.9 MN/m^2 (± 1 ksi). Although temperature-induced changes in wave speed affect the probe, the differential travel time measurement technique, along with the stress-free reference measurement, provides a means to cancel these undesirable effects.

The ability of the probe to measure absolute stresses has not been demonstrated at the present time. Although the variations in absolute travel time measurements are possibly due to variations in stress along the length of the rail, that question will be answered only with a more extensive comparison of the ultrasonic measurements with absolute stress measurements.

References

[1] Egle, D. M., and D. E. Bray. "Nondestructive Measurement of Longitudinal Rail Stresses." Interim report, DOT project DOT-OS-40091, report no. FRA-OR&D-76-270 (June 1976) PB-272061.

[2] Egle, D. M., and D. E. Bray. "Measurement of Acoustoelastic and Third-Order Elastic Constants for Rail Steel." Journal of the Acoustical Society of America 60(3): 741-44 (September 1976).

[3] Egle, D. M. and D. E. Bray. "Nondestructive Measurement of Longitudinal Rail Stresses: Application of the Acoustoelastic Effect to Rail Stress Measurement." Final report, DOT project OS-40091, Federal Railroad Administration, report no. FRA/ORD-77/09.1 (January 1978) PB-281164/AS.

[4] Bray, D. E. "Ultrasonic Pulse Propagation in the Cold-Worked Layer of Railroad Rail." DOT report no. FRA/ORD-77/34.II (January 1978).

[5] Egle, D. M., and D. E. Bray. "Application of the Acoustoelastic Effect to Rail Stress Measurement." Materials Evaluation 37(4): 41-46, 55 (March 1979).

[6] Bray, D. E., D. M. Egle, and L. Reiter. "Rayleigh Wave Dispersion in the Cold-Worked Layer of Used Railroad Rail." Journal of the Acoustical Society of America 64(3): 845-51 (September 1978).

"Limitations on the Use of Ultrasonic Stress Measurements Techniques"

Robert W. Benson
Bonitron, Inc.

Ultrasonic stress analysis techniques have now been available for more than 20 years. Very little use has been made of these techniques, even though there are many applications for which they appear to be well suited. When first developed, all new techniques are put to the test of being tried on problems for which other competing methods have failed. In attempting to apply new methods to the most difficult problems, failure is usually encountered and the techniques are subsequently discarded as being no better than others that have failed. At least to some degree, ultrasonic stress analysis has been applied to problems for which there is yet no answer, and this has resulted in a lack of confidence similar to that associated with other new methods that have been considered.

This paper is concerned with those aspects of ultrasonic stress analysis that have been encouraging and attempts to define some of those limitations, which should aid in avoiding the unsuccessful applications.

Ultrasonic Stress Analysis

The basic method of stress analysis using ultrasonic waves is a direct analogy to observing stress patterns in optically transparent solids using polarized light. One advantage is that almost all structural solids are ultrasonically transparent so that the methods may be applied directly to structures of interest rather than models.

Another advantage is the fact that the ultrasonic measurement results in a measurement that is stress sensitive rather than strain sensitive. Much of what is known concerning metallic structures is based upon an assumption that the stress is related to strain by a constant, such as is used with resistive strain gages. The use of such devices must characterize stress history from the time of application, and only by careful laboratory techniques can the state of stresses at time of application be determined. Since the ultrasonic method is directly related to stress, it is possible to determine the state of stresses at any time, thus revealing a possibility of determining residual stresses in the structure that can be considered to be attributable to previous history.

A general description of the methods of ultrasonic stress analysis can reveal some of the advantages. First, the most simple form of stress measurement is accomplished in a uniform rectangular specimen subjected to a uniform external force, as illustrated in figure 1. An ultrasonic crystal vibrating in a shear mode is coupled to the specimen. This causes a wave to propagate across the specimen, be reflected, and be received by the same crystal. The particle vibrations can be selected at any angle, but may be selected to be either parallel to or perpendicular to the applied force. The increase or decrease in travel time versus stress can be measured versus stress, as is plotted in figure 2. For an external compressive force, the parallel particle motion results in a decrease in travel time, whereas the perpendicular particle motion results in an increase in travel time although of smaller magnitude. The difference in travel time as well as the change in travel time for each component is linearly related to applied force.

If the ultrasonic crystal produces a pure shear wave, it will be linearly polarized and will remain so in propagating through the specimen so long as the particle motion is either parallel to or perpendicular to the stress within the specimen. If, however, the crystal is rotated so that the particle motion is at some angle with respect to the stress, then the state of polarization will change successively from linear to elliptical to circular to elliptical and back to linear polarization, as illustrated in figure 3. If the ultrasonic wave is produced as a pulsed wave train and the successive reflections are observed, the decay due to attenuation will be observed when the state of polarization is chosen along one of the principal axes of stress. For any other orientation, the successive pulses may be greater or less than the preceding pulse height due to the change in state of polarization of the wave. The third advantage is that the principal axes of stress may be located by the observation of the decay of multiple reflections of the ultrasonic wave.

If the plane of polarization is rotated and the decay is uniform for all orientations, then there is no birefringence and the material appears to be stress free.

This brief description of the behavior of ultrasonic shear waves is the basis for measurements of stress in metals. Similar effects can be produced near the surface, using waves that propagate in a thin layer near the surface and for which the particle motion is also transverse to the direction of propagation. Surface wave analysis, however, is much more complex due to the refraction of the waves. Stress gradients that exist near the surface cause a variation in velocity of propagation versus depth in the material. This velocity variation causes a refraction, or bending of the wave front, so that it either penetrates farther into the material or is confined to the surface like a wave guide.

Since the depth of penetration is frequency dependent, stress gradients as well as stress magnitude may be determined.

Limitations

A laboratory demonstration of ultrasonic stress measurement would impress the most skeptical observer. Provided that the right material is selected, a stress of less than 50 pounds-force per square inch (psi) can be detected, as is produced by squeezing a piece of bar stock between one's fingers.

The first major limitation is associated with the material to be studied. The stress-acoustic constant -- that is, the relationship between ultrasonic velocity and stress -- is dependent upon the material. Some alloys of some materials have relatively large effects and some materials do not even behave in a manner for which an effect can be defined.

For materials that have not been reported in the literature, it is necessary to perform a laboratory study to determine whether or not the material is birefringent and, if so, to determine the magnitude of the effect. If the precision of measurement is not sufficient for the amount of the effect, practical measurements may not be possible. It is further possible that the attraction is so great at frequencies for which time resolution is acceptable that signal strength limits the accuracy. Although increased frequency may appear to give improved accuracy, it may be found that attenuation effects limit the frequency at which successful measurements may be made.

The second major limitation is concerned with the shape of the specimen and the orientation of stresses within the specimen. If surfaces are flat and parallel, measurements are simplified. In general, thicknesses of less than 1/4 inch present problems in time resolution. Surface roughness comparable to a wave length, in general a few thousandths of an inch, can further reduce the accuracy of measurements. Geometries involving complex shapes should be avoided at least until simple geometries have been mastered. A thorough understanding of stress and stress distributions is a necessity if proper measurements are to be selected. It must be remembered that stress is not a scalar quantity, not even a simple vector quantity, but in general is described by a tensor. It is only when the stresses can be simplified enough by the selection of orientation and sample geometry, that simple measurements will suffice. Although present computer-aided techniques can allow for complex analyses, only the most sophisticated can expect to be successful.

The third limitation is concerned with ultrasonic wave propagation. Ultrasonic waves undergo reflection and refraction within the solid as they propagate. Under certain conditions it is possible that a surface wave can be converted to a shear wave traveling into the material and at a different velocity. Such conversions in the mode of propagation make analysis even more difficult.

The most troublesome problem in using ultrasonic waves for stress measurement is the fact that the wave propagation is sensitive to factors other than stress. If a sample is examined by ultrasonic measurements when no external forces are present, it would be desirable that the remaining effects are due to residual stresses due to the formation of the sample. Unfortunately, such factors as preferred grain orientation produced by the formation processes result in an effect that cannot be differentiated by the ultrasonic measurement from a true residual stress. If these effects were small in comparison to the desired effect, they could be ignored, but in most cases the processes resulting in desirable structural shapes produce a variety of metallurgical inhomogeneities in addition to residual stresses. It is important, therefore, to deal with these factors.

Researchers primarily concerned with the testing of basic properties of materials are familiar with the fact that basic mechanical tests used to determine the elastic and inelastic properties of materials, including yield strength, ultimate strength, etc., are subject to these same variables -- that is, preferred grain orientation, residual stress, etc. Preliminary observations under laboratory conditions indicate that there is a qualitative relationship between the ultrasonic

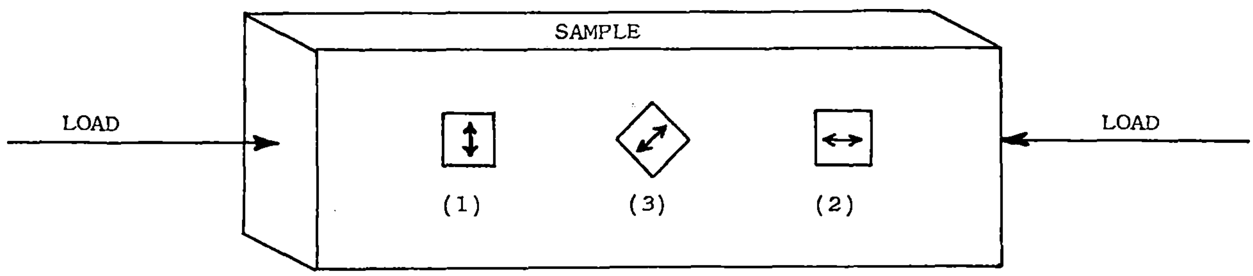

FIGURE 1. POSSIBLE DIRECTIONS OF SHEAR CRYSTAL PLACEMENT ON A SAMPLE

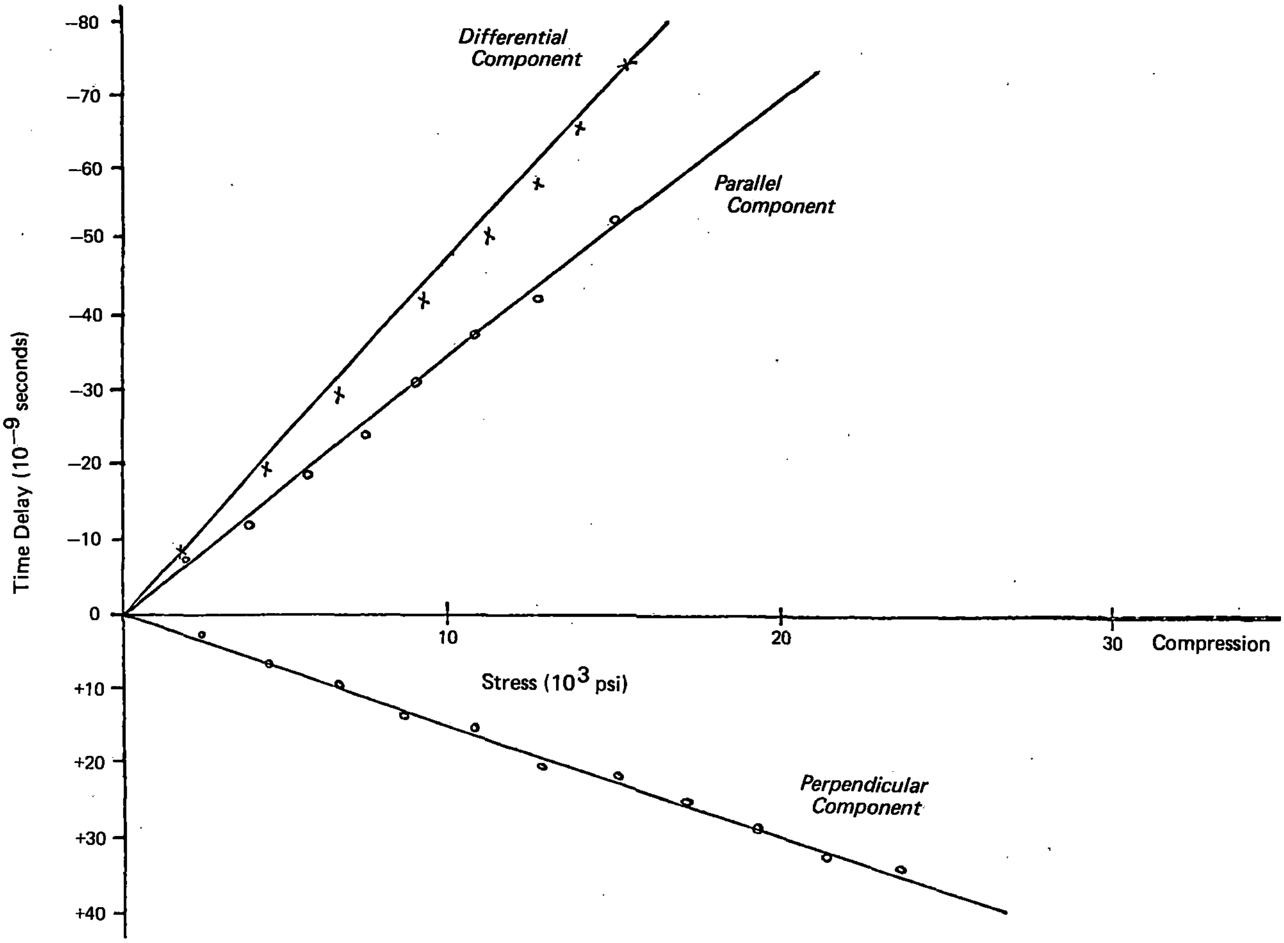

FIGURE 2. VARIATION IN TRAVEL TIME VERSUS STRESS OF VARIOUS COMPONENTS OF A SHEAR WAVE IN 7075 ALUMINUM ALLOY

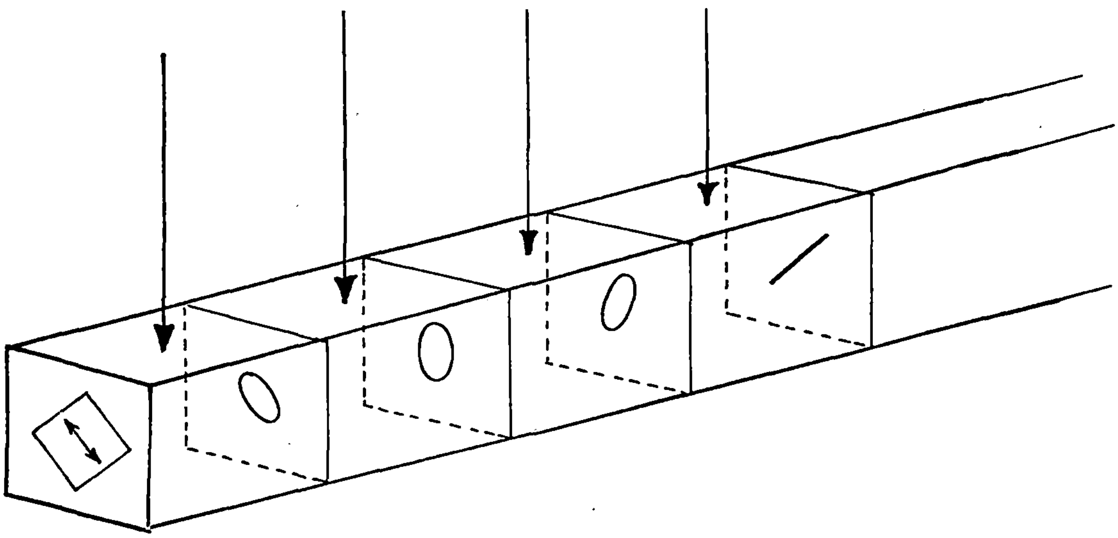

FIGURE 3. POLARIZATION OF A SHEAR WAVE AS IT PASSES THROUGH A MEDIUM

measurements and variations that may be produced in the mechanical tests. The following is an example of the procedures that were followed.

Tensile and compressive test specimens were cut from a large flat plate, 1/2 inch in thickness. Half of the specimens were taken with their major axis along the length of the plate and half were taken with their major axis transverse to the length of the plate. Ultrasonic measurements were made indicating that birefringence was present with the axes along the major axes of the specimen. It was further determined that the magnitude of the birefringence was equal to that obtained by an external pressure of 10,000 psi.

It is assumed that the formation of the ingot and the successive rolling or extruding processes introduce residual stresses, since each piece is stressed beyond the elastic limit. It is also known that the same processes result in preferred grain orientation; that is, the individual crystallites tend to align themselves with respect to the rolling direction. The elastic

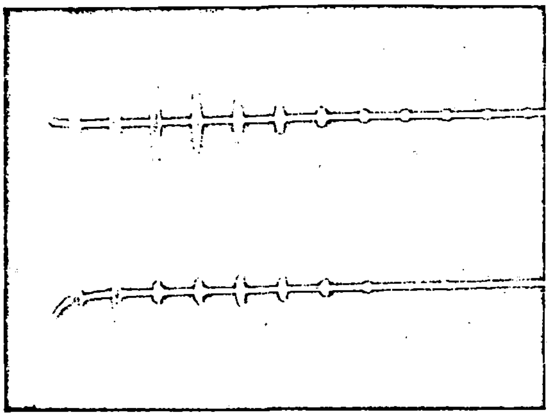

FIGURE 4. OSCILLOSCOPE PHOTOGRAPH SHOWING DECAY PATTERN OF A SHEAR WAVE IN 1/2 INCH PLATE

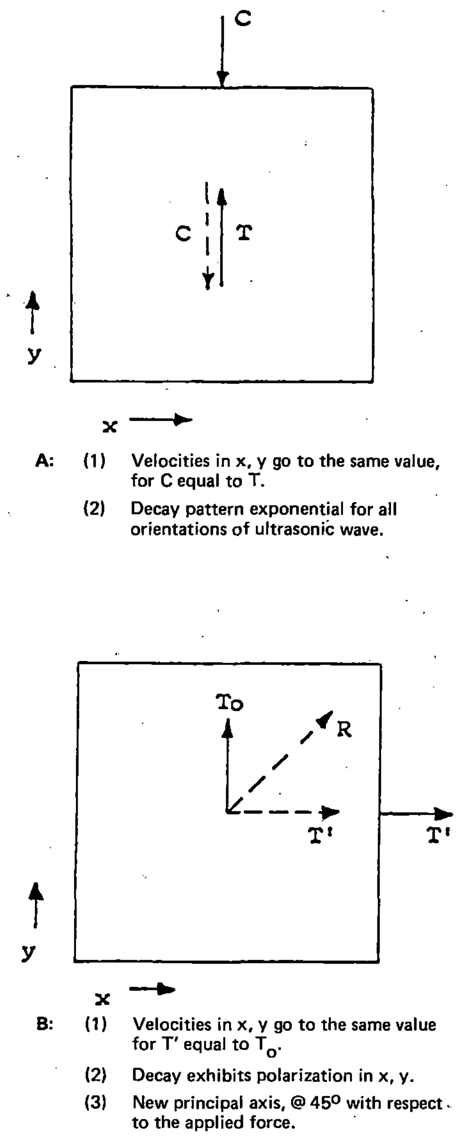

FIGURE 5. DETERMINATION OF CORRECT VECTOR FOR INITIAL STATE OF SAMPLE AS RECEIVED FROM MILL

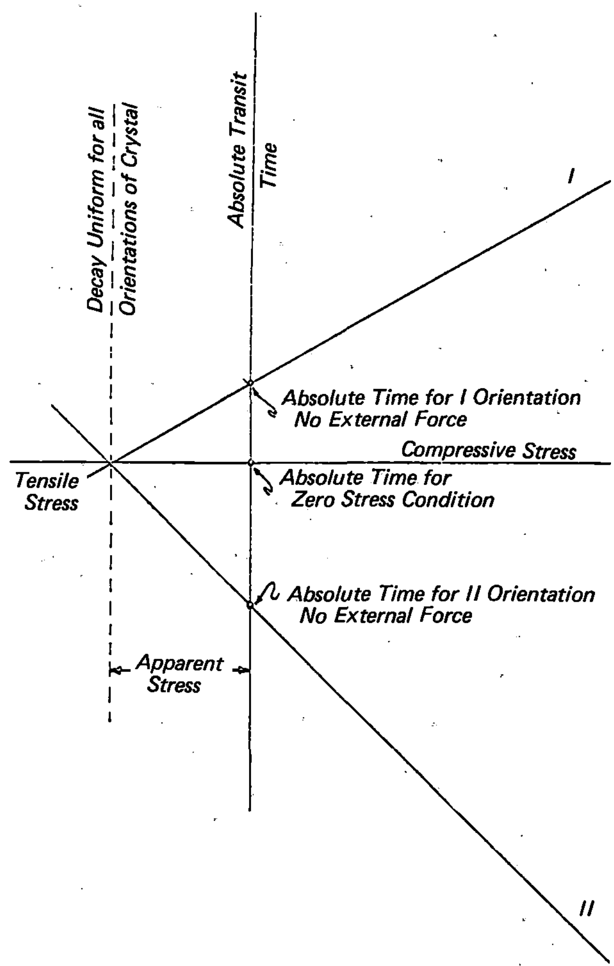

FIGURE 6. ILLUSTRATION RESULTING IN TRUE STRESS VECTOR IN TENSION ALONG 11 AXIS WITH MAGNITUDE T_o

constants of the crystallites vary with orientation and result in velocity variations for ultrasonic waves in a manner similar to that observed for an applied stress. In general, the apparent stress appears quite uniform throughout the samples. In such cases, the effect cannot be stress alone, for the summation of the forces across a cross section must vanish. Such effects as grain orientation, therefore, are added to those that are actual residual stresses within the sample.

The samples taken from the plate have a total effect due to actual residual stresses and all other causes that appears to be due to an equivalent pressure of 10,000 psi. It is unknown, however, whether this is due to an apparent state of tension along the major axis or a state of compression along the lateral dimension of the sample. Figure 5 illustrates the two assumptions that may be made. If an equal and opposite force is applied, the material can be made to appear stress free. For our samples, an application of a compressive force along the y-axis in part A of figure 4 resulted in achieving an apparent stress-free sample. When a tensile force was applied to the lateral surfaces, the resultant principal axis was formed.

After marking each of the test specimens with an appropriate arrow showing the magnitude and the direction of the apparent stress, a stress-strain curve was obtained on each test specimen. Qualitatively, the strain appeared to be related to the vector addition of the apparent residual stress and the externally applied stress. Although our observations are limited and qualitative in nature, it would appear that the mechanical behavior of a structure is influenced by the external load, the residual stresses, and all other elastic effects that influence the elastic behavior of the structure. The ultrasonic methods of measurement allow for new methods of analysis, providing that careful laboratory tests are performed.

Practical field application cannot be expected to be successful without adequate laboratory documentation of actual simulated results that can be substantiated. It is believed that ultrasonics will find its place in the testing of materials and, in addition, the actual performance of field testing.

"Special EMAT Configurations for Optimum Detection of Ultrasonic Birefringence"

R. B. Thompson
Rockwell International Science Center

Introduction

The previous two papers have dealt with the use of ultrasonics in detecting stresses, both in rails and in general. This paper will not cover this same material. Instead, it will rely on the previous papers as background. The emphasis will be placed on a new type of transducer which overcomes some of the coupling problems that are typically experienced in implementing those techniques. Topics to be discussed include the general properties of this new transducer, the unique fact that it can excite some wave types and polarizations that are not conveniently excited by piezoelectric transducers, and advantages that it offers in implementing stress-detection techniques.

Transducer Principles

Figure 1 illustrates the principle of the electromagnetic acoustic wave transducer (EMAT) [1]. Consider for the moment a non-magnetic metal part. Suppose that a wire has been placed adjacent to the material. Also suppose that a current has been driven through the wire at the desired ultrasonic frequency, ω, and that a magnet establishing a static magnetic field has been placed nearby. Eddy currents will then be induced within the metal and, because of the static field, there will be dynamic forces, the so-called Lorentz forces, exerted on the material. Ultrasonic waves are launched as a reaction to these sources, and the polarizations of these waves can be modified by changing the direction of the magnetic field. This phenomenon is very familiar. These forces are the same forces that drive an electric motor. This is not an exotic physical phenomenon by any means.

The phenomenon has several major advantages. It can be used to excite ultrasonic waves with no contact to the metal, so a couplant is not needed. In principle, one can generate waves using a transducer mounted on a car traveling at 60 miles per hour down a rail. The ultrasonic phase shifts that always occur when a couplant is used are avoided, so one can make more reproducible measurements. The transducer does not load the sample. One does not have to worry about one transducer interfering with a measurement made by another transducer.

If the metal part is magnetic, magnetostrictive forces exist as well as the Lorentz forces discussed above [2]. This can be understood by noting that, when current passes through the wire, there are magnetic fields that encircle the wire and penetrate into the material. If the material is magnetized by the static magnetic field, as indicated in figure 1 by the symbol M_0, the dynamic magnetic fields will cause the magnetization to have a slight oscillatory component. Through magnetostrictive forces, ultasonic waves can be launched as a response to this magnetization modulation.

Through each of these mechanisms, the same transducer structures can excite a number of different types of waves. In this discussion, the emphasis will be placed on the waves generated by the Lorentz forces since they exhibit much simpler behavior and are easier to understand. The magnetostrictive forces are also present in rails and should be considered. But the same waves can be obtained with slightly different transducer configurations.

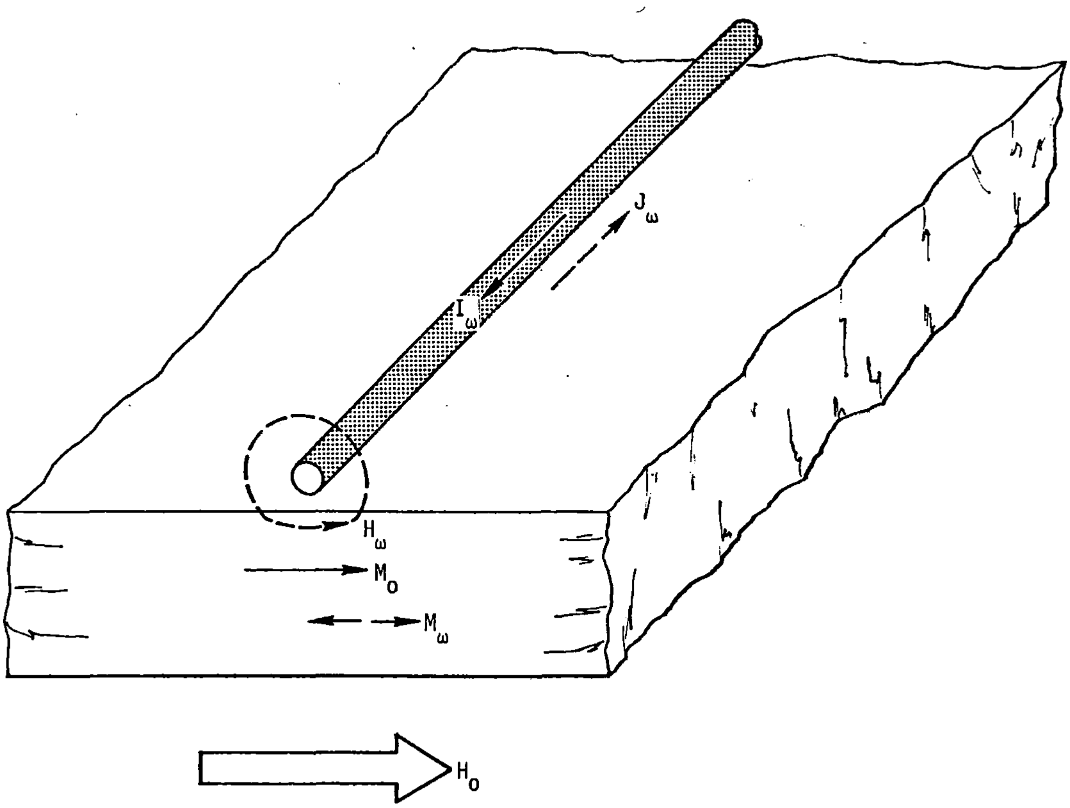

FORCE ON LATTICE: LORENTZ FORCE

MAGNETOSTRICTION

FIGURE 1. PRINCIPLES OF OPERATION OF AN EMAT

Transducer Configurations

Figure 2 shows a number of different transducer geometries that can be obtained by generalizing on the wire-magnet combinations shown in figure 1 [3]. Consider for the moment the excitation of an ultrasonic wave normal to the surface of a part. As shown at the left of figure 2, one of the transducer geometries that has been utilized the longest in this field is the spiral coil EMAT. The coil carrying the dynamic current has a spiral shape and is placed underneath a uniformly polarized magnet whose field is perpenducular to the part surface. In this case, the eddy currents induced in the part will flow in circular paths. The force, which is perpendicular to both the eddy currents and the magnetic field produced by the permanent magnet, will have the radial distribution shown at the bottom of the figure. These radial forces launch a radially polarized ultrasonic shear wave normal to the metal surface.

In the context of birefringence, such a wave has some advantages, particularly if one independently knows the axis of the stress. One can now simultaneously excite both shear wave components with just one transducer, without any need for rotating the transducer. This allows the relative velocity of the two components to be rapidly measured.

If, however, one would like to generate a plain polarized wave, one could do a number of things. The next column of the figure shows a scheme in which two elongated spiral coils are combined and arranged so the wire elements are parallel underneath the magnet. Here the combination of the magnetic field and the eddy currents produce a constant amplitude shearing force distribution that launches plane polarized shear waves normal to the surface.

If, instead of generating uniform current distributions, one creates a distribution in which the currents alternate back and forth,

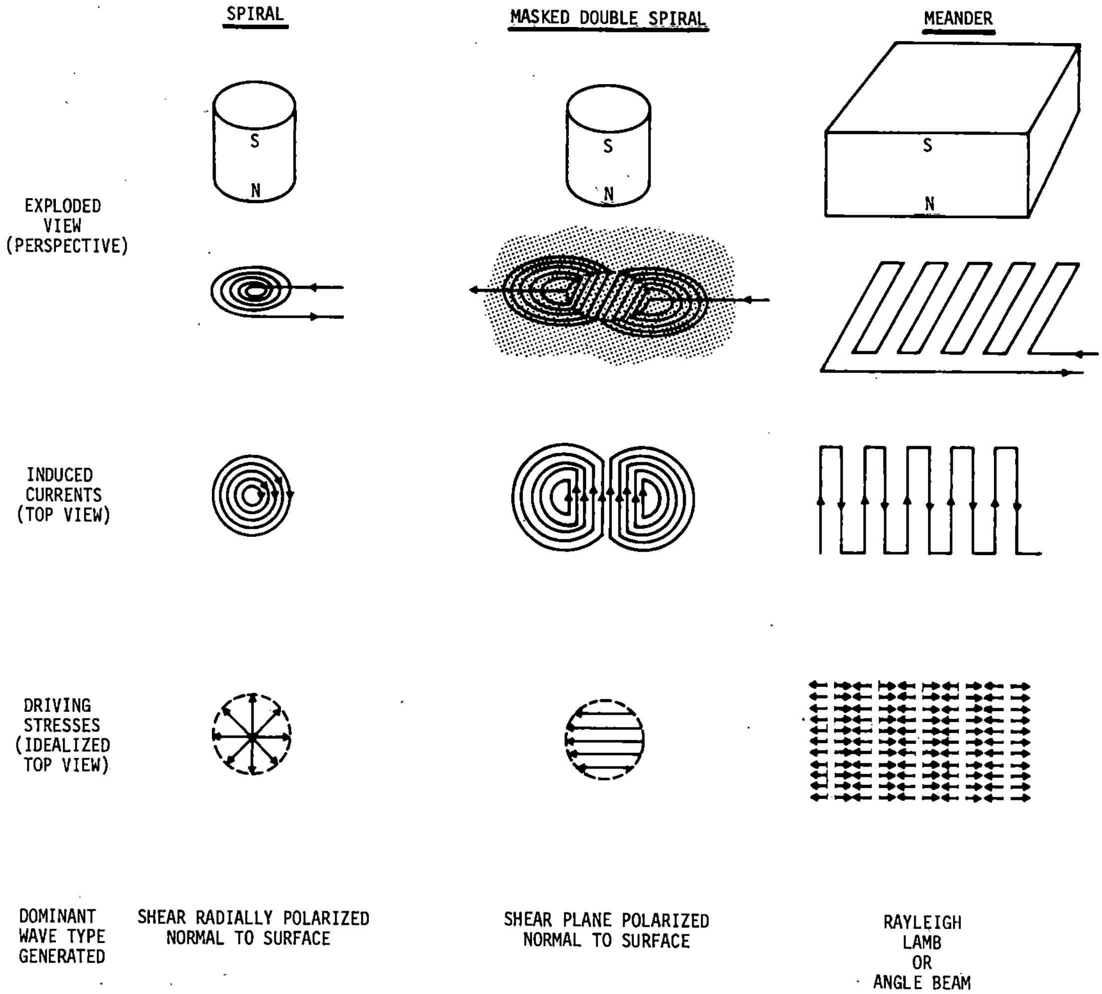

FIGURE 2. THREE REPRESENTATIVE EMAT GEOMETRIES

as shown at the right, one can produce surface stresses that are periodic in the plane of the surface. This is analogous to a phased array antenna used in radar, and can excite surface waves or bulk waves propagating at angles with respect to the surface. It will be the topic of a later discussion.

Figure 3 gives some data, obtained with a spiral coil, that show the utility of this transducer in birefringent measurements [3]. The sample was a 0.5-inch-thick aluminum plate. The coil was excited by a current impulse. The ultrasonic echo train consisted of signals that had traversed the sample multiple times. Since the receiver was on the side of the plate opposite the transmitter, the first signal has propagated through 0.5 inch of metal, the second echo has propagated through 1.5 inches of metal, and so forth. Closer inspection of the expanded scale displays in elements (c), (d), and (e) of the figure shows that each echo is broken up into a pair of signals. This pair of signals is produced by two orthogonal shear wave components that travel at a slightly different velocity. In this sample, the birefringence was induced by texture. However, it could have just as easily been a stress-induced birefringence, and it illustrates the fact that EMAT's can very easily excite, detect, and resolve two shear wave components traveling with different velocities.

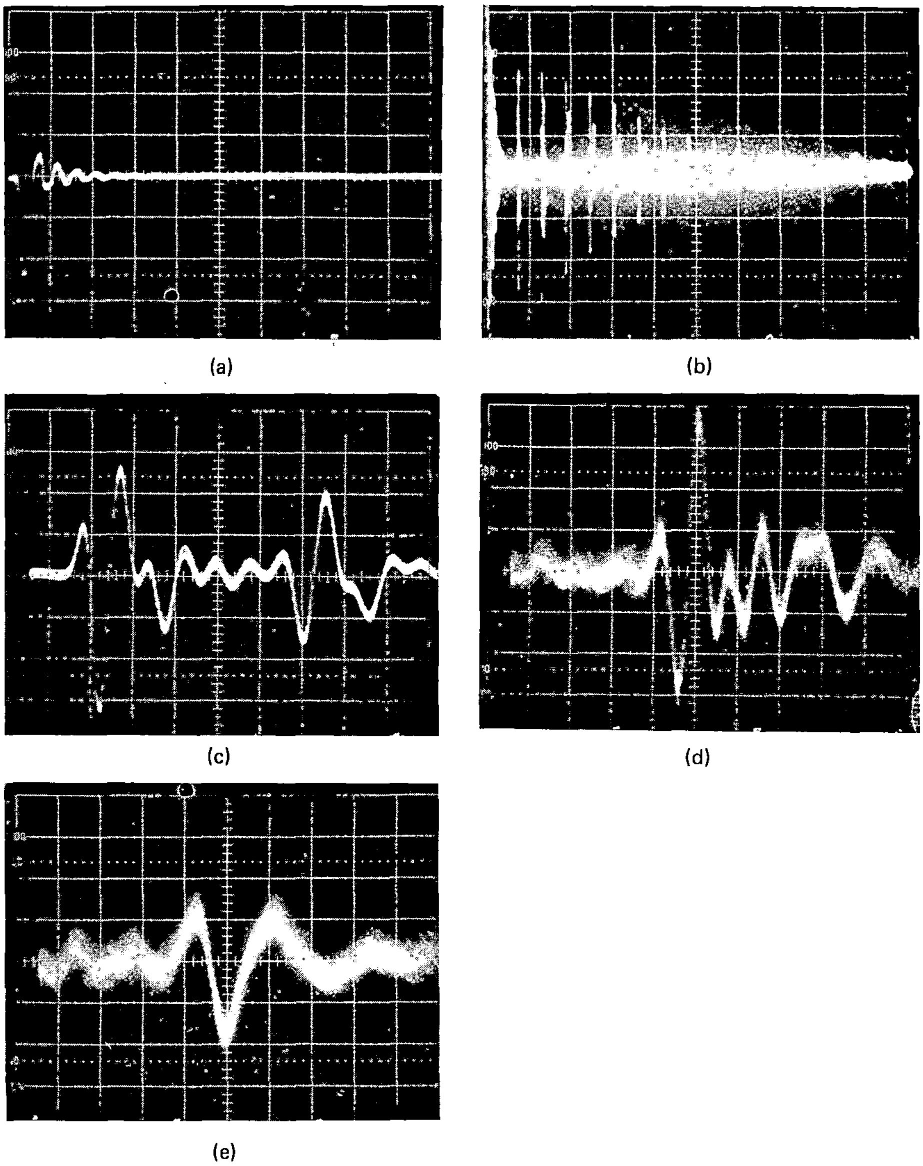

FIGURE 3. ULTRASONIC BIREFRINGENCE IN A TEXTURED ALUMINUM PLATE OF 0.5-INCH THICKNESS:

(a): CURRENT PULSE EXCITING EMAT (2 AMPERES/DIV, 0.2 MICROSECOND/DIV)

(b): ULTRASONIC ECHOES (20 MICROSECONDS/DIV)

(c): EXPANDED VIEW OF FIFTH ROUND TRIP ECHO PAIR (0.2 MICROSECOND/DIV)

(d), (e): EXPANDED VIEW OF NINETEENTH ROUND TRIP ECHO PAIR (0.2 MICROSECOND/DIV)

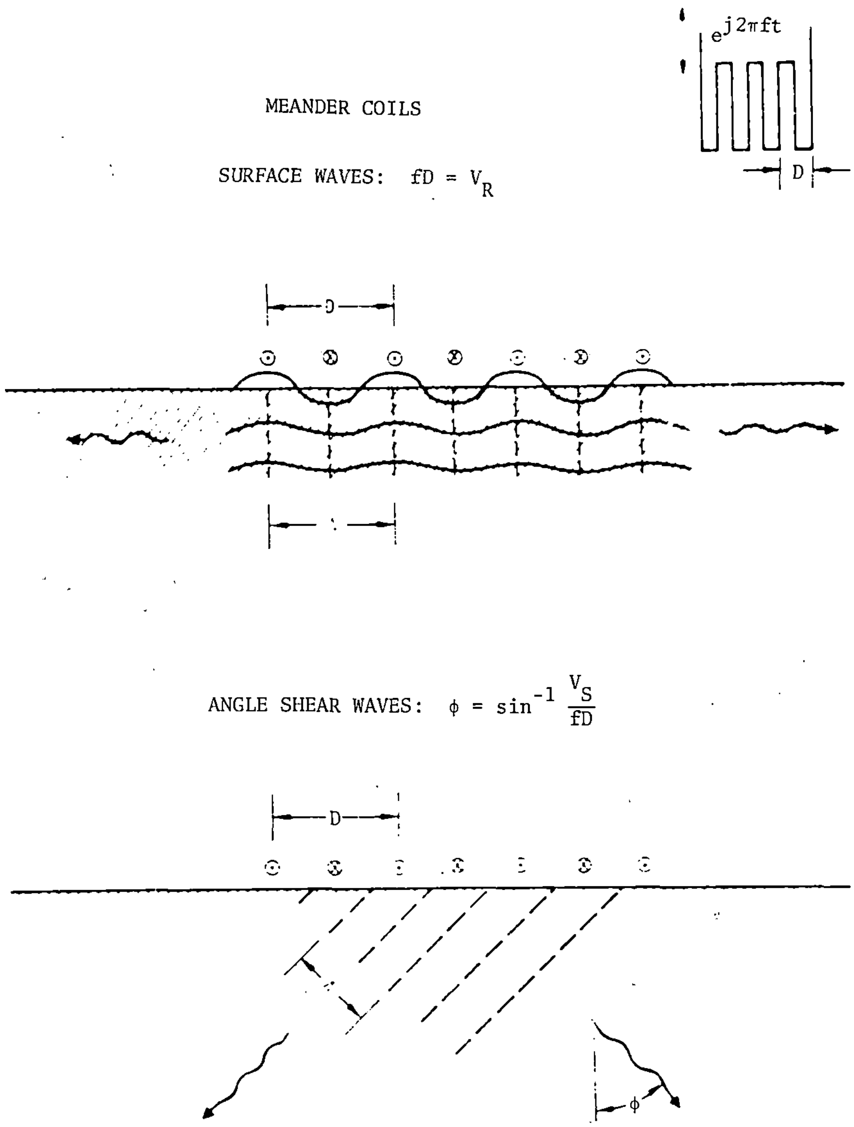

Principle of generation of surface waves and angle bulk waves by meander coil electromagnetic transducers.

FIGURE 4. MEANDER COIL EMAT: RAYLEIGH WAVE GENERATION (TOP) AND ANGLE BEAM GENERATION (BOTTOM)

Another effect is also illustrated in figure 3. It may not be directly germane to the inspection of rails for stresses, but it is rather interesting and worth noting. After a few trips through the sample, the echoes appeared quite similar. However, after 19 round trips, the two signals looked considerably different. (They are shown in two separate photographs in the figure because they are spread so much in time.) One pulse has totally changed in shape, presumably because of an anisotropic grain structure of the aluminum. This effect may be useful for studying grain structures in the future.

As noted above, surface waves and angle beams have a major role to play in the detection of stresses. Figure 4 shows what is known as the meander coil EMAT [4]. The coil is wound in a serpentine fashion with a period D. As illustrated in the cross-sectional view of the coil on a part, one sees that the current flows in

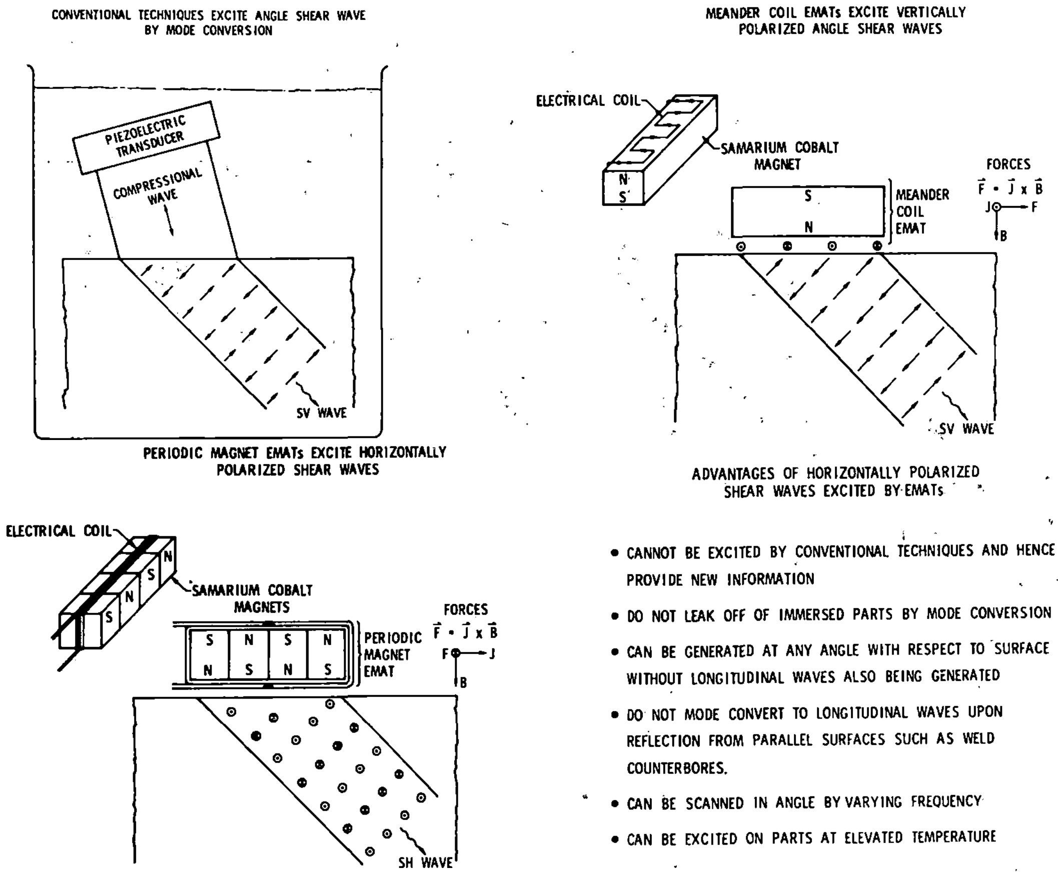

FIGURE 5. COMPARISON OF TRANSDUCER FOR GENERATING ANGLE BEAMS

alternate directions in adjacent wires. The frequency is adjusted such that the product of the frequency times the period of the coil is equal to the surface wave length, so one can launch a Rayleigh wave from each end of the coil.

If, however, the frequency is increased, there will no longer be constructive interference between Rayleigh waves launched from under the individual wires. Instead, a shear wave will be launched propagating into the material. The angle of that shear wave is determined by the driving frequency, and is equal to $\sin^{-1}(\frac{V_s}{fD})$, where f is the frequency, V is the shear wave velocity, and D is the coil period.

There are other types of ultrasonic waves that propagate in metals that are rather difficult to excite by conventional means, but that may be useful in stress detection. A transducer that excites some of these is illustrated in figure 5. At the top left is shown the traditional way of exciting an angle shear beam in a material. A piezoelectric transducer excites a compressional wave in either a fluid or plastic wedge material. This strikes the surface of the part at an angle, mode converts, and refracts to produce a shear wave propagating in the material, which is polarized in the plane of the figure. The transducer

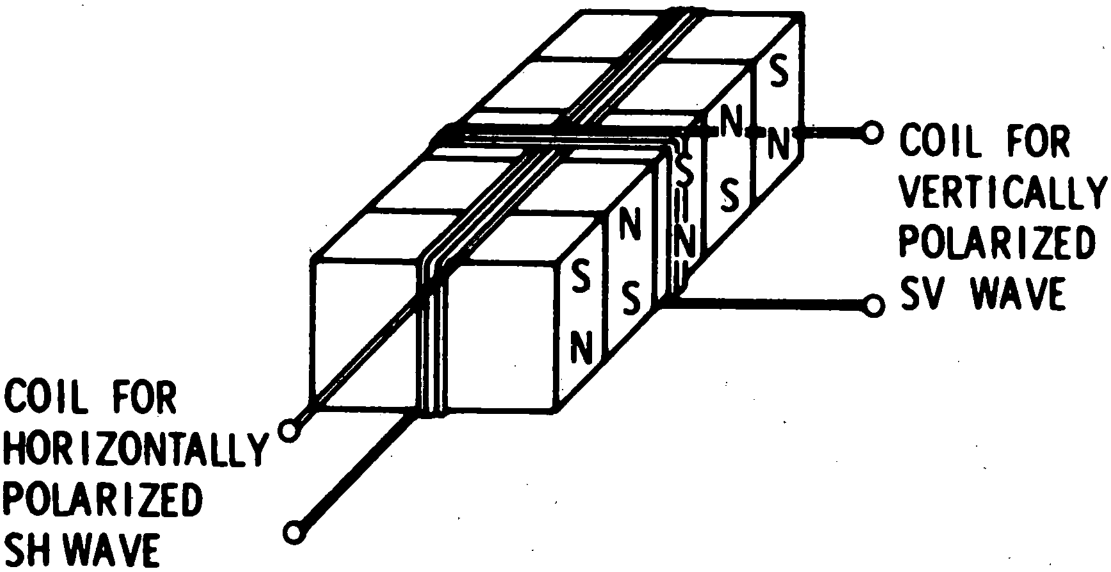

FIGURE 6. TRANSDUCER FOR SIMULTANEOUSLY EXCITING VERTICALLY AND HORIZONTALLY POLARIZED SHEAR WAVES

just discussed, the meander coil transducer with a uniform magnet, excites the same type of wave.

An alternate EMAT design uses a periodically polarized magnet and in a uniform coil (figure 5, bottom left) [5]. The periodicity is the same as that of a meander coil, but now the forces are perpendicular to the plane of the figure. A shear wave is launched, which is polarized parallel to the surface of the part. This is known as a horizontally polarized shear wave.

This suggests that it may be possible to perform birefringent measurements at angles other than 90 degrees with respect to a surface. (One case in which this has been done will be presented later in this paper.) As in the case of the spiral coil, the unique feature that makes this possible is the capability to impress shearing forces on the solid with no couplant. That capability greatly simplifies the implementation of many shear wave techniques.

Some of the general advantages of horizontally polarized shear waves for nondestructive evaluation (NDE) are listed in the lower right-hand corner of the figure. Several are more germane to flaw detection than stress detection problems and will not be discussed further. However, others do warrant additional comment.

The horizontal shear waves can be generated at any angle with respect to the surface of a part without accompanying generation of longitudinal or Rayleigh waves. Hence, one can often obtain cleaner signals that make it possible to measure velocities more precisely. They also do not mode convert when they reflect from surfaces parallel to their polarization. This again leads to cleaner signals.

Any of the EMAT transducers can be used at elevated temperature, and also at very reduced temperature. For example, if one were in an arctic environment and trying to use liquid couplants for rail inspection, the liquid may freeze. However, EMAT's will work at arbitrarily low temperatures and do not experience this problem.

The final type of transducer that will be discussed is a transducer consisting of a periodic magnet structure on which two coils have been wound, as shown in figure 6. Analyzing the

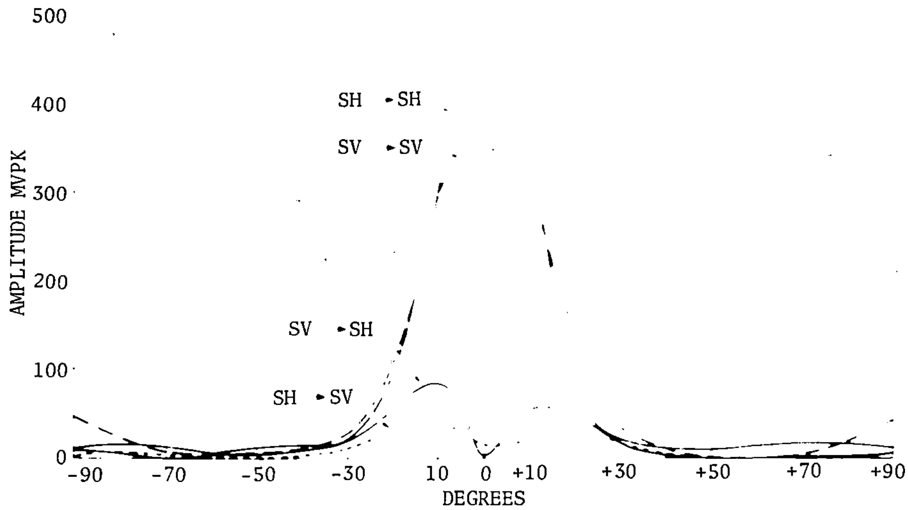

RADIATION PATTERNS

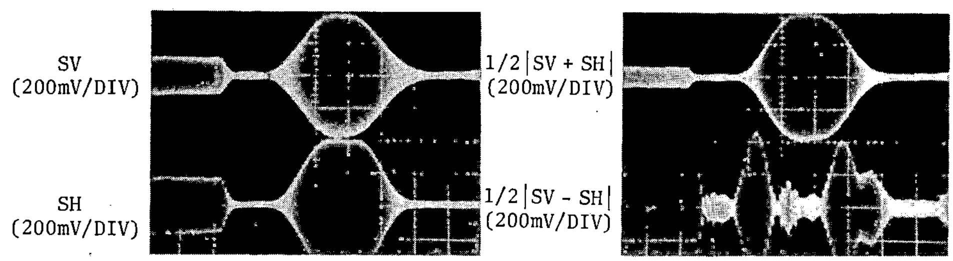

ALL 20μ sec/DIV

FIGURE 7. CALIBRATION OF ELLIPSOMETER CHANNELS

direction of the forces, one finds that one of the coils will excite a vertically polarized shear wave and the other coil will excite a horizontally polarized shear wave. It is thus possible to use one transducer to independently excite both types of shear waves and implement a birefringence technique [6].

Figure 7 presents some design data taken with such a device. In this case, the concept presented above has been slightly modified as shown in figure 8, by using a transducer consisting of separate but adjacent channels to generate the two wave types. In this pitch-catch system, the vertically polarized shear wave signal is transmitted from the vertically polarized channel of one transducer to the vertically polarized channel of the other, and likewise for the horizontally polarized shear wave.

The strength of the signals transmitted between the channels is plotted in figure 7 as a function of angle. The strength of the SH to SH signal is slightly greater than that of the SV to SV signal, but this can be compensated for very easily by modifying the gain of the respective receivers. The degree of orthogonality of the two channels is also indicated by presenting the SV to SH results. In theory, this should be zero on axis, with small but finite values at other angles, and the experiments bear this out well.

This transducer has been used to monitor the birefringence due to texture in a metal plate. Figure 9 presents the results. Here the output of the SH to SH channel has been summed with that of the SV to SV channel, with appropriate phase such that a null is produced on a reference plate. As the device is rotated on the textured sample, the null is destroyed by a birefringent induced relative phase shift in the two channels. This graph is presented to illustrate the simplicity and accuracy of the technique. A velocity shift of 0.1 percent was easily measured in a few seconds. One could easily make an order of magnitude or better improvement without too much difficulty. The limit at the present time is the mechanical rigidity of the fixture that controls the distance between the transducers.

A probe such as this, or a simple modification, could be applicable to the detection of stress in rails. For example, the device could be placed on the web and used to excite waves propagating perpendicular to the rail axis. One component would be polarized parallel to the stress and the other perpendicular to the stress, and stress-induced birefringence should be observed. Many other approaches can be conceived and should be investigated.

Practical Considerations

One limitation of the EMAT approach is that transduction efficiencies are somewhat less than

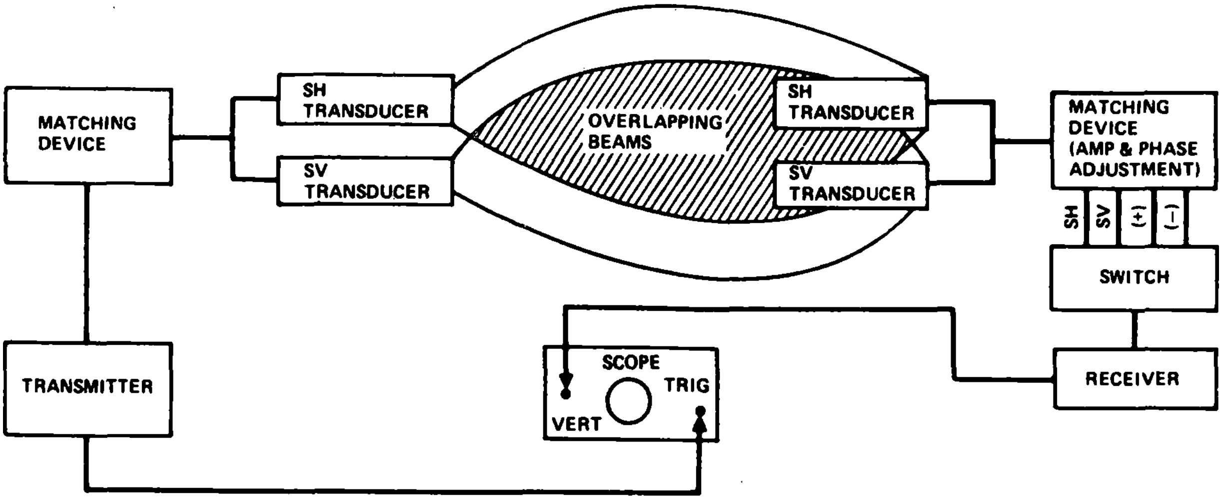

FIGURE 8. BLOCK DIAGRAM OF ULTRASONIC ELLIPSOMETER

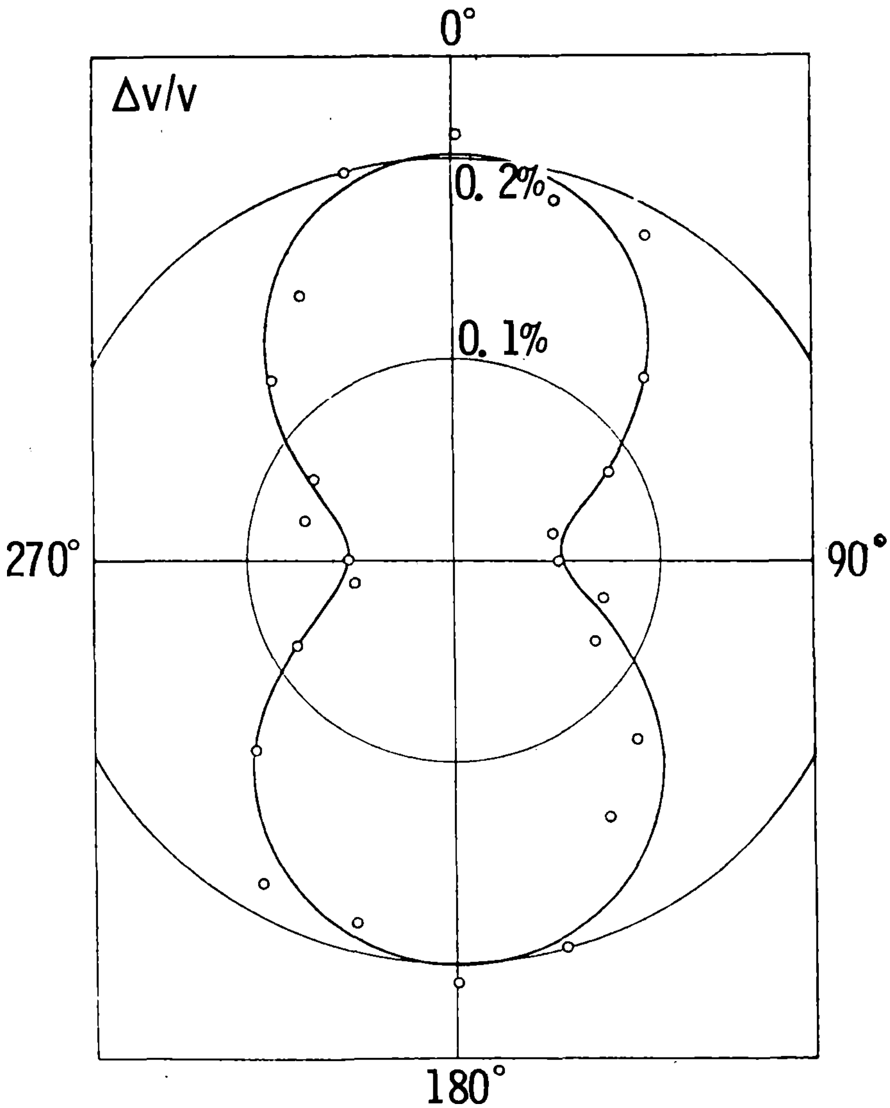

FIGURE 9. MEASUREMENT OF TEXTURE INDUCED BIREFRINGENCE IN AN ALUMINUM PLATE

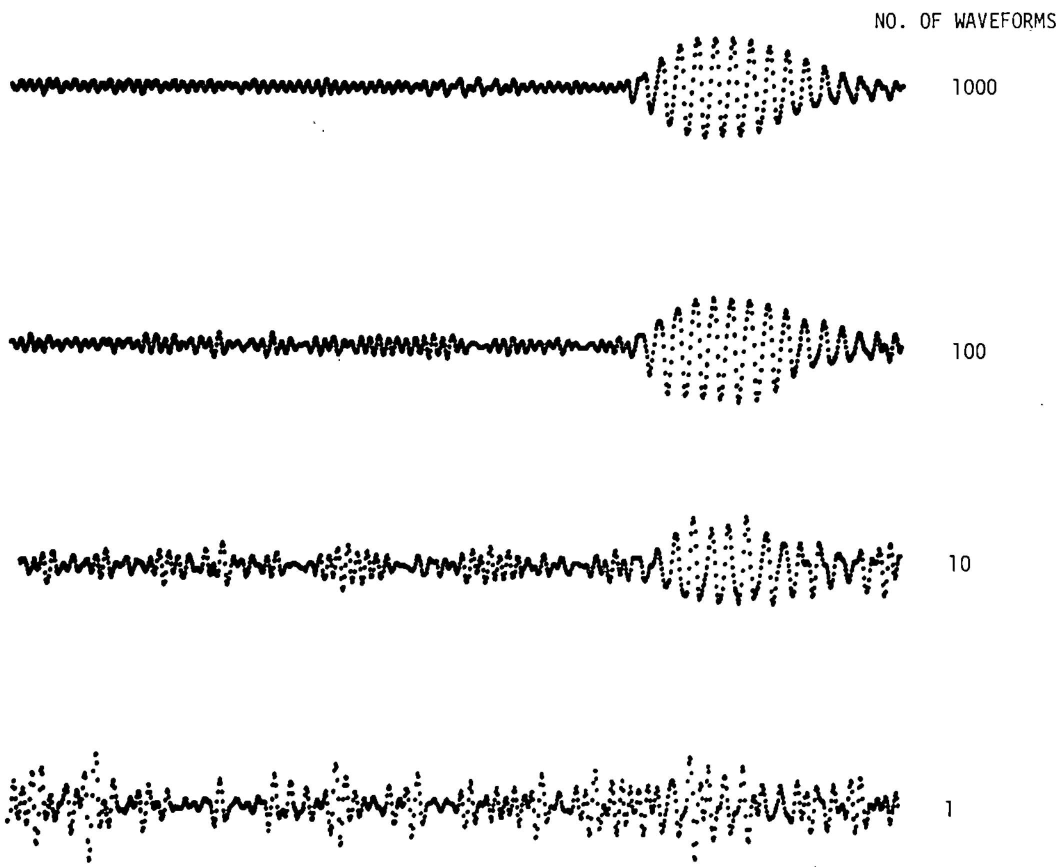

FIGURE 10. SIGNAL-TO-NOISE RATIO IMPROVEMENT THROUGH AVERAGING

those of piezoelectric probes. However, good, clean signals can be obtained, as can be seen from the figures in this paper, which are quite useful for velocity measurements. Sometimes, if one encounters a situation in which the signals are weak, one can use signal averaging techniques to enhance signal-to-noise ratio. Figure 10 presents an example of the improvement that can be gained using a technique based on digital signal processing. By averaging 1,000 repetitions of the same measurement, the noise was substantially suppressed. This produced a signal of sufficient quality to be the basis for precise velocity measurements. With presently available hardware, such averages can be performed in essentially real time at typical ultrasonic repetition rates. Thus this improvement shown in figure 10 can be obtained in about 1 second. A long period of time is not required.

A practical question that is often asked is, "How does the strength of coupling vary with the distance between the transducers and the parts?" The answer in principle is the same but in practice is rather different for transducers that generate waves propagating normal to part surfaces and transducers that generate beams propagating at angles to or along the surface. The basic physics dictates that the coupling decreases exponentially as lift-off increases. This occurs because the electromagnetic fields in the gap between the coil and the metal must satisfy Laplace's equation. The key parameter is the distance scale over which the fields decay. As may be expected, this is on the order of the distance over which the currents change direction in the coil.

For a spiral coil, this distance is on the order of 1 centimeter. Signal strengths are relatively insensitive to lift-off, with separations of 1 millimeter being easily tolerated.

For the meander coils, or the periodic magnet structures, lift-off is much more sensitive because of the rapid spatial variations of the eddy currents or bias fields. A useful rule of thumb is that one loses about 1 decibel in signal per mil of lift-off per megahertz of frequency for a pulse-echo or pitch-catch measurement. At frequencies above 1 megahertz, this implies that, although no couplant is required, the transducer must be very close to the part.

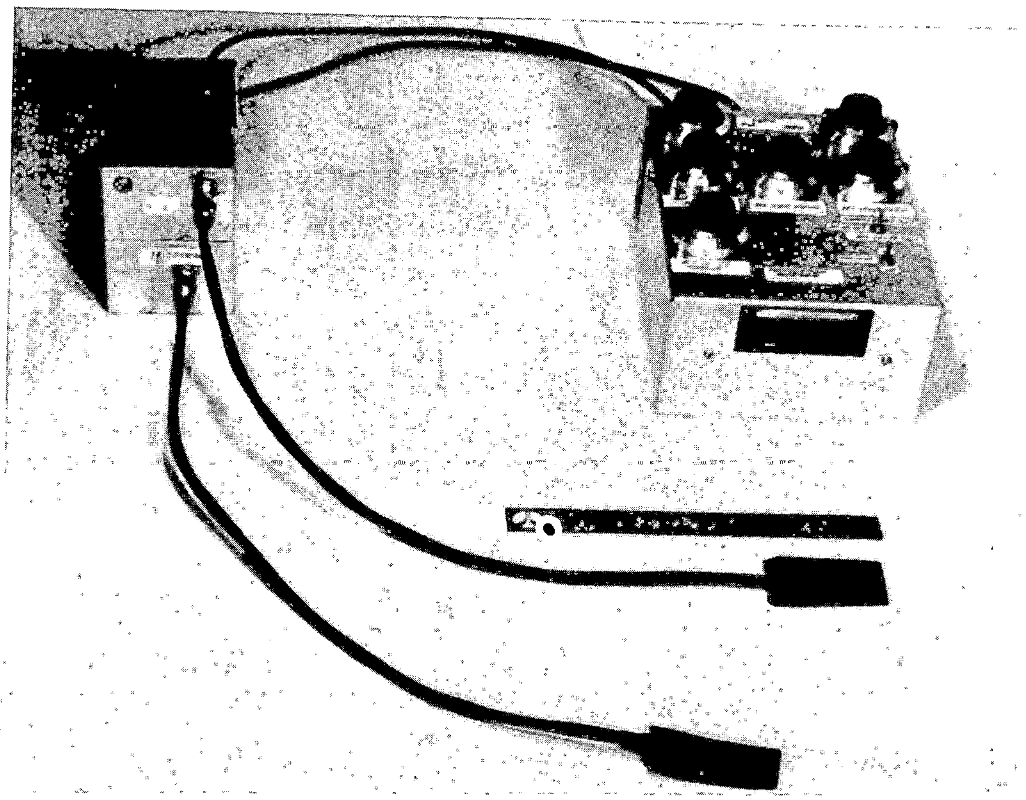

FIGURE 11. PROTOTYPE EMAT ELECTRONICS PACKAGE

The fact that the lift-off loss increases with frequency occurs because of the shorter periodicities of the transducer. If one can operate at lower frequencies, say 100 kilohertz, then the lift-off problem becomes much less severe. A 100-mil lift-off produced only 10 decibels of loss under those conditions. Systems at these frequencies have been developed for inspecting buried gas pipelines, and similar approaches should be applicable to rails.

Present Status of Hardware

To conclude the paper, a few pieces of hardware that have been developed for other applications will be shown to define the present status of the EMAT technology [7].

Figure 11 shows an early electronics package. Included is a pair of EMAT coils (the magnets are not shown) a dedicated transmitter/receiver circuit, and a correlation receiver. The coils can be made of flexible pieces of printed circuit board that are very convenient in curved geometries, such as certain parts of rails.

Figure 12 shows the results of some flaw detection performed on a rail with this equipment. Included is an oscilloscope photograph showing the ultrasonic signal reflected from a 1/8-inch hole in the web. This demonstrates that very nice, clean signals can be obtained with EMAT's in the rail geometry.

Figure 13 shows a prototype of a fully packaged EMAT system. In this flaw detector, a surface wave is excited at a frequency of 1 megahertz. The ultrasonic probe consists of a coil, such as shown in figure 10, and a permanent magnet. The probe is designed to be unidirectional, so that waves are generated and detected only in one direction. The instrument contains all of the transmitter and received electronics and digital circuitry necessary to convert the received information into a measurement of the distance to the flaw from the probe and a measurement of the strength of the ultrasonic signal. These are presented in a digital display.

Conclusions

The configurations that one could use in the measurement of stress in rails could perhaps be quite different, but these general concepts will apply. The EMAT provides a probe that can excite both new wave types and operate at high speeds -- properties that may prove invaluable in future rail inspection systems.

References

[1] Thompson, R. Bruce. "Noncontact Transducers." In 1977 Ultrasonics Symposium Proceedings, pp. 74-83. New York: IEEE, 1977.

[2] Thompson, R. Bruce. "Mechanisms of Electromagnetic Generation and Detection of Ultrasonic

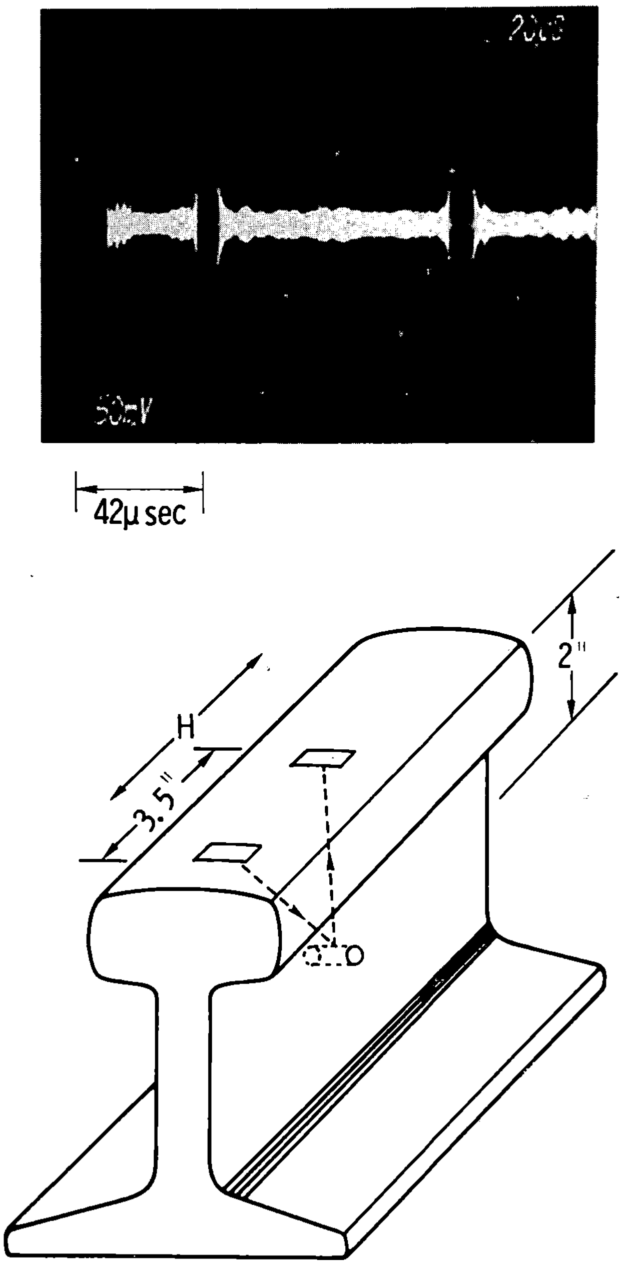

FIGURE 12. DETECTION OF SIMULATED FLAW IN RAIL WEB

Lamb Waves in Iron-Nickel Alloy Polycrystals." Journal of Applied Physics, vol. 48 (1977), pp. 4942-50.

[3] Thompson, R. B., and C. M. Fortunko. "Optimization of Electromagnetic Transducer Systems." In Proceedings of the ARPA/AFML Review of Progress on Quantitative NDE. Air Force Materials Laboratory, report no. AFML-TR-77-44 (1977), pp. 142-47.

[4] Thompson, R. Bruce. "A Model for the Electromagnetic Generation of Rayleigh and Lamb Waves." IEEE Transactions on Sonics and Ultrasonics, vol. SU-20 (1973), pp. 340-346.

[5] Vasile, C. F., and R. B. Thompson. "Excitation of Horizontally Polarized Shear Waves by Electromagnetic Transducers with Periodic Permanent Magnets." Journal of Applied Physics, vol. 50 (1979), pp. 2583-88.

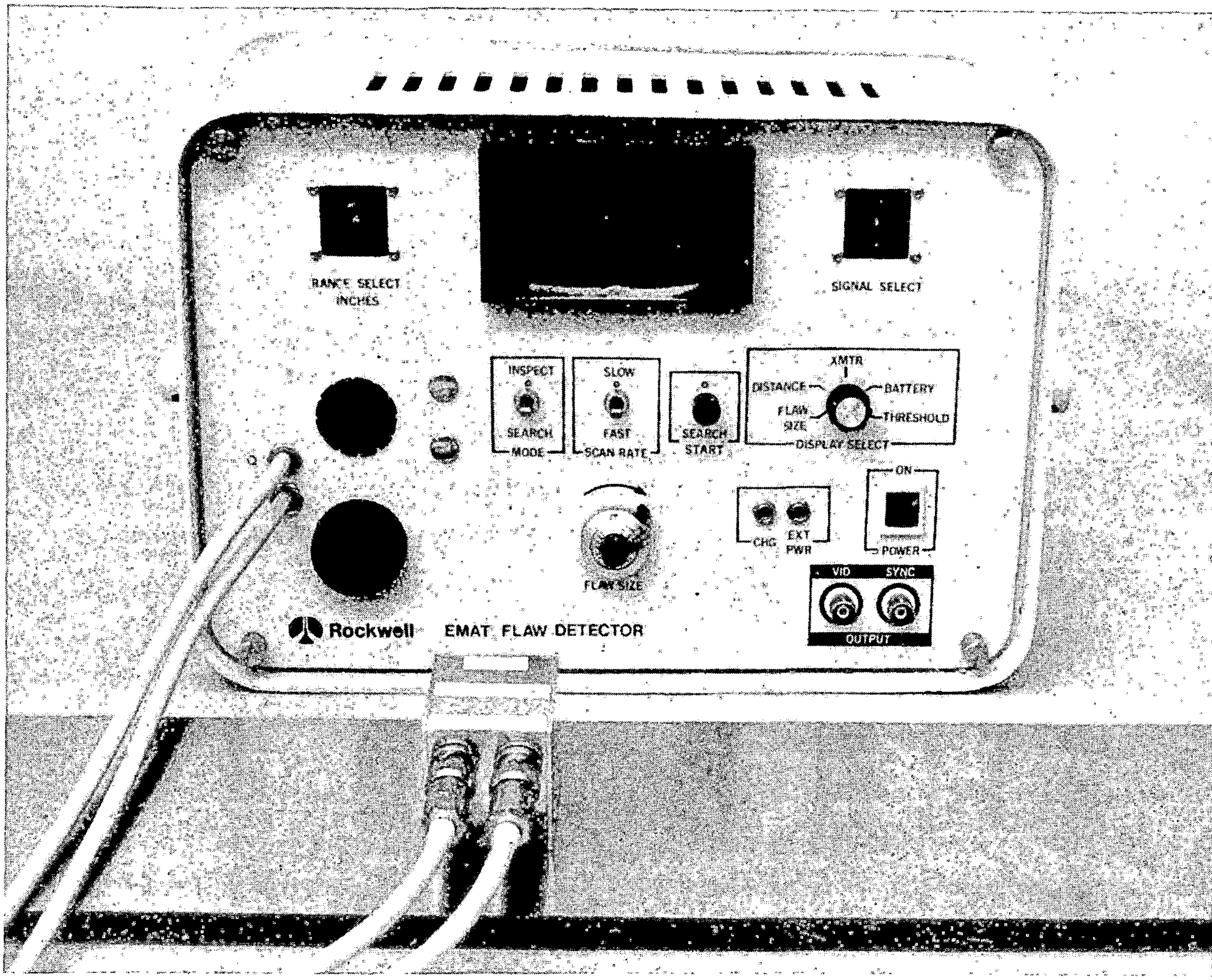

FIGURE 13. FULLY PACKAGED EMAT FLAW DETECTOR

[6] Thompson, R. B., and C. F. Vasile. "An Elastic-Wave Ellipsometer for Measurement of Material Property Variations." Applied Physics Letters, vol. 34 (1979), pp. 128-30.

[7] Thompson, R. Bruce, and George A. Alers. "EMAT Transducers for Ultrasonic Inspection of Structural Materials." In Proceedings of the National Electronics Conference - 1979, pp. 213-18. Oak Brook, Illinois: National Electronics Consortium, 1979.

"Measurement of Residual Stress by Noncontact Sensing of Magnetrostrictive Properties with EMAT's"

R. B. Thompson
Rockwell International Science Center

Introduction

In comparison with the preceding paper there is a second, conceptually distinct, way to use EMAT's in the detection of residual stress. This involves using them as sensors of the stress-dependent magnetostrictive properties of a magnetic metal, such as rail steel [1], [2], [3], [4], [5].

Figure 1 schematically illustrates the experimental configuration. Suppose a surface wave is being excited with the EMAT and that the magnetic bias is provided by an electromagnet whose strength can be varied by changing the dc durrent that drives it. Suppose also that the amplitude of the wave generated is detected by a second transducer. In this discussion, detection will be assumed to be performed by a piezoelectric wedge, but other transducer types, including EMAT's, could be used. If the strength of the magnet bias is varied, the ultrasonic signal strength will change in the manner shown at the bottom of the figure. At high fields, there will be a linear relationship between the bias field strength and the ultrasonic signal amplitude. At lower fields, one finds peaks and fine structure in the graph. The underlying physics is that, at high fields, one is in the Lorentz force regime, where driving forces are directly proportional to the bias field. For lower bias fields, the magnetostrictive properties of the material become dominant and lead to the observed structure. Since magnetostriction is very sensitive to stress, the features of this structure can be used in the estimation of stress.

To avoid possible confusion with respect to the preceding paper, it should be noted that not all regions of the curve are equally sensitive to stress. Thus, at the large maximum, the efficiency is relatively stress insensitive. There is also no stress sensitivity in the Lorentz force regime. Consequently, the stress-dependent effects discussed in this paper do not interfere with the previously discussed applications of EMAT's in birefringent techniques.

Physical Principles

The role that magnetostriction plays in determining the transduction efficiencies has been established in a series of scientific studies [6]. The details of the modeling and confirming experiments will not be presented here, but it should be noted that the driving magnetostrictive forces are related to the derivatives of a magnetostrictive stress tensor, and that the amplitude of the wave generated is proportional to an overlap integral involving the depth dependence of these magnetostrictive forces and the velocity profile of the ultrasonic wave.

Figure 2 presents the results of one comparison between theory and experiment. The dots on the graph show the results of experimental measurements of the ultrasonic wave amplitude as a function of the bias magnetic field. The solid line is the theoretical prediction, which contains as parameters the magnetostrictive coefficients of the material. In this case, the magnetostrictive coefficients have been experimentally measured on the same sample with strain gages. The agreement between theory and experiment is excellent except at low bias fields, where irreversible effects become dominant. The dotted line on the graph shows the theoretical predictions when the magnetostrictive coefficients were calculated based on a polycrystalline average of single crystal responses. From 10,000 oersteds down to the 300-oersted bias at which the large peak occurs,

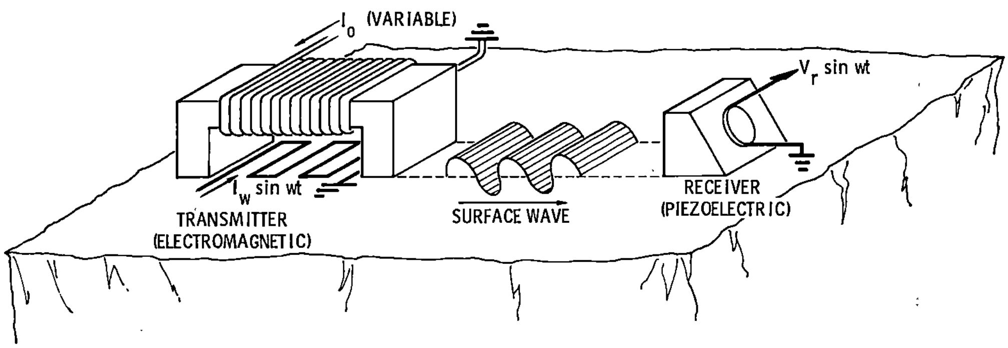

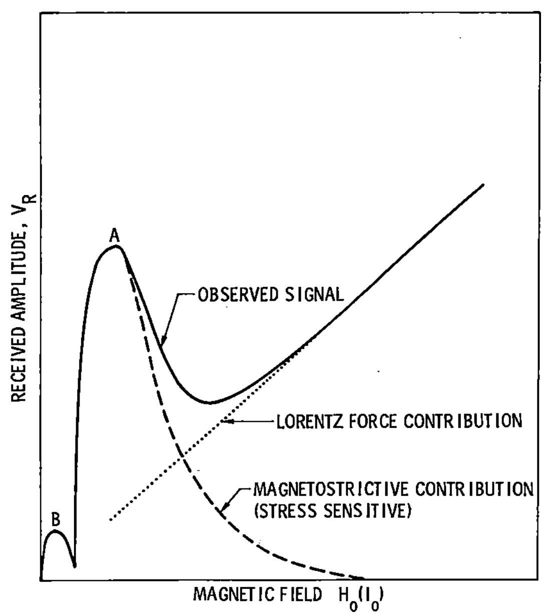

FIGURE 1. EXPERIMENTAL APPROACH:
CONFIGURATION (TOP) AND
TYPICAL VARIATION OF ULTRASONIC SIGNAL STRENGTH WITH BIAS FIELD (BOTTOM)

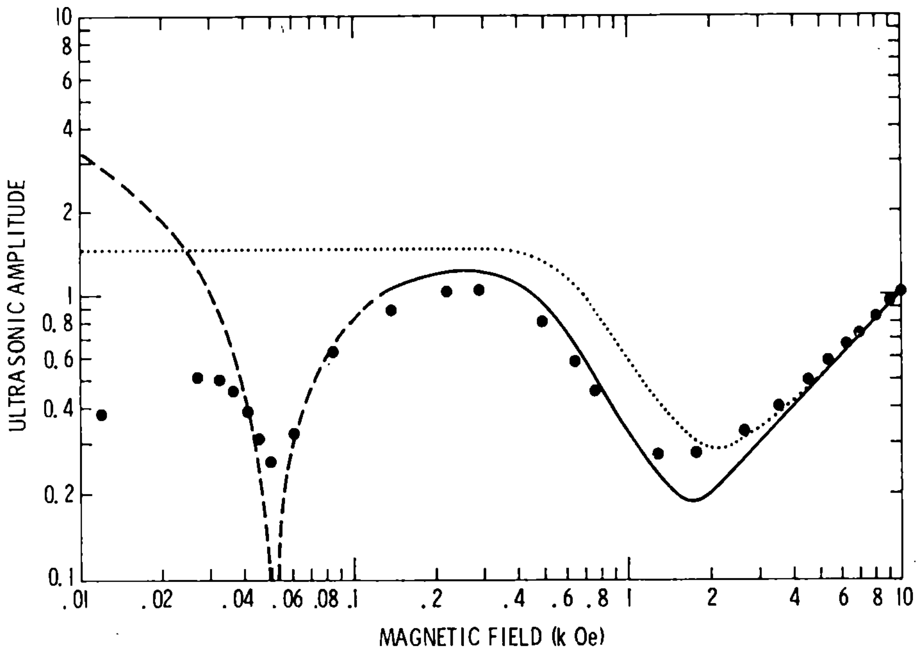

FIGURE 2. VARIATION OF ULTRASONIC AMPLITUDE IN 1018 STEEL PLATE AT 130 KILOHERTZ (DOTS = EXPERIMENTAL POINTS; CURVES = THEORETICAL RESULTS AS DESCRIBED IN TEXT)

the agreement is quite reasonable. The disagreement that occurs at lower fields is expected as a result of the fact that the model includes only domain rotation effects.

The availability of an analytical model provides the basis for studying the effects of stress on the transduction efficiency, as well as such other parameters as texture and cold working. This differentiates the magnetostrictive approach from a number of other magnetic approaches that do not have such an analytical basis.

Figure 3 presents some experimental data, which demonstrates the stress sensitivity of magnetostriction [7]. Here, the change in length of an Armco iron bar has been measured as a function of the bar's magnetization at three different stress levels. At zero stress, iron has the rather peculiar physical property that it first lengthens and then contracts during magnetization. However, if one has just 10 ksi of tension, this initial expansion is totally suppressed and the material contracts monotonically during magnetization. Conversely, if one has a 10 thousand pounds-force per square inch (ksi) compressive force, one enhances this initial expansion. Thus the stress dependence of the magnetostrictive properties is large. By combining this knowledge with the fact that magnetostriction strongly influences transduction efficiency, it is clear that a nondestructive test for stress can be developed based on measurement of transduction efficiency.

Before presenting experimental data demonstrating this new approach, it is important to consider the physical basis for this unusual property of iron that leads to an expansion followed by a contraction during magnetization. An understanding of this effect will provide a foundation for understanding the stress effects.

Figure 4 illustrates the magnetostriction during magnetization of iron [1]. Consider first a single crystal that is being magnetized along a cubic axis. In iron, the magnetic anisotropy energy is such that the magnetization tends to align itself along the cubic axes. In the demagnetized state, one would expect there to be an equal distribution of magnetization along each of these axes. As one starts to magnetize the sample, magnetizations along the six directions parallel to cubic axes are no longer energetically equal. The least energetically favorable state is oriented at 180 degrees with respect to the applied field direction. The first process during magnetization is a 180-degree reversal of domains in this state so that they become aligned with the field. No change in

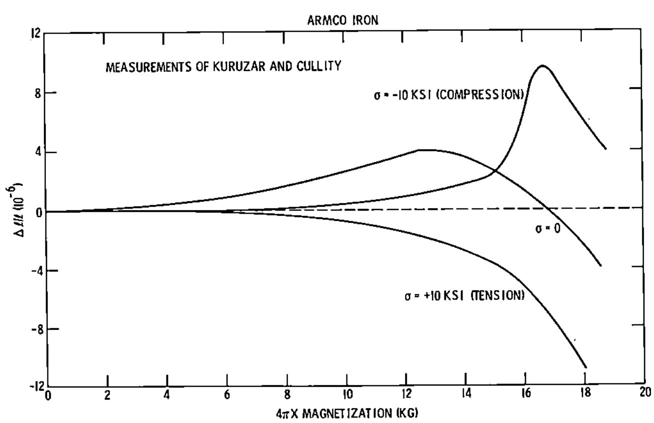

FIGURE 3. STRESS DEPENDENCE OF MAGNETOSTRICTION

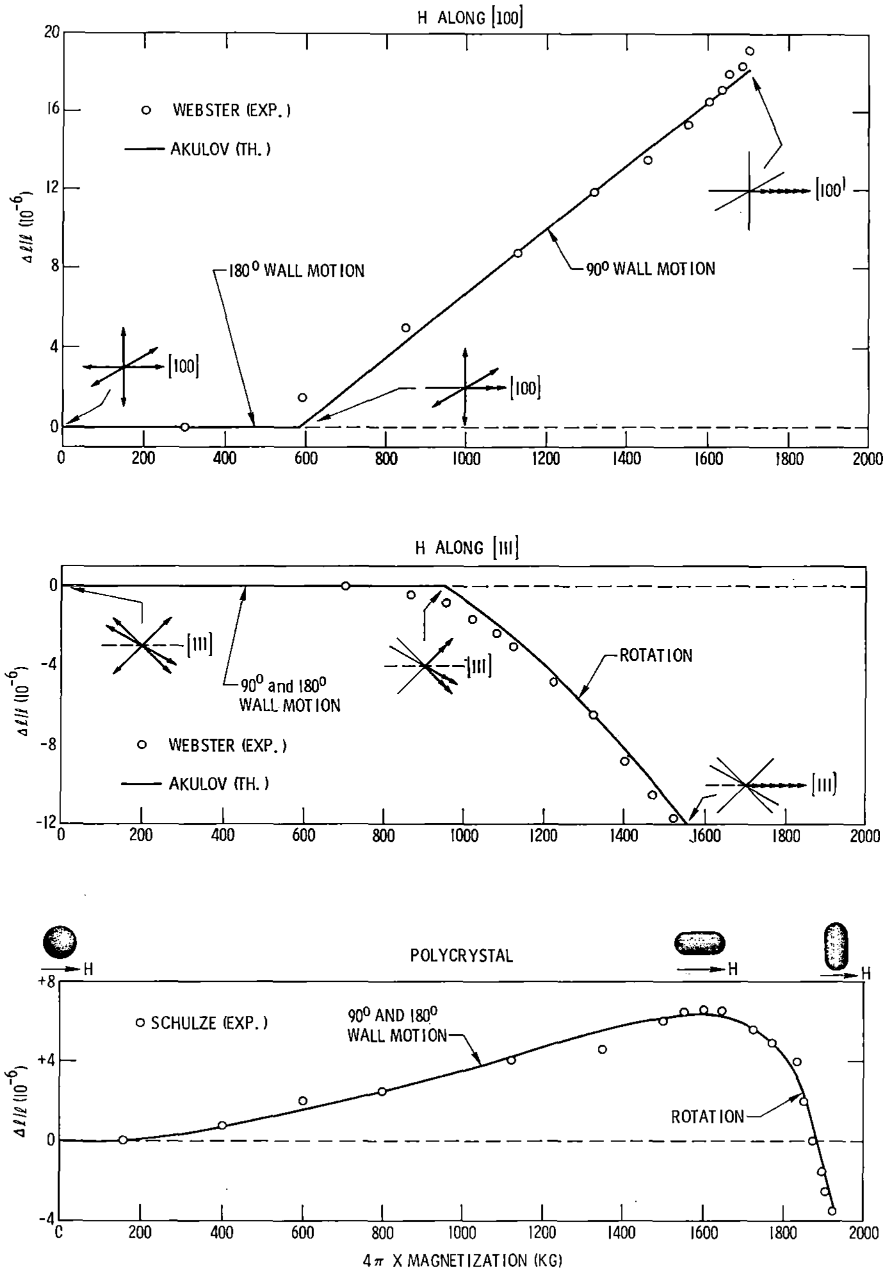

FIGURE 4. PHYSICAL BASIS FOR STRESS-FREE MAGNETOSTRICTIVE BEHAVIOR OF IRON:

TOP: SINGLE CRYSTAL MAGNETIZED ALONG CUBIC AXIS
MIDDLE: SINGLE CRYSTAL MAGNETIZED ALONG BODY DIAGONAL
BOTTOM: POLYCRYSTAL

length takes place during this process since magnetostriction is independent of the sign of the spin along a given direction. Subsequently, the domains oriented at 90 degrees with respect to the applied field direction move toward parallel alignment by 90-degree wall motion, and this is accompanied by a magnetostrictive expansion proportional to the magnetization change. The absolute change in length is determined by the single crystal magnetostrictive constant λ_{100}, whose value is determined by the strength of the spin-orbit coupling.

The situation is somewhat different when the single crystal is magnetized along its body diagonal. Again, in the demagnetized state, the magnetization is uniformly distributed among the six possible cubic axes. These can be divided into two sets of three each: One triplet that is at equal obtuse angles with respect to the

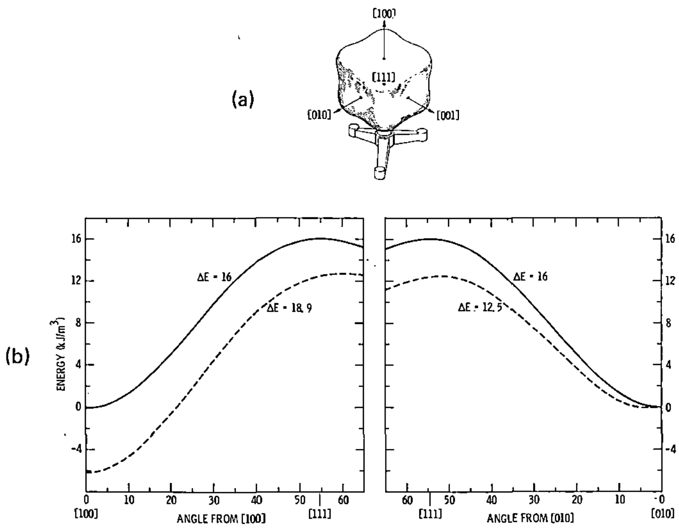

FIGURE 5. CHANGE IN MAGNETIC ANISOTROPY ENERGY INDUCED BY A STRESS OF 20 KSI ALONG THE (100) DIRECTION:

(a): THREE-DIMENSIONAL ENERGY SURFACE WITH AND WITHOUT STRESS
(b): STRESS-INDUCED ENERGY CHANGES IN TWO CROSS SECTIONS

applied field and a second triplet that is at equal acute angles. As the field increases, the first process is the elimination of the triplet at obtuse angles in favor of that at acute angles. Again, no length change occurs during this early stage of magnetization. Subsequently, all of the magnetizations rotate from the easy axes to the field direction. During this process, the material shortens in accordance with the negative sign of the magnetostrictive constant l_{111} of iron.

The fact that the iron lengthens when magnetized along the cubic axis and shortens when magnetized along the body diagonal is a direct consequence of the highly anisotropic behavior of the spin-orbit coupling, which is phenomenologically reflected in the opposite signs of λ_{100} and λ_{111} [8]. The polycrystalline response is an average of these and many other single crystal responses. The complex behavior results from the (100) response being dominant at low fields and the (111) response being dominant at high fields. The rich structure is quite helpful in the measurement of stress since it leads to many features that can be easily measured.

Figure 5 provides a little more detail [5]. In the three-dimensional plot of the magnetic anisotropy energy of iron, it can be seen that the states of minimum energy lie along the cubic axes as discussed above. Also shown is a graph of the energy as it varies in cross sections containing both the cubic axes and body diagonal, both with and without stress. For the stress-free case, the energy has minima along the (100) of (010) directions and a maximum in the (111) direction. When a tensile stress of 20 ksi is applied along the (100) direction, the energy surfaces shift as a result of the magnetoelastic effect. The energy of the (100) direction has now been lowered, while no change has taken place along the (010) direction. Since the energy of magnetization of the two axes is no longer equal, the magnetization will preferentially align along the (100) direction.

Figure 6 illustrates how this stress-induced change in magnetic energy modifies magnetostrictive behavior [1]. Consider again a crystal that is being magnetized along the (100) direction. For zero stress, the demagnetized state will consist of an equal distribution of magnetization along the cubic axes. When fully magnetized, all the magnetization will be in the (100) direction of magnetization. The plot of length change versus magnetization is the same as that shown in figure 4.

Suppose now that there is a large tension applied along the (100) direction. This will suppress the energy in the (100) and ($\bar{1}$00) directions so that the demagnetized state has magnetization only in these two directions. As the sample is magnetized, there is no change in length because the only change that occurs is 180-degree domain wall motion that produces no magnetostriction. Thus the presence of the tension suppresses the magnetostrictive lengthening.

Conversely, if there is a large compressive stress applied along the (100) direction, the demagnetized state will consist of only magnetization perpendicular to this direction. Magnetization will take place through domain rotation processes, and the length change will be greater than for the stress-free case. The results illustrate, on a microscopic scale, the mechanism of the large stress dependence of magnetostriction.

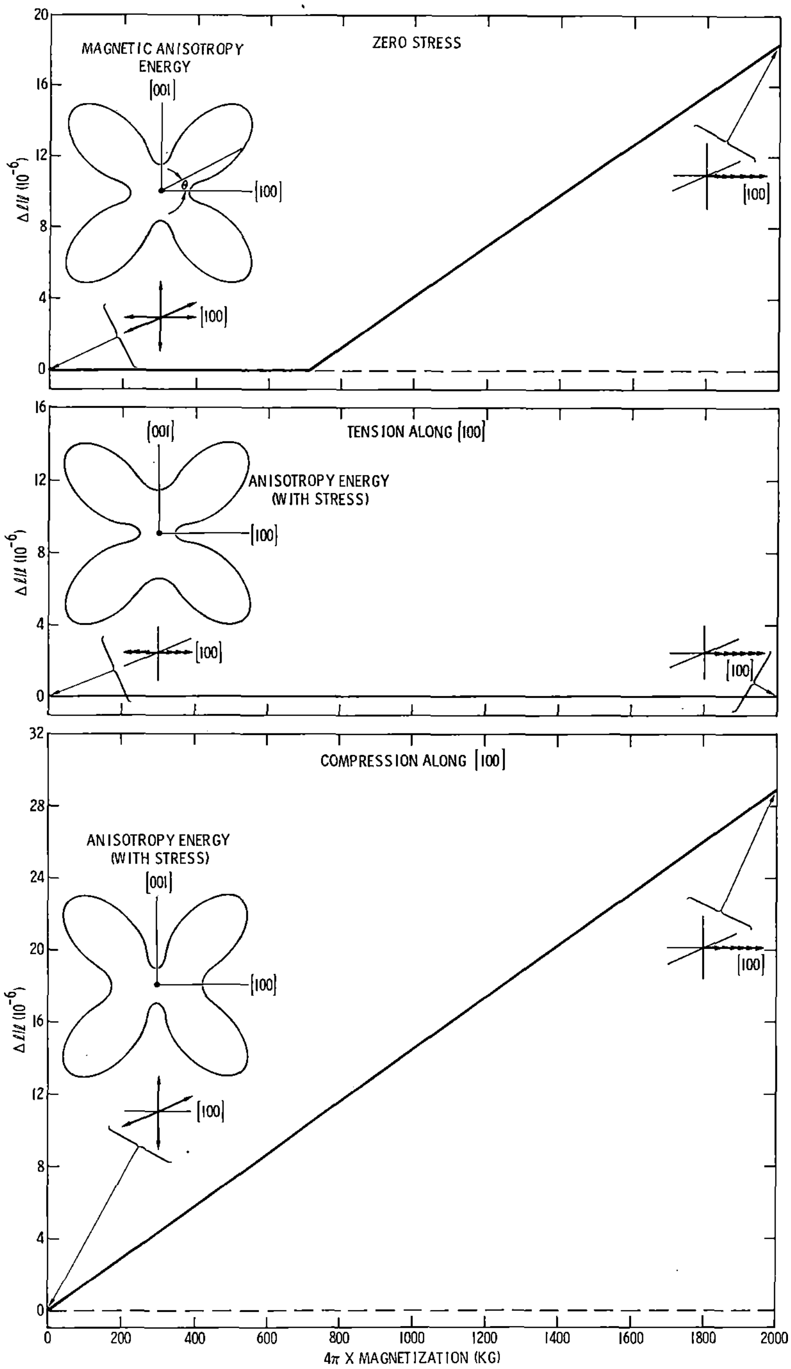

FIGURE 6. EFFECT OF STRESS ON SINGLE CRYSTAL MAGNETIZED ALONG CUBIC AXIS:

TOP: NO STRESS
MIDDLE: LARGE TENSILE STRESS PARALLEL TO FIELD
BOTTOM: LARGE COMPRESSIVE STRESS PARALLEL TO FIELD

Experimental Results

A number of experiments have been performed to verify that these principles do, in fact, lead to a technique for the measurement of stress. Figure 7 illustrates the apparatus that consists of a sample in a 4-point bending jig. For a given load, an EMAT can be placed on one side or the other of the sample so that it is either in tension or compression. Then the bias magnetic field, produced by an electromagnet, is varied and the strength of the ultrasonic signal is measured as a function of magnetic field strength. In this case, a separate piezoelectric transducer

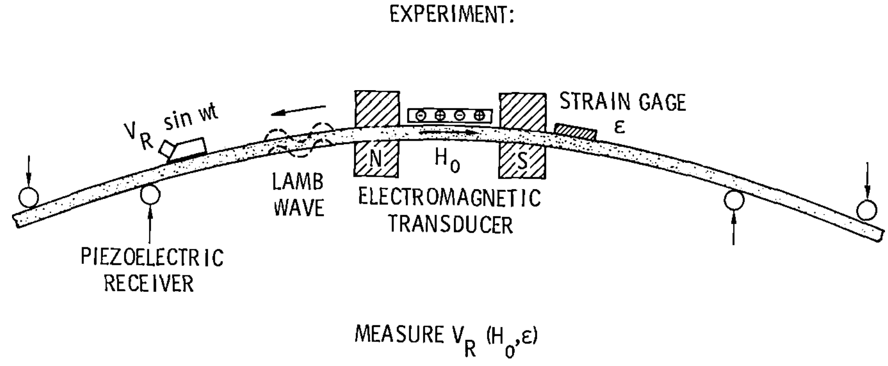

FIGURE 7. EXPERIMENTAL CONFIGURATION

was used to sense the wave amplitude. Another EMAT could have been used, but was not necessary, in order to study the physics.

Figure 8 illustrates the type of experimental results that are obtained. The solid curve shows a plot of ultrasonic amplitude as a function of the magnetic field for zero stress. There is a weak peak at low fields and a very strong peak at higher fields. If one applies a tensile load, the small, low field peak vanishes and the shoulder of the large peak shifts to lower fields. In other words, the large peak broadens. On the other hand, if one applies a compressive load, the large peak narrows and the small, low field peak becomes larger and more accentuated.

There is clearly a lot of information about the state of stress in these plots. The question is, how does one parameterize and interpret it? Only the first initial steps have been taken, but some points are already clear. For example, one does not want to use absolute wave amplitude as a parameter because lift-off, surface roughness, diffraction, and other effects can influence the experimental data independent of stress. Instead, a normalization procedure has been adopted as shown in figure 9. The maximum value of the large peak has been defined to be unity and all other amplitudes are measured relative to this value. The characteristic parameters are then chosen to be magnetic field values that produce a specified value of normalized wave amplitude. For example, one such parameter is called $H_{1/3}$. This is defined as that magnetic field at which the efficiency is one-third of its peak value. Another parameter is $H^{+}_{4/5}$. This is the magnetic field value at which the amplitude is reduced to 80 percent of its peak value. The plus indicates that one is on the high field side of the peak rather than below it. It is these parameters that will be related to stress in the remainder of the paper.

Figure 10 presents the results of some early measurements on samples of Armco iron and 1018 steel. One thing that one notices is that there are some differences in the responses of these two alloys. Such compositional and microstructural affects are characteristic of all magnetic techniques, and they must be taken into account in applications. Having recognized this, it is appropriate to consider the data in a little greater detail. In the Armco iron, there is a very smooth variation of the parameter $H_{1/3}$ with stress. However, there is also an offset of 14 ksi between data taken on the compressive and tensile sides of the sample. In order to independently determine whether this represented a real difference in the stress condition of the two sides, or an experimental artifact, X-ray stress measurements of stress were made. Using the Fast Stress unit (originally developed by General Motors), a stress difference of 17 ksi between the two sides was observed. This strongly supports the claim that EMAT efficiency measurements can be used to determine stress.

On the 1018 steel sample, an offset in the data shown in figure 10 was also observed. However, on this sample, the Fast Stress unit did not produce meaningful data because of the presence of heavy machining marks on the surface. This establishes that the EMAT technique is less sensitive to changes in surface condition than the X-ray measurements. A closely related point is the fact that the EMAT technique averages the stress in a surface layer on the order of a few

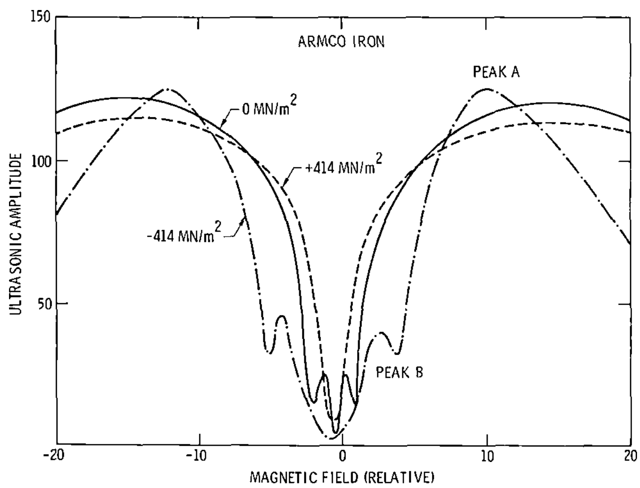

FIGURE 8. TYPICAL PLOTS OF ULTRASONIC AMPLITUDE VERSUS MAGNETIC FIELD IN ARMCO IRON AT THREE STRESS LEVELS

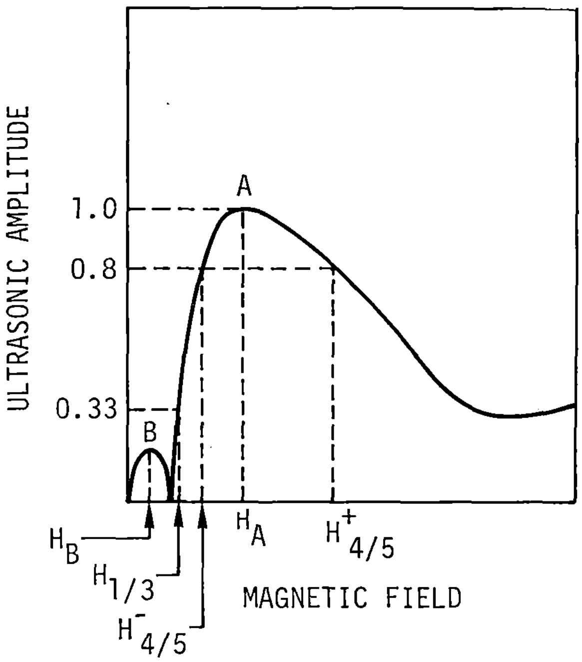

FIGURE 9. DEFINITION OF EXPERIMENTAL PARAMETERS

mils in thickness, much thicker than the layer averaged by X-rays. Thus the EMAT measurements are less strongly influenced by highly localized surface stresses.

Figure 11 presents the results of measurements of the stress dependence of $H_{1/3}$ on A569 steel. Again, a rather smooth variation with stress is observed. In this case, there is a very rapid variation of $H_{1/3}$ between about -20 ksi and +20 ksi, with a much slower variation at higher stresses. Furthermore, the curve becomes multi-valued for tensile stresses. This is a problem since it implies that a particular measured value of $H_{1/3}$ could correspond to two different possible stress levels. Clearly other parameters must be used if a unique stress determination is to be made.

Figure 12 shows the behavior of one such parameter, $H^+_{4/5}$. For tensile stresses, there is now a monatonic variation with stress. Measurement of this parameter, and $H_{1/3}$, would uniquely determine the stress.

This sample was large enough so that measurements could be made both parallel and perpendicular to the rolling direction to assess how significantly texture would influence the measurement. As seen in figures 11 and 12, there was a texture effect, but it was not terribly severe.

In all measurements reported thus far, the direction of stress and the direction of ultrasonic wave propagation were parallel to one another. Figure 13 represents experimental results

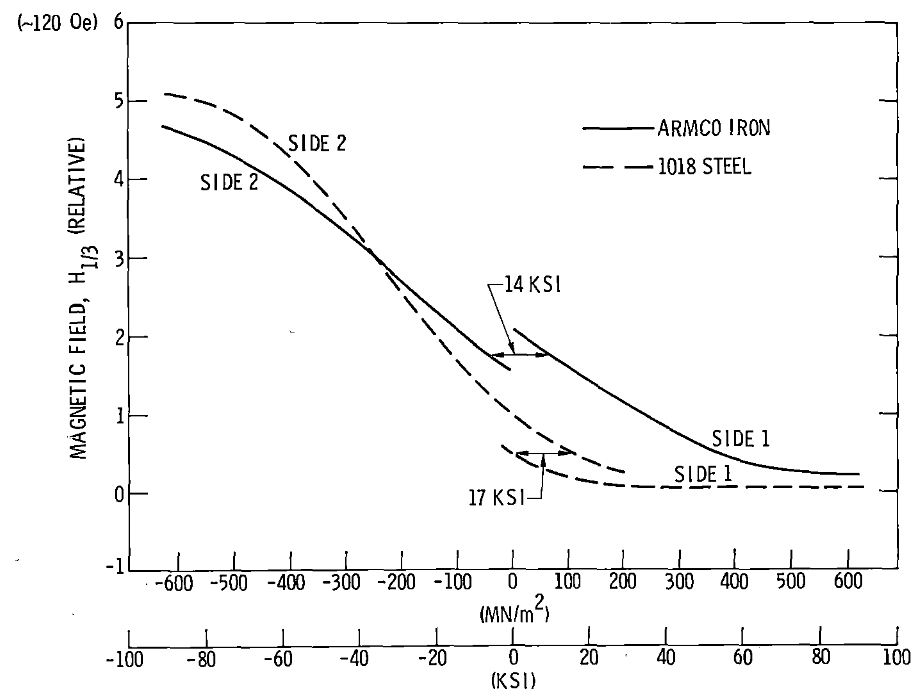

FIGURE 10. VARIATION OF $H_{1/3}$ VERSUS STRESS IN ARMCO IRON AND 1018 STEEL

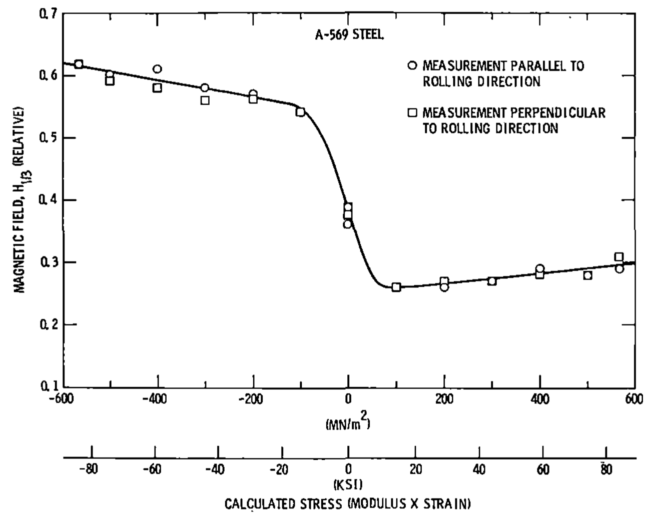

FIGURE 11. VARIATION OF $H_{1/3}$ VERSUS STRESS IN A-569 STEEL

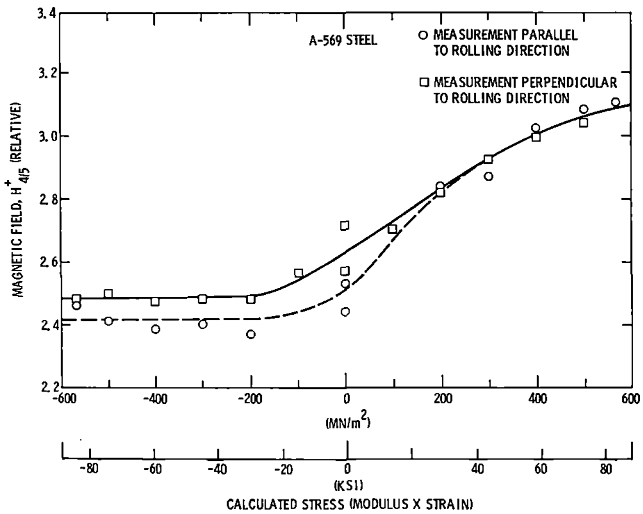

FIGURE 12. VARIATION OF $H^+_{4/5}$ VERSUS STRESS IN A-569 STEEL

on the same sample when the measurement direction was rotated by 90 degrees from the stress direction. In this case, $H^+_{4/5}$ was relatively insensitive to stress. This suggests that stress directions, as well as magnitudes, can be determined by this technique.

Conclusions

Many magnetic techniques for stress measurement have been studied -- for example, those based on the Barkhausen effect. Measurement of magnetostriction with EMAT's does not fully solve the problem, but it provides access to some very important information that may not be provided by the other techniques. Figure 14 illustrates this in a pair of plots showing the variation of both the magnetization and magnetostriction of Armco iron as a function of applied field [9]. In each case, several curves are plotted with stress as a parameter. It is clear that stress causes a much greater change in the magnetostrictive response than it does in the magnetization. The magnetostriction is apparently sensing the presence of stress more directly.

Figure 15 presents an interpretation of this result. Consider two initial states of material. In one state, imagine that the demagnetized state has a domain configuration in which the domains of closure are as shown at the left in the figure. This would be typical of a material with zero applied stress. In the second state, imagine that a compressive stress is present. Since the compressive stress inhibited the formation of the domains of closure of the original material, the domains would close in the orthogonal plane. This sample would thus have a different initial length. (This difference is in addition to the usual elastic difference resulting from the applied-load.) When magnetized to saturation, both samples would have the same length. A measurement of change in length during magnetization could be

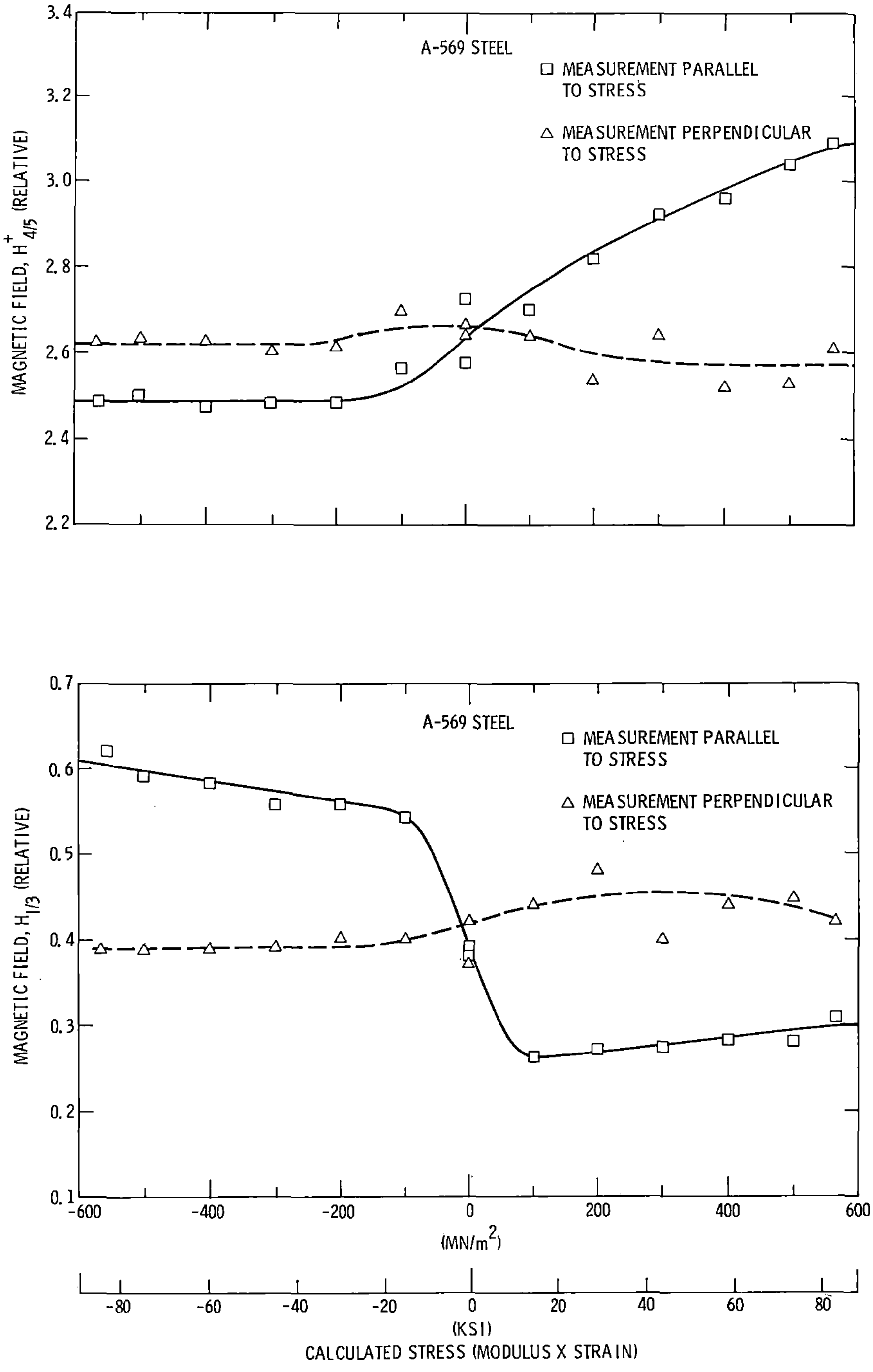

FIGURE 13. VARIATION OF $H_{1/3}$ AND $H^{+}_{4/5}$ VERSUS STRESS IN A-569 STEEL FOR MEASUREMENTS PARALLEL AND PERPENDICULAR TO APPLIED STRESS

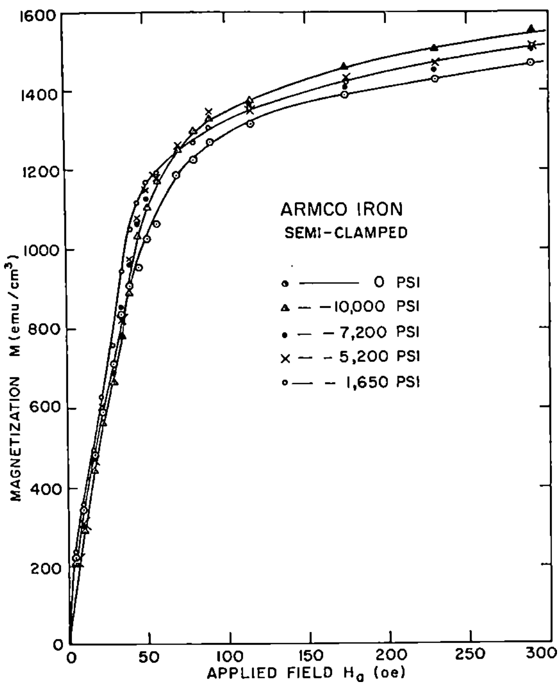

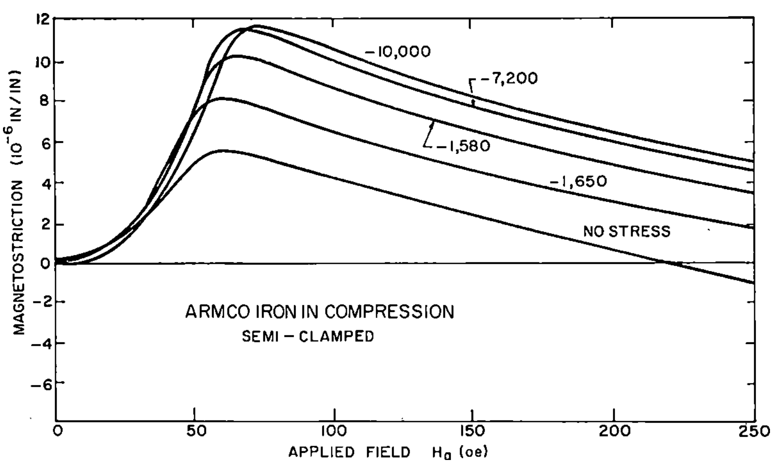

FIGURE 14. COMPARISON OF STRESS DEPENDENCIES OF MAGNETIZATION AND MAGNETOSTRICTION IN ARMCO IRON

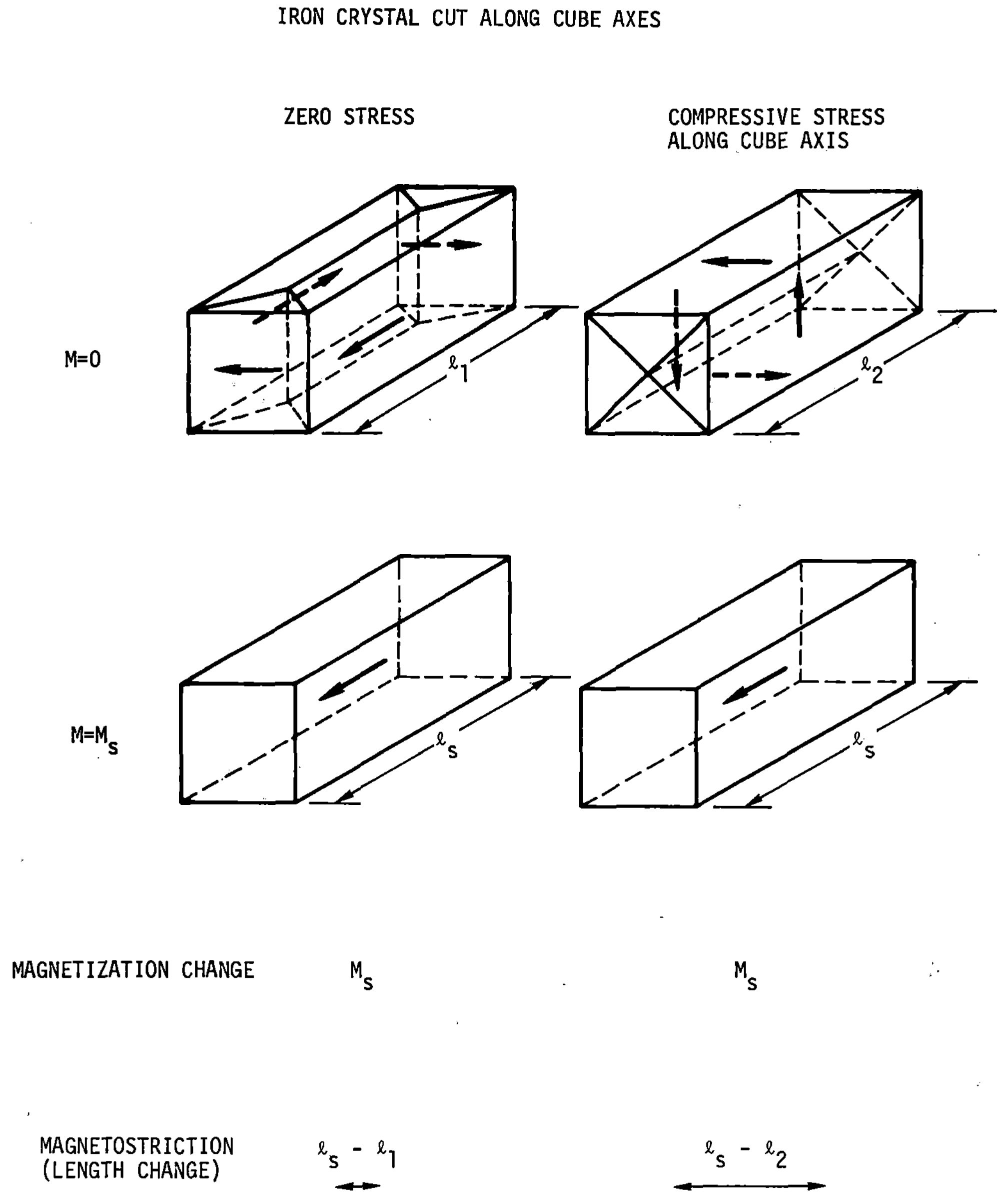

FIGURE 15. MICROSCOPIC COMPARISON OF EFFECT OF STRESS ON MAGNETIZATION AND MAGNETOSTRICTION

used to distinguish between them. However, a measurement of change in magnetization would not provide such a differentiation since, in each case, the magnetization goes from zero to its saturated value. Clearly, the magnetostriction has leverage on new magnetic information that cannot be obtained by simple magnetic measurements. This presents significant opportunities for measuring stress states, which should prove of use in the inspection of rails.

References

[1] Thompson, R. B. "Residual Stress Detection by Measurement of Efficiency of Electromagnetic Generation of Ultrasound." In Proceedings of the ARPA/AFML Review of Progress on Quantitative NDE. Air Force Materials Laboratory, report no. AFML-TR-75-212 (1976), pp. 33-45.

[2] Thompson, R. B. "Electromagnetic Generation of Ultrasound." In Proceedings of a Workshop on Nondestructive Evaluation of Residual Stress. San Antonio, Texas: Nondestructive Testing Information Analysis Center, Southwest Research Institute, 1976.

[3] Thompson, R. Bruce. "Strain Dependence of Electromagnetic Generation of Ultrasonic Surface Waves in Ferrous Materials." Applied Physics Letters, vol. 28 (1976), pp. 483-85.

[4] Buck, O., and R. B. Thompson. "Acoustic Interactions with Residual Stresses in Metals." In Nondestructive Evaluation of Materials, pp. 257-82. New York: Plenum Press, 1979.

[5] Thompson, R. B. "Detections of Strain by the Measurement of the Magnetostrictive Generation of Ultrasonic Surface Waves." In 1976 Ultrasonics Symposium Proceedings, pp. 585-89. New York: IEEE, 1976.

[6] Thompson, R. Bruce. "A Model for the Electromagnetic Generation of Ultrasonic Guided Waves in Ferromagnetic Metal Polycrystals." IEEE Transactions on Sonics and Ultrasonics, vol. SU-25 (1978), pp. 7-15.

[7] Kuruzar, M. E., and B. D. Cullity. "The Magnetostriction of Iron under Tensile and Compressive Stress." International Journal of Magnetism, vol. 1 (1971), p. 323.

[8] Bozorth, R. M. Ferromagnetism. Princeton, New Jersey: P. Van Nostrand, Inc., 1951.

[9] Allen, C. W., R. Haborak, and W. H. Kao. "The Effect of Stress on the Magnetostriction of Iron, Nickel, and 49 Permalloy." Report no. THEMIS-UND-70-9 (Notre Dame, 1970) AD-711094.

"British Railways' Experience in the Measurement of Longitudinal Rail Forces"

G. S. Lane
Research and Development Division
British Railways

Introduction

An essential feature of continuously welded rail (CWR) is the property of restrained thermal expansion. Over a typical rail temperature range, this leads to the existence of large tensile and compressive forces and the possibility of rail breaks or buckles. British Railways (BR) has considerable interest in the control of longitudinal rail forces, and this paper gives an account of recent BR experience in their measurement.

The Importance of Rail Forces

On BR, CWR is installed so that the temperature at which there is no overall longitudinal rail force is 80°F (26.5°C). This temperature is usually, but erroneously, referred to as the stress-free temperature. A more accurate description is the term, force-free temperature. Hydraulic tensors are used, and these allow the force-free temperature to be accurately controlled to better than ± 5°F. However, experience has shown that, in service, changes in force-free temperature can occur for a variety of reasons, such as rail creep, curve movement, track maintenance, or ground subsidence.

The force-free temperature can be used as a yardstick that fully indicates whether the track is safe from the point of view of longitudinal rail forces. If the force-free temperature increases, there is the possibility that excessive tensile forces in winter will cause rail breaks. If a decrease occurs, excessive compressive forces in summer may lead to track buckling. The buckle is generally considered to be the more dangerous occurrence; because of this, the force-free temperature of 80°F is chosen to be higher than the average rail temperature.

The factor that controls track buckling is the overall longitudinal rail force across the whole rail section (not rail stress), which of course depends on force-free temperature and actual rail temperature. The preferred way of assessing the safety of a given length of CWR is to measure both the rail force and the temperature and from these determine the force-free temperature. Bearing in mind the time of the year and its relation to likely rail temperatures, the safety can then be assessed. Theoretical work on BR has indicated that, if rail temperatures are more than 50-70°F (depending on track design and maintenance standards) above the local force-free temperature, buckling may occur.

All rail force data on BR is processed and assessed in this way.

Measuring System Requirement

Any measuring system designed to monitor the safety of CWR from the point of view of the effects of restrained thermal expansion must satisfy certain requirements. These will be divided into two categories -- necessary and desirable. The necessary requirements for such a system are as follows:

a. Nondestructive. A system must either be train-borne (the preferred form) or, if this is not possible, track-mounted in such a way that readings can be taken without interruption to traffic.

b. Measurement of total force over the whole rail section. This is the force that directly controls the tendency to buckle.

c. Measurement of average rail temperature over the whole rail section. There is no way in which the safety of CWR from possible buckling can be assessed from force measurements alone. BR feels strongly that accurate average rail temperatures should be measured at the same time as rail forces.

d. Tolerance of railway environment. Both severe weather conditions and heavy service loading (including the effect of dynamic loadings due to wheelflats, etc.) can severely affect instrumentation systems.

e. Good long-term stability. Minimal drift over several years is desirable.

f. Sensitivity. It should be possible to measure the force-free temperature to ± 5°F (± 3°C). This is approximately equivalent to a force of ± 50 kilonewtons and stress of ± 7 meganewtons per square meter (± 1 ksi), where both force and stress are averaged over the whole rail cross section.

The desirable requirements for a measuring system are:

a. The instrumentation should be as simple and straightforward as possible and be easily portable.

b. The whole system should be capable of installation and use by normal track maintenance staff with minimal training,

c. If the system is track-mounted, it should be possible to provide a remote reading facility via a data logging and telemetry link.

The BR Rail Force Transducer (RAFT) System

BR has developed a track-mounted transducer system for the measurement of average rail force. The transducer is fully temperature compensated, but a special version, entirely compatible with the standard instrumentation, has been produced that measures average rail temperature.

These transducers satisfy most of the requirements listed above. They are mounted in a 29-millimeter hole drilled in the web of the rail, and they operate on a vibrating wire principle. Changes in rail force (and temperature for the temperature transducer) lead to distortion of the hole and also to changes in the period of vibration of the wire can be related to the quantity to be measured through a calibration characteristic. A coil/magnetic circuit system is used to electromagnetically pluck the wire and detect the period of vibration.

The basic system is illustrated in the accompanying illustrations. Figure 1 shows the rail force transducer complete and with coils removed. Figure 2 shows the rail force transducer mounted in rail. Figure 3 shows the standard measuring instrument for manual readings.

The force transducer is calibrated in situ using a hydraulic rail tensor to apply calibration loads. This automatically insures that the average rail force is subsequently measured. Figure 4 shows typical calibration characteristics. (Note that there are two wires -- "sensing elements" -- in each transducer.) A sensitivity at least equal to the requirement given above can be obtained.

Because of the time-consuming nature of manual readings, BR has developed a telemetry/data logging system so that rail force and temperature data can be obtained in the office. Data reduction can also be time-consuming, so the system has been extended to include a microcomputer to analyze the data. Programs have been written to the detailed requirements of the civil engineer and the first site with the full system applied is to be operational in April 1979. Figures 5 and 6 show the development version of the system, illustrating the site equipment and office equipment, respectively.

BR Experience -- Problems and Developments

BR experience to date has shown that the RAFT system is viable and gives rail forces and temperatures to a sufficient degree of accuracy to monitor CWR for safety from buckling. BR has encountered several problems with the system, and these have led to further developments of the system that are currently being pursued.

With the present design, an individual onsite calibration of each force transducer is required. This is time-consuming and requires track possession. Currently BR is investigating an improved wire clamp arrangement that will give greater consistency of the wire "end fixity" conditions. This should lead to a consistent calibration characteristic (and also reduce possible wire slip, which can lead to zero drift).

In 1977, several transducers were installed in the Facility for Accelerated Service Testing (FAST) track at the Transportation Test Center near Pueblo, Colorado. These suffered deterioration in service in two ways. Internal and external

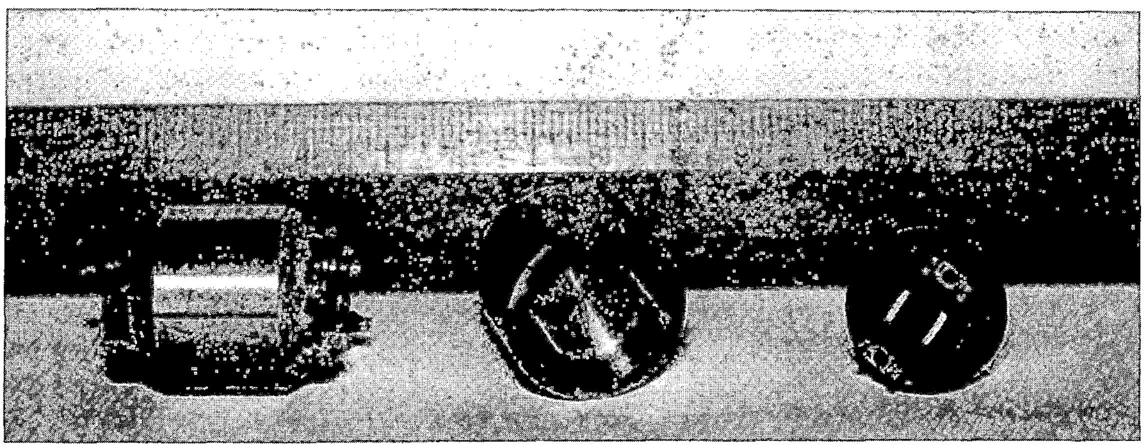

FIGURE 1. RAIL FORCE TRANSDUCER -- COMPLETE AND WITH COILS REMOVED

rusting took place, and some instances of loss of wire tension were noted. The rusting we have been able to associate with a more severe proof testing procedure instigated specifically for the FAST track transducers to cater to the arduous conditions of temperature and loading. This treatment led to failures in the sealing of the transducers allowing ingress of moisture. The solution is to amend procedures so that the transducers are sealed after proof loading. The possibility of loss of wire tension should be reduced by our new clamping arrangements.

BR has found the standard surface-mounted magnetic rail thermometers unreliable unless very carefully insulated from sun and wind, etc. In addition, they are not suitable for remote reading. These factors led to the design of the temperature-measuring vibrating wire transducer. Problems have been experienced with this device because the transducer responds to both force and temperature and it is not easy to separate the effects of each, and because the softer wire may be more susceptible to slip in the clamp under service loading. To avoid these problems, the temperature transducers have so far been installed in dummy 1-meter lengths of rail positioned between the running rails. We are currently experimenting with a transducer incorporating a temperature-sensitive wire at about 60°F to the horizontal that will be unaffected by changes in rail force. A transducer with one normal (horizontal) wire and one Invar wire at this angle should give both rail force and temperature.

An Example of the Use of the RAFT System

The force-free temperature of CWR can be influenced by many factors, all of which can result in an unsafe condition. Examples of these are curve movement between times of high and low rail temperatures; rail creep due to traction forces, braking, gradients, etc.; and maintenance operations. BR is interested in all of these possibilities. However, as an illustration of the way in which the RAFT system is being used at present, this section describes some recent results obtained in an area where CWR is affected by mining subsidence.

Although similar problems may not occur widely in the United States, there are many areas on BR at the moment where CWR lines carrying high-speed passenger traffic are affected and where very large gound strains occur. If a significant fraction of these strains were transferred to the rail, a high probability of track buckling or rail breaks would exist. Where this is the case, the standard practice would be to remove the CWR and replace it with jointed track, thereby incurring the large penalties of cost, additional track

FIGURE 2. RAIL FORCE TRANSDUCER MOUNTED IN RAIL

maintenance, and degraded track quality and vehicle ride. The RAFT system presents an alternative of retaining CWR, monitoring safety through regular measurements of rail force and temperature, and re-stressing the track only when necessary. Without a rail force and temperature measuring system, there is no way of assessing the safety of CWR influenced by ground strain.

Figures 7, 8, 9, and 10 refer to a site that was instrumented in 1978 with the twin objectives of monitoring the CWR for safety and checking the relationship between rail and ground strains. The latter objective required the installation of monuments to check ground subsidence and strain and also the installation of a larger number of rail force transducers than would be used purely for a safety monitor.

Figure 7 shows the relationship between the instrumented length and the mine working.

Figure 8 shows the predicted ground strain expressed as an equivalent change in force-free temperature, assuming that the ground and rail strains are equal (a worst case assumption). The present situation, February 1979, is shown and also the maximum compressive strain predicted. These data were produced by the Mining Engineers Department of BR using a full three-dimensional ground subsidence/strain model. At some stage, the track will clearly become unsafe.

Figure 9 shows the ground strain and rail strain plotted against distance for the readings taken in January and February 1979. The ground strains were obtained using steel tape measurements between monuments; they suffer from some scatter due to severe weather conditions. Again the results are expressed in terms of equivalent change in force-free temperature, assuming that rail strain equals ground strain.

The correlation apparent in figure 9 is shown more clearly in figure 10, where the rail strain is plotted directly against the ground strain. A good correlation exists that indicates that some 60 percent of the ground strain is experienced by the rail. This experiment is in its early stages and more accurate data will become available as the ground strain increases.

The performance of the rail force transducers at this site has so far been excellent.

Summary

The necessity for and requirements of a rail force and temperature measuring system have been

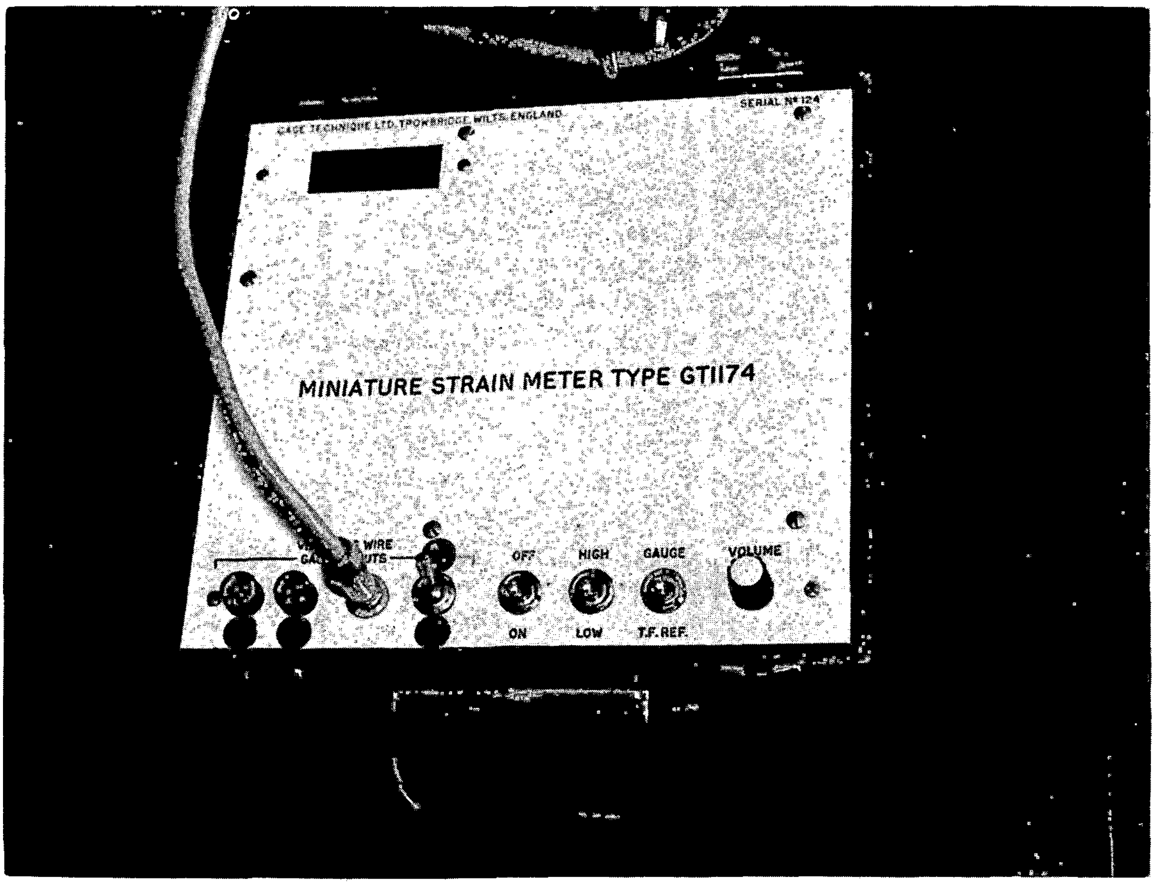

FIGURE 3. STANDARD MEASURING INSTRUMENT FOR MANUAL READINGS

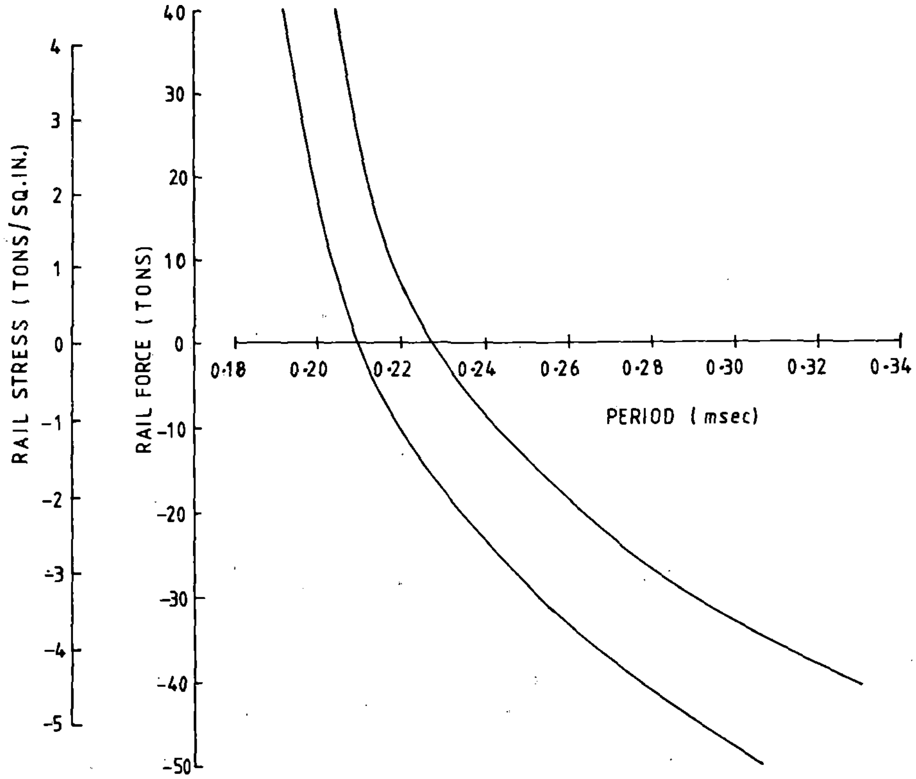

FIGURE 4. RAFT CALIBRATION CHARACTERISTIC -- BILSTHORPE RAFT NO. 18 (TWO SENSING ELEMENTS)

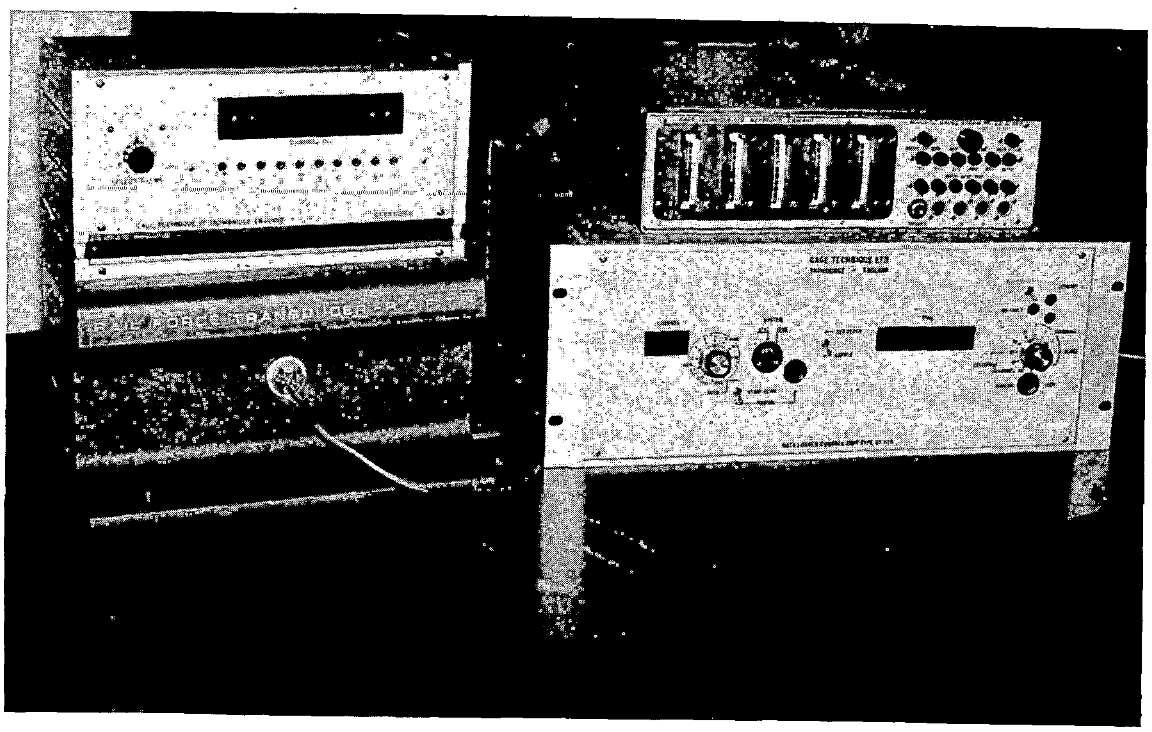

FIGURE 5. TELEMETRY SYSTEM: SITE EQUIPMENT

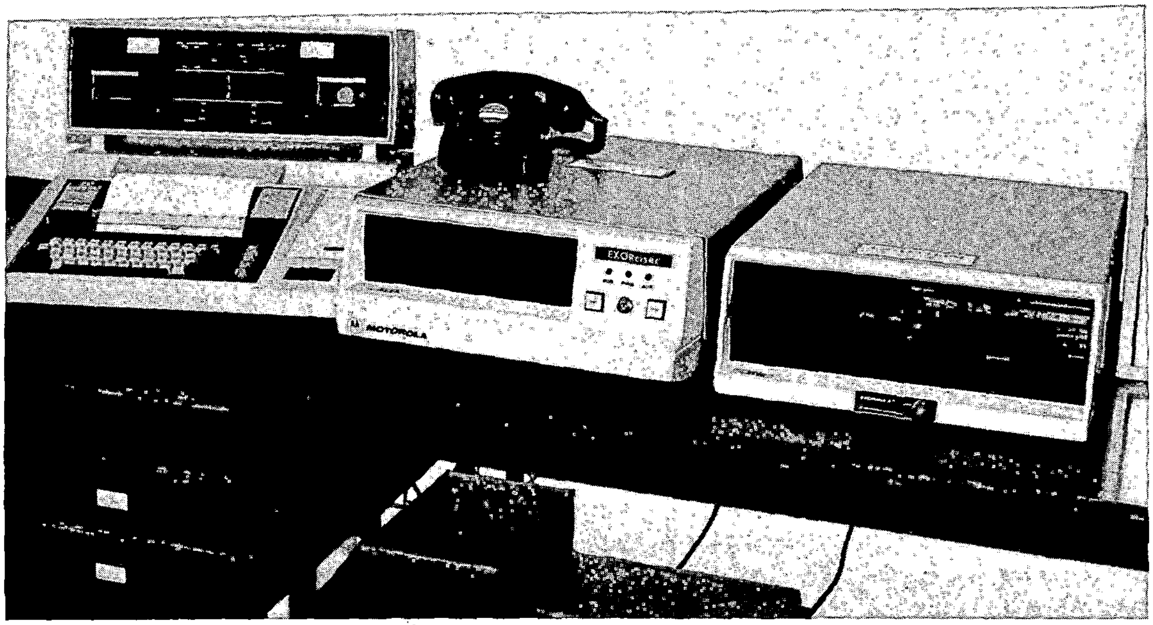

FIGURE 6. TELEMETRY SYSTEM: OFFICE EQUIPMENT

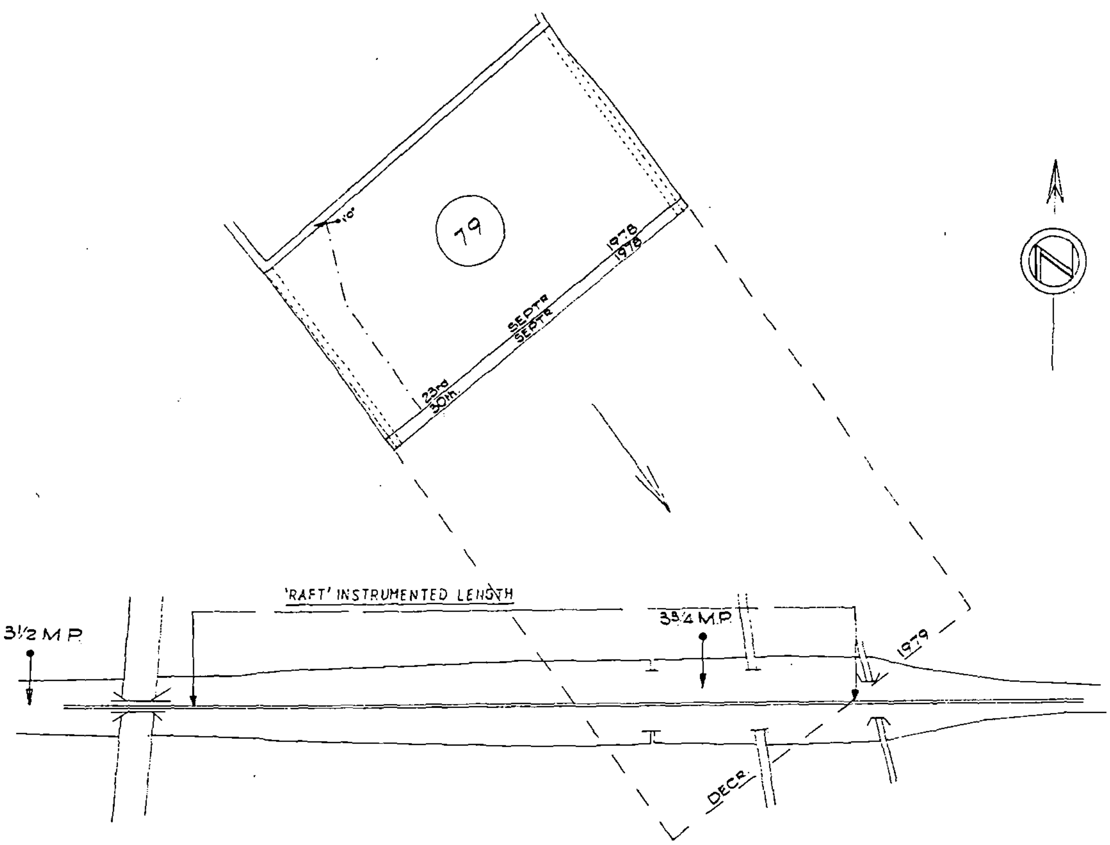

FIGURE 7. BILSTHORPE COLLIERY BRANCH LINE: PROBABLE FACE ADVANCE

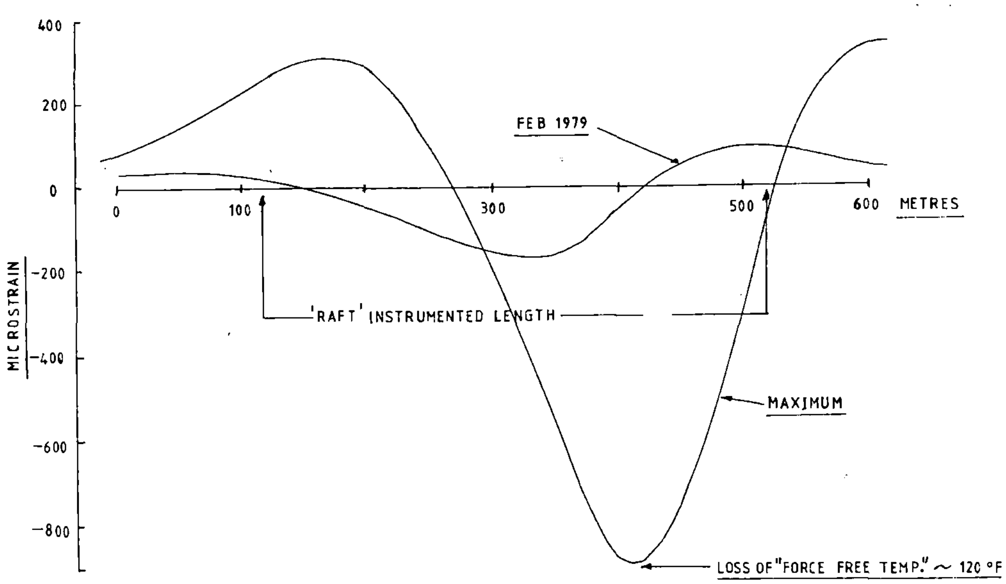

FIGURE 8. BILSTHORPE COLLIERY BRANCH LINE:
PREDICTED GROUND STRAIN

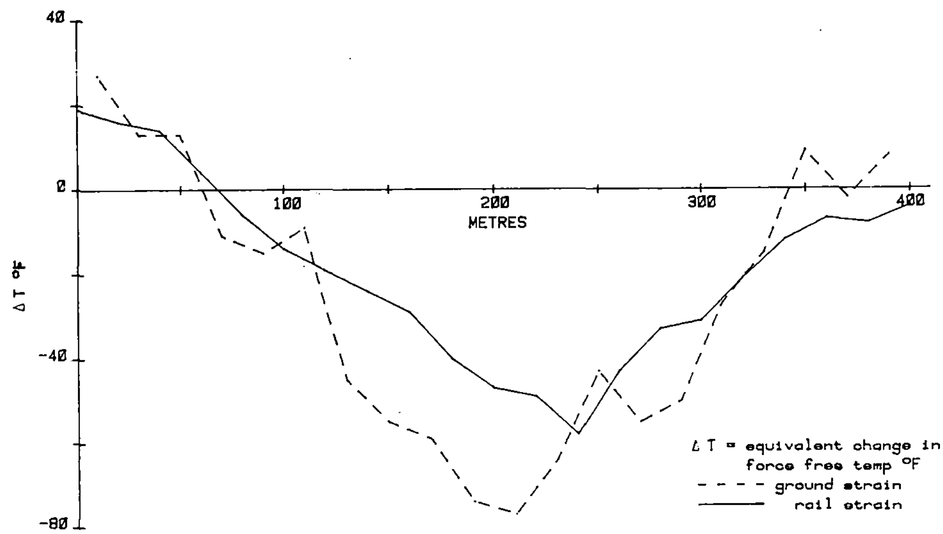

FIGURE 9. BILSTHORPE COLLIERY BRANCH LINE:
GROUND AND RAIL STRAINS, FEBRUARY 6, 1979

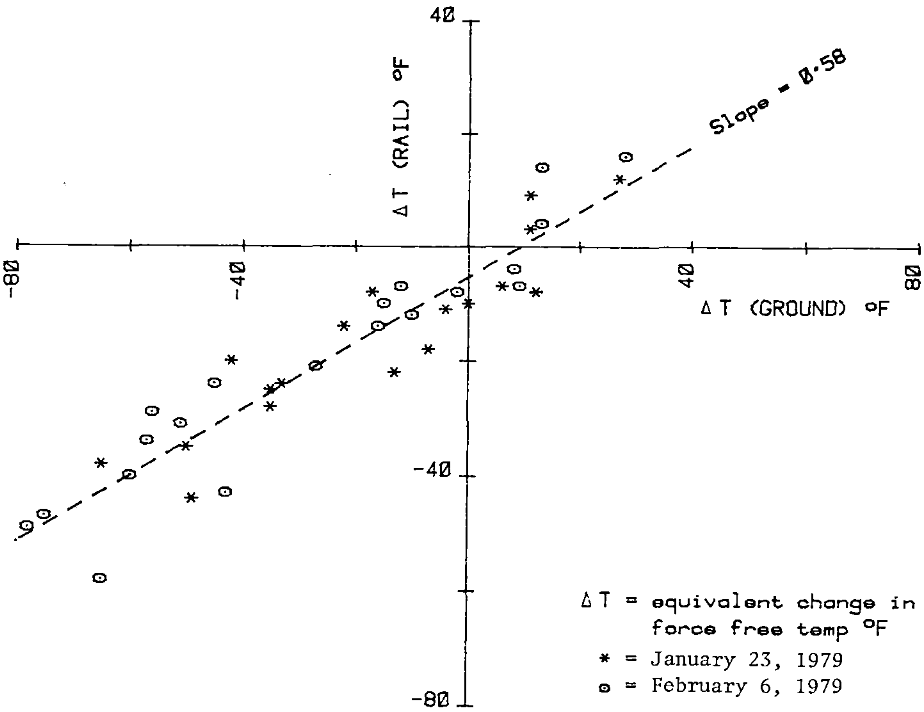

FIGURE 10. BILSTHORPE COLLIERY BRANCH LINE: COMPARISON OF GROUND AND RAIL STRAINS

set out and the BR RAFT system described. The RAFT system satisfies most of the requirements, but it does require a hole drilled in the rail web. The major advantages of the system are the ease with which it can be adapted to measure rail temperature, the ease with which manual readings can be made, the insensitivity of readings to adverse conditions, and the remote reading facility.

BR experience has been described briefly in terms of recent problems and developments, including the use of the system in areas affected by mining subsidence. In these areas, the RAFT system is providing BR with a financial saving while maintaining safety and a good track standard.

PANEL DISCUSSION

The participants in the panel discussion included authors D. E. Bray, R. W. Benson, R. B. Thompson, and G. S. Lane; conference panel members D. P. McConnell (chairman) (Transportation Systems Center, U.S. Department of Transportation), H. Berger (National Bureau of Standards, U.S. Department of Commerce), B. R. Forcier (Bessemer and Lake Erie Railroad Company), and D. H. Stone (Association of American Railroads); and supplemental session panel members H. H. Chaskelis (Naval Research Laboratory) and T. Yang (ENSCO, Inc.).

T. YANG: I have a question on the transducer for rail force. If you have a continuously welded rail already installed and you are not too sure of the force status, what is the procedure used to calibrate the absolute force?

G. S. LANE: Our attitude to this is that in many, many applications, measuring changes is sufficient. Obviously, without actually cutting the rail and physically making it force-free, there is no way of determining absolute values. However, if at any time the rail is cut and made force-free, you can then relate all previous and subsequent data to that particular situation and then you have got absolute measurements.

I can give you an example of our mining subsidence problem. The subsidence may well occur on a particular piece of track which is, as far as a civil engineering experience goes, quite safe and correctly stressed. We know that at a given time it is likely to be affected by mining subsidence and the stress conditions will change. If we install our gages before this time and then watch what happens as the line is affected by subsidences, this quite adequately monitors the safety of the line.

T. YANG: I also have a couple of questions for Dr. Thompson on the transducer. I was interested in the size requirement, for instance, in using it in ultrasonic flaw detection for penetration. How big or how small will it have to be in order to get enough energy into the rail?

R. B. THOMPSON: The larger the transducer, of course, the stronger the signal one obtains.

In the EMAT application program in which we have expended the most effort, which is the program directed at inspecting artillery projectiles (again, a low-carbon steel probably very similar in properties to rail), we use transducers which have about an inch by an inch aperture. They are fairly large.

Under that condition, we have about 60 or 70 decibels of dynamic range. That is, a signal directly propagating from a transmitter to a receiver in the form of a bouncing shear wave produces a signal that is about 60 decibels above the noise. That number will decrease proportional roughly, to the area of the transducer. So if one had a half-inch by a half-inch transducer, one would lose a factor of four in voltage. One can scale to other sizes accordingly. The minimum size depends ultimately on the signal-to-noise ratio required to achieve the necessary measurement sensitivity or accuracy.

T. YANG: What about the energy requirement? How does it compare, again, to the typical piezoelectric crystal? Does it take a lot more current or less current?

R. B. THOMPSON: In the work that we have done, we have used a high-powered transistor circuitry to drive the transducers. The circuits which we have designed typically deliver a few kilowatts of peak pulse power. The average power is much lower because of the low-duty cycle, probably a little bit higher than for a piezoelectric unit, but not that much. In fact, we have a battery-operated system that can run for 12 hours without a charge.

The British have developed a system for inspecting red-hot steel rod as it comes out of a furnace. There they find it advantageous to use transmit pulses containing megawatts of peak power. This is needed because they are looking for small flaws in very attenuating material. In our projectile system, similar powers would increase the dynamic range to 100 decibels. The EMAT coil will withstand more power than we are presently delivering to it, but we do not now need the added sensitivity.

T. YANG: What is the efficiency of the transducer, comparing its being used as a sender and as a receiver?

R. B. THOMPSON: You can ask that question in two different ways. If you are asking about the absolute efficiency of energy conversion when used with a 50-ohm transmission line, the efficiency of both transmission and reception is the same because the EMAT is a reciprocal device.

However, piezoelectric transducers are often not described from that point of view. Instead, one often compares crystals by comparing their open-circuit received voltage for a given ultrasonic pressure. In these terms, quartz is better than lead zirconate titanate, although the latter has a higher efficiency of energy conversion.

I do not describe EMAT's that way, since we do not use high impedance receiver amplifiers. The efficiency is best described in terms of a transfer impedance that is defined differently than the figures of merits usually used for piezoelectric crystals.

T. YANG: It is not exactly that, either. It is really a matter of a through transmission. Let's say that you switched the receiver to a piezoelectric-type transducer; could you improve the detection?

R. B. THOMPSON: Piezoelectrics are definitely more sensitive than EMAT's. For the case you describe, the improvement might be 20 decibels or 30 decibels. Although EMAT's have lower sensitivities, we can use higher transmit powers, as I have indicated. The EMAT is a low-impedance device, so the electrical noise is also lower in a matched receiver. Consequently, we can gain back some of the difference. Whether one has the desired sensitivity depends on the particular application.

H. H. CHASKELIS: I have just two or three comments. The first is a historical note. The Navy is very interested in stress measurements and actually, in the late '50's and early '60's we did a lot of work very similar to that going on today.

Dr. E. W. Kammer, who did the work, has since retired. However, I was able to contact him and learn from his experiences. The three comments I have are due to my discussions with Dr. Kammer.

First of all, generally speaking, what we are interested in doing here is measuring some kind of a change, either velocity or amplitude. A rough order of magnitude of that change would be 2 percent. If we wish to do this accurately, we must insure that there are no other changes that will upset this measure. Using Kentucky windage, we can say only that this should be an order of magnitude less. We must be aware if there is anything that bothers us that might change within, let's say, two-tenths of 1 percent. An order of magnitude less.

In these first three papers, there were many things that were implied. I have a question now to each of the three authors.

To Don Bray, our background has shown that, although you might measure time very accurately, the actual path length that the ultrasonic wave goes through appears to vary, principally due to the transducer properties. That is, we might physically locate the transducer at point X and Y, but it will respond at a minutely different time to the pulse excitation. This is due to the impedance differences, let's say, of the two transducers, to the homogeneity of the transducer itself, the coupling, etc. That is, it is an inherent change in the apparent path length. We can measure the time accurately but we do not really know the actual path length; that has an upsetting effect, especially if you change from one transducer to the other.

We used quartz crystals that were supposedly homogeneous. When we went to barium titanate or other ceramics, that was even worse. It even gets to be worse when one tries to use surface wave transducers because there one is not sure when the thing will start responding.

D. E. BRAY: Your point, I think, relates to either the material variability or to other variations along the path length. In any situation such as this, where you demand high accuracy, it is absolutely essential that you consider the material property variations.

In addition, the path length problem that you mentioned is another serious situation. We went to a differential-type transducer in order to overcome many of the difficulties encountered along the beam path. In order to fully describe the advantages of the differential transducer, consider first that the entering sound beam becomes, in effect, a uniform bulk wave shortly after it enters the rail web surface. The receiving transducers are of identical design and should have a similar effect on the received waveform. Therefore, the subtraction of arrival times at the two similar transducers should yield results that are relatively free of surface effects. This design, of course, has no benefit in relation to material variations along the path length. Our results tend to indicate that this probe has worked well, since we were able to obtain data showing a fairly good level of repeatability.

Furthermore, in the field test, we always took the data on both sides of the rail. Hence, if you have irregularities on one side -- for example, if the rail was slightly bowed prior to installation -- then these stress effects will also subtract out.

So I think your concern is correct. The best way one can become confident of individual data is to obtain sufficient general data to where one knows what the rail population should look like. Only then can one tell if this is going to be a serious problem.

H. H. CHASKELIS: Dr. Benson, we noticed among the many changes which occur that, with respect to the Young's modulus, if you slice up your material a little bit at a time you will notice that there are minute changes from point to point or from section to section. I just heard about this a few weeks ago, but I have not seen any work done to verify how the Young's modulus happens to change within the rails that we are trying to make measurements on. If you took a 3-foot section and made, say, a hundred samples and tried to measure the modulus, what change would you expect to get out of each hundred samples? And how would that affect the ultimate measure that we wish to establish?

R. W. BENSON: I think I would first like to say "yes" and then go ahead and tell you that, in the written version of the paper, I got into a little more technical detail than I attempted to do in presenting the talk.

There are many, many refinements to all of the techniques we have talked about today and I think that one of the questions that all of us are attempting to answer is how do ultrasonic techniques compare with other techniques in general. I think there are many cases where ultrasonic techniques are overlooked and we are looking at some of the same problems, whether you look at them ultrasonically or by X-ray detection.

Now, just because I talk about ultrasonics, I do not think your question is singling out that it is an ultrasonic problem. It is a stress problem. We all have it and it is something to be well aware of and yes, we have done experiments and yes, there are things you can do about it.

H. H. CHASKELIS: To Dr. Thompson, one of the other changes that we noticed that really upset our experiments has to do with the change in velocity due to magnetic fields. It may be both good and bad with the system that you are working on but, it will adversely affect the other two ultrasonic systems. That is, depending on the magnetic field, the velocity as well as attenuation will change. This may upset the other measuring techniques since the rails are quite magnetized at times.

However, it can be used beneficially (although still a problem area) in your particular system where you are forcibly magnetizing the rail for brief periods of time. For example, if you wish to make a velocity measurement, you have a dynamic situation as you launch the wave (using EMAT), as opposed to a static one for ceramic transducers. Furthermore, the attenuation will also change at that time and so that is another serious problem.

R. B. THOMPSON: As I understood it, there are really two aspects to your question. One has to do with the effect of magnetic field induced attenuation changes and the other has to do with velocity changes.

The second paper that I presented, dealt with using the efficiency of transduction as a stress measure. Under these conditions, it is obvious that attentuation changes would change the amplitude of the signal transmitted between the transducers, and would therefore contribute to an error in the inferred transduction efficiency.

In general, I certainly agree that those changes exist. In my experience, they are generally much smaller in magnitude than the types of changes we are measuring. In fact, in one set of experiments, we directly measured the magnetic field dependence of the attentuation in 1018 steel. It was detectable, although barely. The changes in signal strength due to changes in transduction efficiency were an order of magnitude greater than those due to attenuation. I think this satisfies your criterion.

The existence of field-induced velocity shifts is a much more serious problem when applying the birefringence or other velocity measurement techniques. One is trying to measure a very small effect very precisely, and I imagine that field-induced changes may be comparable to stress-induced changes.

The way in which I would try to overcome this potential problem in an EMAT system would be to use an electromagnet to produce the static bias field. By increasing this bias to a sufficient level, the material could be magnetically saturated so that any preexisting magnetic conditions in the rail are essentially erased. As you alluded, that might well be an advantage in that one would at least know the magnetic state of the rail rather than letting it be a random, uncontrolled variable.

D. P. McCONNELL: I think one of the problems that crops up with any of these techniques that look at the influence of stress on the material properties of the rail steel, such as wave propagation speed or magnetic properties, is that rail steels are inherently "dirty" steels; they are far dirtier than any of the aerospace or construction-grade steels which have been used in trial experiments to date. I believe the large material variability to which Don Bray alluded is a substantial problem for any technique which is looking at either small changes in behavior with stress or techniques which are limited to looking at the surface or local properties of the rail. The variation in local properties along the rail may alter the measured behavior far more significantly than the relatively modest changes in behavior with stress.

I would address one question to the panel as a whole: With the current state of the art of available techniques, do you feel that this material problem is manageable in a field measurement system?

D. E. BRAY: The obvious response is that that question cannot really be answered at this time. One must know how the rail population appears to his particular method before that question can be adequately answered. We have tested one track at Pueblo (Transportation Test Center) which is a very rigid track. Installation specifications there were much more strict than typically existing in main-line installations. We have shown that you can obtain good data under those circumstances. But, until you get to know the general rail population, it is an academic point to debate the overall quality of our measurements.

D. H. STONE: First, I would like to comment on some of the comments regarding the variabilities of the rail. I would like to address this question to Bob Benson or Don Bray.

The problem is, we have more than one kind of rail. We have heat-treated rail, for example, which is going to have an entirely different residual stress pattern that may cause some mode-conversion problems and cause some difficulties there. My question is, do residual stresses exist in the rail and to what extent are they going to affect the measurement of longitudinal force? Essentially, I think you are going to be measuring both, but they are two different things.

R. W. BENSON: Stresses never are just the simple longitudinal force you are looking for. In general, in the rail that has gone through the formation processes that it has, you are not going to find a uniaxial force if you include residual stresses. They will be at least biaxial and probably triaxial. Consequently, if all you do is make velocity measurements, you are quite often going to get to the place where you can make very precise measurements which do not answer the question that you have asked. You must really measure residual stress if you are going to answer the problem I think you are trying to answer.

D. H. STONE: The other side of the coin is, you have always got to measure it at the same spot.

R. W. BENSON: No, I do not think that is necessary. Now you are back talking about technique. There are many techniques available to overcome things that we do not like, but they may slow us down. We may only go 59 miles per hour.

D. H. STONE: The question I have for Dr. Lane from British Railways is, have you had any problems with bolt hole-type cracks (star cracks as I think the British call them) emanating from the hole you have drilled to put your rail force transducer in?

G. S. LANE: I ought to give a one-word answer to that: "No." But I could say a few more words. The star crack problem is normally associated with rail ends at bolted rail joints. The situation there is much more severe than the situation where we drill a hole in a piece of continuously welded rail, for several reasons. Firstly, we produce a much higher quality hole. We use a special tool -- like a cross between a reamer and a broaching tool -- for producing this hole. It is basically a cut reamer device which produces a hole of very high quality, very close tolerance, and as far as we have been able to ascertain, a hole which is crack-free, particularly on the significant corner pieces.

The other point which I should make is that the situation at the center of a piece of long-welded rail is very different from a bolted rail joint. At the rail joint, one has firstly the reduced bending stiffness which even without any effective dipped rail ends will produce a dip in the track as the wheel goes over it and therefore produce dynamic increments to wheel/rail force so there is very much more severe loading on the hole at a rail joint than there is at a rail-force transducer.

D. H. STONE: My final question, for Don Bray, is, you mentioned that you have an accuracy of about ± 3 nanoseconds. What is 3 nanoseconds in terms of tons or some other unit per square inch, and what percentage of that do you attribute to air and electronics and variability in the rail steel?

D. E. BRAY: The accuracy figure of ± 3 nanoseconds corresponds to about 1,000 force-pounds per square inch. The way we arrived at that figure was through a series of laboratory tests. For a long period of time, a student who was working for us would merely come in in the morning and remove and replace the probe on the rail. This test lasted for several weeks. We did it with several applied stresses. Finally, we came up with the mark IV probe, which is the one with which we achieved this accuracy of ± 3 nanoseconds.

It has been too long since we went through a complete analysis, so I really cannot say whether the larger amount of error is in the instrumentation or in the material. I would expect that the most trouble is still in the interface of the probes on the rail surface.

B. R. FORCIER: I have two questions. One, going back to the coupling distance, the web of the rail, which seems to be the area that everyone is shooting for now, involves the following. A new rail is probably not too bad, and it has been pointed out that the scale has no effect but that, over a period of time, rail could become pitted. There is the brand that exists on one side and the heat numbers and so on on the other. So, given any velocity at all when you are moving the probe, there is going to be some problem. Has this been addressed?

R. W. BENSON: You can make a transducer that is like a wheel and you can roll it down the rail just like a wheel if you would like. If you use conventional laboratory techniques, you are going to have problems. If you use your imagination and some ingenuity like this work that is done on the EMAT, there is no telling what you can do.

B. R. FORCIER: My second question is for Dr. Lane. From the railroader's standpoint, the axial force measurement is probably the one that we are looking for in sum total. Regarding the insert of the force measurement transducer, has it been thought of to make it a transmitter so that a moving vehicle could read the signal put out by the transducer?

G. S. LANE: The problem with what you are suggesting, I think, is the problem of exciting the wire into vibration. If you could excite it in a way different from the electromagnetic pulses which are used at the moment, yes, you could conceive of various ways of picking up the vibration. But the problem at the moment is, you have to produce a fair amount of power into the coils in the transducer to effect the pluck and I do not see how you could do that from a moving vehicle. Our approach has been to connect the transducer up permanently and its instrumentation through a logging system and a telemetry link. I believe this is an alternative approach with a similar sort of aim.

UNIDENTIFIED SPEAKER: You can't mount a battery-mount or a battery-powered device on the side of the rail because something will slice it or it will get broken. If it was a battery-powered device, you could obviously trigger it by radio and do any number of things.

G. S. LANE: Yes. In fact, our telephone connection is just that, in fact, triggered by telephone. You are right about the problems, because last week we had some vandalism on one of our sites and some of the equipment was stolen. In fact, we are going to bury some of it.

H. BERGER: I think that it is apparent from the laboratory work that has been done that ultrasonics offers a good tool for the kind of measurements we are talking about. The problem is really not one of sensitivity but one of sorting out what that signal is telling you. I am very attracted to the EMAT possibilities because of the concept of putting in waves with different polarization, for example, in order to get more interpretive information.

My first question is, how sensitive is the EMAT in a practical environment like a rail system?

You have commented on the lift-off problem. Are there problems in the nonuniformity of the rail? For example, the fact that the surface may be hardened or pitted could influence the quality of the ultrasonic signal that is put into the rail and the received signal.

My second question follows up on the one that Henry Chaskelis asked. The question of the Young's modulus certainly affects all of the measurements that we are talking about. What is the level of variation of the Young's modulus in a typical rail steel?

D. H. STONE: Although I do not have a good feeling for that, I do know that the chemistry or the chemical composition of a rail down a 39-foot section (a standard length) varies quite a bit. This, in turn, is going to indicate problems with the Young's modulus.

H. BERGER: Yes but what is the order of the change -- 1 percent or 2 percent?

D. H. STONE: I think probably in that range, 2 to 3 percent.

R. W. BENSON: Can I ask a question? I know there are lots of things to worry about in precision but how precise a measurement do you need, practically?

H. BERGER: Henry Chaskelis said he wanted a measurement to two-tenths of 1 percent. That seems impossible in view of the variations we have been discussing.

R. W. BENSON: Yet, you have no useful measurement right now. What would you settle for tomorrow?

H. BERGER: I really don't know what is needed.

R. W. BENSON: Ten percent? Twenty percent?

T. YANG: Take the problem that you are probably going to install it at a neutral temperature, say 80°F or whatever number you just happen to choose. What is the potential error? For any particular day, you can have easily a 20° to 30° error in the installation that the crew was trying to get it in. They say, "Okay, so there is a 20° difference." So that is the kind of uncertainty we are dealing with, I think.

R. W. BENSON: There are some applications, not necessarily railroads, where people are happy if you can tell them this is in tension instead of compression. That is all they need to know. Now, are you saying you need to know that it is less than 80 percent of yield strength?

T. YANG: No, it is the temperature.

All right, let's say that you know that you are in trouble by design when it gets to 120° but maybe you will when it is only 100°, so you have a 20° buffer so you would like to know before that. Then it is a decision of how big or how safe a margin you can afford.

R. W. BENSON: Some of the questions are concerned about percent accuracy and tenth of a percent accuracy. Maybe these are not important if you want to go fast and inspect all of the rail; maybe 50 percent or some ceiling that you tell us you cannot go above is sufficient to answer your question. Or maybe all you need to do is to have a system that says, "If I ever get in tension when the sun is not shining, I have got a problem." I am trying to make it easier for us to answer your question, but I do not know what the question is.

D. P. McCONNELL: The question of required accuracy has come up a number of times. One of the principal factors which governs this requirement are the physical phenomena which one is trying to monitor with such a measurement. I think the phenomenon with which people are most concerned in rails is the compression -- the buckling problem. This phenomenon will largely govern the required accuracy.

Allan Zarembski, can you help us out?

A. M. ZAREMBSKI (Association of American Railroads): Yes, as a sort of a rule of thumb, I would generally have to say that what we are looking for, if we can pin it down to about between 25,000 and 50,000 pounds compressive force per rail, would translate to between 2.5 and 5 ksi in stress or 10°F or 20°F in temperature. This is probably a realistic first-cut set of numbers.

If we get less resolution than 50,000 pounds force, I suspect the utility of the measurement device to guide track maintenance forces is probably pretty severely hampered. It would almost go back to the rule of thumb saying, "Don't work on the rail at temperatures above the laying temperature," which is a rule of thumb that has been adopted in certain railway administrations. Therefore, going back to the stress numbers, we probably are looking at 5 ksi -- even though, as Dr. Lane indicated earlier, 1 ksi would be a next objective. However, I think at this stage, this will suffice.

R. B. THOMPSON: Let me return, for the moment, to the original part of Harold Berger's question regarding the potential which EMAT's represent. There is a difference in how an EMAT and a piezoelectric probe work on a rough surface. Let us consider that the surface of a rail has a high degreee of roughness. With a couplant, one must ask whether the couplant gets into all the nooks and crannies of the rail surface. If it does not, there will be local cold spots in the beam. Even if it does, one will find that the ultrasonic wave front is not planar, since some portions have traveled a greater distance in the low-velocity couplant than others.

The EMAT does not have the first problem. Eddy currents flow in continuous paths and, if there is a small pit, will simply flow under it and follow the contour of the part. The wave will always be generated at the part surface. However, if this surface is rough, wave fronts of the generated waves will again deviate from the planar condition. Thus there may be a corrugation of the wave front. Diffraction will generally smooth that out, but that is a source of error in velocity measurements that has to be evaluated.

In summary, I would say that one is likely to get better signals with EMAT's on rougher surfaces than one may obtain with other approaches.

Nevertheless, there will be a source of error in velocity measurements, having to do with wave front corrugation, that needs to be evaluated. If that corrugation is in the order of a wave length, then it will begin to decrease the signal strength, as it would for any type of transducer.

H. BERGER: What about the hardened surface? Does that cause you any problem?

R. B. THOMPSON: As long as it has a reasonable electrical conductivity, there should be no problem. Forget the magnetostrictive effects for the moment and suppose that one has a big enough magnetic field so that the generation is produced by Lorentz forces. The question then becomes, how does the efficiency of transduction depend upon the electrical conductivity? The result that Bruce Maxfield (formerly of Cornell University, now with Lawrence Livermore Laboratories) obtained many years ago is that, as long as the electromagnetic skin depth is small with respect to the ultrasonic wave length, transduction efficiency is insensitive to conductivity. This is because the total eddy currents induced in a metal by a current in an adjacent wire are independent of conductivity. The only thing that changes is the volume in which they are distributed.

If that volume is close to the surface with respect to a wavelength -- that is, the skin depth is sufficiently small -- then its exact value does not really matter.

UNIDENTIFIED SPEAKER: If there is any real equivalent to case hardening on the outside, you may change the last response that you can get plus the weight values.

R. B. THOMPSON: That would be the same in any ultrasonic measurement. An EMAT system would certainly be sensitive to that to the same degree as any other ultrasonic system. Once a wave is launched, its behavior is independent of the transducer.

D. P. McCONNELL: I think that Don Bray has demonstrated that some of the phenomena he observed were due to the presence of a distinct cold-work layer in the head causing a case-hardening-type behavior. It was for that reason that the interest centered on the web.

QUESTION-AND-ANSWER PERIOD

N. SENAPATI (Battelle Columbus Laboratories): I have a comment on Dr. Bray's paper. I think that is probably one of the various models and I think it is around 6 to 10 percent. Typical variation in the velocities in a commercial piece of material is around 3 percent. We have done extensive studies for nickel and velocity variation was one of the problems. To come up with a process whereby we can reduce the velocity variations to less than 0.2 percent is a major task.

R. B. THOMPSON: What magnitude did you say?

N. SENAPATI: Up to 6 percent change. That is what I am going to talk about in my presentation [in the second session of this conference], but there is further change in attenuation, too.

R. B. THOMPSON: I certaintly believe that, but I was saying that the change in transduction efficiency is much larger. I did not mean to imply that there was no change due to attenuation variations, but only that these were much smaller in magnitude.

N. SENAPATI: But the velocities in this I believe are much smaller than that. When that goes on, the velocity change is particularly due to the stress effect -- say, 10,000 psi.

D. E. BRAY: We are running, say, about 3 nanoseconds per 1,000 psi. Did you say on the order of 10 psi?

N. SENAPATI: No, I said about changes of velocity due to 10,000 psi.

D. E. BRAY: On the order of 1 percent.

N. SENAPATI: Yes, so we are still talking about a small percentage change in velocity, together with some attenuation changes to be considered. In fact, that is probably going to be the way to go in terms of the ultrasonics -- to look at the change in attenuation rather than change in velocity.

L. H. BENNETT (National Bureau of Standards): Dr. Thompson mentioned the sensitivity to the composition and alluded to sensitivity to metallurgical history. Is there not also sensitivity to magnetic history, especially in steels? You might not have so much in the Armco iron, which is very soft magnetic material, but in the steels won't you have a great sensitivity to the magnetic history?

R. B. THOMPSON: That is generally true. However, the way in which we make measurements suppresses this effect. If you will recall, I derived features from a curve of magnetization versus magnetic field. We first saturated the material and then reduced the biassing field and recorded the features of the plot of signal amplitude versus the value of the decreasing field. Any initial domain structure that existed was eliminated by the mitral magnetization to saturation. Although I am not that familiar with rail steels, it is my impression that they are relatively soft magnetically, not as hard as Alnico, and one can erase the past magnetic history when one brings the material to saturization. In taking all of our data, we first took the magnetization to 90 or 95 percent of saturation.

L. H. BENNETT: I would assume they are not as hard as Alnico or something like that, but you might not erase all the previous magnetic history in a single saturation cycle.

D. H. STONE: I do not know if it is pertinent here, but for the past 40 years or so we have in fact been magnetizing our rails regularly as a way of flaw inspection. Is this going to create a problem for you?

R. B. THOMPSON: Again, it is my impression that I felt we were reaching sufficiently high fields to erase that past history. Obviously, whether or not we were practically reaching that or not cannot be fully answered now. That is something that will need to be investigated in comparing this approach with other techniques.

A. D. KERR (University of Delaware): How many transducers have been installed by British Railways on main lines to date?

G. LANE: I am not sure, exactly. It is in the region of about 300, possibly more. A lot of this is for research purposes and a certain amount of installation is for actual service use, as I indicated before.

D. P. McCONNELL: To amplify Dr. Kerr's question, in those locations where gages are used, such as the instances of mining intrusion, what is the measurement density in terms of both the spatial placement of gages that you currently use and how frequently do you sample them.

G. S. LANE: It varies a lot. We tend to

combine the for service use with research purposes, so we tend to put them a little bit closer together than we otherwise would have done. They are in the region of a rail length apart; that is, 20 meters or 60 feet apart. But we have the spacings up to a quarter of a mile for simply looking at certain effects. Each case has got to be judged on its merits. That is about all you can say.

A. D. KERR: What are the observed wave speeds in the rail head and rail web?

D. E. BRAY: As to the question on the Rayleigh wave, initially, let me say that, on the working surface itself, you will have variations in velocities from 2,500 meters per second to almost 3,000 meters per second -- almost a 20 percent variation. You do not see a large amount of variation in the Rayleigh wave velocity on the side of the rail where you do not have this cold-worked effect. An additional consideration is that the Rayleigh wave is relatively insensitive to stress changes as compared to the other types of wave propagation. However, with respect to the web of a hot-work rail, you do not see the large amount of variation that you do on the head of the rail.

Typically, the Rayleigh wave speeds in steel are around 2,900 meters per second. Where you do not have any cold-working or any severe anisotropy, you would not expect to see a severe change in the Rayleigh wave speed. So I would say that the speed would be 2,900 meters a second plus or minus a small percentage on the side of the head. I would expect it to be about the same as the side of the web.

R. GREEN (Johns Hopkins University): I would like to make a couple of comments. One of the problems that every technique is going to have to face is that, if anything else changes the measurement other than the stress, that has got to be accounted for. The worst thing you have with almost any real material is antisotropy, and therefore you have to worry about more than one module.

Unlike most other techniques that will be discussed today, the ultrasonic techniques are based on nonlinear elasticity, not on linear elasticity, so the really important major items have to be worked out with the ultrasonic technique.

TECHNICAL PAPERS

"Stress Measurements in Railroad Rails Indicated by Barkhausen Noise Analysis"*

William D. Perry
John R. Barton

Southwest Research Institute

Introduction

Continuously welded rail (CWR) does not contain expansion joints, and significant stresses are induced by the wide range of seasonal temperatures. At low temperatures, such stresses can contribute to rail fracture and possible derailments; also, at high temperatures, local lateral displacement of track (crookedness) can cause derailments. During installation of continuously welded rail, the temperature of the rail is controlled by a cold-water spray or heating torches (depending on the ambient temperature) in an effort to achieve a rail temperature approximately midway between the anticipated seasonal temperature extremes. Other practices, such as deliberately cutting the rail some time after installation to observe the opening or closure of the ends, removing or adding a small section as appropriate, and then rewelding the ends, has sometimes been utilized to minimize the overall effect of thermally induced stresses. For some time, various railroads and also the Association of American Railroads have attempted to develop approaches to measuring the thermally induced stresses. The purpose of the investigations summarized in this report was to assess the potential of the Barkhausen noise analysis method for indicating the thermally induced stresses in CWR.

Briefly, with this method a controlled magnetization is applied to the region of the part being examined and a small probe is used to sense the Barkhausen noise caused by abrupt movement of magnetic domain walls; analysis of the Barkhausen noise during controlled experiments has established that high-amplitude signatures are associated with tensile stresses, low-amplitude signatures are associated with compression stresses, and intermediate signatures are obtained from unstressed regions. Prior work covering several years has established the effectiveness of the Barkhausen method for indicating residual and applied stresses in a wide range of materials and components; furthermore, limited experiments have showed that the method is sensitive to stresses applied in a bending mode to a specimen of railroad rail. Recently, experiments were conducted to assess the effect of selected parameters on the Barkhausen indications. Included were the effect of temperature with rail specimens unrestrained by end loads, and the effect of end loads applied at a constant temperature.

*Presentation at conference delivered by John R. Barton.

The Barkhausen Noise Analysis Method

The magnetic properties of ferromagnetic materials (practically all steels, some cast irons, nickel, and some nickel alloys) are best described by the magnetic domain theory. This theory, which has substantial experimental confirmation, postulates that the material is made up of local regions called ferromagnetic domains, each magnetized to saturation but aligned according to the state of local magnetization. Adjacent domains are separated by a highly localized magnetic transition region called a domain wall or Bloch wall. Even in the demagnetized state, all domains are still magnetized to saturation, but the orientation of the individual domain magnetization vectors is random; this results in the net magnetization of the specimen being zero. The application of a magnetic field or a stress can change the configuration of the domains, principally by wall movements.

The fact that magnetic domain walls can be forced to move under the influence of a changing applied magnetic field or a stress provides the fundamental basis for the Barkhausen noise method of residual stress measurement. In 1917, Barkhausen discovered that voltages induced in an electrical coil encircling a ferromagnetic specimen produced a noise when suitably amplified and applied to a speaker, even though the magnetization applied to the specimen was changed smoothly. From such experiments, he inferred that the magnetization in the specimen does not increase in a strictly continuous way, but rather by small, abrupt discontinuous increments, now called Barkhausen jumps. Such jumps are caused principally by the discontinuous movements of mobile magnetic boundaries (Bloch walls) between adjacent magnetic domains and occasionally by the initiation of new magnetic domain walls. Furthermore, the direction and magnitude of the mechanical stress existing in a macroscopic ferromagnetic specimen strongly influences the detailed dynamics of the domain wall motion and correspondingly influences the Barkhausen noise.

Figure 1(a) shows three photographs of magnetic domains (made visible by a magneto-optic method) on the surface of a carefully prepared single crystal of silicon-iron and illustrates the manner in which domains change under the influence of an applied stress. The magnetic field was applied from left to right in the illustration, and this was also the axis of the applied compressive stress. Arrows have been placed on some domains to indicate the direction of magnetization within the domain. A careful examination of these photographs shows marked changes occurring as the compressive stress is increased; for example, the domains are principally oriented approximately 45 degrees upward and to the left in the top photograph, while several domains have grown in a direction oriented upward and to the right in the lower illustration. As these domains move, Barkhausen pulses are generated.

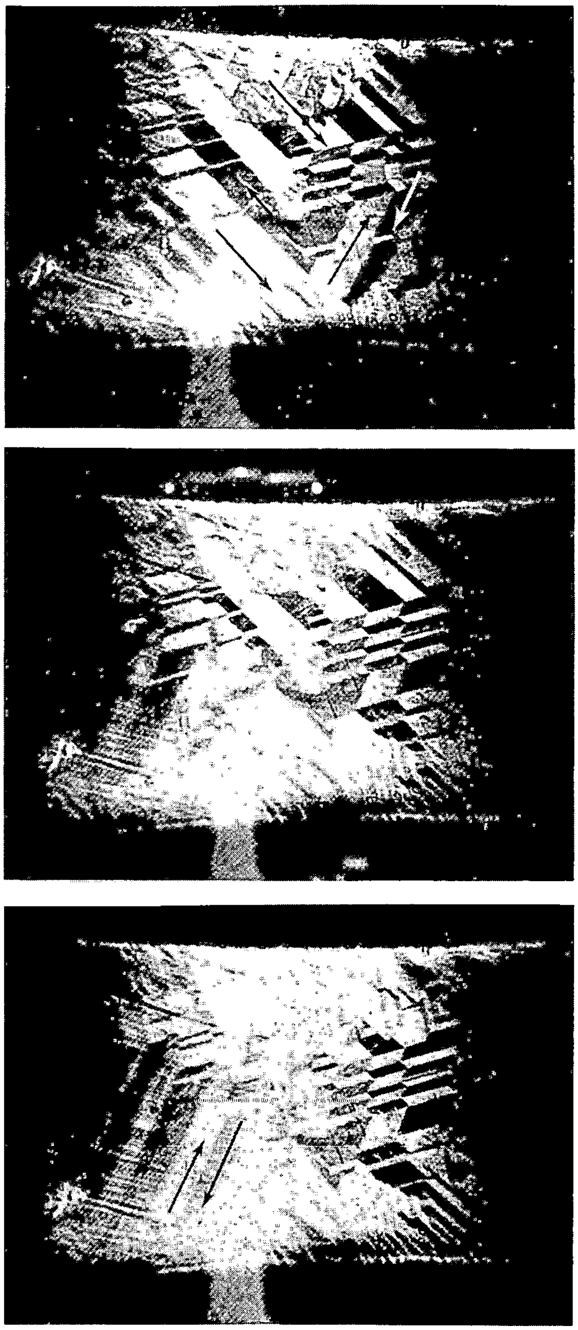

Compressive stress of 900 psi

Compressive stress of 1700 psi

Compressive stress of 2600 psi

229 lbs

FIGURE 1(a). INFLUENCE OF STRESS ON MAGNETIC DOMAINS IN SiFe SINGLE CRYSTAL SPECIMEN

Figure 1(b) shows many of these pulses sensed by an induction coil near the surface of a low carbon steel bar. These Barkhausen pulses are electronically processed and presented on a peak reading meter or on an oscilloscope.

A variety of instrumentation systems have been used in Barkhausen noise research, and a block diagram of the instrumentation used in most of the exploratory investigations is shown in figure 2. A photograph of the most recent model instrument with a digital indicator is presented in figure 3.

A calibration curve obtained on the cantilever bending specimen is shown in figure 4. Note the characteristic curve "flattening" at compressive stress near 50 percent of the yield stress.

Preliminary Experiments on Rail

The first experiments were conducted on sections of rail approximately 8-10 years ago. The experimental arrangement in which bending stresses are applied by center loading a rail section supported at both ends is shown in figure 5. Graphs of

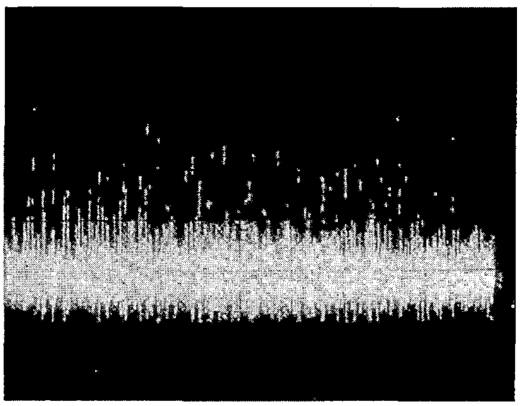

10 mv/cm vertical sensitivity
1 msec/cm sweep rate (horizontal)

FIGURE 1(b). BARKHAUSEN NOISE PULSES

the Barkhausen indication versus load for several locations (B, D, E, and F) around the rail section are presented in figure 6. Results from this experiment showed qualitative agreement between the readings and the stresses caused by the bending load; namely, point D decreases, points B and E (near the neutral axis) showed only small changes, and point F showed a significant increase.

Recently, controlled but limited experiments have been conducted, and these will be summarized in the following sections.

Test Specimens and Equipment for Quantitative Experiments

A test specimen was prepared from a 4-foot length of used, continuously welded rail. The ends of this specimen were machined square to minimize nonsymmetrical column loading and four strain gages (temperature compensated for steel) were mounted at appropriate locations around the midsection of the rail to monitor strain and also detect bending. Three temperature sensors were mounted at equally spaced locations along the length of the test specimen.

Primary equipment and instrumentation used in the experiments consisted of the following:

a. A 200,000-pound Baldwin load test machine for applying controlled end loads to the rail specimen.

b. An electronic strain indicator with a digital readout for the four strain gages.

c. An indicator for sensing temperature of the rail at three locations on a specimen.

d. A model 200 Barkhausen noise analysis instrument with associated probe and digital readout for obtaining Barkhausen measurements of stress.

A dry-ice pack was used to cool the rail and flexible heating elements were placed around the rail to increase the temperature. A photograph illustrating the experimental arrangement is presented in figure 7. Figure 8 is a photograph of a typical Barkhausen measurement being obtained with the probe positioned manually.

Experiments

The first experiment undertaken was to determine the influence of test specimen temperature on the Barkhausen indications. In this experiment, the test specimen was unrestrained and the temperature was reduced using dry ice to approximately 20°F. The temperature was monitored using the three temperature sensors spaced along the rail. The temperature was then allowed to increase until the test specimen temperature was 40°F. At this point, Barkhausen data were obtained from the unrestrained section of rail. The specimen was then warmed using flexible

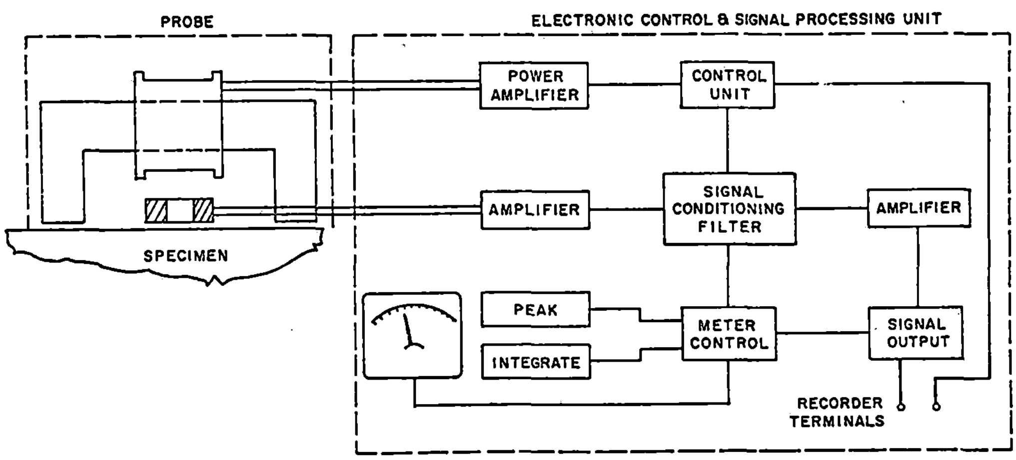

FIGURE 2. BLOCK DIAGRAM OF MEASUREMENT SYSTEM

electrical resistance heaters wrapped around the rail. The temperature was carefully monitored using the temperature sensors, and Barkhausen data were obtained as the temperature of the specimen was raised from approximately 40°F to approximately 120°F. Results from this experiment are plotted in figure 9 and indicate a slight increase of Barkhausen values with increase of temperature. It should be noted again that the specimen for this experiment was unrestrained and was heated slowly and uniformly, with the temperature being monitored at three different positions. Thus, the specimen should have little or no thermally induced stresses, and any change observed in the Barkhausen signal amplitude can be attributed to the temperature of the test specimen only. As can be observed in figure 9, this effect is slight.

The next experiment undertaken was to reduce the temperature of the test specimen to slightly below 40°F; then the test specimen temperature was allowed to rise until it was exactly 40°F. At this point, the test specimen was restrained from expanding by end loads applied with the Baldwin machine (adjusted incrementally to apply just enough load to restrain expansion) as the temperature of the test specimen was increased to approximately 120°F. Thus, by restraining the test specimen and raising the temperature 80°F, compressive stresses are thermally induced in the specimen. The cross-sectional area of the rail is 13 square inches, using a coefficient of thermal expansion of 7 x 10^{-6} inches per inch -°F, a temperature rise of 80°F, and a specimen length of 48 inches, the length of the specimen would increase by 0.027 inch if unrestrained. But if the specimen was restrained to a length of 48 inches, the resulting compressive stress would be 16,800 pounds-force per square inch (psi). Using the cross-sectional area of 13 square inches, the total force generated by the 80° F rise in temperature is 218,000 pounds. Since the load limit of the hydraulic loading machine shown in figure 7 is 200,000 pounds, the temperature rise was limited to 77°F.

During this experiment, several parameters were monitored. Barkhausen data were obtained from several positions on the rail while the temperature sensors and strain gages were monitored. Strain gages were used to confirm that the beam was being loaded symmetrical and was not beginning to buckle. No indications of nonsymmetrical loading were detected during the experiments. The actual end load was adjusted at approximately 5°F intervals using the calibrated hydraulic system of the test equipment. The results of these Barkhausen data are shown in figure 10. These data indicate a trend of reduced Barkhausen signals with increasing compressive stress, although there is significant scatter. Since the Barkhausen probe was manually positioned during measurements, one source of the

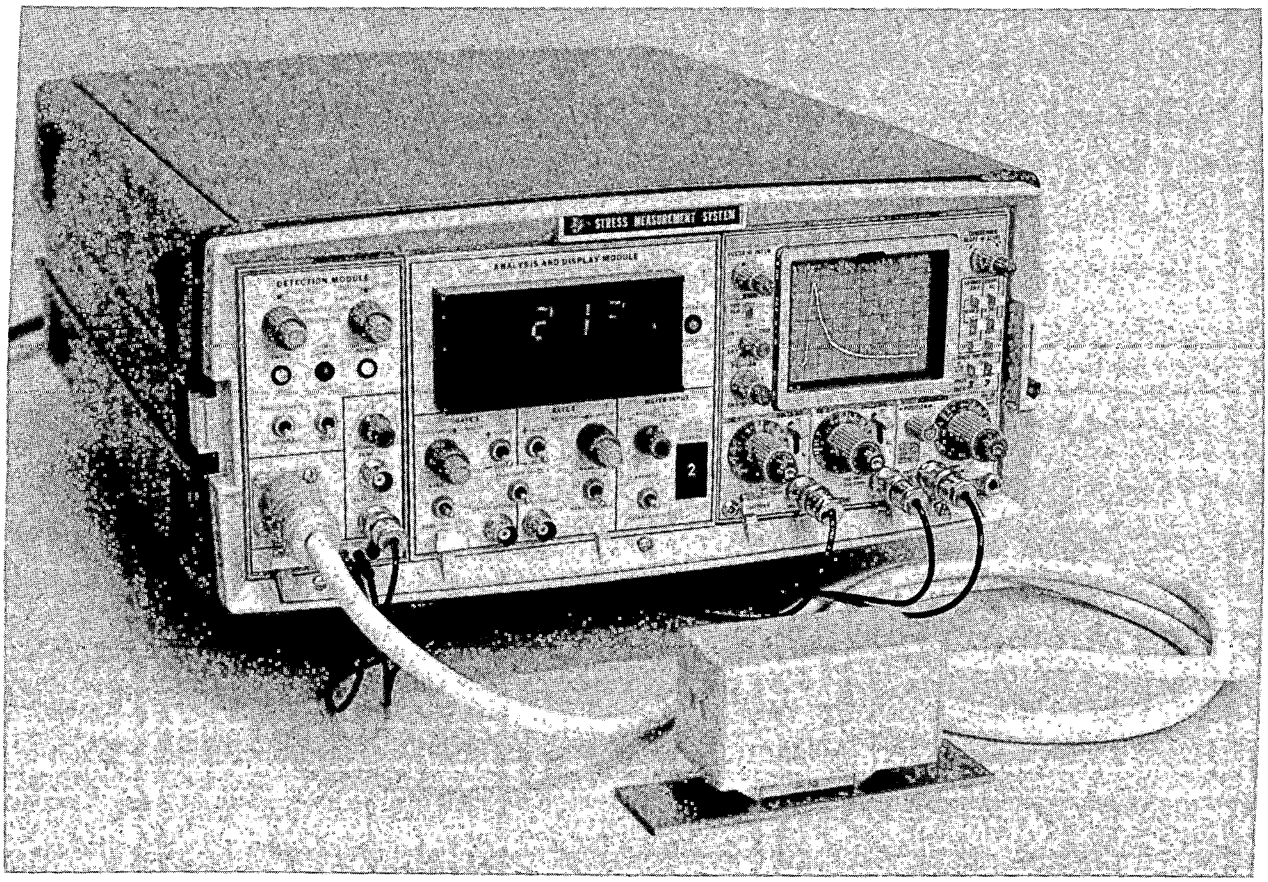

FIGURE 3. BARKHAUSEN NOISE STRESS MEASUREMENT SYSTEM WITH HAND-HELD PROBE

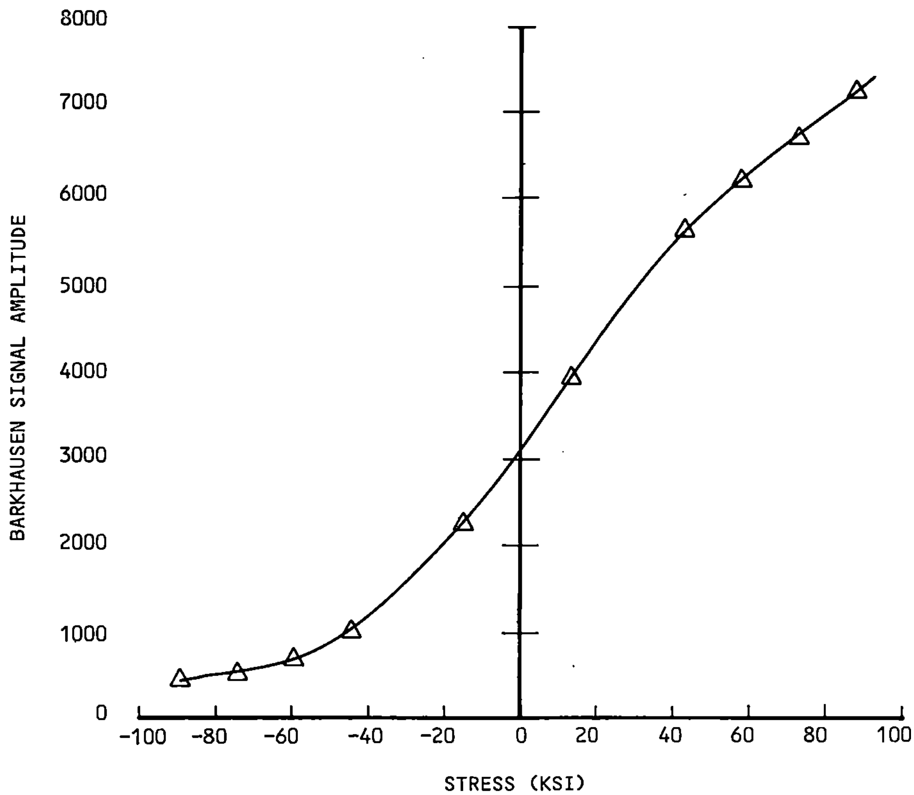

FIGURE 4. BARKHAUSEN SIGNAL VERSUS STRESS
(CANTILEVER BAR SPECIMEN AISI 4340 [200 KSI YIELD])

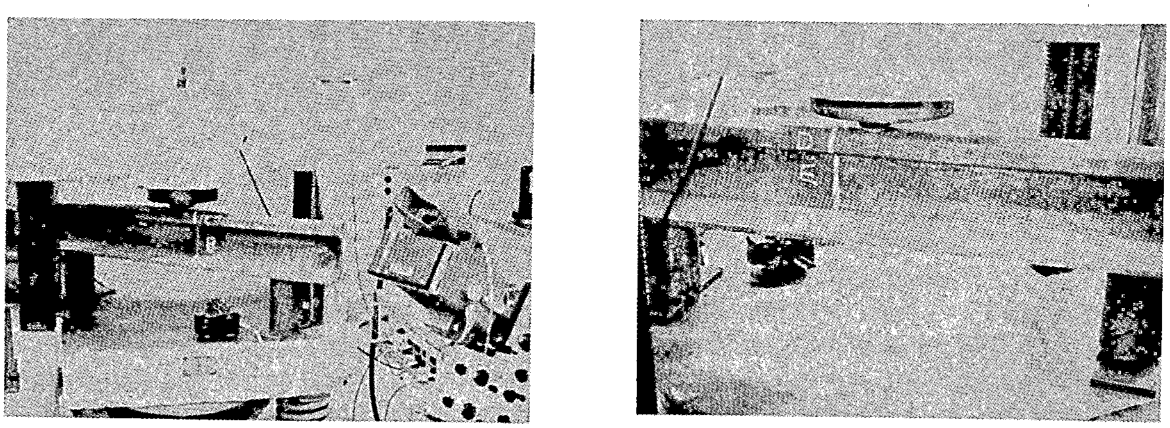

FIGURE 5. EXPERIMENTAL SETUP FOR APPLYING STRESS TO RAILS

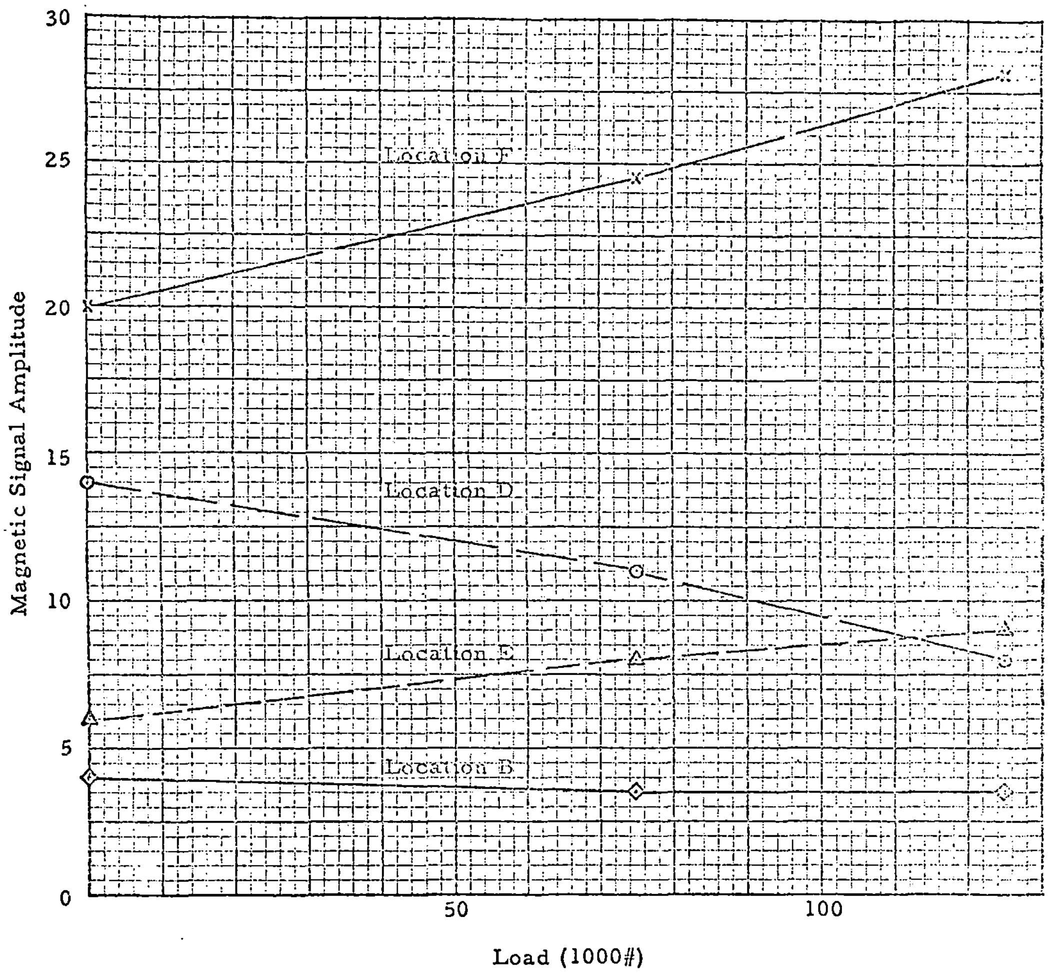

FIGURE 6. MAGNETIC SIGNAL VERSUS APPLIED LOAD (NEW RAIL)

data scatter was attributed to the inability to reposition the probe precisely. To further determine whether the data scatter was primarily a positioning problem, the test probe was rigidly fixed, mechanically, to the test specimen and load versus Barkhausen data were obtained at constant room temperature (the influence of temperature on the Barkhausen readings had been previously determined to be slight). This approach of taking Barkhausen data at a single location as the applied stress is changed eliminates the data scatter caused by repositioning. A typical curve obtained using this method is shown in figure 11. Scatter of these data points is very small.

To further investigate the problem of data scattering associated with positioning of the Barkhausen detection probe, a set of data was taken with the test specimen unrestrained. Barkhausen data were taken at six locations around the specimen and this pattern was repeated at four positions along the specimen. This data pattern was repeated three times so that three individual readings were taken at each combination of position and location. Again, these data showed that the spread caused by relocation of the probe was substantial. In an effort to reduce this scatter problem, a probe with approximately twice the pickup area was fabricated and installed in the Barkhausen hand-held unit. The experiment was repeated with the operator carefully repositioning for each measurement. This experiment showed that the data scatter had been reduced somewhat by the use of a larger pickup coil, but that it remained significant.

Finally, the experiment was repeated using a simple positioning fixture to allow the operator to reposition more precisely at each location. Approximately 160 measurements were obtained. Typical results demonstrating reproducibility are shown in table 1 (page 72). These data showed excellent repeatability from measurement to measurement. Thus, it was concluded that repositioning of the probe to precisely the same location is important to minimize data scatter caused by local variations at the surface of the rail.

Load experiments were conducted with the specimen in the Baldwin machine using the larger pickup coil. Data were obtained from several locations around the rail for two different positions down

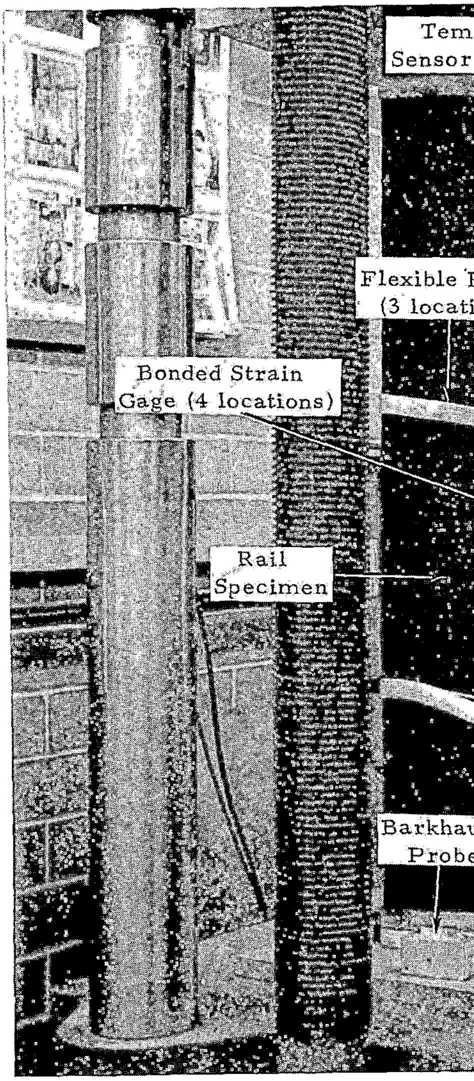

FIGURE 7.

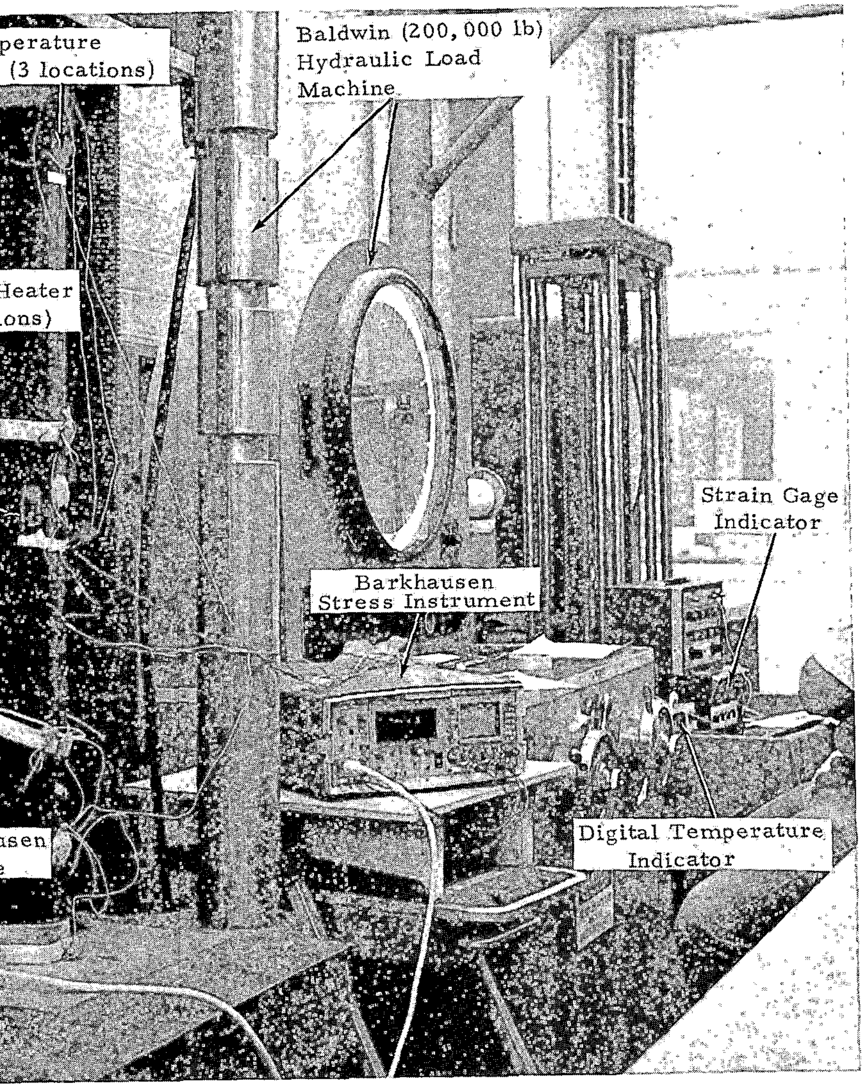

. OVERALL EXPERIMENTAL ARRANGEMENT

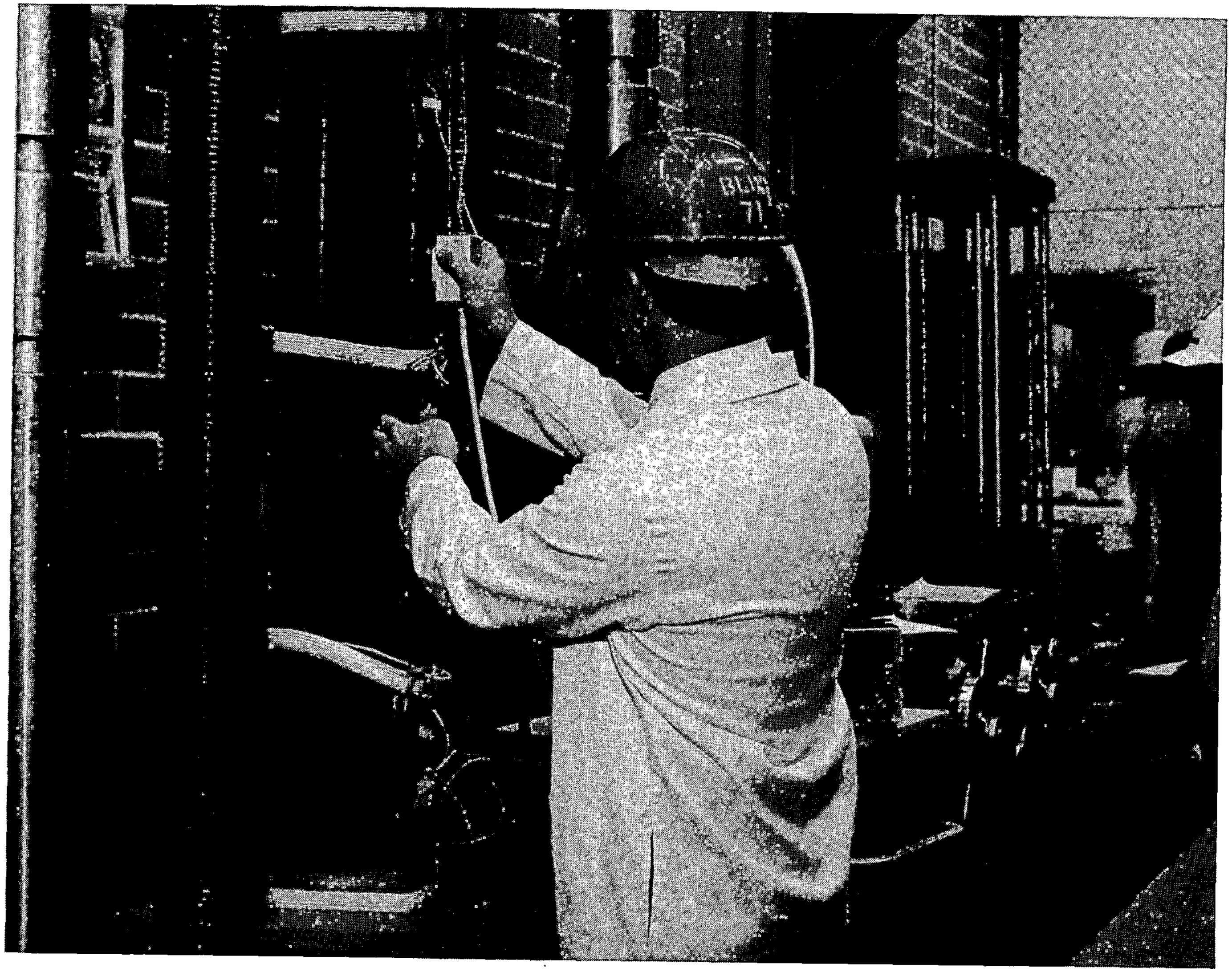

FIGURE 8. BARKHAUSEN MEASUREMENT BEING MADE ON RAIL

BARKHAUSEN SIGNAL AMPLITUDE VERSUS TEMPERATURE
RAIL SPECIMEN NO STRESS
7/21/77 1HZ 1AMP P-P

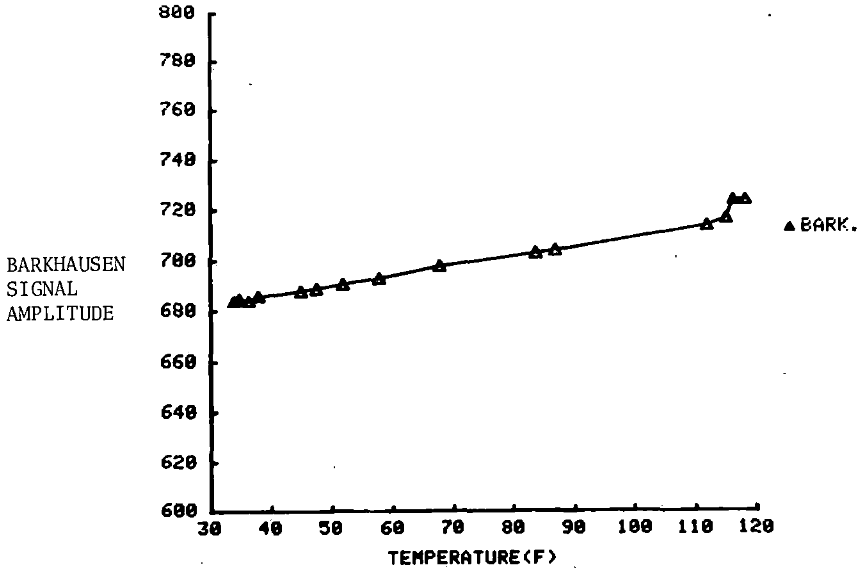

FIGURE 9. BARKHAUSEN SIGNAL AMPLITUDE VERSUS TEMPERATURE FOR UNRESTRAINED RAIL SPECIMEN

BARKHAUSEN SIGNAL AMPLITUDE VERSUS THERMALLY INDUCED STRESS
RAILROAD RAIL SPECIMEN #1
8/12/77

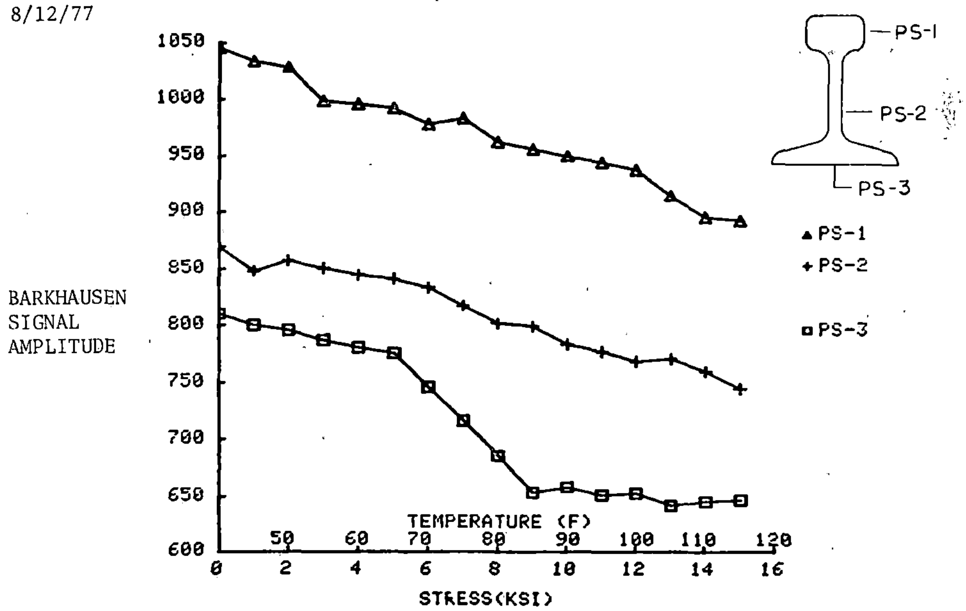

FIGURE 10. BARKHAUSEN SIGNAL AMPLITUDE VERSUS TEMPERATURE/STRESS FOR RESTRAINED RAIL SPECIMEN

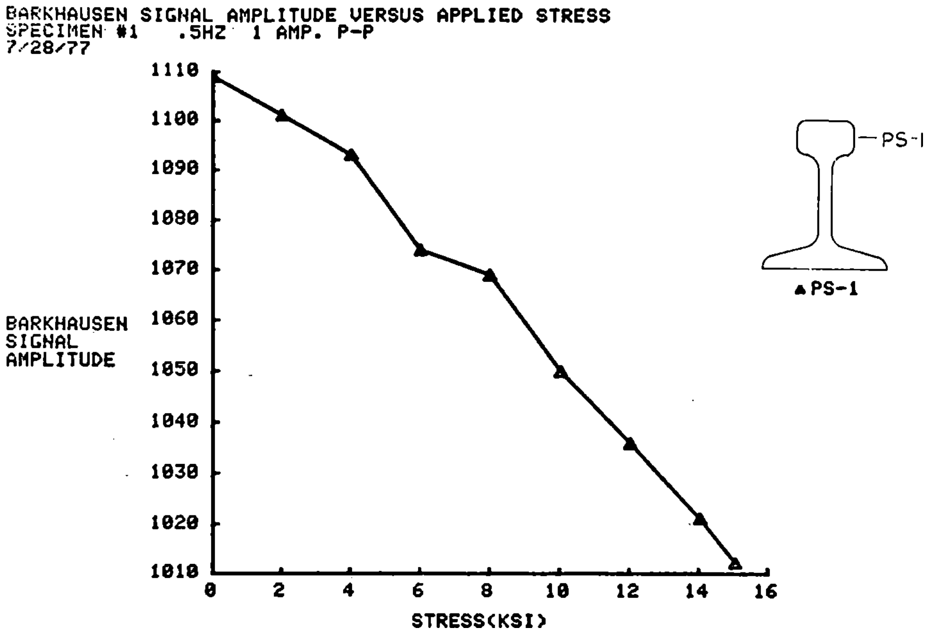

FIGURE 11. BARKHAUSEN SIGNAL VERSUS
STRESS WITH PROBE IN FIXED LOCATION FOR DURATION OF TEST

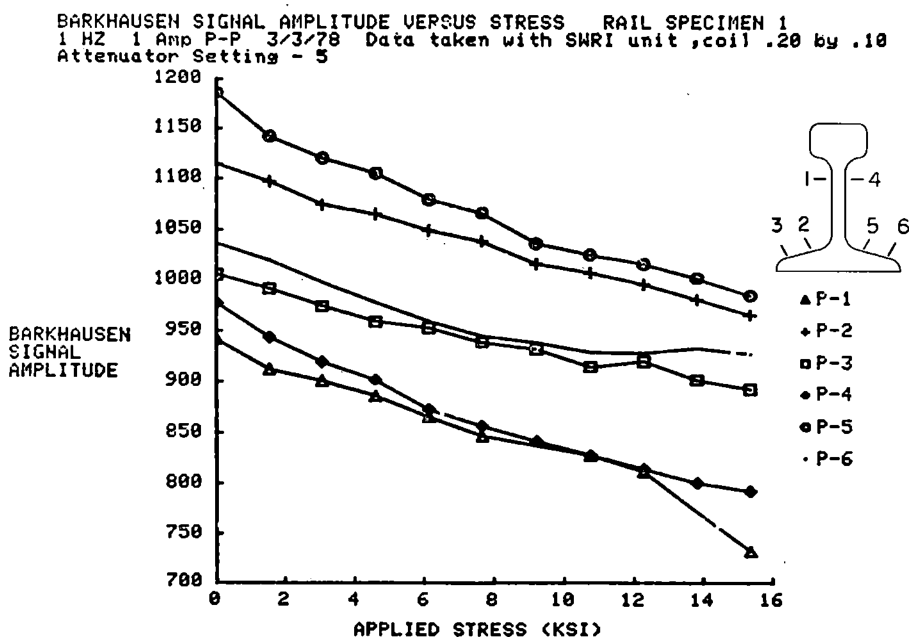

FIGURE 12. BARKHAUSEN SIGNAL AMPLITUDE VERSUS
APPLIED STRESS FOR SIX LOCATIONS AT POSITION 1

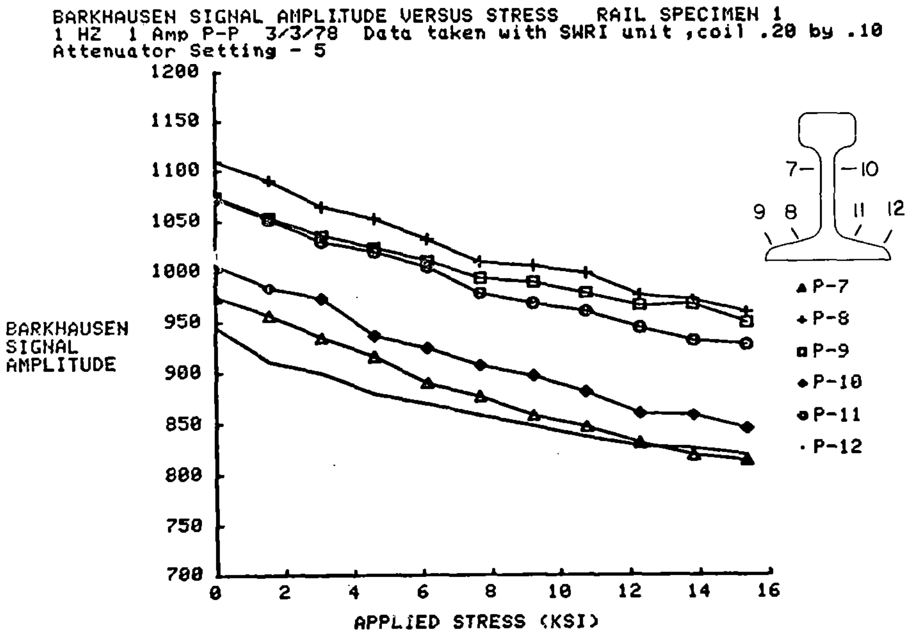

FIGURE 13. BARKHAUSEN SIGNAL AMPLITUDE VERSUS APPLIED STRESS FOR SIX LOCATIONS AT POSITION 2

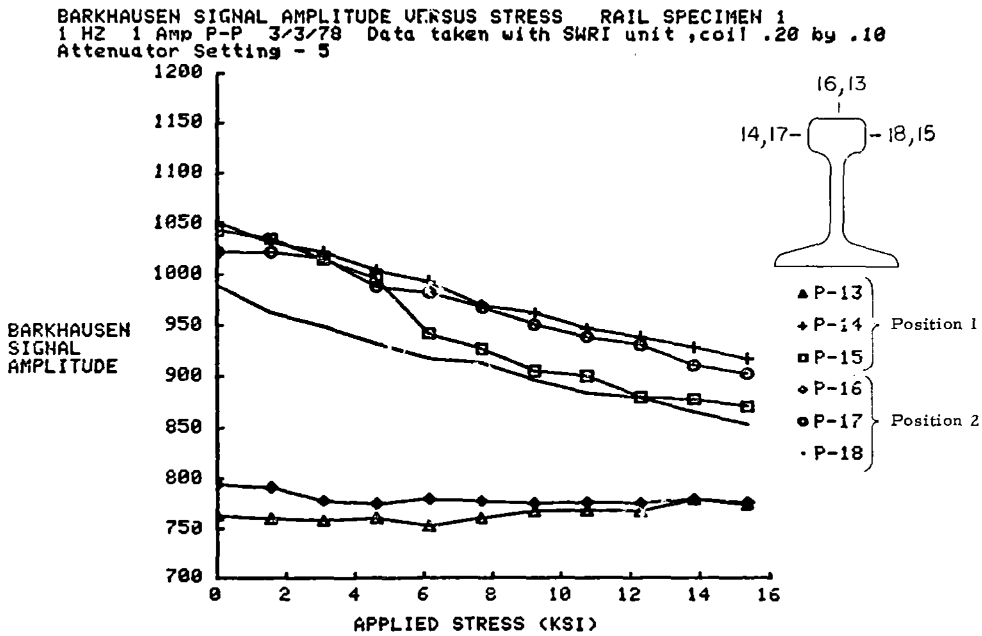

FIGURE 14. BARKHAUSEN SIGNAL AMPLITUDE VERSUS APPLIED STRESS FOR THREE LOCATIONS AT TWO POSITIONS

the length of the rail. Results are shown in figures 12, 13, and 14. The Barkhausen response to applied stress as shown in these figures indicates a relatively good response to increasing compressive stress in all the locations except on the rail head. At this point, little change is indicated in the Barkhausen signal with increasing compressive stress. This effect is probably caused by the fact that this area is in a state of very high residual compressive stress caused by wheel cold working on the surface; accordingly, the material is in a stress condition where the Barkhausen noise does not change as the compressive stress increases.

TABLE 1

REPRODUCIBILITY DATA

Trial	Position 1	2	3	4	5
Trial #1	850	1,000	938	940	1,016
Trial #2	838	1,000	934	936	986

An overall appraisal indicates that the best and most consistent Barkhausen indications of applied stress are obtained from the web and flange regions of the rail.

Conclusions

The conclusions drawn from the above-described work are as follows:

a. The Barkhausen method offers excellent potential for rapid nondestructive measurement of thermally induced stresses in continuously welded rail.

b. Barkhausen readings vary from point to point on the rail.

c. Only nominal cleaning of the rail to remove grease and sand is required.

d. Reproducible indications will require careful repositioning of the Barkhausen probe.

e. Temperature of the specimen alone has only a slight effect on the Barkhausen indications.

Recommendations

The author's recommendations are:

a. A field investigation should be conducted to assess the effectiveness of the Barkhausen method for measuring stresses on in-track rails at several sites.

b. The sites should be selected on the basis of maximum temperature change within a 6-month period.

c. Barkhausen measurements should be made at several locations around the cross section and at several locations along rails. The web may be the best location for measurements because this region is protected somewhat more than other locations and is relatively flat.

d. Probes should be modified to include a larger sensor (to average local variations) and a fixture should be used for precise relocation from time to time.

e. The hydraulic rail stretcher should be used to obtain calibration data at rail measurement locations.

Acknowledgments

The financial support of the Southern Pacific Transportation Company for part of the work summarized in this report is gratefully acknowledged. The most recent work was under the direction of W. D. Perry; he was assisted by F. A. Balter, T. C. Doss, and D. H. Heihn, all of Southwest Research Institute, San Antonio, Texas.

"The Application of a Nondestructive Evaluation Technique Utilizing the Phenomenon of Internal Friction for Detecting the Incipient Failure of Railroad Rails Caused by Residual Stress"

L. L. Yeager
Daedalean Associates, Inc.

Before we get into the actual application of residual stress, I will go through a little bit of the background on the internal friction.

Figure 1 summarizes the basics of the internal damping technique.

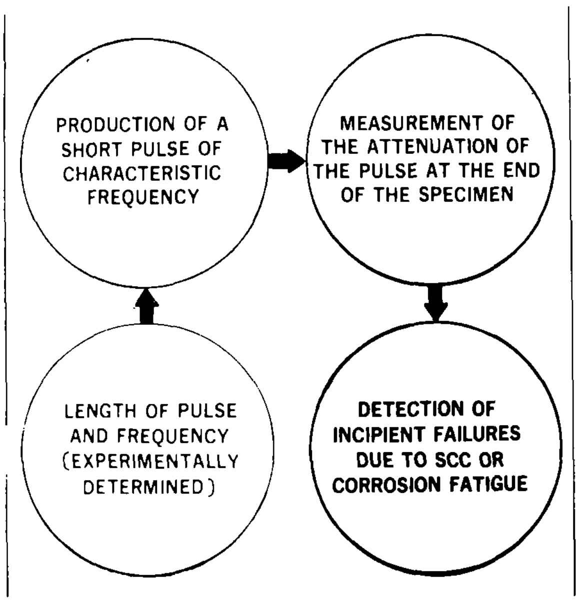

FIGURE 1. INTERNAL DAMPING TECHNIQUE

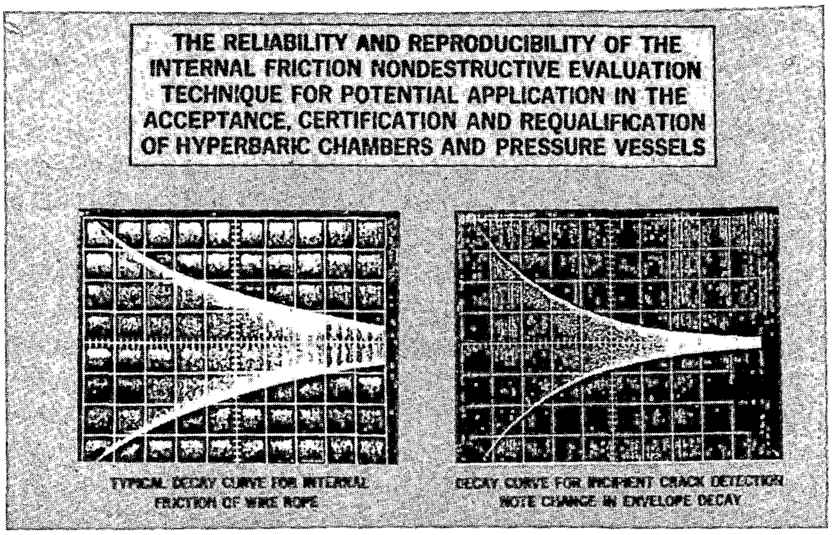

FIGURE 2. REPRESENTATIVE DAMPING DECAY CURVES INDICATING CHANGES IN INTERNAL FRICTION FOR INCIPIENT CRACK DETECTION

In figure 2 are shown two typical decay curves taken from the cathode-ray tube (CRT) of an oscilloscope. The left-hand picture shows a typical trace before a crack initiation. The right-hand picture shows a typical trace after crack initiation.

The actual measurements that have been taken on these pictures are the fundamental measurements used to determine the internal friction, or specific, damping capacity number (to be explained later), which is used in determining residual stress in materials. In this figure, it is important to note here the change between the two pictures.

The specific damping capacity measurement is taken from an input sinusoidal input to a specimen. In figure 3, we see a log decrement decay curve -- typical measurements that are made and include an amplitude measurement, A_O, taken at the initiation. Some amplitude, A_N, would be taken a number of decay cycles down the decay curve. The rest of the mathematics involved ΔW divided by W, which we are calling specific damping capacity and would be equal to $1 - e^{-2\alpha}$. The log decrement, α, would be defined as follows:

$$\alpha = \frac{1}{N} \ln \left(\frac{A_O}{A_N}\right).$$

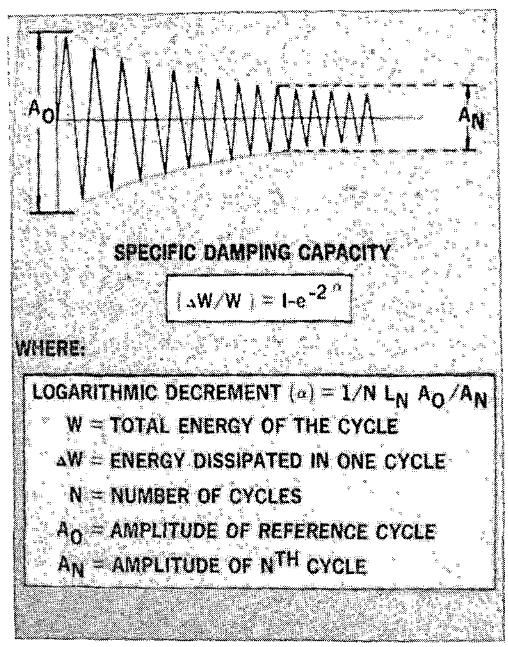

FIGURE 3. CALCULATION OF SPECIFIC DAMPING CAPACITY $(\frac{\Delta W}{W})$

$$\left[\frac{\Delta W}{W}\right]_{est.} = a(LC_N) + b$$

WHERE: $\left[\frac{\Delta W}{W}\right]$ = ESTIMATED SPECIFIC DAMPING CAPACITY

LC_N = NUMBER OF LOAD CYCLES

a&b = CONSTANTS OBTAINED FROM DATA

THE STANDARD ERROR OF ESTIMATE FOR $\frac{\Delta W}{W}$ AND LC_N:

$$S\left(\frac{\Delta W}{W} \cdot LC_N\right) = \left[\frac{\Sigma\left(\frac{\Delta W}{W} - \left[\frac{\Delta W}{W}\right]_{est.}\right)^2}{LC_N}\right]^{1/2}$$

WHERE: $S\left(\frac{\Delta W}{W} \cdot LC_N\right)$ = STANDARD ERROR OF ESTIMATE

$\frac{\Delta W}{W}$ = MEASURED SPECIFIC DAMPING CAPACITY

$\left[\frac{\Delta W}{W}\right]_{est.}$ = ESTIMATED SPECIFIC DAMPING CAPACITY

THE CONFIDENCE LIMITS ARE DEFINED AS:

$$\left[\frac{\Delta W}{W}\right]_{est.} \pm 3S\left(\frac{\Delta W}{W} \cdot LC_N\right)$$

WHERE: $3S\left(\frac{\Delta W}{W} \cdot LC_N\right)$ = 99.7% OF ALL MEASURED SPECIFIC DAMPING CAPACITY VALUES

FIGURE 4. CONFIDENCE LIMITS FOR NDE DATA

Other calculations are used for determining the confidence limits taken on the specific damping capacity measurements and are shown in figure 4. Some of the parameters of the test that are used are an estimated value, $\frac{\Delta W}{W}$, and confidence limits about that estimated value.

The internal friction damping method utilizes an experimentally determined pulse and a frequency to apply to a particular specimen. At this point, the specimen is insignificant.

The production of the short pulse is then made on the specimen at the characteristic frequency. The different instruments that are used in both inputting and outputting this particular pulse will be explained later. Then we measure the output pulse, measure the attenuation of that pulse at some location along the specimen, and use that attenuation to determine different types of failures; the failure may be some sort of environmentally assisted failure or some form of mechanical failure.

The associated equipment shown schematically in figure 5 includes, in the upper left-hand corner, a beat frequency oscillator, that, in turn, is attached to the frequency counter and some sort of a gating system to gate a signal into a specimen. In this particular case, there are a permanent

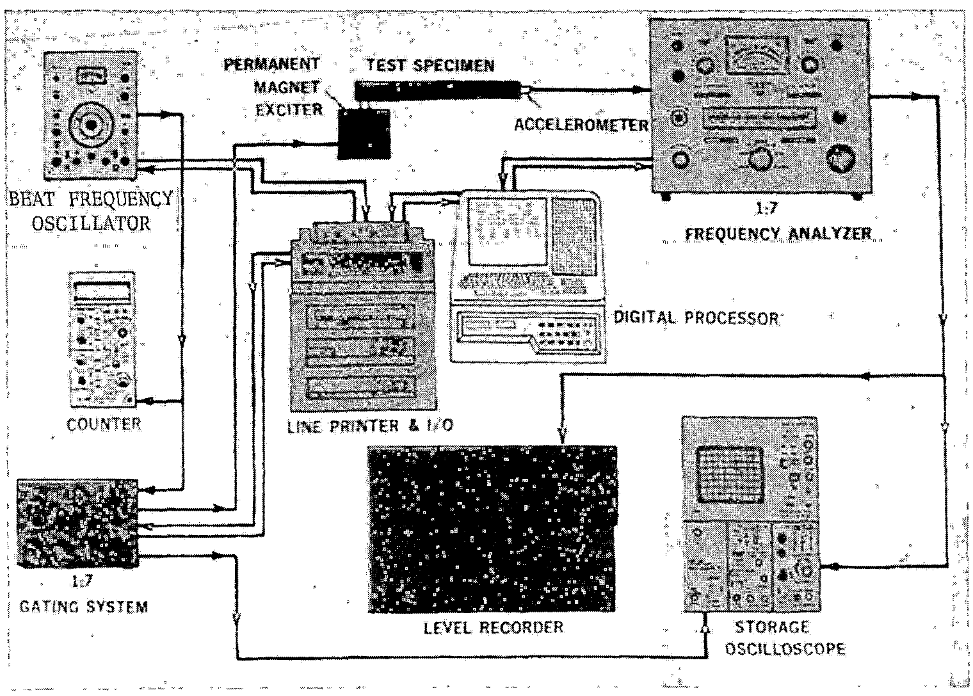

FIGURE 5. NDE SYSTEM CONFIGURATION UTILIZING A COMPUTER-ASSISTED DIGITAL PROCESSOR FOR PREDICTING INCIPIENT FAILURE IN U.S. NAVY COMPONENTS AND STRUCTURES

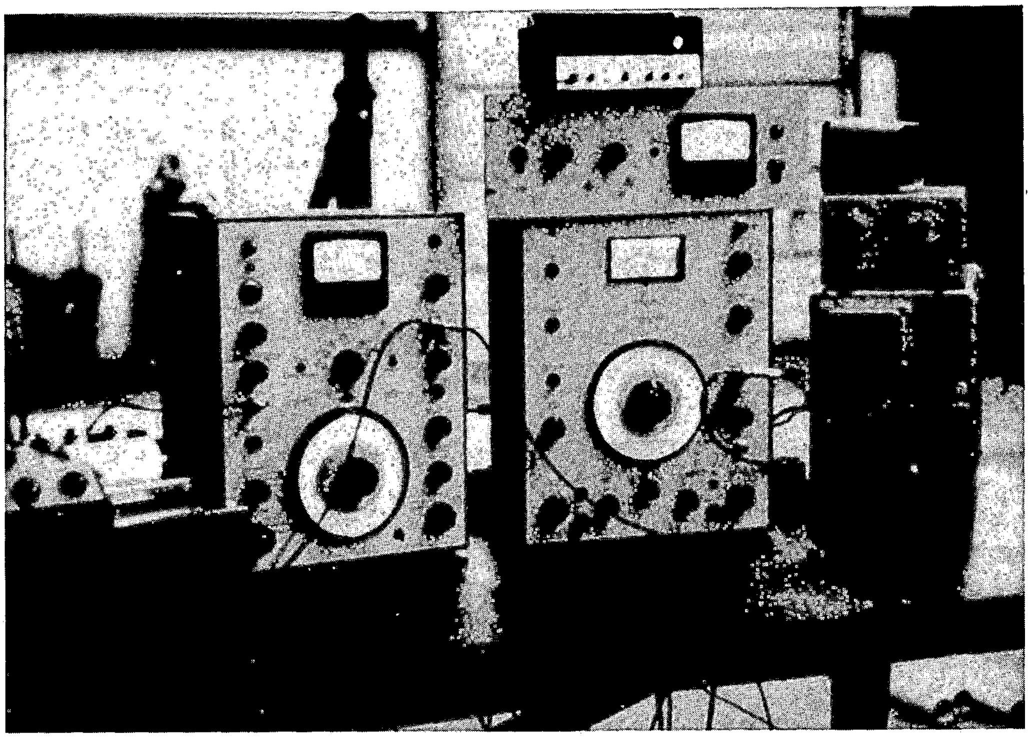

FIGURE 6. DIGITAL PROCESSOR AND I/O FOR AUTOMATING IFD-NDE DATA ACQUISITION AND ANALYSIS

magnet exciter attached to the test specimen, an accelerometer (in this particular case, a piezoelectric accelerometer) attached to the test specimen, and a frequency analyzer that is utilized for picking up the signal output from the specimen, amplifying the signal, and also for filtering out such unwanted transients as noise.

A digital processor also is included (see figure 6), and this would interface with the system in a way of making the entire system complete and automatic. Two other functional pieces (shown in figure 5) are a storage oscilloscope and a level recorder for use in outputting some form of hard copy output.

Note the log decremental decay on the storage oscilloscope screen (figure 7); the measurement shown would be reproduced for analysis at a later time. An additional method of outputting the data is shown in figure 8.

The digital processor (figure 6) enables you to perform a real-time analysis of your output signal using some fast fourier transforms for determining the specific damping capacity of your material. This is a laboratory equipment set and not necessarily something that would be taken to the field.

Figure 9 is a general view of the IFD-NDE hardware.

I will now cover a few of the different programs that we have gone through in developing this internal friction technique for applying it to a number of different failure mechanisms.

In figure 10, we are showing data from a bar specimen that was failed in flexure. The specimen was notched. The specific damping capacity data are shown exceeding the upper confidence limit, indicated by the darkened horizontal band. At this point in the test, the specific damping capacity number exceeded the confidence limit, thus indicating an incipent failure.

To define some of the parameters that we had for this particular test, we see in figure 11 the cross section of the bar specimen. We see the crack growing from the root of a notch and we see the change in the specific damping capacity as a function of the crack growth for this particular bar specimen.

Note that the change of the specific damping capacity is recorded as approximately 4, and near the earlier stages of the test where we had a 1,000th of an inch crack, it had increased to somewhere around 4.5 to 5. Then the specific damping capacity number was increasing from that point throughout the growth of the crack in the specimen.

Some of the other applications included in internal friction damping (IFD) background would be a scale model offshore structure. As shown in figures 12 and 13, we see the digital processing

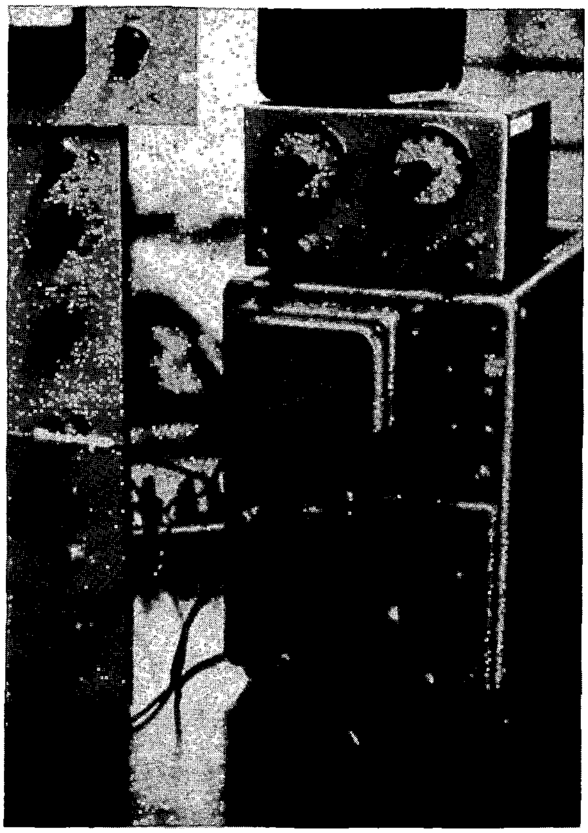

FIGURE 7. TYPICAL LOG DECREMENT SHOWN ON STORAGE OSCILLOSCOPE CRT

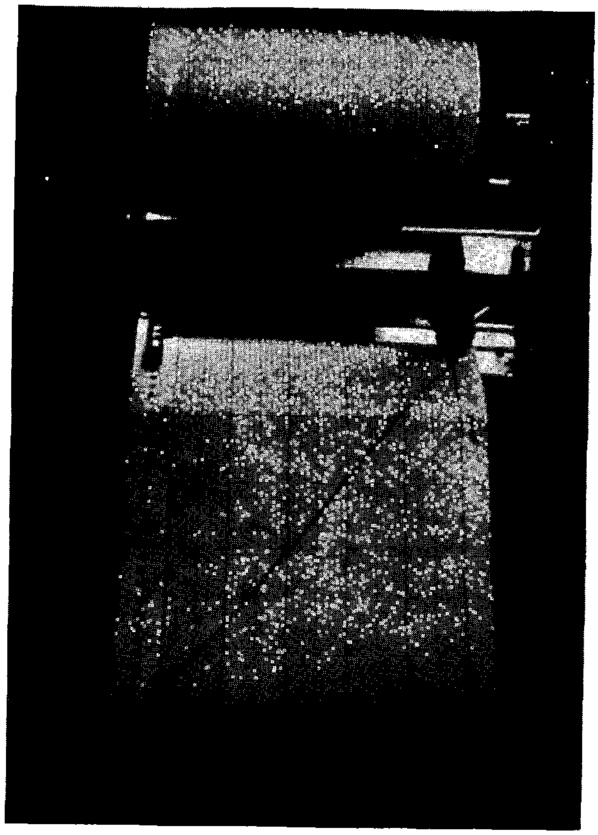

FIGURE 8. ALTERNATE METHOD OF OUTPUTTING HARD COPY DATA THROUGH USE OF LEVEL RECORDER

FIGURE 9. IFD-NDE HARDWARE

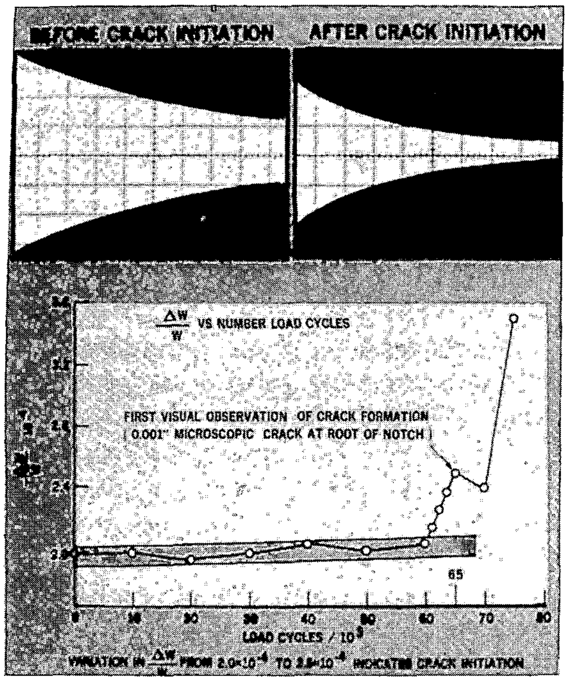

FIGURE 10. TYPICAL IFD-NDE DATA AND OSCILLOSCOPE OUTPUT ILLUSTRATING ORDER OF MAGNITUDE CHANGES EXPECTED

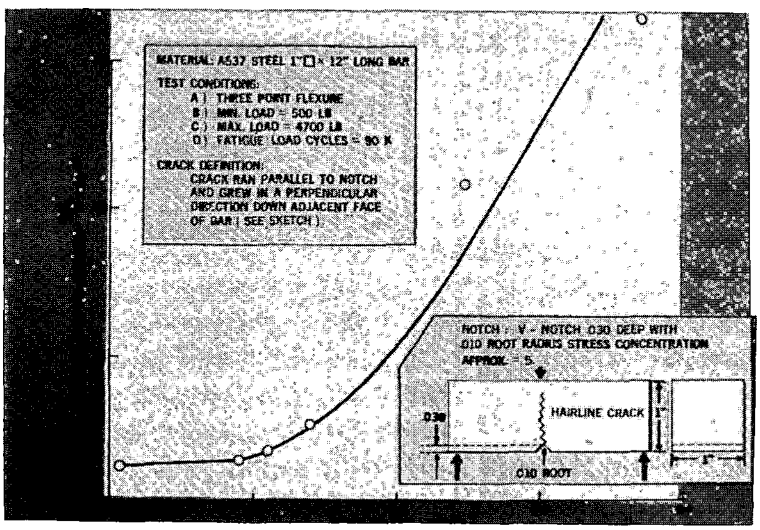

FIGURE 11. SPECIFIC DAMPING CAPACITY ($\frac{\Delta W}{W}$) VERSUS CRACK LENGTH (INCHES) FOR 1-INCH SQUARE x 12-INCH LENGTH BAR SPECIMEN FATIGUED IN THREE-POINT FLEXURE

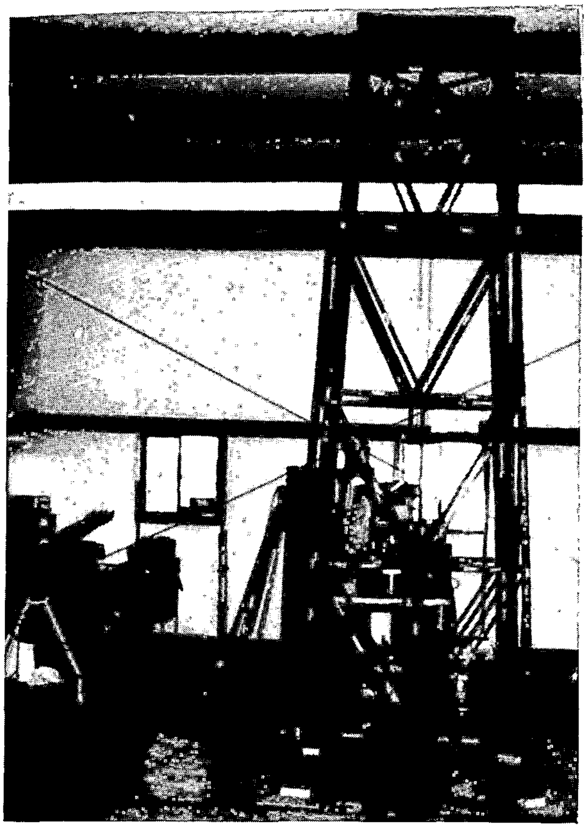

FIGURE 12. 1/14 SCALE OFFSHORE TOWER

FIGURE 13: ILLUSTRATION OF DIGITAL PROCESSOR AS APPLIED TO OFFSHORE TOWER MODEL

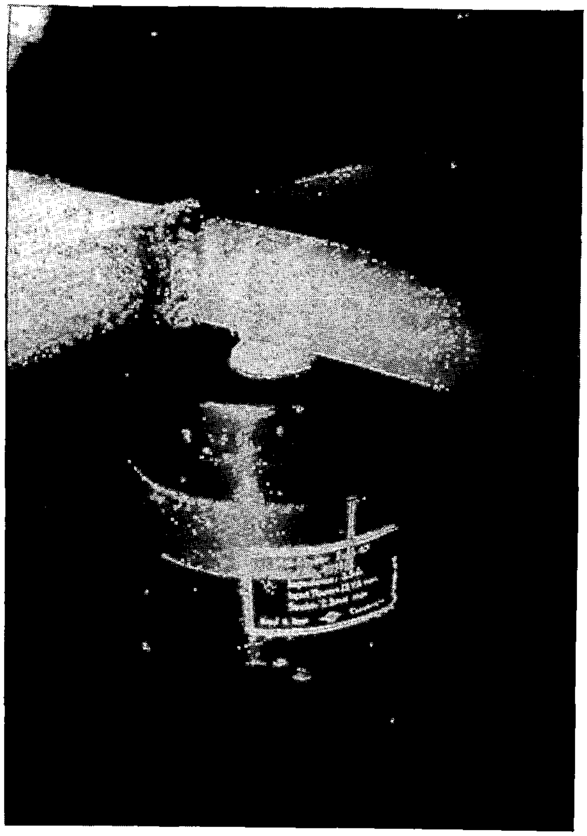

FIGURE 14. INPUT MINISHAKER

equipment applied to this structure. The input device (the actual vibration of this specimen was achieved through a permanent magnet vibrator) is shown in figure 14.

The particular frequency of test is determined from the particular mode of resonance we would care to look at and use for the prediction of failure.

The piezoelectric accelerometer (figure 15), here attached with a permanent magnet, is just stuck on the side of the tower. No particular preparation was made for applying the accelerometer to the tower. The accelerometer is used in accepting data from the tower and putting the data into the frequency analyzer (possibly a frequency spectrum analyzer) and/or the digital equipment for analysis.

The output data again being brought out of the tower would be fed into the digital processor to be analyzed. The frequency, the signal strength coming out, and the attenuation of the signal coming out would be analyzed and a determination of the type of failure would be made.

The frequency domain was analyzed for the purpose of determining frequencies of responses at particular frequencies that would determine whether a bar was failing because of an environmentally assisted failure mechanism or because

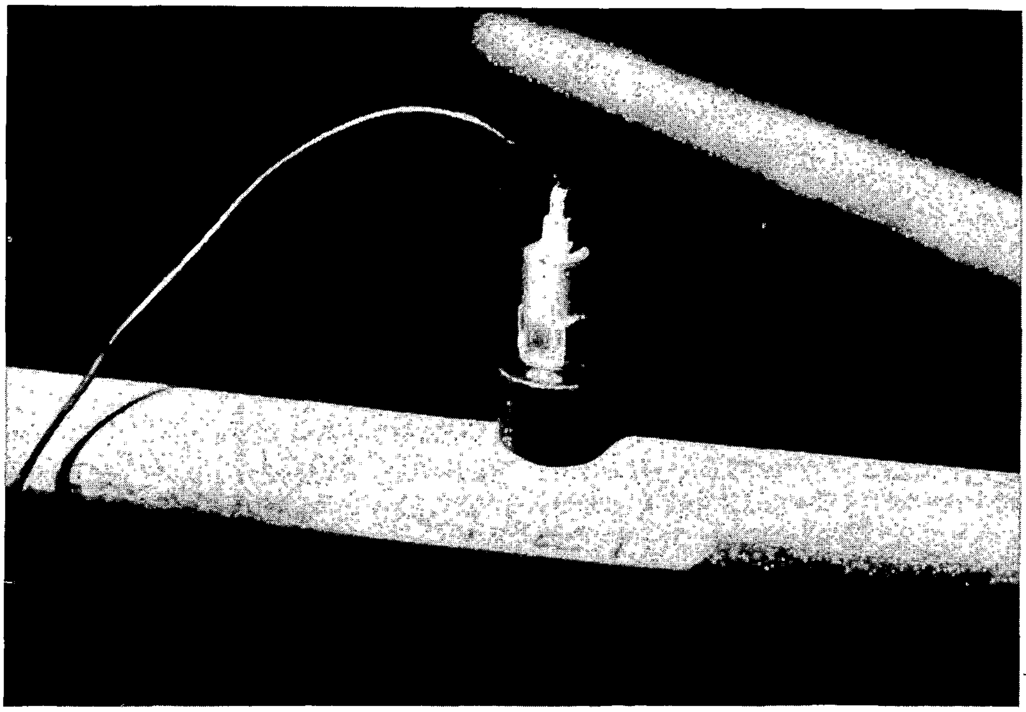

FIGURE 15. MAGNETICALLY ATTACHED OUTPUT ACCELEROMETER

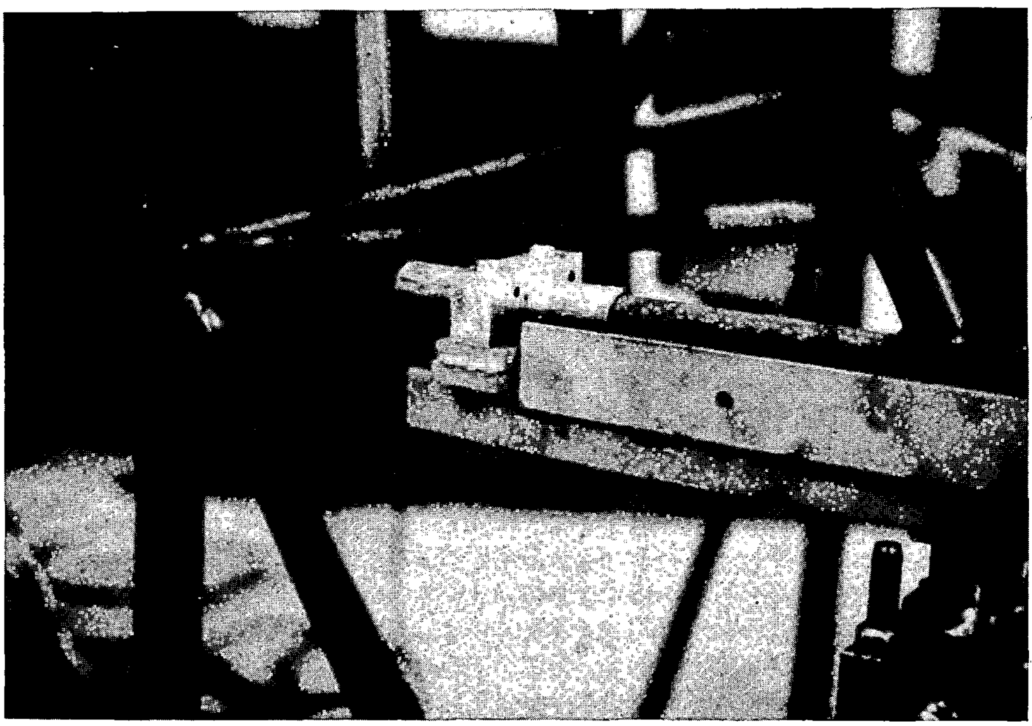

FIGURE 16. ELECTROMECHANICAL FATIGUE APPARATUS

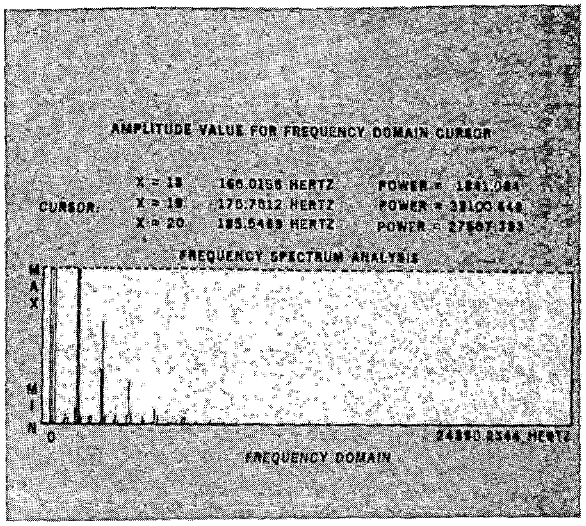

FIGURE 17. OUTPUT FROM FAST FOURIER TRANSFORM PROGRAM SHOWING AMPLITUDE OF THE RESPONSE AS A FUNCTION OF THE FREQUENCY SPECTRUM

MEMBER 30-31 FAILURE (LOCATION OF FAILURE-MIDPOINT MEMBER 30-31)						
INPUT LOCATION	PICKUP LOCATION	FREQ	CYCLES			FAILURE
			0	3000	6000	9900
			SPECIFIC DAMPING CAPACITY			
MDPT MEMBER 24-31	JOINT 30	2325	19.9	21.9	24.7	27.9
MDPT MEMBER 30-39	MDPT MEMBER 30-31	2263	12.3	15.1	16.9	55.9
MDPT MEMBER 30-39	JOINT 30	671	17.8		23.8	17.5
JOINT 30	MDPT MEMBER 30-31	499	11.3	12.8	13.0	12.7
JOINT 30	MDPT MEMBER 30-31 (ACCEL. PARA. TO MEMBER)	2027	40.3	48.9	47.6	53.5
MDPT MEMBER 30-31	JOINT 30	2506	13.5	22.2	14.9	33.1
MDPT MEMBER 30-31	JOINT 30	2215	15.6	19.4	13.8	64.8

FIGURE 18. TYPICAL OUTPUT VALUES OF THE SPECIFIC DAMPING CAPACITY LISTED FOR A MEMBER AND A JOINT OF THE SCALE MODEL OFFSHORE PLATFORM FOR THE VARIOUS NUMBER OF CYCLIC LOAD CYCLES

of a stress corrosion, cracking corrosion, fatigue, or other failure mechanism (such as just pure torsional fatigue or pure flexural fatigue). The fatigue apparatus is illustrated in figure 16. It is intended to simulate the actual failure mechanism experienced by the offshore tower during its load cycle history.

The frequency domain is searched for responses, with typical specimens giving different responses at different frequencies. This becomes evident in figure 17.

Notice in figure 18 the lower two sets of data wherein we have taken data at two different

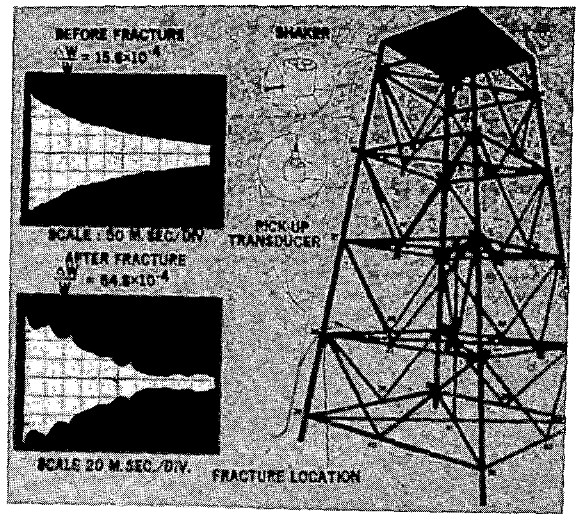

FIGURE 19. IFD DATA FOR TOWER

frequencies -- 2,200 hertz and 2,500 hertz. The specific damping capacity remains relatively constant at both of these frequencies. However, as the member fails, as shown on the far right, the change at 2,500 cycles is one-half of the change that we see at 2,200 cycles. Again, the particular type of failure mechanism would have differing impacts, dependent on the frequency of measurements.

Figure 19 shows the difference in the output oscilloscope pictures taken at that point in the failure of the tower, the lower picture showing the specific damping capacity at about 64×10^{-4} and the upper picture showing it at about 15×10^{-4}. Now, this fourfold increase was actually generated *before a 1,000th of an inch crack* was picked up on the particular member that we were failing in this structure.

The offshore structure had numerous input and output locations. The data that we generated were for eight input locations with eight output locations.

We are doing some work in the area of determining differing types of failure in drillstring pipe for Dr. Reeber of the U.S. Department of Energy. This work involves our applying the internal friction technique to drillstring pipe. These pipes are approximately 32 feet long, with an outside diameter of 4½ inches and tool-joint ends that are approximately 6½ inches in diameter. The tube of the pipe and the tool-joint ends are of differing strength materials. The tool-joint ends have been hardened. The field application has to withstand differing environmental conditions. We found the technique to be very sensitive even in extremes of hot, cold, and bad weather, etc. In this case, the input frequency is achieved through the discrete contact of the drillstring pipe with a permanent magnet vibrator, and the output is picked up through, again, the piezoelectric accelerometer attached with a permanent magnet (see figure 20). The pipes are vibrated approximately 500 cycles per second. In figure 21, an actual field pickup is being placed on the pipe.

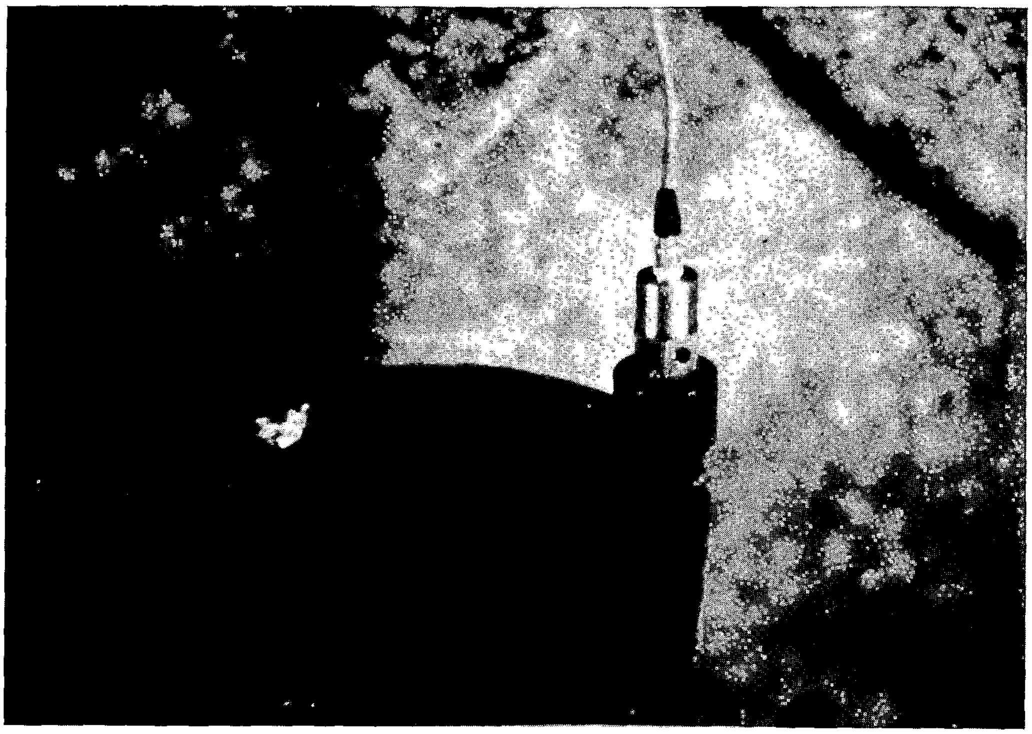

FIGURE 20. LABORATORY OUTPUT DEVICE FOR DRILLSTRING PIPE PROGRAM

FIGURE 21. OUTPUT DEVICE FOR DRILLSTRING PIPE PROGRAM AS USED IN THE FIELD

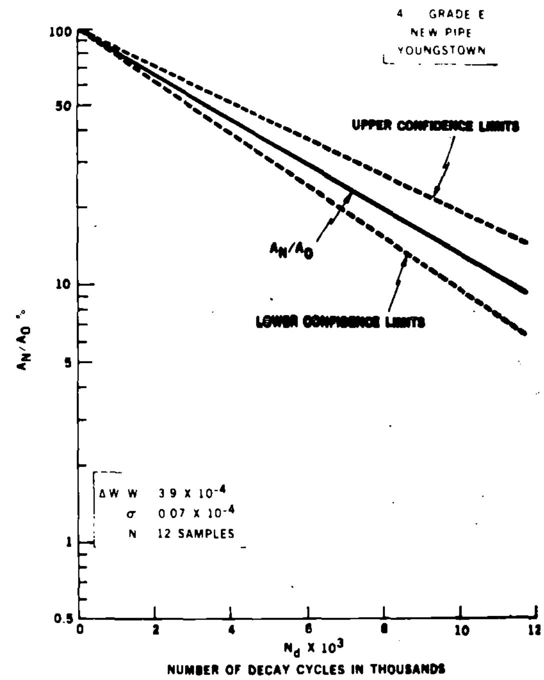

FIGURE 22. A_N/A_O VERSUS NUMBER OF DECAY CYCLES SHOWING CONFIDENCE LIMITS FOR NEW PIPES

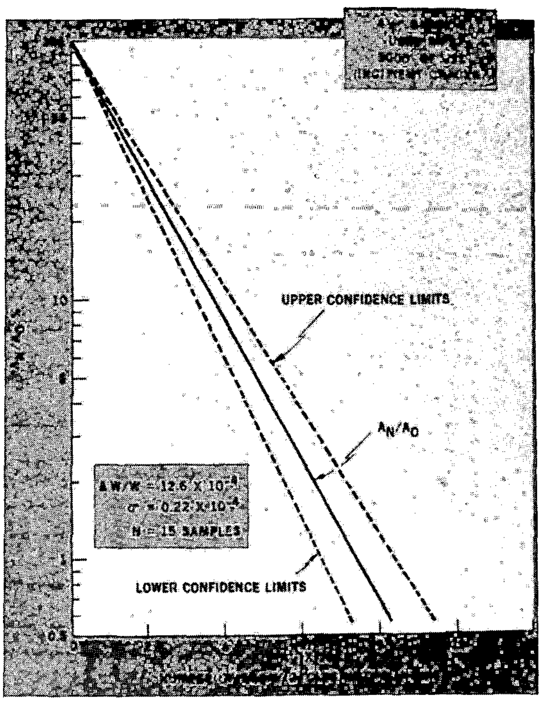

FIGURE 23. A_N/A_O VERSUS NUMBER OF DECAY CYCLES SHOWING CONFIDENCE LIMITS FOR USED PIPES (5,000 FEET OF USE)

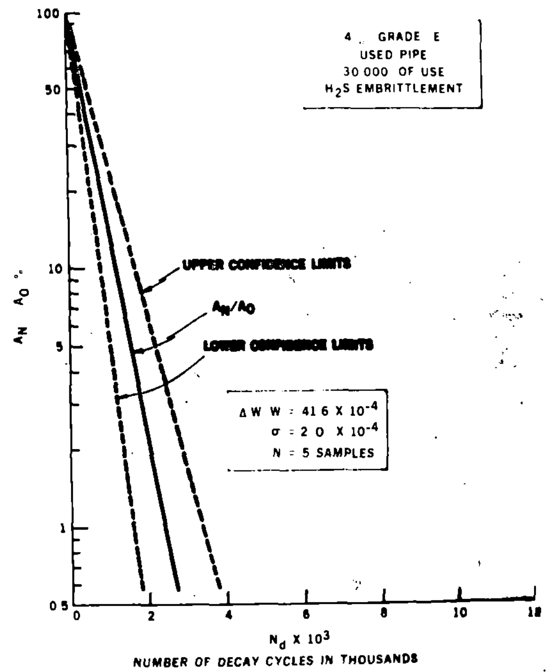

FIGURE 24. A_N/A_O VERSUS NUMBER OF DECAY CYCLES SHOWING CONFIDENCE LIMITS FOR USED PIPES (30,000 FEET OF USE)

Differing types of failure mechanisms are found in these particular pipes; some of them are environmental and some of them are purely mechanical.

Hydrogen sulfide is an environmental hazard that the drilling industry comes up against in drilling through H_2S gas. It tends to embrittle the pipe, causing a brittle fracture in the pipe.

The internal friction technique is sensitive to this environmental parameter. The actual embrittlement of the pipe is picked up in a gross form throughout the length of the pipe, with the internal friction technique showing a very marked change in the response of the pipe.

In figures 22 through 25, we see the data that were generated. The important thing to note here would be the different types of failure mechanisms that have been measured and the different responses to these differing failure mechanisms.

In figure 22, we show data for a new pipe. The slope of this line is the important thing to be looking for. In figure 23, we see for a slightly used pipe (in the terms of use out in the oil field, this pipe had very little usage) a very marked change in the slope of the $\frac{\Delta W}{W}$ value. We see again the confidence limits about this data. Figure 24 shows comparable data for other used pipe.

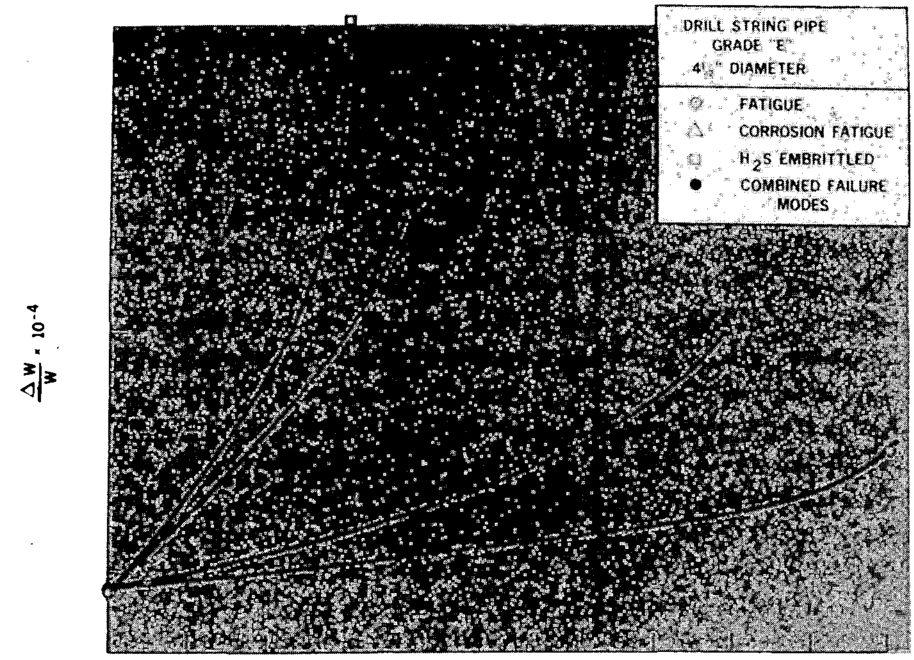

FIGURE 25. FEET OF USE VERSUS AVERAGE SPECIFIC DAMPING CAPACITY FOR ALL GROUPS MEASURED

The internal friction technique showing a response to these different failure mechanisms is plotted out on a form that shows different failure mechanisms together in the same specific damping capacity plots (figure 25).

All pipes start out at approximately the same point, these points being average values.

The internal friction damping of these pipes, changes significantly for different failure mechanisms. The particular failure mechanism of hydrogen sulfide in figure 25 is shown as the most severe.

Illustrated in figure 25 is the failure mechanism versus some length of use of the pipe and in taking a measurement, what we are showing here is that one does not necessarily have to have a baseline. One does not necessarily have to have the complete history of a pipe to go out and pick up a particular failure mechanism.

The internal friction damping technique is more of a comparative type of technique wherein we are looking at different points in time and we are assessing the specimen for different points in time and the specific damping capacity number would not necessarily have to have been followed through from the inception of use of the specimen.

What is evident above is a case of failure of the drillstring pipe. One could go out, take a measurement on that particular pipe, come back at a later point in time (so many more feet of use), take another measurement on that particular pipe, and then assess the location of that pipe in the history of its use; whether or not it is at 20,000 feet, 30,000 feet, or 50,000 feet would then become basically insignificant. But you would tell how fast you were approaching failure with that particular pipe.

Again, we have some combined failure modes. It would not necessarily have to be purely, say, a torsional fatigue or a bending fatigue or a hydrogen sulfide pipe.

One of the important things here that we picked up is that a complete history or a complete background history of the pipe is important -- but not completely necessary.

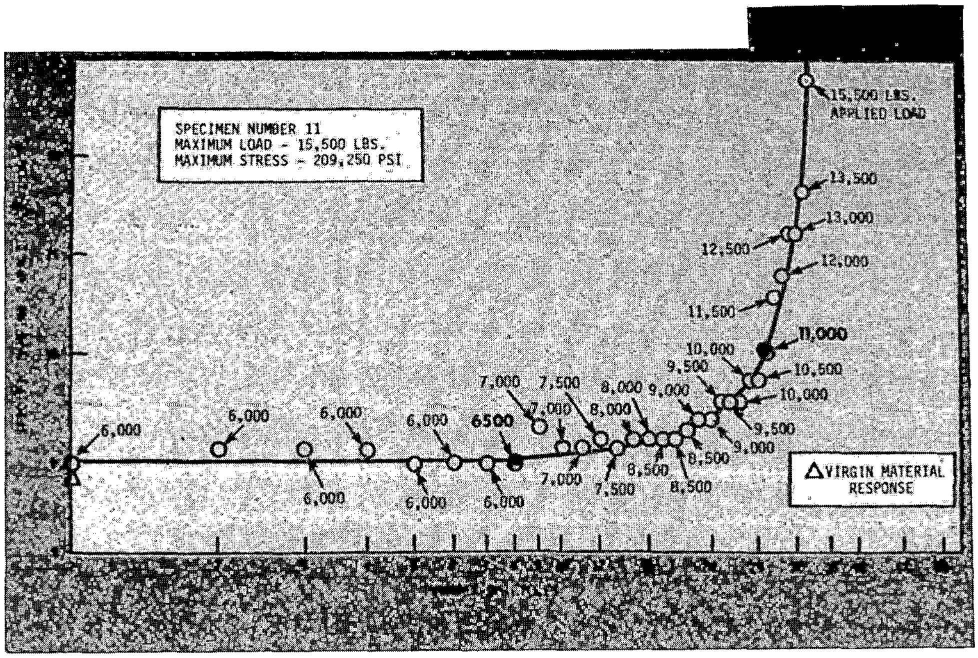

FIGURE 26. CHANGES IN SPECIFIC DAMPING CAPACITY AS A FUNCTION OF LOADING CYCLES OF INCREASING APPLIED LOADS FOR A WELDED SPECIMEN IN THREE-POINT LOADING

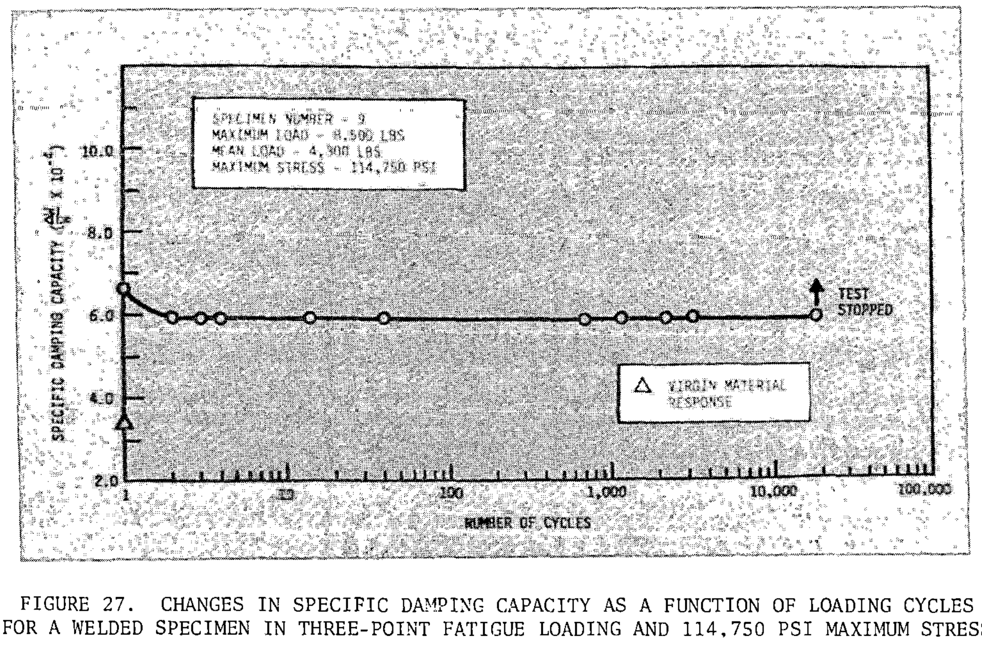

FIGURE 27. CHANGES IN SPECIFIC DAMPING CAPACITY AS A FUNCTION OF LOADING CYCLES FOR A WELDED SPECIMEN IN THREE-POINT FATIGUE LOADING AND 114,750 PSI MAXIMUM STRESS

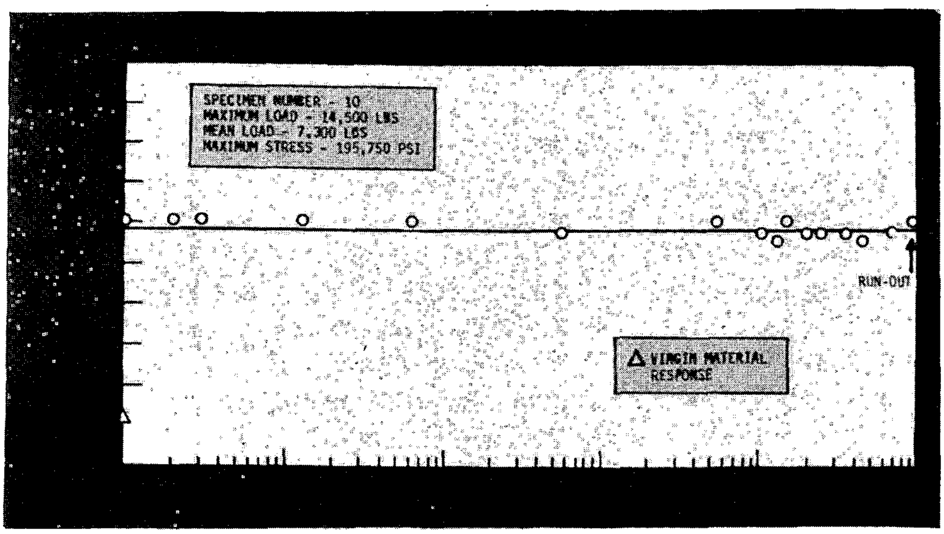

FIGURE 28. CHANGES IN SPECIFIC DAMPING CAPACITY AS A FUNCTION OF LOADING CYCLES FOR A WELDING SPECIMEN IN THREE-POINT FATIGUE LOADING AND 195,750 PSI MAXIMUM STRESS

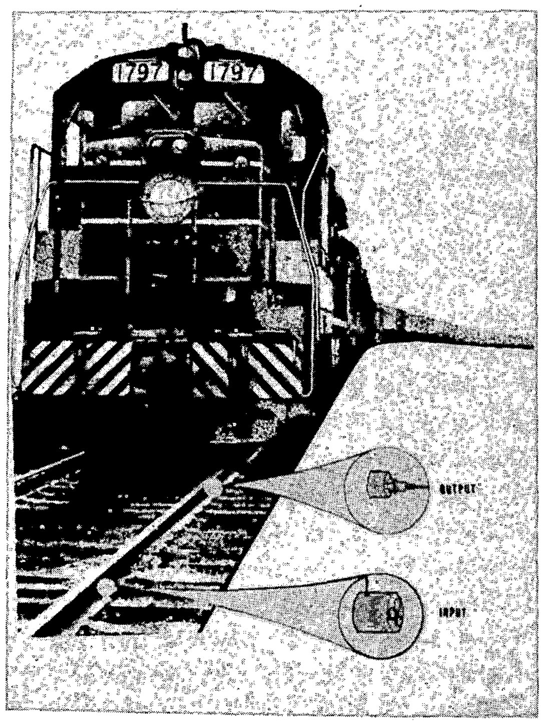

FIGURE 29. APPLICATION OF IFD TECHNIQUE FOR MEASURING RESIDUAL STRESS IN STEEL RAIL

The bulk of the information that I am trying to convey is the measurements of residual stress. In figure 26, we see a basic curve developed for differing stress levels and we see specific damping capacity measurements on the left-hand side for differing numbers of cycles applied. We are showing the residual stress phenomenon here for 1-inch-square bar specimens. We see a specific damping capacity number generated for an individual bar specimen. In figure 27, we see the number developed as approximately 6. In going back to the master curve that we developed, we follow 6 across and we see the number of applied load to be approximately 8,500 pounds.

Then in going back to our measured bar, we find that the actual applied load was, indeed, 8,500 pounds. This would indicate that the specific damping capacity or internal friction damping number may be used to determine the residual stress in materials.

We again applied this at a higher load. In figure 28, we came up with the number 15. With that number, when applied back to the actual master curve, we find a variation of a few percentage points away from the actual data taken.

This application of the residual stress to the specimens provides the incentive for using this particular technique as a measure of residual stress in steel rail specimens, as illustrated in figure 29.

"The Effect of Axial Load on the Flexural Dynamic Response of a Rail"*

Richard Lusignea
Fred Prahl
Ken Maser

Foster-Miller Associates

Introduction

The axial force in continuously welded track that develops as a result of temperature changes can have a considerable effect on track safety. High compressive forces can increase track deflections due to moving vehicle loads and ultimately cause track buckling. Consequently, there is considerable interest within the rail industry in developing a simple instrument for rapidly and nondestructively evaluating the axial stress in track.

Among the techniques that have been considered for performing such are ultrasonics (measuring the effect of axial load on shear and dilatational wave speeds), X-ray diffraction, and resonant frequency/phase velocity measurements.

It is the last-named technique that is considered in this paper. A transversely vibrating beam decreases in resonant frequency with increasing axial force. By measuring the resonant frequency of a beam and comparing it to a reference value, one can determine the axial force in the beam. The same is true for any structure where an in-plane load is coupled with a transverse deflection. In fact, the resonant frequency method is a standard nondestructive technique for determining buckling loads in structural components.

Railroad track can vibrate in a number of transverse modes. From a rail/vehicle dynamics point of view, the mode of interest is the rail vibrating as a continuous beam on an elastic foundation. Here, the fundamental resonant frequencies are low ($\leq$ 100 hertz). They depend strongly on the properties of the fastener, tie, ballast, and subgrade, and the fundamental mode does not involve flexure of the track. This mode, therefore, is not useful for an axial stress measurement.

The higher the mode, the less sensitive are the resonant frequencies to the properties of the fastener, tie, ballast, and subgrade. Thus, the higher frequency range (500-20,000 hertz) may be useful for axial stress evaluation. In this range, however, the wavelengths are still long enough to make the method less sensitive to small flaws or changes in metal grain structure than either ultrasonic waves or X-ray diffraction techniques.

Dynamic Behavior of a Finite Rail

As a first step towards determining the effect of axial load on the dynamic response of a rail, a program was carried out to evaluate the resonant frequencies of an unloaded 10-foot section of 130-pound rail, both experimentally and analytically. It should be noted that field measurements on in-situ rail will probably involve measuring the phase velocity of flexural waves rather than resonant frequencies, because continuously welded rail approximates an infinite rail that supports only traveling waves. However, resonances of a finite rail and the phase velocity of an infinite rail are intimately connected in that resonances are essentially standing waves made up of traveling waves reflecting back and forth between the ends of the rail. The particular traveling waves that reinforce each other to form the standing waves or resonances have wavelengths that are integral multiples of the rail length. It was feasible, therefore, to use a finite rail for the first phase of this program.

Theory. Previous work [1] has indicated that, for frequencies above 1,000 hertz, the effect of rail fasteners, ties, and ballast on the vibration of a rail is very small. For this reason, our analysis and measurement program concentrated on the rail's dynamic behavior in the 1,000-10,000 hertz range. Because wavelengths in this frequency range are not large compared with the rail's cross-sectional dimensions, Bernouilli-Euler beam theory is not accurate enough. A better approximation is Timoshenko beam theory, which includes the effects of shear and rotary inertia, although it is still a one-dimensional model for a three-dimensional elastic body.

*Presentation at conference delivered by Ken Maser.

Consider a beam with area A; second moment of the cross-sectional area about the neutral axis, I; Young's tension modulus E; shear modulus G; and density ρ. The equations of motion for the Timoshenko theory [2] are

$$a_1^2 \left(\frac{\partial^2 \eta}{\partial x^2} - \frac{\partial \phi}{\partial x}\right) = \frac{\partial^2 \eta}{\partial t^2}$$

$$a_2^2 \frac{\partial^2 \phi}{\partial x^2} + a_1^2 k_o^2 \left(\frac{\partial \eta}{\partial x} - \phi\right) = \frac{\partial^2 \phi}{\partial t^2}, \quad (1)$$

where $a_1^2 = \frac{\kappa G}{\rho}$,

$a_2^2 = \frac{E}{\rho}$,

$k_o^2 = \frac{A}{I}$,

κ = a numerical factor that depends on the beam's cross-sectional shape,

η = the transverse displacement, and

ϕ = the rotation.

This set of equations leads to the following dispersion relation:

$$\omega^4 - \omega^2 \left[a_1^2 \left(k^2 + k_o^2\right) + a_2^2 k^2\right] + a_1^2 a_2^2 k^4 = 0 \quad (2)$$

For an infinite beam, $k = 2\pi/\lambda$, the wave number. For a simply supported finite beam, $k_n = \frac{n\pi}{L}$, where L is the beam length and n is the mode number. These are the eigenvalues of the finite beam problem. Note that a plot of ω versus k from equation (2) for the infinite beam would result in continuous lines, while ω versus k_n for the finite beam would produce discrete points that lie on the same lines. Because the dispersion relation is a quadratic in $\omega^2(k^2)$, it has two distinct branches. The phase velocities corresponding to these two branches are shown plotted as a function of wave number in figure 1 and as a function of frequency in figure 2. Note that there is a cutoff frequency below which only mode 1 exists.

An exact analysis of flexural waves in beams using the full three-dimensional theory of elasticity has been found only for circular rods. The mathematics are too complex to allow an exact solution even for a uniform beam with a rectangular cross section. It is worthwhile to examine the phase velocity plot for circular rods, shown in figure 3 [3], [4] because we expect the rail to show somewhat similar behavior. Shown for comparison are the same curves for Bernouilli-Euler theory and Timoshenko theory. Although Timoshenko theory accurately predicts the first propagation mode, it does not predict higher modes accurately; it only predicts one higher mode when in fact there are an infinite number of which two are shown as solid lines in figure 3. Notice also that Timoshenko predicts that the higher mode approaches the longitudinal wave velocity, $\sqrt{E/\rho}$, assymtotically, while exact theory predicts that the shear wave velocity, $\sqrt{G/\rho}$, is the limit. Because of the frequency range in which our measurements on the finite rail were made, we expect to find the type of behavior shown in figure 3. It should also be noted that, because there are many propagation modes that combine at a given frequency or wave number, the displacement pattern can become very complex,

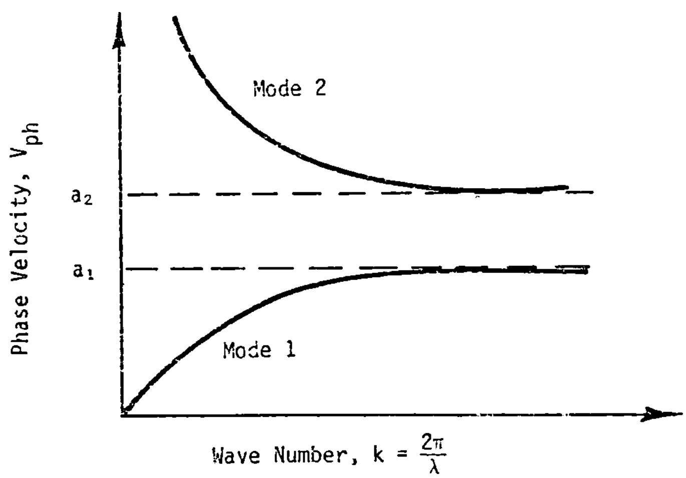

FIGURE 1. PHASE VELOCITIES OF SINUSOIDAL WAVES ON A TIMOSHENKO BEAM AS A FUNCTION OF WAVE NUMBER

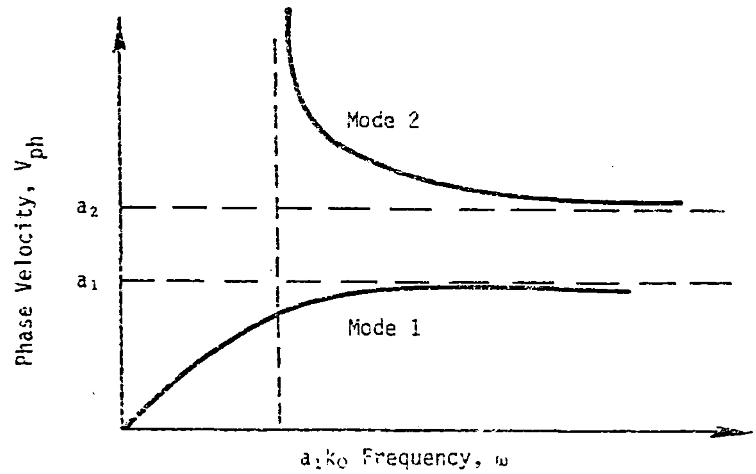

FIGURE 2. PHASE VELOCITIES OF SINUSOIDAL WAVES ON A TIMOSHENKO BEAM AS A FUNCTION OF FREQUENCY

involving translation, rotation, and distortion of the rail cross section. Such behavior was observed and is discussed below.

Measurements. Frequency response measurements were made on the test rail with the following objectives:

a. Determine what effect the length of the test rail has on resonant frequencies (free-free beam harmonics), and how to extrapolate test results on a finite rail to predict behavior for an "infinite" continuously welded rail.

b. Define other "internal modes" of vibration that may show changes in resonant frequency dependent on axial force.

The measurements were carried out on a 130-pounds-per-yard P.S. (Pennsylvania Section) rail, 10 feet in length. The rail was supported by 3/16-inch-thick neoprene pads placed on a work bench at Foster-Miller's shop facility. A Wilcoxon model F7/Z7 shaker impedance head was used to excite the rail and to make resonance and mode shape measurements. A Wavetek sweep frequency generator was used to drive the piezoelectric shaker. A Wilcoxon model 165 accelerometer was used to make the necessary mode shape measurements.

Figure 4 shows the setup used for resonant frequency measurements. The frequency range, 1-10 kilohertz, was swept very slowly (approximately 20 minutes for a complete sweep) with the shaker impedance head mounted at each of five locations at the center of the rail, as shown in figure 5.

Figures 6 and 7 show the responses for the head vertical and head horizontal points only.

The resonant frequency plots are more precisely dynamic compliance plots, in that the graphs show displacement divided by force as a function of frequency. Peaks on the graphs indicate resonances where the structure vibrates with relatively large amplitude and small force. The amplitude of vibration is measured indirectly by double integration of the acceleration signal from the impedance head. The force is measured by a piezoelectric force transducer in the impedance head and is of the order 0.01 to 1 pound.

The next step in the laboratory tests was to determine mode shapes at the observed resonant frequencies.

The mode shape describes how the structure vibrates when driven at a resonant frequency. It shows points of maximum displacement and points of no displacement (nodes). When a pure mode is excited, all points on the structure that are not

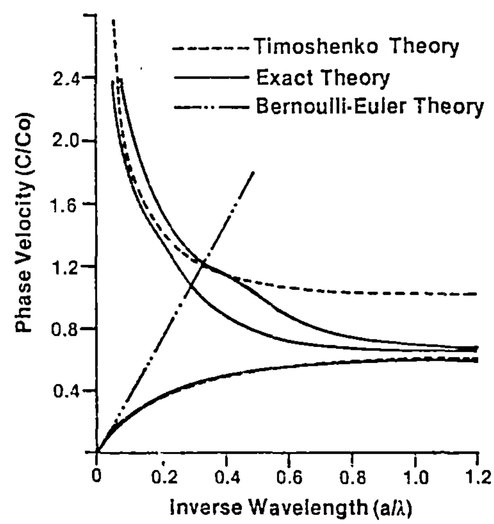

FIGURE 3. PHASE VELOCITY CURVES FOR FLEXURAL ELASTIC WAVES IN A SOLID CIRCULAR CYLINDER OF RADIUS a (from Y. C. Fung, Foundations of Solid Mechanics, Englewood Cliffs, New Jersey: Prentice-Hall, Inc., 1965)

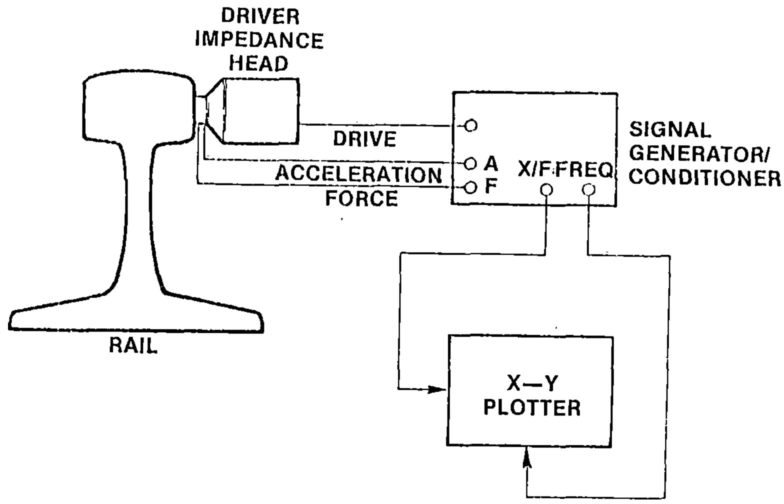

FIGURE 4. FREQUENCY RESPONSE MEASUREMENT SETUP

nodes are either in phase with the driving point or 180 degrees out of phase. Mode shapes were determined both longitudinally and around the cross section at the driving point.

Figure 8 shows the setup for making longitudinal mode shape measurements. The resonant frequency is found, and then the roving accelerometer is moved down the rail away from the driving point. The value of A_R/A_D (A_R = acceleration of roving accelerometer, A_D = acceleration at the driving point) is plotted as a function of position of the roving accelerometer, and the phase relationship between A_R and A_D is determined by monitoring the two on an oscilloscope. As the rail was excited at the center, we observed only the odd-numbered modes; the even modes of a free-free beam have a node at the center (see figure 9). Typical reduced data for representative mode shapes with horizontal and vertical excitation are shown in figures 10 and 11.

Figure 12 shows the setup for making cross-sectional mode shape measurements. Instead of A_R/A_D being plotted directly, the two were tabulated for eight points around the cross section. Figure 13 shows how a mode shape is plotted from such a table. These shapes (shown in figure 14) can be described as follows:

a. Horizontal Excitation, Head and Web:

(1) H_1 and H_2 - Flexure and torsion of the rail combined with static deformation of the cross section.

(2) H_3 - Head and foot act as independent beams coupled by the bending stiffness of the web.

(3) W_1 - Bowing of the web.

b. Vertical Excitation, Head and Foot:

(1) V_1 - Pure rail flexure

(2) V_2 - Foot behaves as a plate driven at the center.

(3) V_3 - Head and foot act as independent beams coupled by the vertical stiffness of the web.

(4) F_1 - Foot behaves as a long plate driven at one edge and built in at the other.

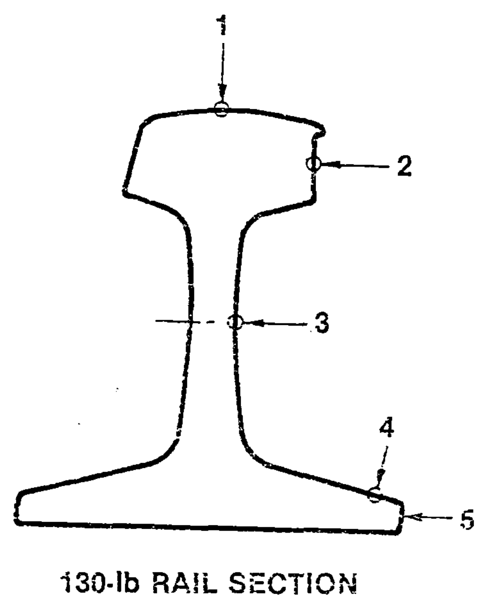

FIGURE 5. LOCATIONS FOR IMPEDANCE HEAD MOUNTING

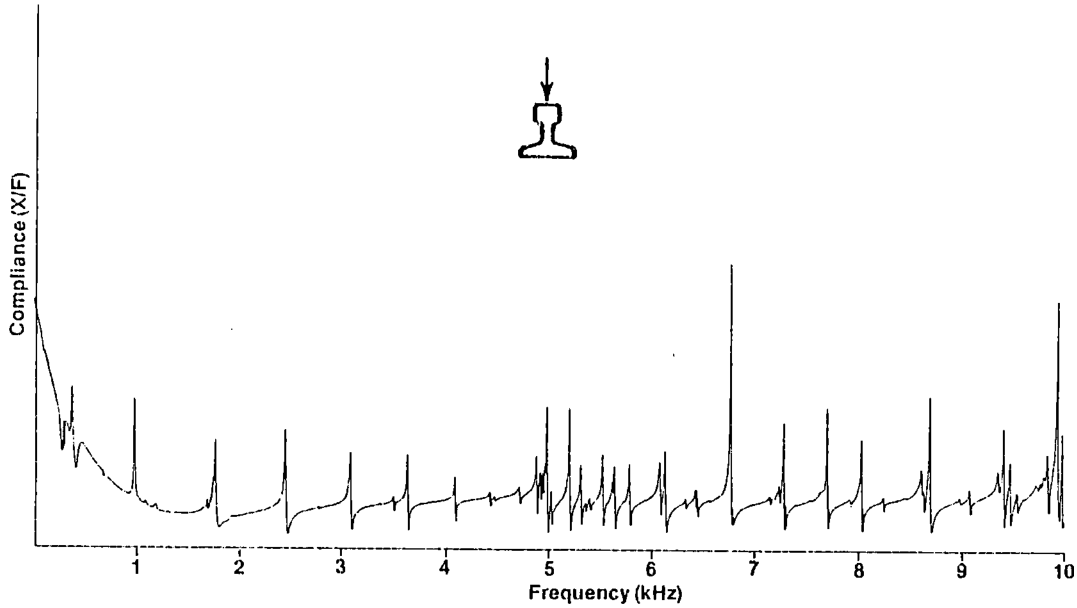

FIGURE 6. FREQUENCY RESPONSE OF TEST RAIL:
VERTICAL EXCITATION OF RAIL HEAD

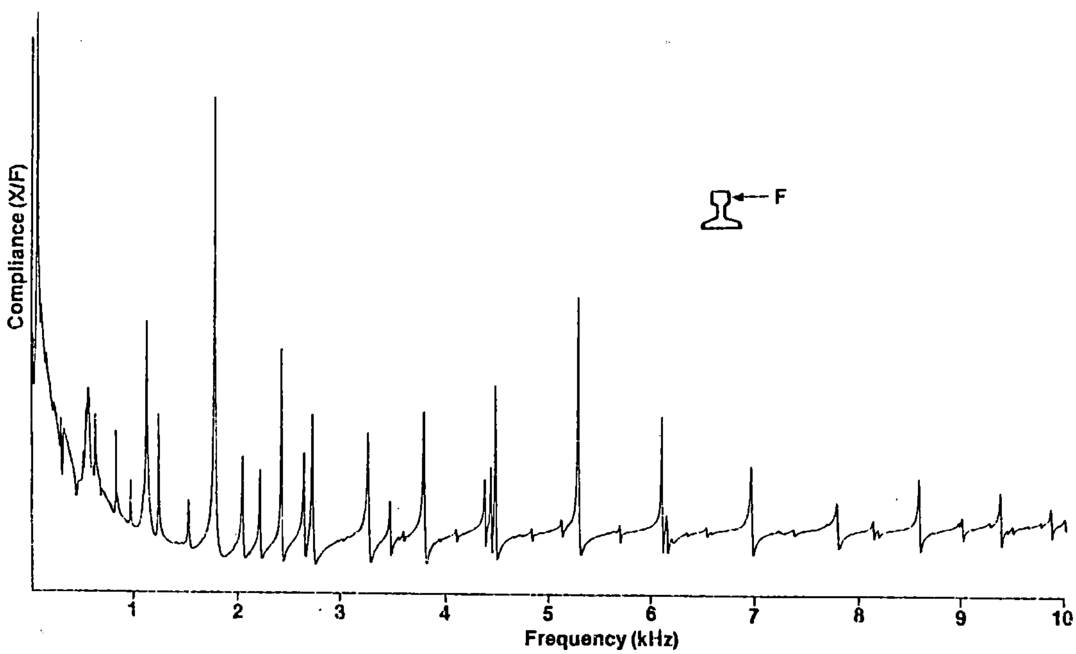

FIGURE 7. FREQUENCY RESPONSE OF TEST RAIL:
HORIZONTAL EXCITATION OF RAIL HEAD

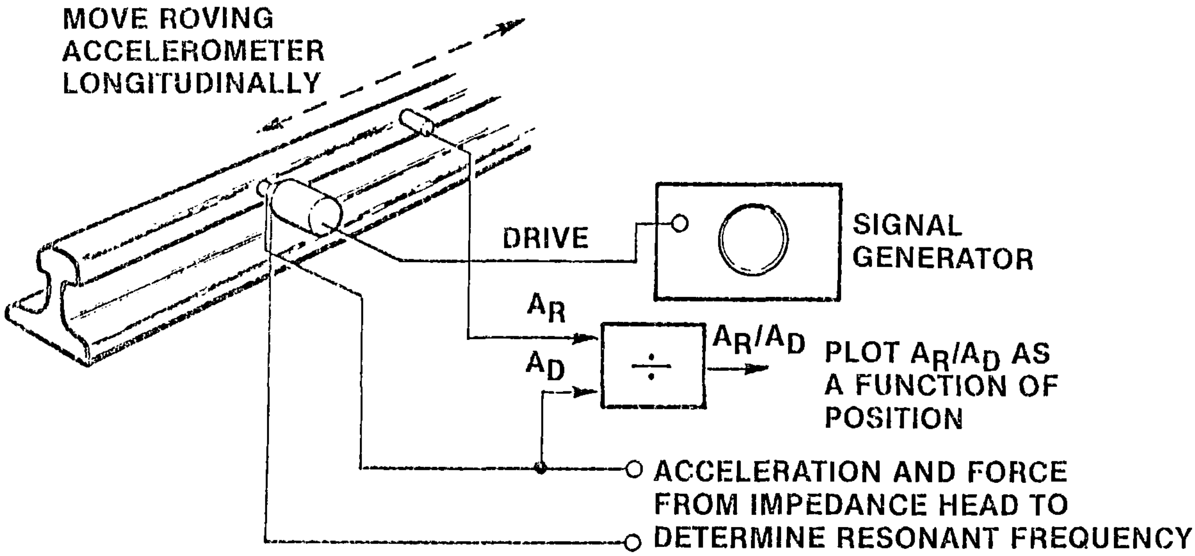

FIGURE 8. SETUP TO DETERMINE LONGITUDINAL DEPENDENCE OF TRANSVERSE VIBRATION AT RESONANCE

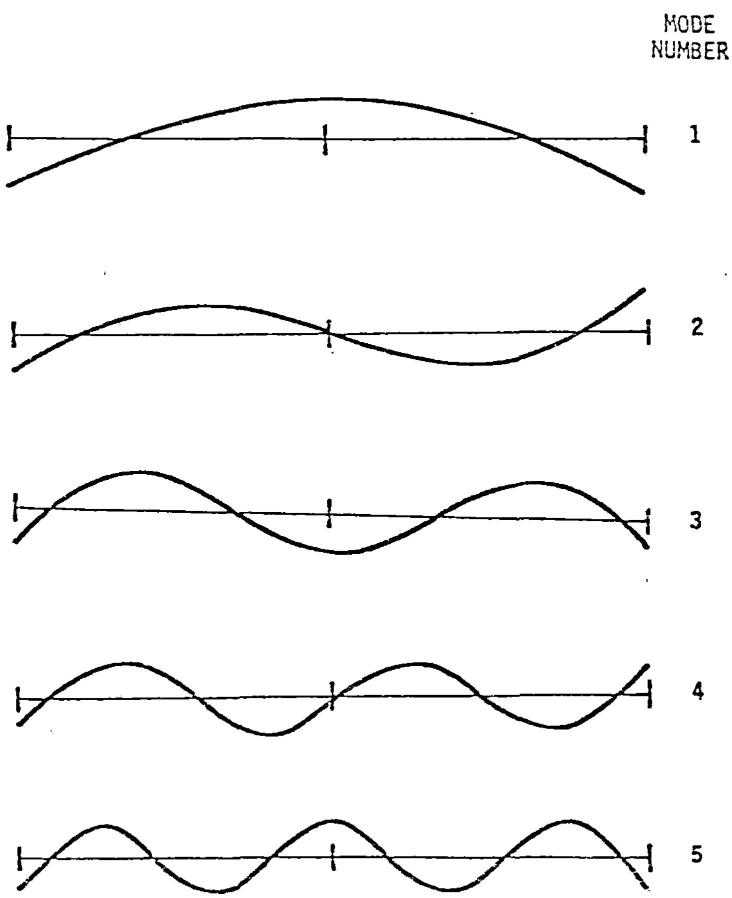

FIGURE 9. LONGITUDINAL MODE SHAPES OF A FREE-FREE BEAM

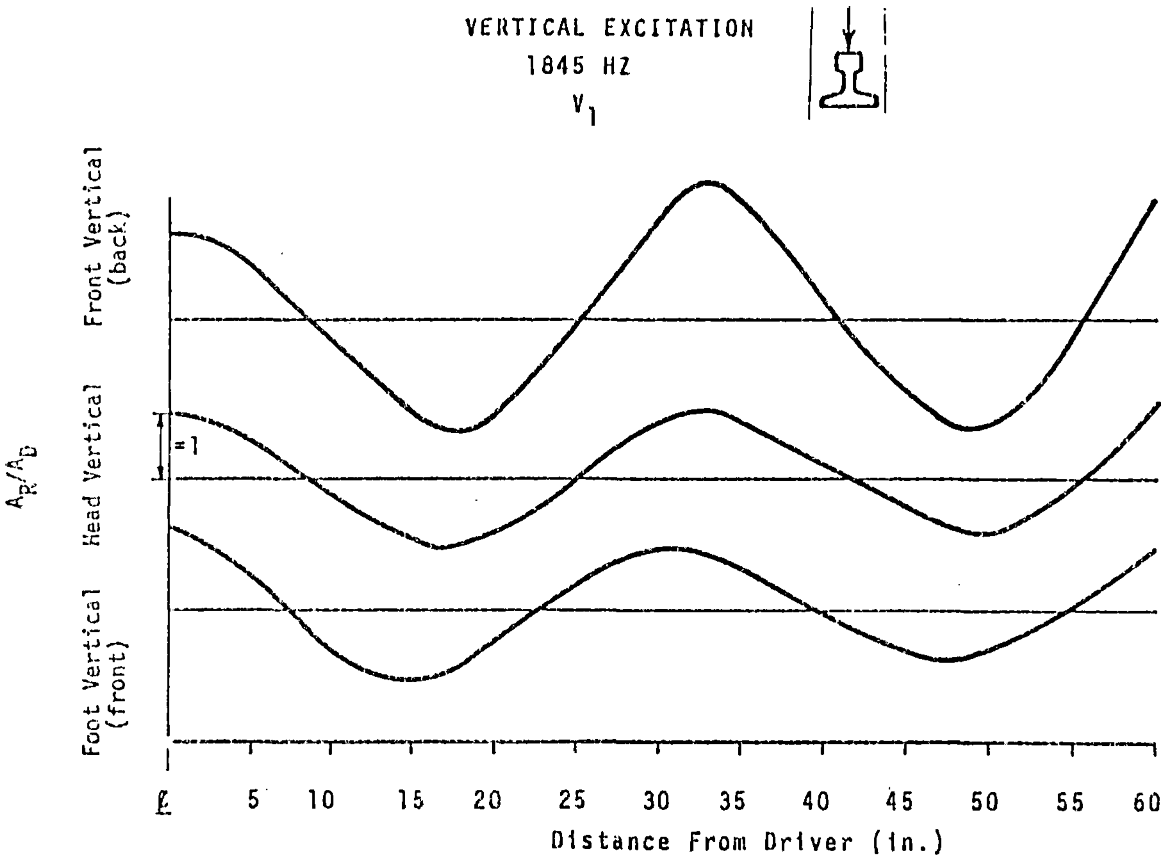

FIGURE 10. LONGITUDINAL MODE SHAPES WITH VERTICAL EXCITATION

The results of the measurement program are summarized in tables 1 and 2. Figures 15 through 17 are plots of phase velocity versus frequency for each of the four excitations. These plots all have a strong similarity to that shown in figure 2. In fact, for vertical excitation at the head of the rail, the cutoff frequency for mode 2 of Timoshenko theory may be calculated from figure 2 as $\omega = a_1 k_0$ or $f = \frac{1}{2\pi}\sqrt{\frac{\kappa GA}{\rho I}}$, assuming that $\kappa = 0.39$ and $f = 5198$ hertz, which agrees with the measured cutoff frequency shown in figure 15.

Effect of Axial Load on Resonant Frequencies

Theory. According to the theory and the measurements presented above, higher order propagation modes than those predicted by Timoshenko beam theory occur in rail sections excited in the 1-10 kilohertz frequency range. Because the exact solution is not obtainable for a beam with a cross section as complex as a rail's, another analytical approach must be found. The observed cross-section deformation and some analytical work performed by Goldstein [5] raised the possibility that the rail could be modeled as simpler beams vibrating on an internal elastic coupling. Some possibilities are:

a. The rail head vibrates horizontally or vertically on the web while the foot remains stationary (considered by Goldstein).

b. The head and the foot behave as Bernouilli-Euler beams vibrating on the elastic foundation of the web.

(H_1) TYPE VIBRATION

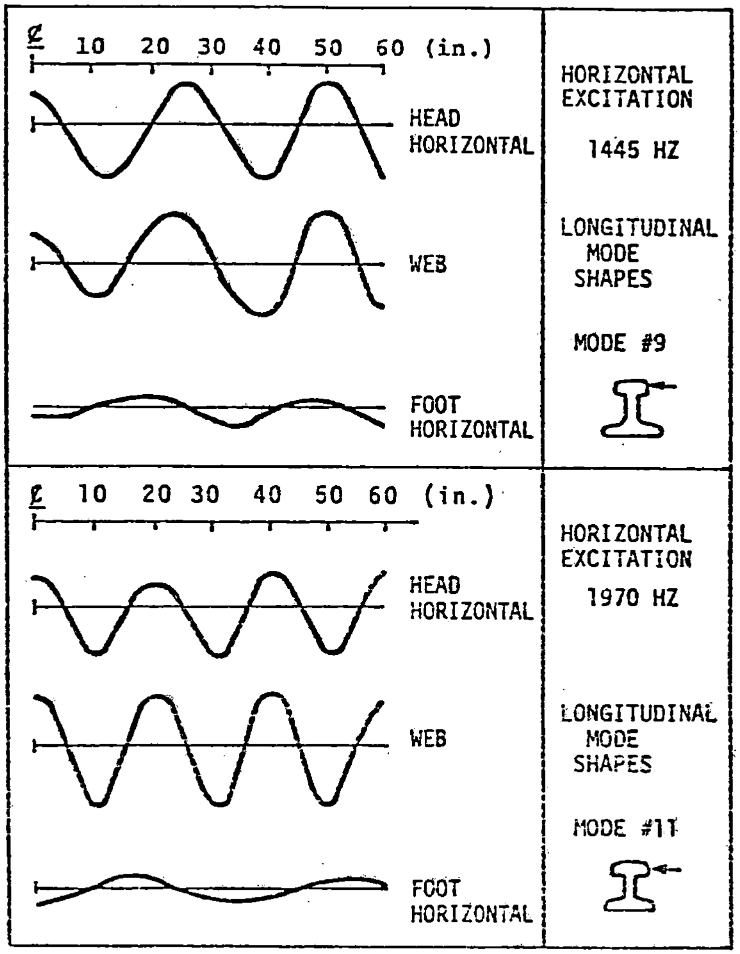

FIGURE 11. LONGITUDINAL MODE SHAPES WITH HORIZONTAL EXCITATION

It was hoped that these relatively simple models would agree with the observed resonant behavior of the rail and provide an analytical framework for calculating the effect of axial load.

In order to model the rail head vibrating on the elastic foundation of the web with axial load, Goldstein [5] considered the compliance of a Bernouilli-Euler beam on an elastic foundation subjected to a compressive axial load. The governing equation is

$$EI \frac{\partial^4 W}{\partial x^4} + P \frac{\partial^2 W}{\partial x^2} + kW + \rho \frac{\partial^2 W}{\partial t^2} = 0, \qquad (3)$$

with the following boundary conditions at $x = 0$:

$$EI \frac{\partial^3 W}{\partial x^3} = \frac{1}{2} \hat{P} e^{i\hat{\omega} t} \text{ and } \frac{\partial W}{\partial x} = 0.$$

Here, x = distance along rail axis,
E = the modulus of elasticity in lb/in^2,
I = moment of inertia of the rail in in^4,
P = axial load in rail (positive for compression),
k = foundation modulus in lb/in^2,
W = displacement of rail,
$\hat{P}$ = load applied at $x = 0$, and
$\hat{\omega}$ = radian frequency.

The most important result of this analysis is that there two resonant frequencies for this case:

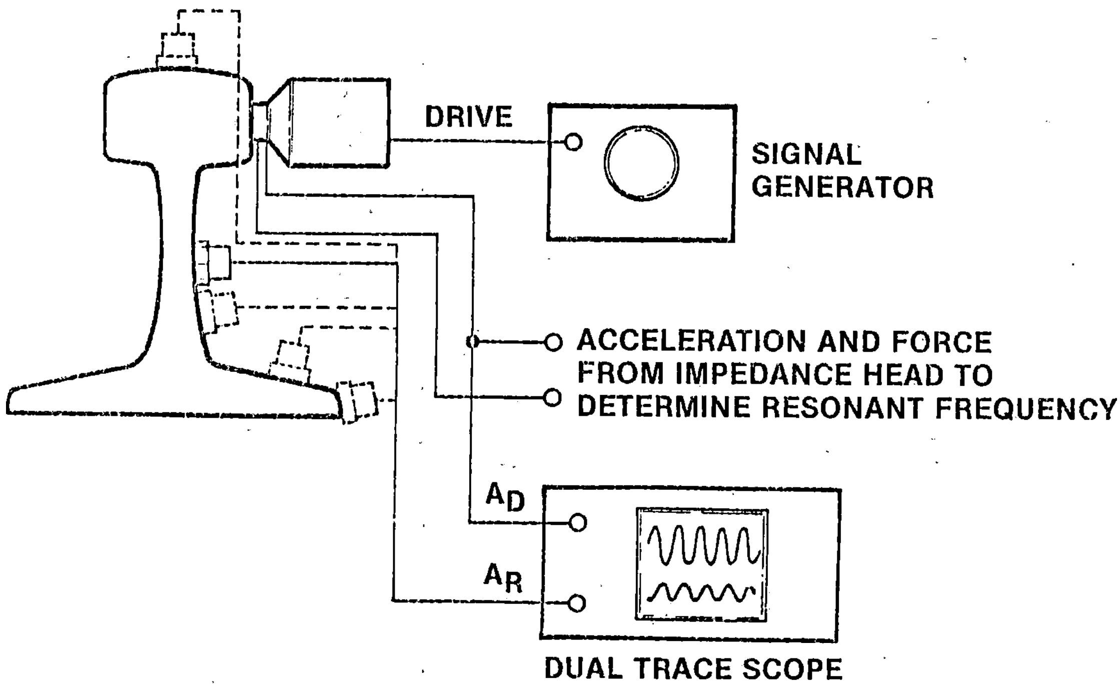

FIGURE 12. SETUP TO DETERMINE CROSS-SECTIONAL MODE SHAPE

$$\omega_1 = \sqrt{\frac{k}{\rho}} \quad \text{and} \quad \omega_2 = \omega_1\sqrt{1-\frac{P^2}{P_{cr}^2}}, \tag{4}$$

where ω_1 is the resonant frequency of the rail moving as a rigid body on the elastic foundation, and ω_2 is identified with the buckling load. Note that, if $P = P_{cr}$, then $\omega_2 = 0$, whereas, if $P = 0$, then $\omega_2 = \omega_1$ and there is only one resonant frequency.

In contrast with the infinite beam on an elastic foundation with axial load as discussed above, we will now consider a simply supported finite beam on an elastic foundation and subjected to axial load [6]. If Bernouilli-Euler theory is assumed, the governing equation for this case is identical to equation (3), but for a finite beam of length, L, the boundary conditions for simple supports are as follows:

$$Y(0) = Y''(0) = 0, \text{ and } Y(L) = Y''(L) = 0. \tag{5}$$

Assuming a steady-state solution, mode shapes satisfying equation (5) are

$$Y(x) = \sin\frac{n\pi x}{L}.$$

Substitution of this in equation (3) yields the following result for resonant frequencies:

Mode No.	f (Hz)	a_D 1	a_R/a_D 2	3	4	5	6	7	8
7	960	1.0		0.85	0.23	− 0.42	− 0.61	− 0.96	− 0.65
9	1446	1.0	0.25	1.25	0.95	− 0.45	− 0.75	− 1.00	− 0.35
11	1970	1.0	0.13	0.90	0.48	− 0.32	− 0.50	− 0.70	− 0.18
13	2598	1.0	0.17	1.33	0.33	− 0.27	− 0.47	− 0.60	− 0.27
15	3134	1.0	0.47	1.35	0.70	− 1.41	− 2.18	− 2.82	− 1.18

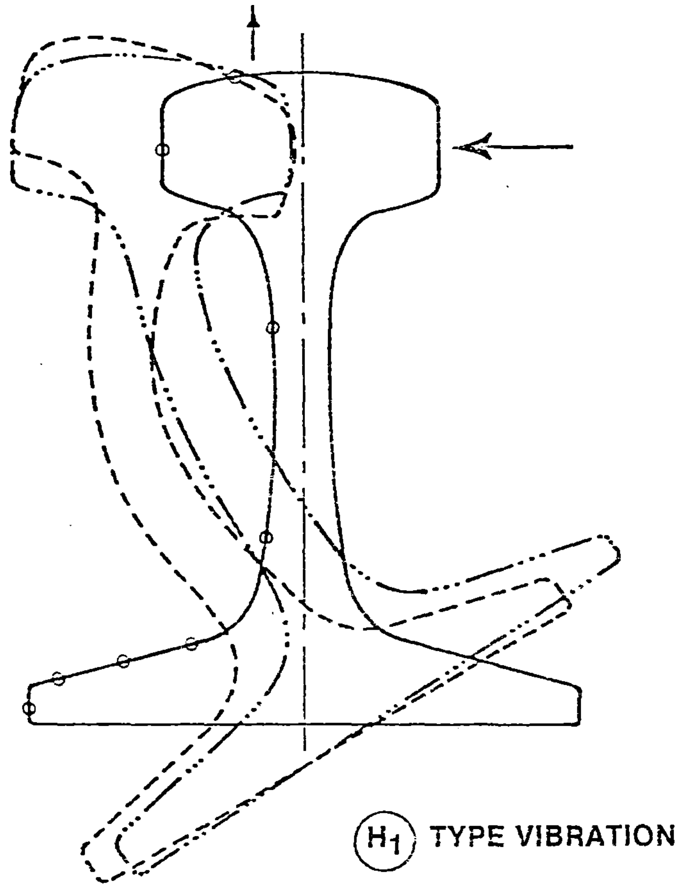

FIGURE 13. HORIZONTAL EXCITATION CROSS-SECTIONAL MODE SHAPE (EXAGGERATED)

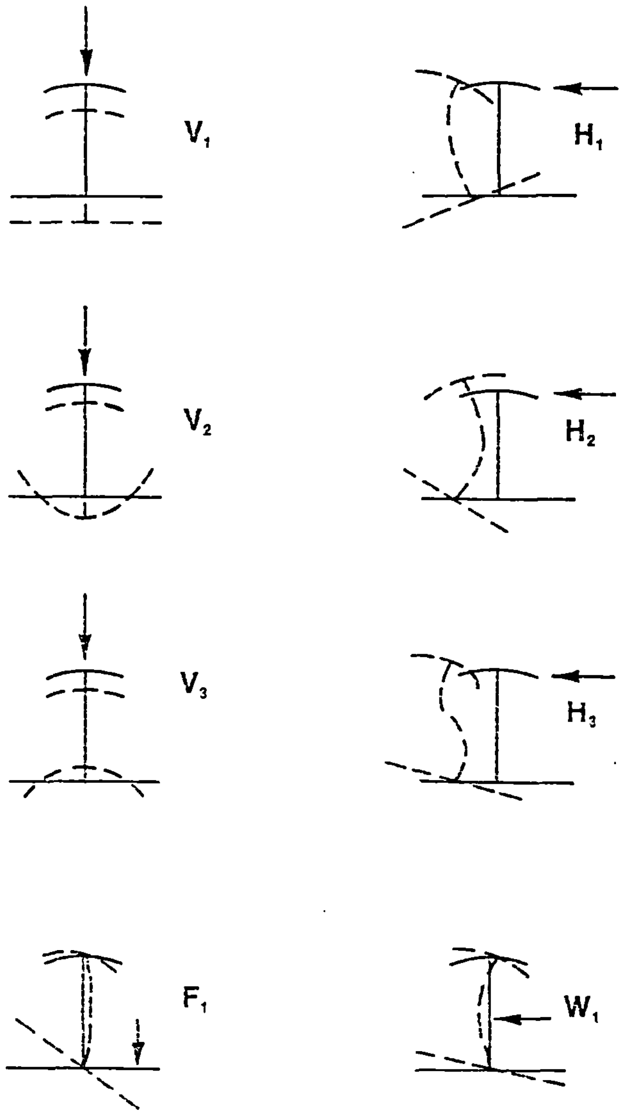

Types of Vibration for Vertical
and Horizontal Excitation

FIGURE 14. CROSS-SECTIONAL MODE SHAPES

TABLE 1. SUMMARY OF VERTICAL VIBRATION MEASUREMENTS

DRIVING AT HEAD, VERTICAL

	f Hz	n	λ in.	V_{ph} 1000 ips
	1158	5	43.6	50.5
	1841	7	32.0	58.9
V_1	2520	9	25.3	63.7
	3149	11	20.9	65.8
	3730	13	17.8	66.4
	4231	15	15.5	65.6
	5467	7	32.0	175
	5679	9	25.3	144
	5830	11	20.9	122
	5962	7	32.0	191
	6060	11	20.9	127
V_2	6202	13	17.8	110
	6491	15	15.5	101
	7060	17	13.7	96.8
	7507	19	12.3	92.4
	7889	19	12.3	97.1
	8168	21	11.2	91.2
	8762	23	10.2	89.5
	9432	25	9.41	88.8
V_3	9960	5	43.6	435.

DRIVING AT FOOT, VERTICAL

	f Hz	n	λ in.	V_{ph} 1000 ips
V_1	1158	5	113.6	50.5
	1530	7	32.0	49.0
	1760	3	68.6	121.
V_1	1849	7	32.0	59.2
	2073	5	43.6	90.4
	2175	9	25.3	55.0
	2430	7	32.0	77.8
V_1	2520	9	25.3	63.8
	2775	11	20.9	58.0
V_1	3149	11	20.9	65.8
	3686	17	13.7	50.5
	4034	17	13.7	55.3
	4193	19	12.3	51.6
V_1	4231	15	15.5	65.6
	4412	17	13.7	60.4
	4667	21	11.2	52.3
	4943	19	17.3	60.8
	4994	19	12.3	61.4

f = frequency
n = mode number

λ = wavelength
V_{ph} = phase velocity

TABLE 2. SUMMARY OF HORIZONTAL VIBRATION MEASUREMENTS

DRIVING AT HEAD, HORIZONTAL

f Hz	n	λ in.	V_{ph} 1000 ips	
960	7	32.0	30.7	
1445	9	25.3	36.6	H_1
1970	11	20.9	41.2	
2550	13	17.8	45.4	
2775	9	25.3	70.2	H_2
3135	15	15.5	48.6	H_1
3795	11	20.9	68.8	H_2
3810	15	15.5	60.0	
4335	17	13.7	59.5	H_1
4860	15	15.5	75.3	
5675	21	11.2	63.3	
6400	23	10,2	65.4	
6420	23	10.2	65.6	
7155	25	9.41	67.3	
7890	27	8.73	68.8	

f = frequency
n = mode number
λ = wavelength
V_{ph} = phase velocity

DRIVING AT WEB, HORIZONTAL

f Hz	n	λ in.	V_{ph} 1000 ips
1445	9	25.3	36.6
1538	5	43.6	67.0
1760	3	68.6	121.
1970	11	20.9	41.2
2073	5	43.6	90.4
2433	7	32.0	77.8
2550	13	17.8	45.4
2769	9	25.3	70.0
2868	9	25.3	72.6
3135	15	15.5	48.6
2376	11	20.9	70.6
3687	17	13.7	50.5
4035	13	17.8	71.8
4188	15	15.5	67.9
4267	1	160.	683.
4335	17	13.7	59.4
4414	3	68.6	303.
4652	5	43.6	203.
4945	19	12.3	60.2
4998	7	32.0	160.

$$f_n^2 = \frac{a^2(n\pi)^4}{2\pi}\left[1 + k^*(\lambda_n/2\pi)^4 - P^*(\lambda_n/2\pi)^2\right], \quad (6)$$

where $a^2 = \frac{EI}{\rho L^4}$, $P^* = \frac{P}{EI}$, and the other parameters are as defined in the above discussion of the finite beam on an elastic foundation with axial load. The percentage decrease in frequency attributable to axial load is given by:

$$\left(1 - \frac{1}{\varepsilon}\right) \times 100 = \%$$

where

$$\varepsilon = \sqrt{\frac{1+k^*(\lambda_n/2\pi)^4}{1+k^*(\lambda_n/2\pi)^4-P^*(\lambda_n/2\pi)^2}} \quad (7)$$

This is plotted in figure 18 for two of the measured higher order modes. Although, as shown above, Bernouilli-Euler beam theory is not adequate to describe the dynamic response of a rail, it does allow an order of magnitude estimate of the effect of axial load.

We will now consider some more exact theories, beginning with two beams separated by an elastic foundation.

To obtain simply the quantitative effect of axial load and to obtain the modal shapes, we consider a simply supported beam system as shown in figure 19. Here, one beam represents the rail head, the other the rail foot. The web is modeled as an elastic (massless) coupling with stiffness k. The governing equations are as follows:

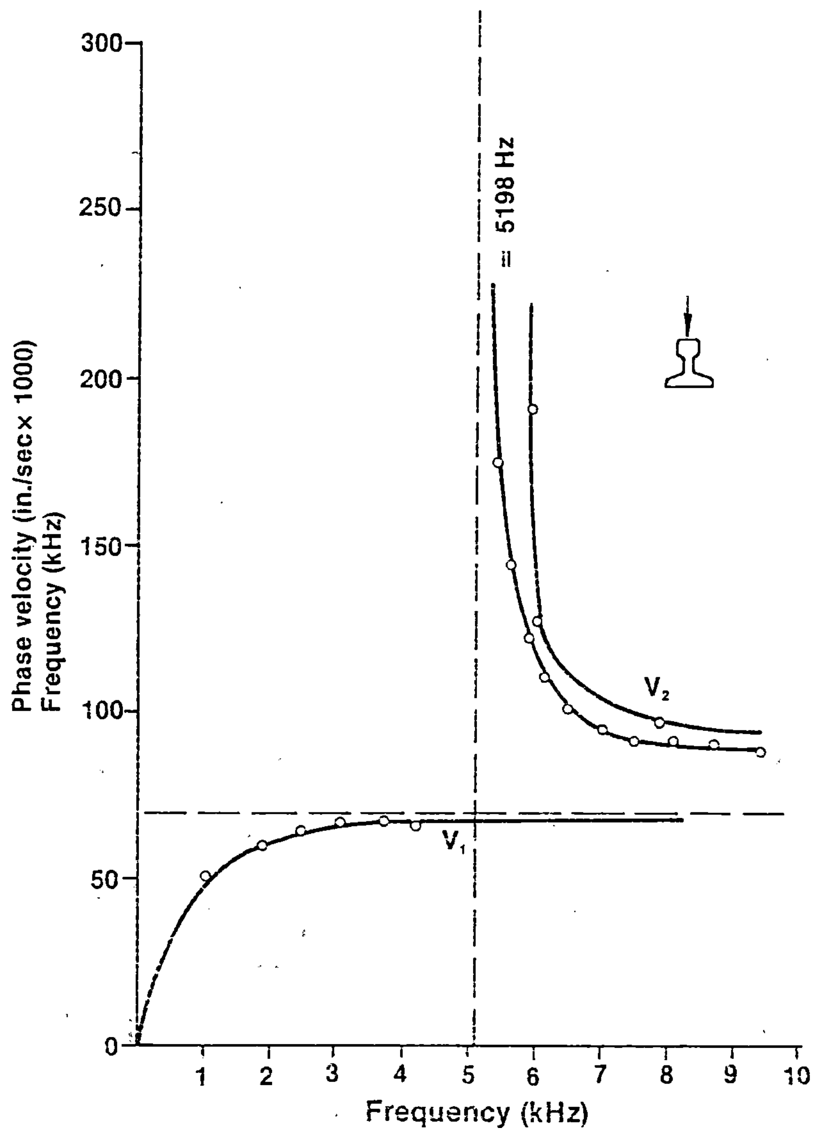

FIGURE 15. PHASE VELOCITY VERSUS FREQUENCY: VERTICAL EXCITATION AT RAIL HEAD

$$EI_1 \frac{\partial^2 v_1}{\partial x^4} + P_1 \frac{\partial^2 v_1}{\partial x^2} + k\,(v_1 - v_2) = -m_1 \frac{\partial^2 v_1}{\partial t^2}\,, \text{ and} \tag{8}$$

$$EI_2 \frac{\partial^4 v_2}{\partial x^4} + P_2 \frac{\partial^2 v_2}{\partial x^2} - k\,(v_1 - v_2) = -m_2 \frac{\partial^2 v_2}{\partial t^2}\,,$$

where $m_1 = \rho A_1$, $m_2 = \rho A_2$, and all constants are as defined under equation (3) above. The solution for this system is

$$v_i = V_i \sin\left(\frac{n\pi x}{L}\right) \sin \omega t\,,$$

and the frequency-wavelength relation is

$$2\omega^{*2} = 1 + \frac{1}{\alpha\beta} + k_1^*\left(1 + \frac{1}{\beta}\right) - P_1^* - \frac{1}{\beta}\hat{P}_2^* \pm \left\{\left[\left(1 - \frac{1}{\alpha\beta}\right) + k_1^*\left(1 - \frac{1}{\beta}\right) - P_1^* + \frac{1}{\beta}\hat{P}_2^*\right]^2 + \frac{4k_1^{*2}}{\beta}\right\}^{1/2}, \tag{9}$$

where,

$$P_1^* = \frac{P_1\lambda^2}{EI_1}\,, \quad P_2^* = \frac{P_2\lambda^2}{EI_2} = \alpha p P_1^* = \alpha\hat{P}_2^*\,; \quad \alpha = \frac{EI_1}{EI_2}\,, \; p = \frac{P_2}{P_1}$$

$$k_1^* = \frac{k\lambda^4}{EI_1}\,, \; k_2^* = \frac{k\lambda^4}{EI_2} = \alpha k_1^*$$

$$\omega^{*2} = \frac{\omega^2}{a_1^2}\,; \quad a_1^2 = \frac{EI_1}{m_1\lambda^4}\,,$$

$$\beta = \frac{m_2}{m_1}\,, \; \lambda = \text{wavelength}\,.$$

Equation (9) can be rewritten in terms of the beam parameters and the axial stress in each beam due to the axial loads, P_1 and P_2:

$$2\omega^2 = \left(\frac{E}{\rho}\right)\left[\left(\frac{I_1}{A_1} + \frac{I_2}{A_2}\right) + k_1^*\left(\frac{I_1}{A_1} + \frac{I_1}{A_2}\right)\right]\frac{1}{\lambda^4} - \left(\frac{\sigma_{1x}}{\rho} + \frac{\sigma_{2x}}{\rho}\right)\frac{1}{\lambda^2} \pm \sqrt{\left(\frac{E}{\rho}\right)\left[\left\{\left(\frac{I_1}{A_1} - \frac{I_2}{A_2}\right) + k_1^*\left(\frac{I_1}{A_2} - \frac{I_1}{A_2}\right)\right\}\frac{1}{\lambda^4} + \left(\frac{\sigma_{1x}}{\rho} - \frac{\sigma_{2x}}{\rho}\right)\frac{1}{\lambda^2}\right] + 4\frac{A_1}{A_2}k_1^*}\,. \tag{10}$$

Note that, if $\sigma_1 x = \sigma_2 x$, then the axial stress term under the square root sign equals 0.

Another more exact theory involves the effect of axial load on Timoshenko beam theory. The governing equations for a Timoshenko beam subjected to axial load are

$$a_1^2\left(\frac{\partial^2\eta}{\partial x^2} - \frac{\partial\phi}{\partial x}\right) = \frac{\partial^2\eta}{\partial t^2}\,, \text{ and}$$

$$a_2^2\frac{\partial^2\phi}{\partial x^2} + a_1^2 k_o^2\left(\frac{\partial\eta}{\partial x} - \phi\right) + k_1^2\frac{\partial\eta}{\partial x} = \frac{\partial^2\phi}{\partial t^2}\,, \tag{11}$$

where η is the beam's displacement, ϕ is its rotation and

$$a_1^2 = \frac{\kappa G}{\rho}\,, \; a_2^2 = \frac{E}{\rho}\,, \; k_o^2 = \frac{A}{I}\,,$$

$$k_1^2 = \frac{P}{\rho I}\,, \; k = \frac{2\pi}{\lambda}\,, \text{ the wave number.}$$

The dispersion relation, including the axial load, is

$$\omega^4 - \omega^2\left[a_1^2(k^2 + k_o^2) + a_2^2k^2\right] + a_1^2a_2^2k^4\left(1 - \frac{k_1^2}{a_2^2k^2}\right) = 0\,. \tag{12}$$

This is in the same form as equation (2), except for the appearance of the axial load effect in the last term. Equation (12) may be used to find the phase velocity,

$$V_{ph} = \frac{1}{\sqrt{2k}}\sqrt{\left[\omega_o^2\left(\frac{I}{A}k^2 + 1\right) + \frac{E}{\rho}k^2\right] \pm \sqrt{\left[\omega_o^2\left(\frac{I}{A}k + 1\right) + \frac{E}{\rho}k^2\right]^2 - 4\omega_o^2k^2\left[\frac{I}{A}\left(\frac{E}{\rho}\right) - \frac{\sigma_x}{\rho}\right]}} \tag{13}$$

where σ_x is the axial stress.

More insight into the physics of the problem can be gained by considering the effect of an elastic foundation on an axially loaded rail. As shown in the discussion of the two preceding theories, the axial stress appears in the frequency or phase velocity relations as a term on the order of σ/ρ added to a term on the order of E/ρ. σ/ρ is much smaller than E/ρ for loads that approach the track buckling load. The effect of an elastic foundation is to lower the E/ρ, as is indicated below. We will use Bernouilli-Euler theory because it clearly demonstrates the effect. The phase velocity for a simple beam on an elastic foundation is as follows:

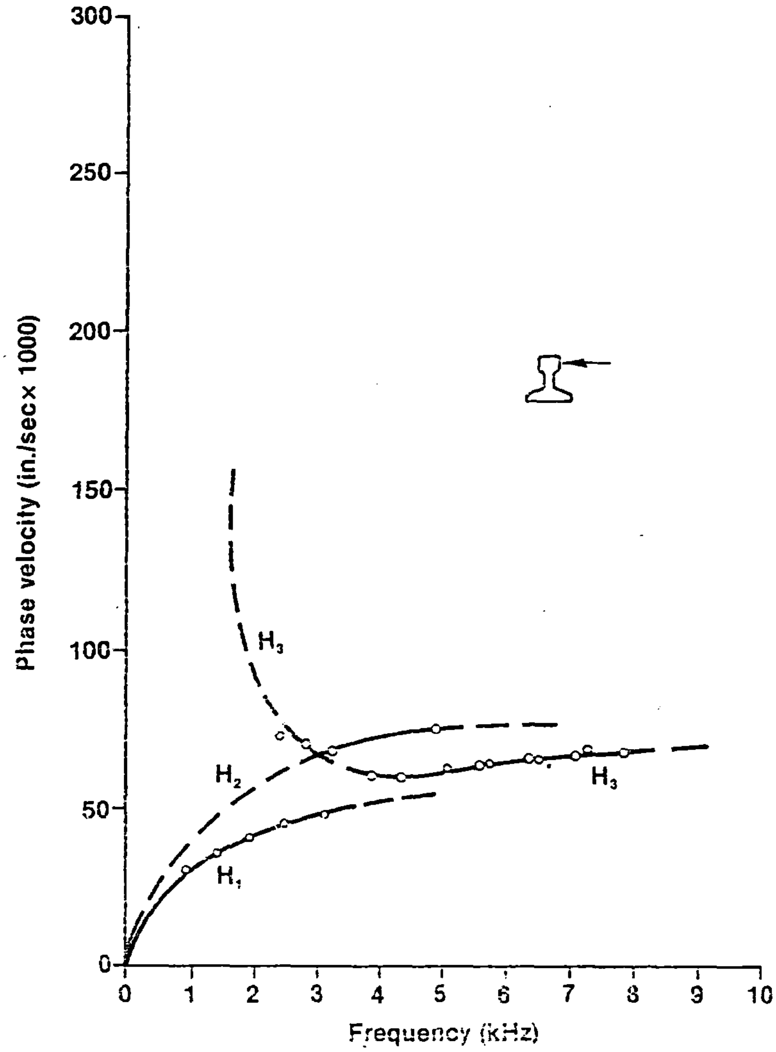

FIGURE 16. PHASE VELOCITY VERSUS FREQUENCY: HORIZONTAL EXCITATION AT RAIL HEAD

$$V_{ph} = \sqrt{\left[\frac{EI}{\rho A} k^2 + \frac{\alpha}{\rho A k^2}\right] - \left(\frac{\sigma_x}{\rho}\right)}$$

$$= \sqrt{C_1{}^2 + C_2{}^2} \qquad (14)$$

C_1 and C_2 are shown plotted versus wave number in figure 20. The effect of the elastic foundation is to provide a dip in the C_1 curve where C_1 and C_2 become relatively close in value.

Measurements on Axially Loaded Rail. Measurements were made on an axially loaded 10-foot rail section with the following objectives:

a. To determine experimentally the sensitivity of the rail's dynamic response to axial load.

b. To validate the analytic models considered.

c. To see if there may be nearfield (that is, nonpropagating) effects that were not accounted for in the analysis and that may be sensitive to axial load.

The measurements were carried out on the same 10-foot rail section used for the program described in the above discussion of cross-sectional mode shapes. A simple fixture, shown in figure 21 was designed and built to provide compressive loads up to 200,000 pounds. Figure 23 is a photograph of

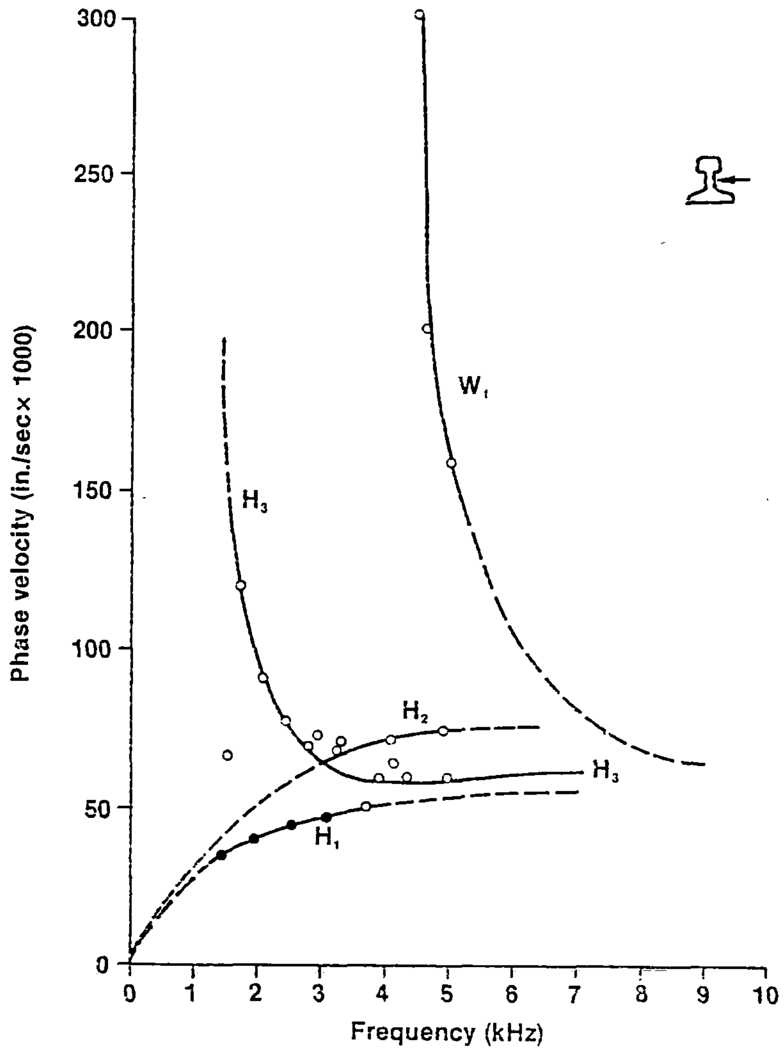

FIGURE 17. PHASE VELOCITY VERSUS FREQUENCY: HORIZONTAL EXCITATION AT WEB

the test fixture with rail in place. The fixture consists of two 3-inch steel plates connected by four 1-3/4-inch diameter steel rods welded to the plates (see figure 21). The overall length of the fixture is approximately 11 feet 3 inches. A third 3-inch plate, free to slide on the rods, is located between the two fixed end plates. The 10-foot rail fits between one of the end plates and the sliding plate, supported by angle irons mounted to the plates. Between the sliding plate and the other end plate is placed a 100-ton Enerpac hydraulic jack connected to a hand pump. Figures 23 and 24 show the jack and the hand pump. The jack loads the sliding plate, which in turn loads the rail.

The equipment used to excite the rail and to measure its response is the same as described in the discussion of cross-sectional mode shapes. Loads in the rail were monitored with three strain gage bridges, the output signals of which were sent to a Vishay model SB-1 switch and balance unit and a Vishay model P-350A strain indicator. One bridge measured axial load and the other two measured bending moments about the vertical and horizontal axes. Figure 25 shows the strain gages mounted to the rail, as well as the Wilcoxon impedance head used to excite the rail. Figure 26 shows the strain gage signal conditioning equipment.

The pressure applied to the hydraulic jack was monitored by a pressure gage, and axial load was recorded during testing by noting the hydraulic pressure (this was more convenient than reading strain). The relationship between hydraulic pressure in pound-force per square inch (psi) and axial load in thousand pounds-force per square inch (kips) was determined from strain gage measurements (see figure 27) and was found to be linear.

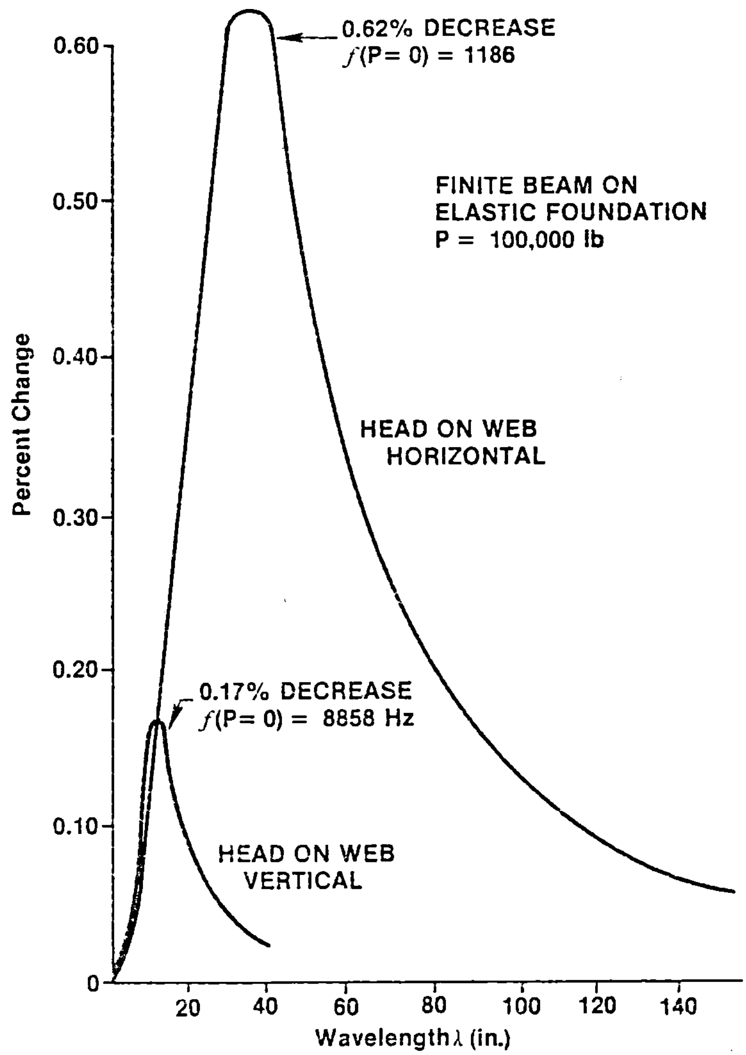

Percent Change in Resonant Frequencies or Phase Velocity Due to Axial Load

FIGURE 18. PERCENTAGE CHANGE IN PHASE VELOCITY

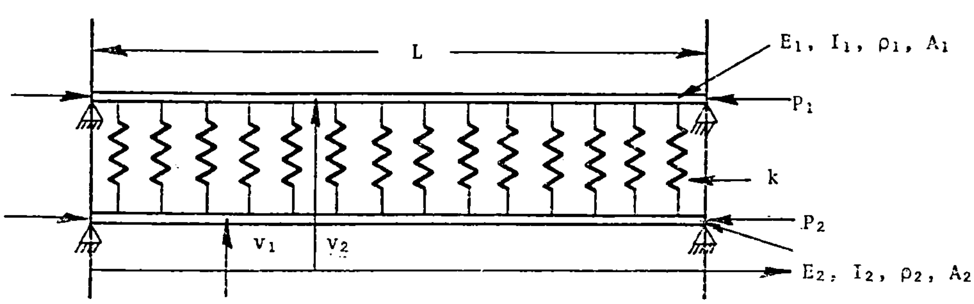

FIGURE 19. TWO BEAMS CONNECTED BY A LINEAR ELASTIC COUPLING

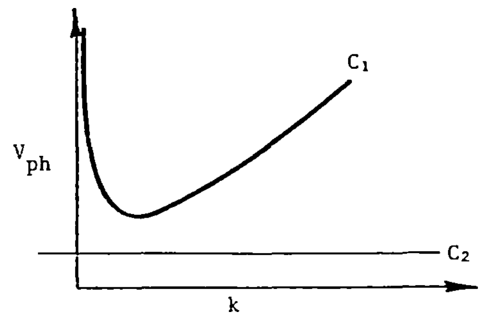

FIGURE 20. PHASE VELOCITY VERSUS WAVE NUMBER

In addition to axial load, bending moment was measured using strain gages at the center of the rail, and was found to be negligible (equivalent to a 200-pound lateral force) compared to axial load (214,000 pounds).

Measurement of resonant behavior and associated longitudinal and cross-sectional mode shapes was carried out in the same fashion discussed above. Data were collected systematically by driving the rail at the five points shown in figure 5 at axial loads from 0 to 221 kips. The resonant frequency and wavelength were measured and recorded and the phase velocity was calculated. Table 3 shows a typical set of recorded and reduced data.

The reduced data are presented in the frequency versus phase velocity plots of figures 28 through 31. Each plot was made from data gathered with excitation at one of four driving points and load levels from 0 to 185 kips.

The fundamental modes of cross-sectional vibration shown previously in figure 14 were again observed, and their sensitivity to axial load was investigated. Although the resonant frequencies of the rail appeared to shift greatly with increased axial load (see figure 32, for example), computed phase velocities did not vary proportionately. We believe that the frequency shifts are due to the changing end conditions of the rail in going from 0 kip to the 185-kip axial level. Phase velocity is independent of end conditions because shifts in frequency are accompanied by compensating shifts in flexural wavelength. Thus, deviations from the phase velocity behavior of a particular mode should be a true indication of axial load dependence, whereas deviations in resonant frequency alone are artifacts of the experimental setup.

We did not observe significant or consistant deviations in phase velocity behavior as a result of increased axial load. This is illustrated in figure 33, which shows that frequencies and phase velocities do shift as a result of axial load but remain very close to the curve defined by the locus of zero load points.

Other changes were noticed that are not as quantifiable as the phase velocity curves. These are briefly described below:

a. Irregular longitudinal mode shapes occur when the rail is under load. The 5-7 kilohertz range with foot vertical excitation exhibited several longitudinal mode shapes with irregular spacing of nodes.

b. Poorly defined longitudinal mode shapes appear under load. The 5.5-6.0 kilohertz range

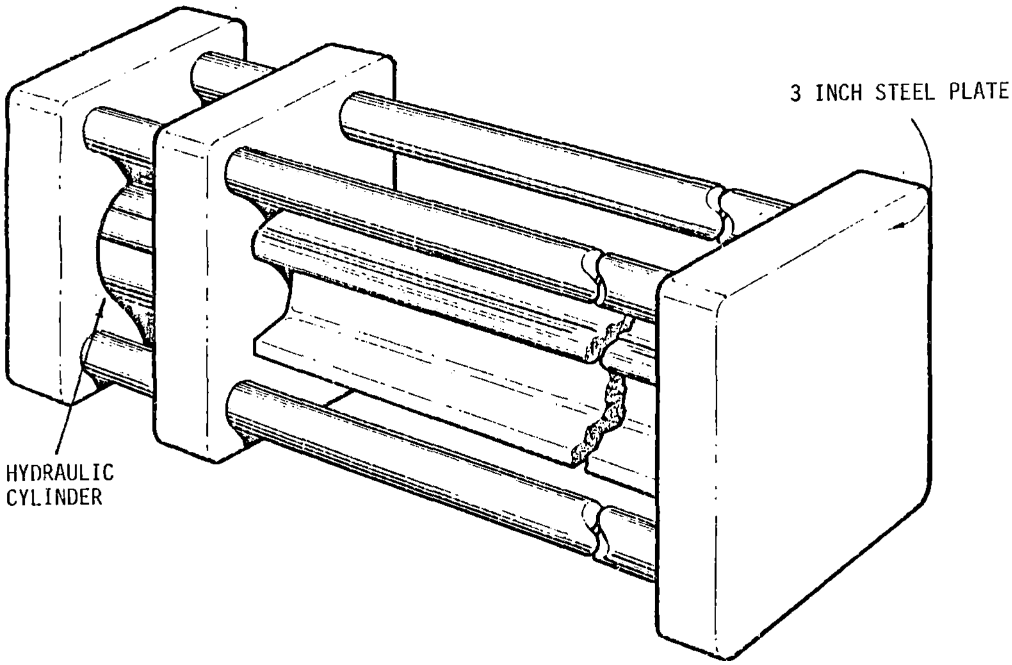

FIGURE 21. TEST FIXTURE TO PROVIDE AXIAL LOAD ON RAIL

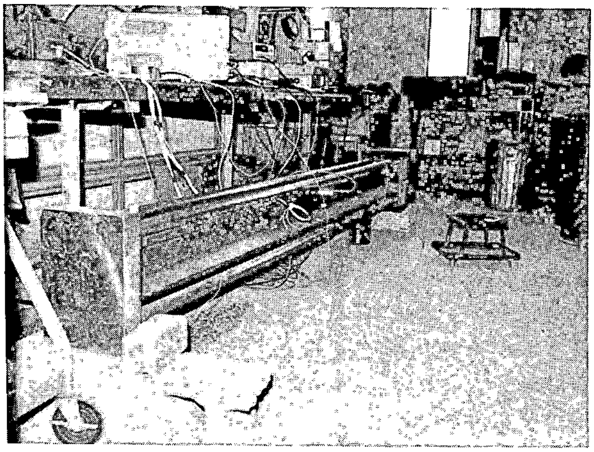

FIGURE 22. OVERALL VIEW OF TEST FIXTURE

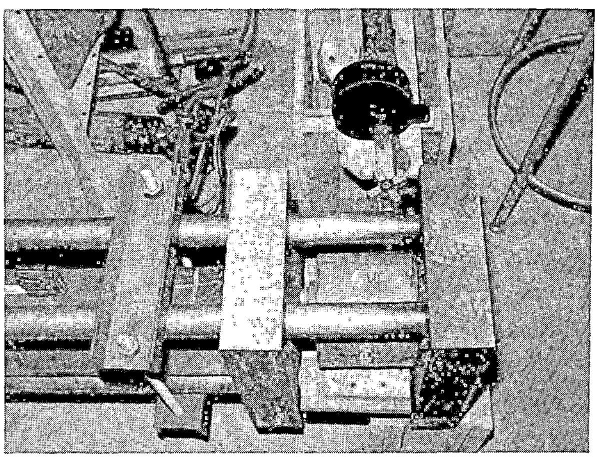

FIGURE 23. 100-TON HYDRAULIC CYLINDER

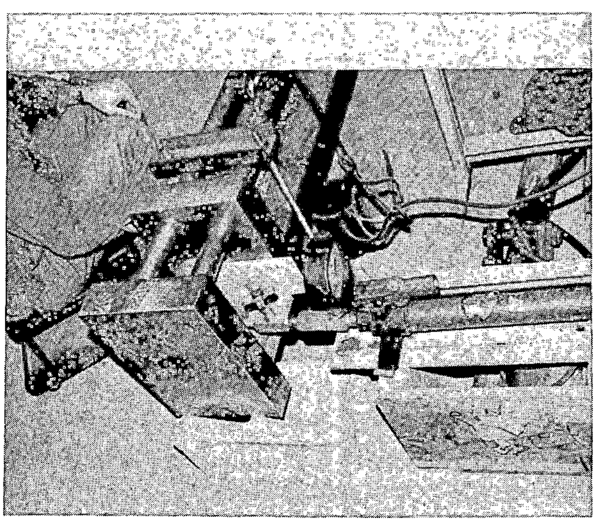

FIGURE 24. HAND PUMP AND GAGE FOR HYDRAULIC CYLINDER

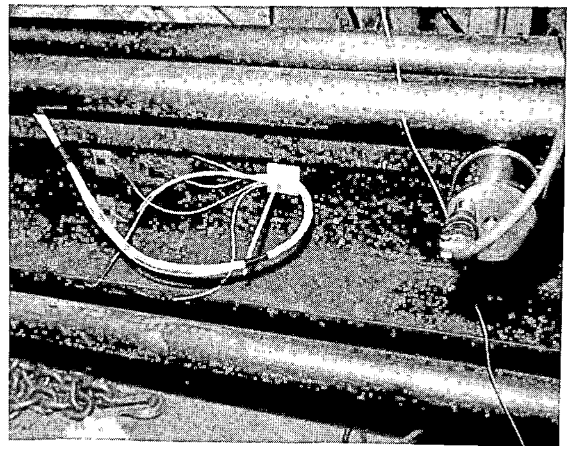

FIGURE 25. STRAIN GAGE ARRAYS AND IMPEDANCE HEAD

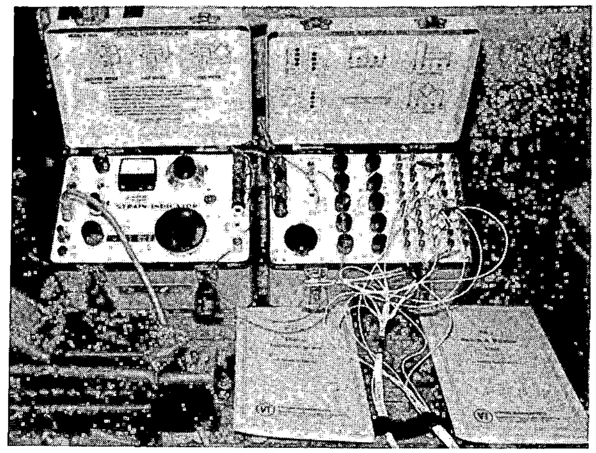

FIGURE 26. SIGNAL CONDITIONERS FOR STRAIN GAGES

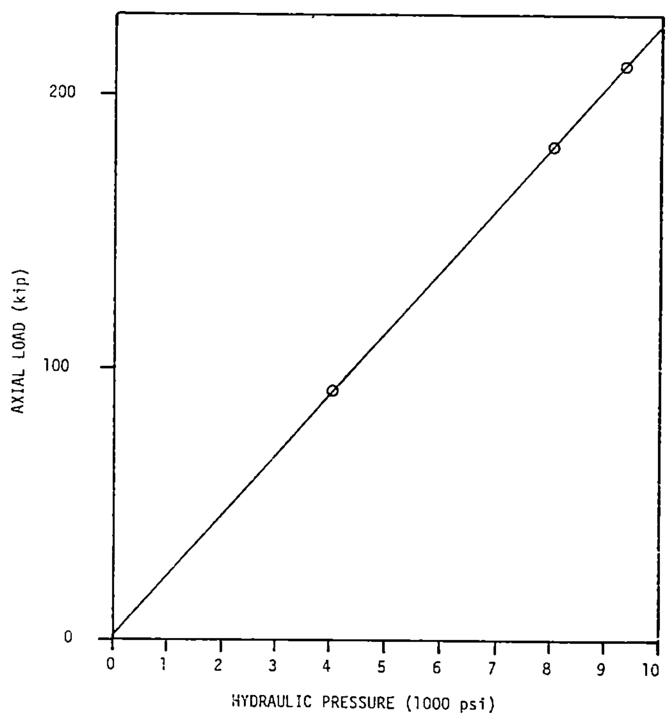

FIGURE 27. RELATIONSHIP BETWEEN HYDRAULIC PRESSURE AND AXIAL LOAD IN RAIL

TABLE 3. TYPICAL SET OF RECORDED AND REDUCED DATA

DRIVING POINT: HEAD VERTICAL

AXIAL LOAD: 3000 psi = 70 kip

Measured Frequency (kHz)	Measured Wavelength (in)	Computed Phase Velocity (1000 ips)
1754	33.10	58.06
1860	32.57	60.58
2421	26.10	63.08
3035	21.60	65.56
3623	18.36	66.53
4146	16.00	66.34
6809	14.13	96.23

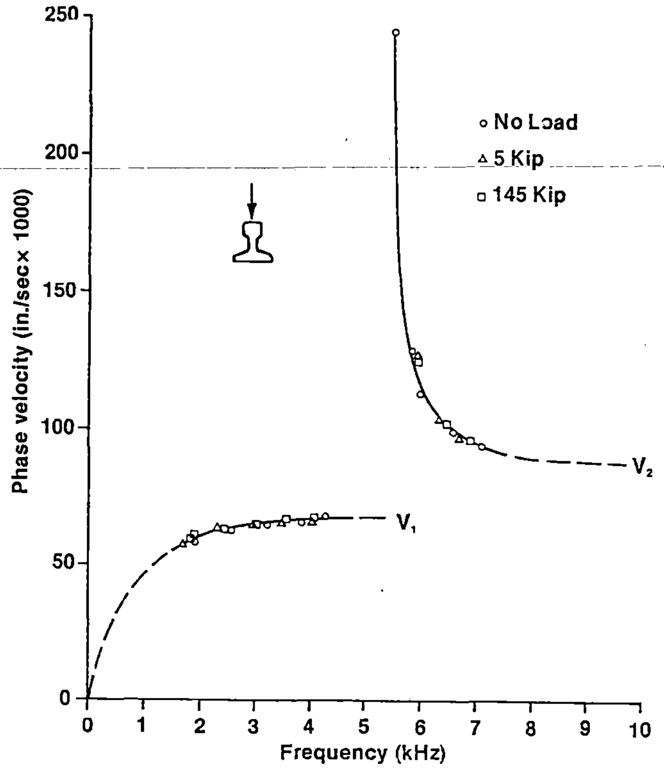

FIGURE 28. PHASE VELOCITY VERSUS FREQUENCY: VERTICAL EXCITATION AT RAIL HEAD WITH AXIAL LOAD

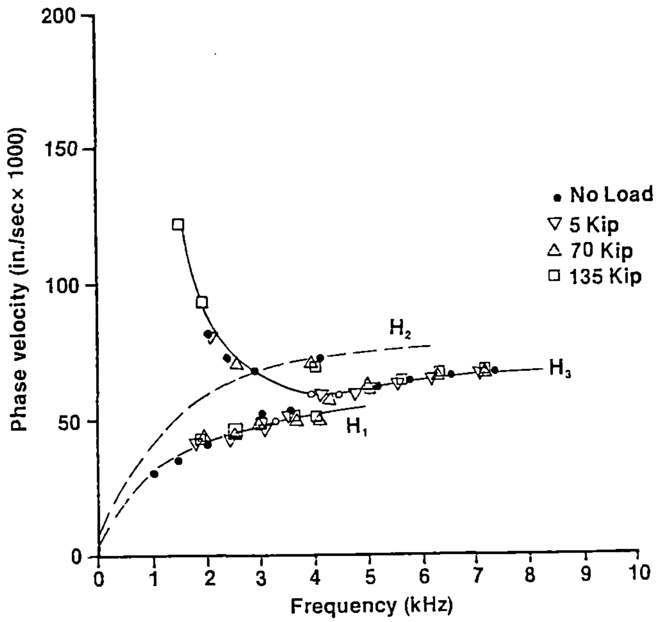

FIGURE 29. PHASE VELOCITY VERSUS FREQUENCY:
HORIZONTAL EXCITATION AT THE RAIL HEAD WITH AXIAL LOAD

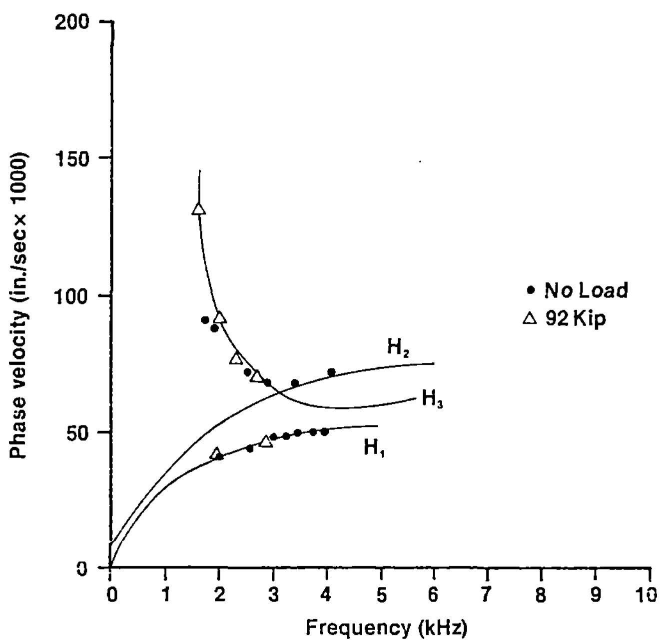

FIGURE 30. PHASE VELOCITY VERSUS FREQUENCY:
HORIZONTAL EXCITATION AT THE WEB WITH AXIAL LOAD

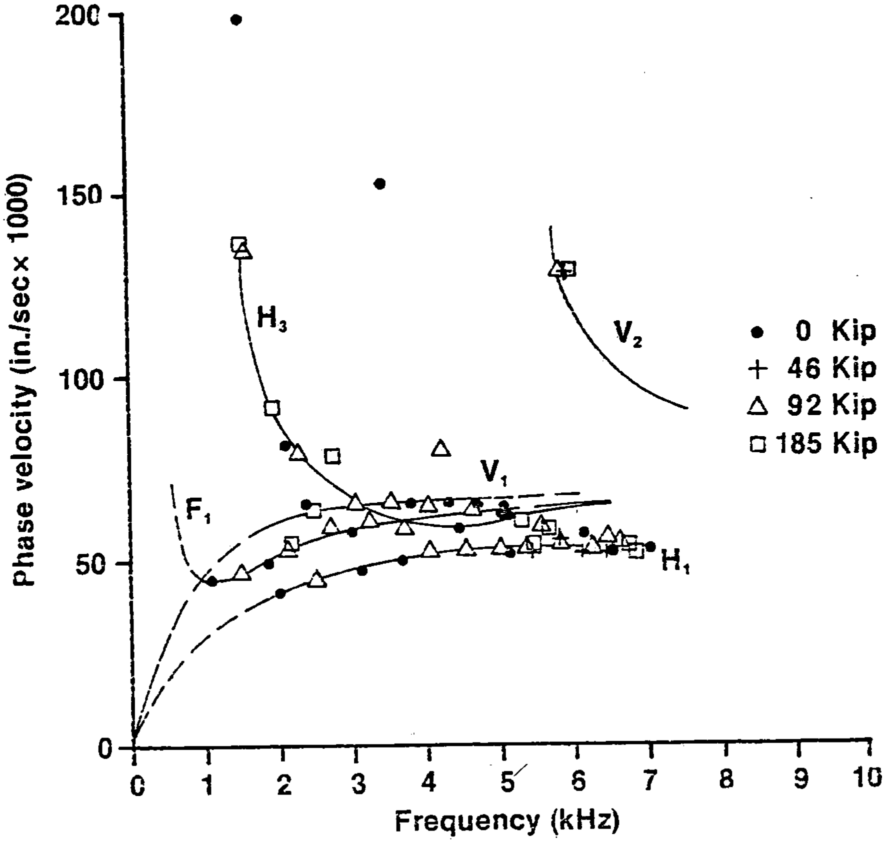

FIGURE 31. PHASE VELOCITY VERSUS FREQUENCY: VERTICAL EXCITATION AT FOOT WITH AXIAL LOAD

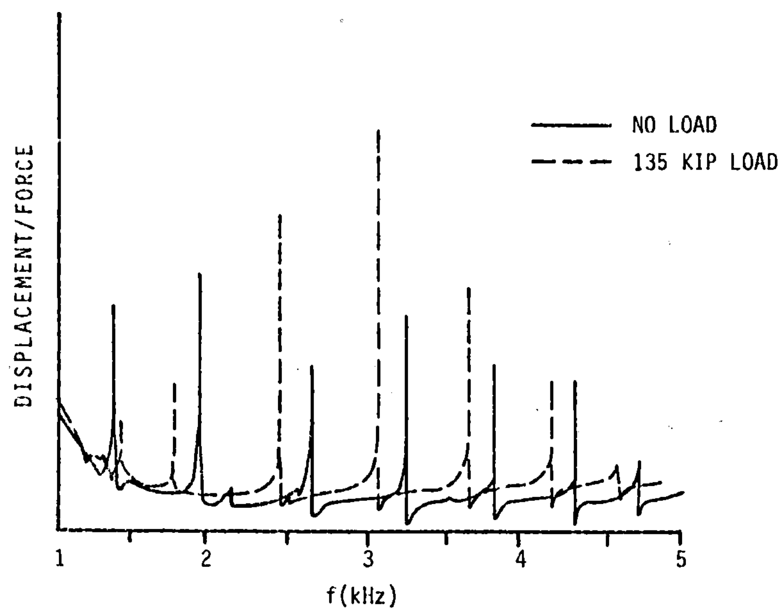

FIGURE 32. RESONANT FREQUENCY SHIFTS ATTRIBUTABLE TO CHANGES IN LOAD APPLIED BY THE TEST RIG

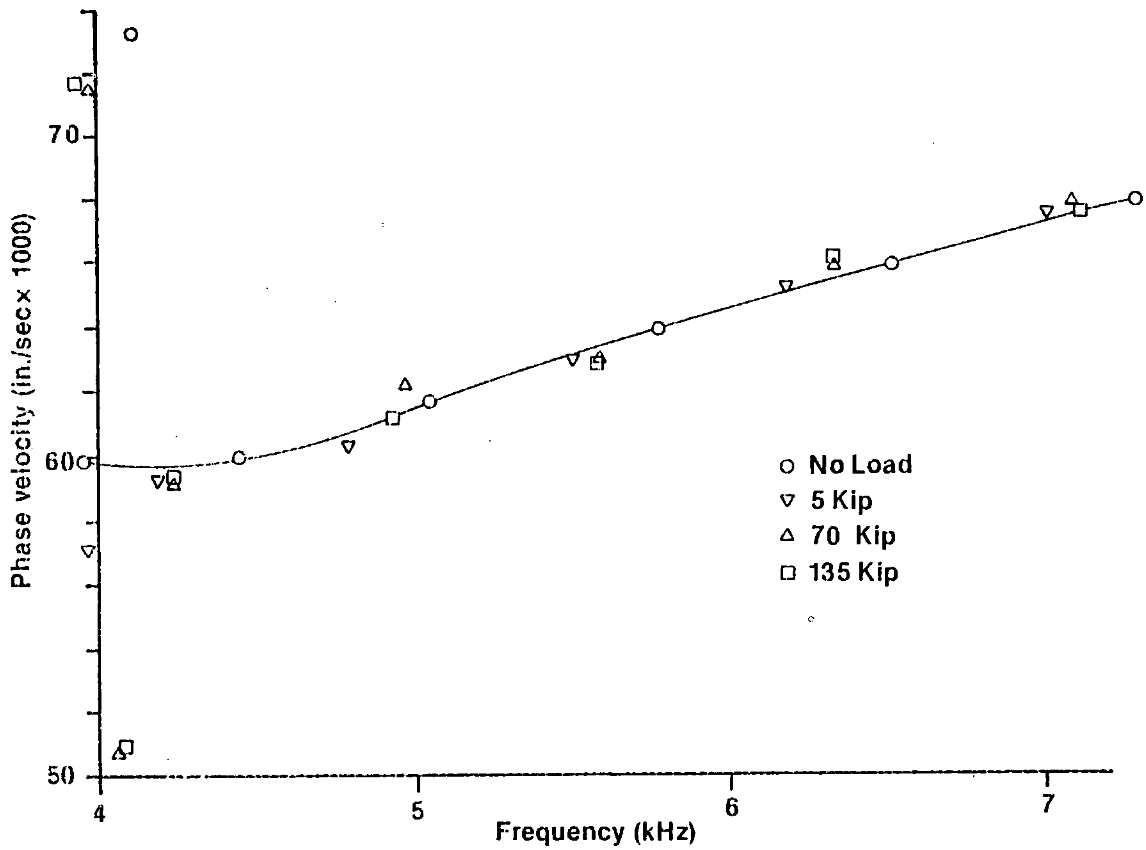

FIGURE 33. H3 BEHAVIOR UNDER AXIAL LOAD

with head vertical excitation showed clearcut longitudinal mode shapes without load, but nodal points could not be determined with the rail under load.

c. Resonant peaks were attenuated in the 1.0-1.5 kilohertz range at all driving points under load.

d. The average level of the frequency response curves changed proportionately with load at certain ranges between resonant peaks. This indicates that changes in axial load may be more easily inferred from the dynamic compliance than from phase velocity measurements.

References

[1] Remington, P. J., et al. "Wheel/Rail Noise and Vibration Control. Urban Mass Transportation Administration, report no. UMTA-MA-06-0025-73-15, interim report (May 1974).

[2] Crandall, S. H., et al. Dynamics of Mechanical and Electromechanical Systems. New York: McGraw-Hill, Inc., 1968.

[3] Fung, Y. C. Foundations of Solid Mechanics. Englewood Cliffs, New Jersey: Prentice-Hall, Inc., 1965.

[4] Abramson, H. N. "Flexural Waves in Elastic Beams of Circular Cross Section." JASA, volume 29, number 1 (January 1957).

[5] Goldstein, G. "Determination of Axial Loads in Rails by Means of Compliance Curve Measurements." Internal memorandum, Transportation Systems Center, Cambridge, Massachusetts, 1978.

[6] Personal communication with Professor T. J. Lardner.

"Magnetoultrasonic Stress Measurement"

Nagabhusan Senapati
Battelle Columbus Laboratories

Introduction

High axial stresses attributable to thermal and mechanical forces have been the primary cause of track buckling and rail pull-aparts. Nondestructive measurement of these stresses has been a pressing problem for the railroad industry. Many such measurement techniques have been proposed and evaluated, with only limited success to date.

The stresses in a continuously welded rail in track are attributable to three major sources:

a. Residual stress from manufacturing anomalies and from the continuous plastic deformation and cold working caused by wheel-rail contact forces.

b. Mechanical forces resulting from rail running and bunching as a consequence of train operations and irregular terrain.

c. Thermal stresses associated with ambient temperature changes.

The residual stress distribution over any cross section of rail is very complex. However, the residual stresses will be in equilibrium over a short length of the rail, and the net axial force from residual stresses should be negligible. Therefore, these stresses do not contribute to buckling.

The axial component of the mechanical and thermal stresses is expected to be distributed fairly uniformly over the cross section of the rail. It is this component of axial stress, or net axial force, in the rail that contributes to buckling and is the principal objective of a measurement technique.

This paper describes a novel technique for measuring the net axial mechanical and thermal stresses independent of any residual stresses and local variations of physical properties. The technique is based on two physical phenomena of ferromagnetic materials -- namely, magnetostriction and magnetomechanical damping. Some preliminary experimental results from a specimen of rail steel are presented. The major advantages of this technique are described, together with recommended future experiments that are needed to further evaluate the feasibility of using this technique for measuring thermal stresses in rails.

Background

The manufacture and service of standard railroad rail produce large variations in the residual stresses along the length and cross section of the rail. Manufacturing anomalies and cold working of the rail head during normal use also introduce large local variations in the metallurgical and physical properties. These variations introduce considerable statistical spread in the ultrasonic velocity and similar properties of the rail. The expected change in ultrasonic velocity owing to the acoustoelastic effect is much smaller than the statistical variations of the ultrasonic velocity owing to unavoidable anomalies. Therefore, in spite of its many advantages, the conventional ultrasonic technique based on the acoustoelastic effect alone has not proven to be practical for evaluating total stress.

However, this basic problem can be overcome. The solution lies in making two independent measurements of a physical property -- as, for example, ultrasonic attenuation -- that is influenced by two independent phenomena strongly coupled to the state of the stress in the rail. The difference between these two measurements of the ultrasonic attenuation under the influence of each of the two independent phenomena made separately, but at identical positions, will be a single-valued function of stress. For ferromagnetic materials such as rail steel, two strongly coupled phenomena that affect ultrasonic attenuation and depend on the state of stress are magnetostriction and magnetomechanical damping.

Physical Basis of the Magnetoultrasonic Technique

The principle of the proposed technique is based on the combination of two known physical phenomena for ferromagnetic materials. These are magnetostriction and mechanical damping.

Magnetostriction, or the Joule Effect, is the strain induced in a ferromagnetic material along the axis of an applied magnetic field. For steel, the sign and magnitude of strain along the axis of the magnetic field are independent of the direction of the field but dependent on the magnetic field strength. The maximum strain under no stress is about ± 8 microinches per inch. However, the strain produced by a magnetic field also depends on the total stress. Therefore, application of a magnetic field will produce a reversible change in the local stress. The magnitude of this change depends on the strength of the magnetic field.

Mechanical damping (attenuation) of the elastic (ultrasonic) waves depends on many physical properties, as well as the total stress in the material. Therefore, in ferromagnetic materials, application of an external magnetic field along a desired direction will change the ultrasonic attenuation owing to the reversible change in the stress distribution as a result of magnetostriction.

The ultrasonic attenuation in rail steel, therefore, is a strong function of the total stress and the applied magnetic field, and the change in ultrasonic attenuation measured with and without the presence of a known magnetic field can be used to measure the total unknown stress. The average value of the residual stress component of the total stress over a short length along the axis of the rail is expected to be zero. However, the average mechanical and thermal stresses along the same axis in general will not be zero. Therefore, it is possible to select an appropriate path for the ultrasonic beam that essentially eliminates the effect

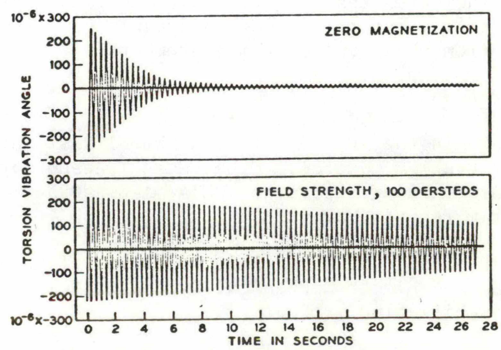

FIGURE 1. DAMPING OF TORSION OSCILLATIONS IN A CARBONYL IRON WIRE AS UNMAGNETIZED (ABOVE) OR MAGNETIZED IN A FIELD OF 100 OERSTEDS (BELOW)

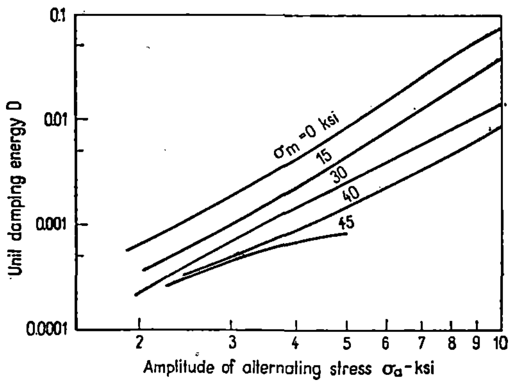

FIGURE 2. EFFECT OF STATIC MEAN STRESS σ_m ON UNIT DAMPING ENERGY OF MAGNETOELASTIC ALLOY TYPE 403

of residual stress on the measurement of change in ultrasonic attenuation. This provides a measurement of the remaining axial stress owing to mechanical and thermal forces alone, subject to the assumption of an equilibrated distribution of residual stresses.

Mechanical Damping. Figure 1 [1] shows the effect of an external magnetic field of 100 oersteds on the damping of torsional vibrations in carbonyl iron wire -- a significant decrease in attenuation in the presence of the magnetic field. Figure 2 [2] shows the effect of mean and alternating stress on unit damping energy in a magnetoelastic alloy type 403. Note that static mean stress decreases whereas alternating stress increases the mechanical loss factor in the ferromagnetic material. To our knowledge, similar data on rail steel have not been published to date.

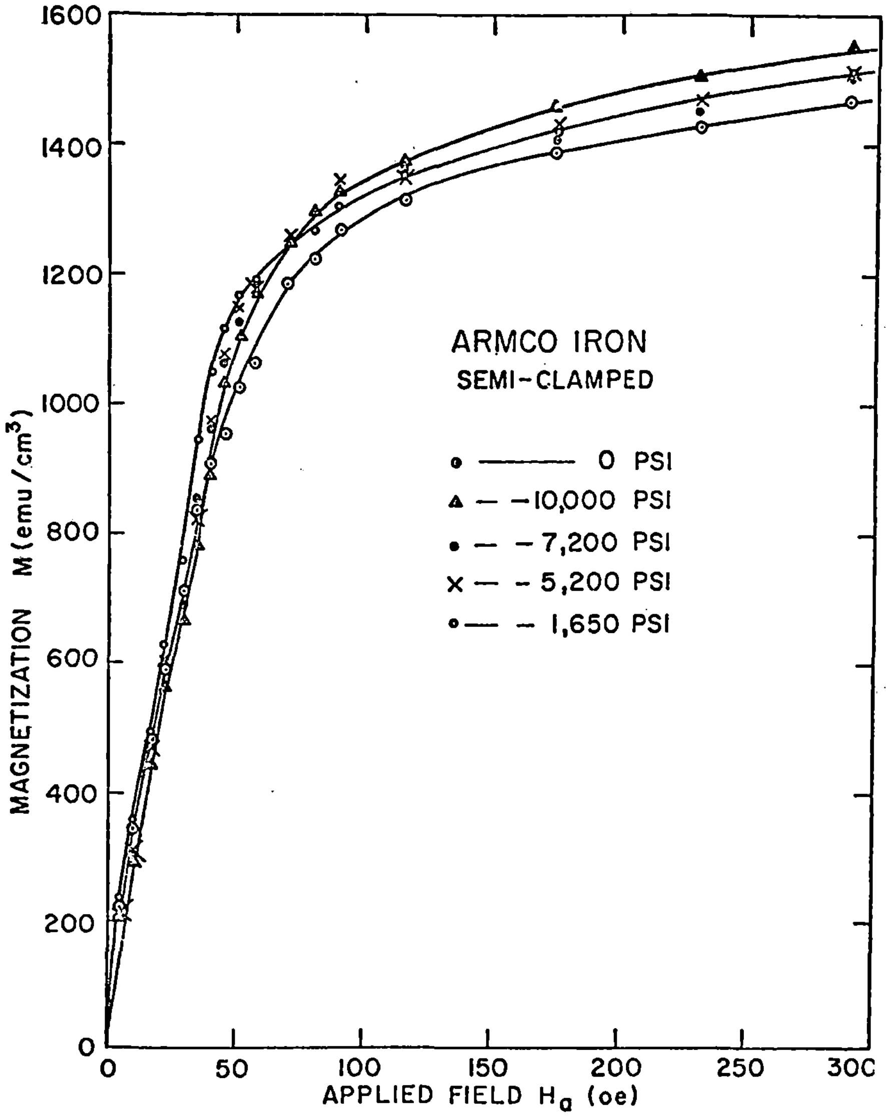

FIGURE 3. MAGNETIZATION OF IRON

Magnetostriction in Iron. The initial magnetization of iron is shown in figure 3 [3]. Stress levels affect the magnetization curve to a small extent, which probably is within the statistical variation of these properties of iron under no stress. However, the magnetostriction property is a strong function of the magnetizing field and stress. Figure 4 [3] shows the typical dependence of magnetostriction on the initial stress (in an Instron testing machine) and magnetizing field in Armco iron. Compressive stress increases the positive magnetostriction significantly, whereas tensile stress suppresses the positive magnetostriction all the way to the negative magnetostriction effect. No data of this type have yet been published for rail steels, but such steels are expected to exhibit a similar behavior.

Experimental Observations

Although the magnetostrictive and magnetomechanical damping properties of rail steel were not available, some simple, preliminary experiments with rail steel have been made at Battelle's Columbus Laboratories to demonstrate the feasibility of this concept. A 0.5-inch-thick plate was milled from the head section of a standard 136-pound rail from the track at the Facility for Accelerated Service Testing (FAST). The milling faces were parallel to the vertical plane of symmetry. The entire plate, about 18 inches long and 1.5 inches wide, was stress relieved at 1,250° F for 14 hours and allowed to furnace cool for 4 days to relieve all residual stresses. A rod, 2 inches long and 0.5-inch square cross section, was carefully machined from this plate for the experimental study. The rate of metal removal was kept as slow as practicable to minimize machining stresses at the surfaces.

Figure 5 shows the schematic of the experimental setup. External compressive stress was applied by clamping the specimen by two bolts as shown in the upper portion of the figure. The stress was varied by adjusting the torque on the bolts. The magnetic field was supplied by a horseshoe electromagnet connected to a variable direct current power supply. The magnet was designed to generate a magnetizing force of 0 to 100 oersteds in the rail steel specimen. An ultrasonic transducer operating at a nominal frequency of 2.25 megahertz was used to measure the ultrasonic attenuation in the rail steel. The ultrasonic transducer, a wideband piezoelectric device, was used in the pulse-echo mode. The ultrasonic pulse generator connected to the transducer sent out electrical impulses at a pulse repetition rate of 1 kilohertz. The pulse generator also was used to trigger an oscilloscope, which displayed the ultrasonic echoes. This arrangement is similar to the familiar A-scope presentation of ultrasonic pulses. Figures 6 and 7 show the typical oscilloscope display of the ultrasonic echoes from different interfaces of the specimen under zero stress and under 28,000 psi compressive stress.

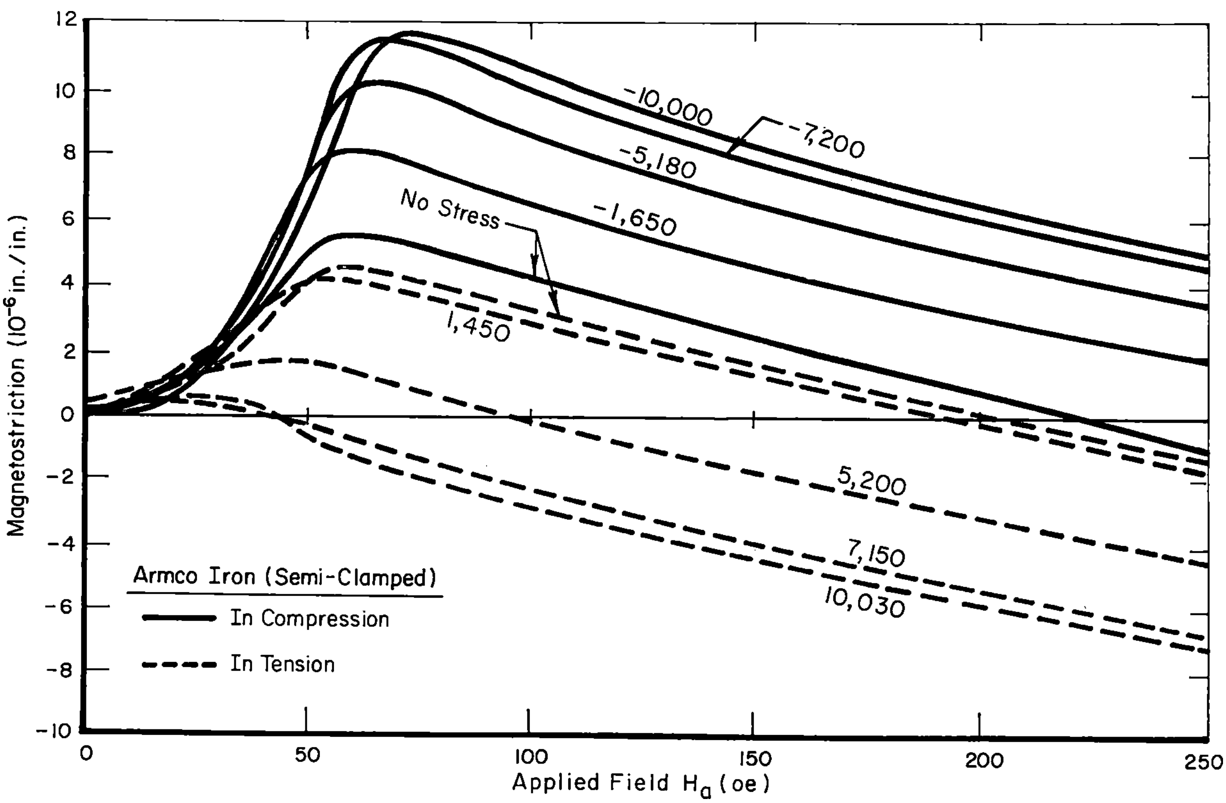

FIGURE 4. EFFECT OF STRESS AND MAGNETIC FIELD ON MAGNETOSTRICTION IN IRON

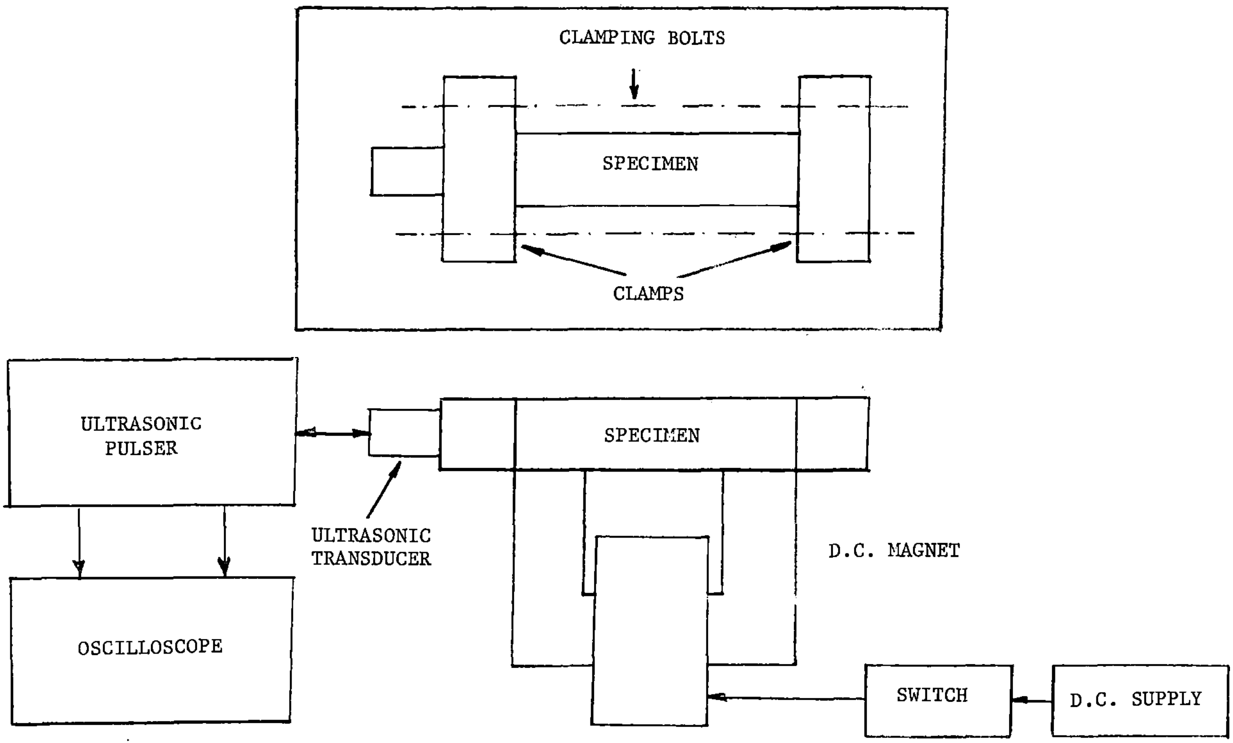

FIGURE 5. SCHEMATIC EXPERIMENTAL SETUP FOR MAGNETOULTRASONIC STRESS EVALUATION

Initially, the compressive stress was adjusted to be almost zero while maintaining the ultrasonic coupling. As shown in figure 6, there was practically no change in echo amplitude under otherwise identical conditions with or without the presence of an external magnetic field. However, when the compressive stress was increased to 14,000 or 28,000 pounds-force per square inch (psi), the amplitude of the echo decreased significantly in the presence of the magnetic field as compared to the echo amplitude with no magnetic field (figure 7).

The percentage change in amplitude of the echo from the back of the specimen caused by an applied magnetic field of 50 oersteds was plotted as a function of applied stress. Figure 8 shows the results of this preliminary experiment. The vertical lines show the actual spread of the experimental data taken at 14,000 psi and 28,000 psi. We believe signal averaging techniques can be used to reduce the spread of the data.

Discussion of Results

Figure 8 shows that the percentage change in ultrasonic echo amplitude attributable to a known change in magnetic field is a monotonic function of the applied compressive stress. Therefore, such a calibration curve can be used to estimate the unknown axial stress, σ, in rails by measuring the percentage decrease in the echo or transmitted ultrasonic amplitude caused by a known magnetic field.

A series of calibration curves can be obtained for both compressive and tensile stresses in rail steel at various known values of magnetic field and ultrasonic frequencies. An optimal ultrasonic frequency can be selected from these calibration curves for a specified range of stress and magnetic fields.

Ultrasonic pulses can be generated easily at a repetition rate of 1 kilohertz. Therefore, two measurements of the ultrasonic pulse amplitude, with and without the magnetic field, can be made within a few milliseconds. The change in the amplitude can be compared manually or electronically to evaluate the unknown stress in the rail. As pointed out previously, the ultrasonic path in the rail can be optimized to minimize the effect of residual stress on the change in ultrasonic amplitude. Therefore, the change in ultrasonic amplitude would depend only on the net mechanical and thermal stresses, but it would be independent of the local variation of physical properties along the path of the ultrasonic beam.

Advantages of the Technique

The key advantage of this technique is that it is based on a difference in ultrasonic attenuation, with and without a known magnetic field, rather than on an absolute value. As discussed previously, the absolute values of attenuation or similar properties depend on many different factors, including the total stress. The application of the Joule Effect enables one to isolate the effect of the total stress, so

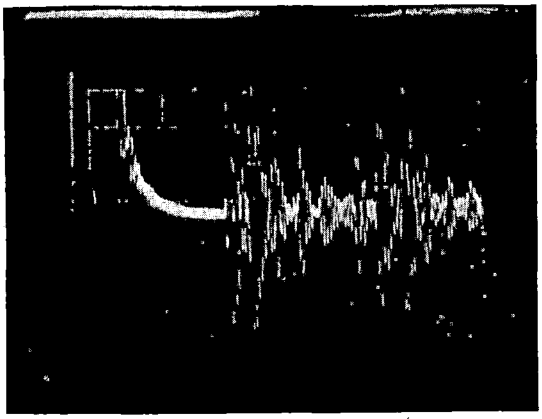

a. Magnetizing Field = 0

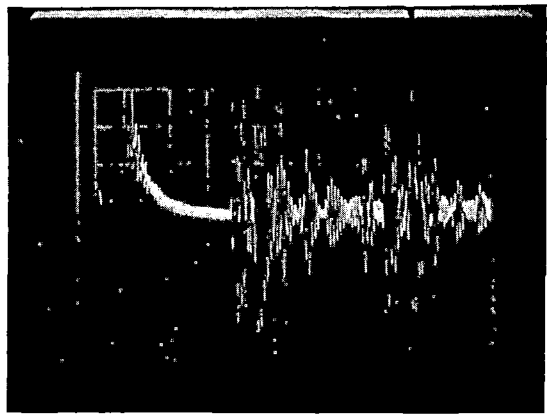

b. Magnetizing Field = 50 Oersted

FIGURE 6. ULTRASONIC ECHOES FROM SPECIMEN OF ANNEALED RAIL STEEL UNDER ZERO STRESS

that the differential attenuation is a single-valued function of the total stress under known conditions of the magnetic field.

Consider that α is the ultrasonic attenuation coefficient, α_0 is the mean of α, and $\Delta\alpha$ is the standard deviation of α. Therefore, assuming a statistical normal variation, a measured value of α will satisfy

$$(\alpha_0 - 3\Delta\alpha) < \alpha < (\alpha_0 + 3\Delta\alpha)$$

with 99.7 percent confidence.

Let the effect of stress on α be given by (assuming a linear model)

$$\alpha' = \alpha + a \cdot \sigma,$$

where σ is the stress and a is the stress coefficient of α. The stress coefficient, a, of α or similar property is very small. Therefore α' is very likely to be within the statistical variation of α given by

$$(\alpha_0 - 3\ \Delta\alpha) < \alpha' < (\alpha_0 + 3\Delta\alpha).$$

Therefore, it is not feasible to differentiate between normal variation of α and the effect of stress on α.

This is a serious drawback of most other techniques for nondestructively evaluating stress that are based on a single measurement. The effect of stress alone on the measured property -- for example, ultrasonic velocity or molecular lattice spacing -- is much smaller than the statistical spread of these properties.

Now consider the combined effect of stress and magnetic field on ultrasonic attenuation. Let the effect of a magnetizing field, H, along the axis of a rail under an axial stress σ be given by

$$\alpha'' = \alpha + a\sigma + f\ (H, \sigma),$$

where f (H, σ) is a nonlinear function of H and σ. α'' may still be within the statistical variation

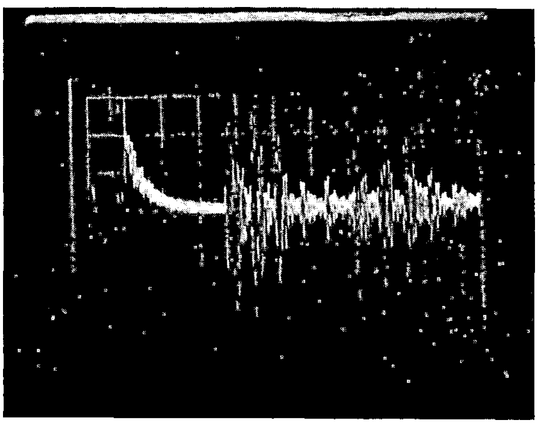

a. Magnetizing Field = 0

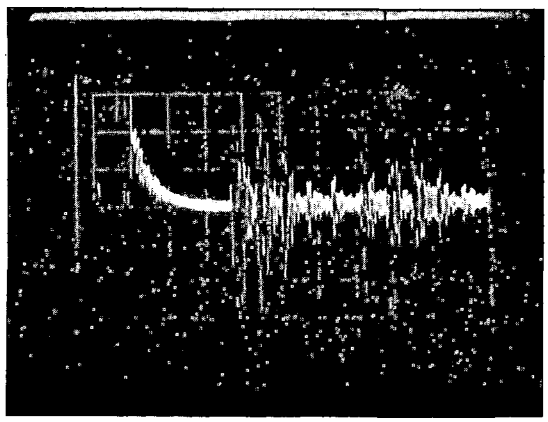

b. Magnetizing Field = 50 Oersted

FIGURE 7. ULTRASONIC ECHOES FROM SPECIMEN OF RAIL STEEL, COMPRESSIVE STRESS = 28,000 PSI

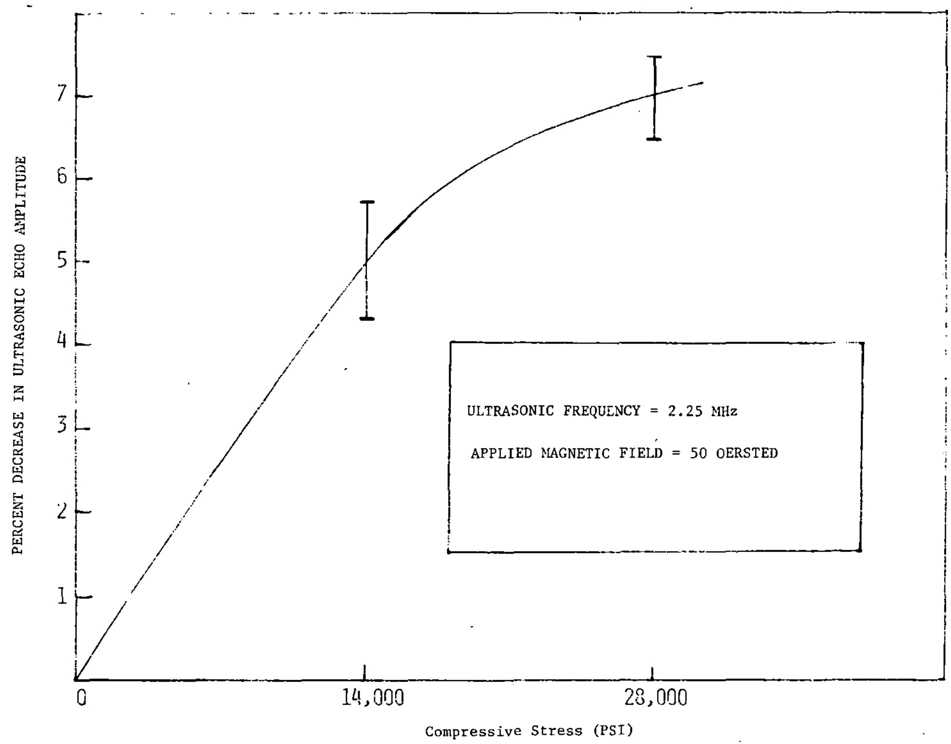

FIGURE 8. PERCENTAGE DECREASE IN ULTRASONIC ECHO AMPLITUDE OWING TO EXTERNAL MAGNETIC FIELD IN ANNEALED RAIL STEEL UNDER STRESS

of α, but the change in attenuation given by

$$\alpha'' - \alpha' = f\ (H, \sigma)$$

is independent of the statistical variation of α.

Note that the difference in attentuation depends both on the magnetic field and the level of stress in the specimen. For a known value of H and the calibration function f (H, σ), σ can be evaluated. The statistical uncertainty of the difference is essentially the uncertainty of the calibration function f (H, σ). However, the measurement is not affected by the local variations of ultrasonic attenuation or other physical properties, because both of the measurements were made under identical physical conditions, except for the application of the magnetic field.

Conclusions

This paper describes the basic physical principles and some preliminary experimental data of a novel technique for the nondestructive evaluation of stress in a ferromagnetic material. The technique is based on two measurements of the ultrasonic attenuation or pulse amplitude at the same location in the rail, with and without the presence of an axial magnetic field. The difference between these two measurements is a function of the net mechanical and thermal stress and is independent of all other local anomalies.

The magnetoultrasonic technique has many promising features. These can be summarized as follows:

a. The technique is nondestructive.

b. The technique eliminates the effect of local variations of physical properties on the measured value of stress.

c. The technique can be implemented to measure the net force with negligible effect owing to residual stress.

d. The technique can be implemented using proven rail inspection hardware (for example, ultrasonic and magnetic flaw detection hardware).

e. The technique is rugged and simple.

f. It is feasible to make continuous or moving measurements in the same way that ultrasonic and magnetic flaw detection is done on rail test cars.

g. The technique requires no surface preparation.

h. The technique requires no zeroing.

i. The technique requires minimum calibration.

References

[1] Bozorth, M. Ferromagnetism. Princeton, New Jersey: Van Nostrand Company, Inc., 1951.

[2] Lazan, B. J. Damping of Materials and Members in Structural Mechanics. New York: Pergamon Press, Inc., 1968.

[3] Allen, C. W., et al. "The Effect of Stress on the Magnetostriction of Iron, Nickel and 49 Permalloy." Office of Naval Research, U.S. Department of the Navy, Project THEMIS final report no. THEMIS-UND-70-9.

"Magnetomechanical Acoustic Emission for Residual Stress Measurements in Railroad Rails and Wheels"*

Kanji Ono
M. Shibata

School of Engineering and Applied Science
University of California at Los Angeles

Introduction

Residual stresses in various structures and components often cause premature failures. In the rail transportation industry, longitudinal compressive stresses in rails have resulted in numerous cases of lateral buckling. Widespread use of continuously welded rail is partly responsible for increased occurrences of buckling owing to constrained thermal expansions [1]. In numbers, failures of railroad wheels occur more often than those of rails. Consequences of some of the wheel failures also are very serious. New wheels have built-in residual compressive stresses in the rim section. However, repeated braking and attendant thermal cycling gradually reduce such compressive stresses. After the residual stresses become tensile, the wheel readily fails whenever a critical crack develops from thermal fatigue [2].

For nondestructive measurement of residual stress, several techniques have been developed. Some of them have been used for industrial applications. X-ray diffraction is the most commonly utilized [3]. Techniques based on shear wave acoustic birefringence [4] and magnetic Barkhausen effect [5] are emerging from the laboratory to field usage. These and other methods are covered in other technical papers being presented at this conference, and some promising applications appear to be in the making.

This paper reports preliminary results of magnetomechanical acoustic emission (AE) phenomenon and its application to residual stress measurement in rails and wheels. The magnetomechanical AE is a mechanical counterpart of magnetic Barkhausen effect [6], [7]. It was first discovered by Lord [8] and its stress dependence was found by Kusanagi et al. [9]. When the level of applied magnetic field is varied, the shift in magnetic domain structures produces ultrasonic waves, which are detected as AE signals. In the absence of a magnetic field, AE attributable to domain wall motion was also reported during tensile testing of iron [10]. Because of the potential of the magnetomechanical AE phenomenon as a new nondestructive method for stress measurement, we have studied the phenomenon in several steels and iron [11]. In this study, we extended the measurement to rail and wheel steels to assess the feasibility of developing a useful instrument for field use.

Experimental Procedures

Rail and wheel steels were used in this study. Samples of rail steel were taken from the head section of a rail section supplied by the Association of American Railroads (AAR), Chicago, Illinois, and utilized in a fatigue fracture study by Lund [12]. Wheel steel samples were identical to those used by Fowler [13]. The samples were identified as Wheel B in the Fowler study. The chemical composition of these materials is given in table 1 (see page 117).

In the as-received conditions, both materials had fully pearlitic microstructures. Rail and wheel samples were annealed at 1,173° kelvin (K)

*A presentation based on this paper was scheduled to be delivered at conference, but neither author was able to attend.

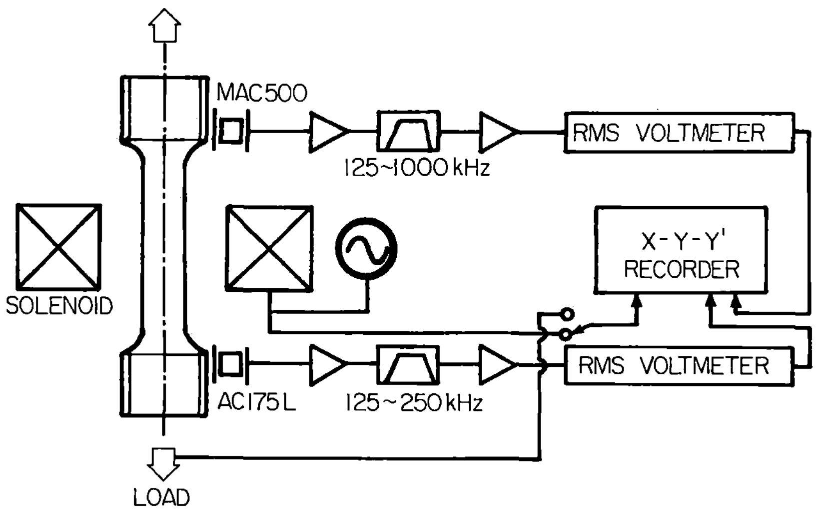

FIGURE 1. SCHEMATIC DIAGRAM OF EXPERIMENTAL SETUP

for 1 hour and furnace cooled. Wheel samples were also oil-quenched after austenitizing at 1,173 K for 1 hour. An oil-quenched sample also was tempered at 773 K or 923 K for 1 hour and air-cooled. Annealed samples were fully pearlitic, whereas the oil-quenched samples were martensitic.

TABLE 1

CHEMICAL COMPOSITION OF SAMPLES

Element	Rail (Head Section)	Wheel (B)
Carbon	0.67	0.74
Manganese	0.90	0.68
Silicon	0.17	0.27
Phosphorus	0.018	0.018
Sulfur	0.024	0.040
Chromium	0.03	0.16
Nickel	< 0.01	0.15
Molybdenum	0.02	0.03
Copper	0.01	0.15

Round tensile specimens of the half-size ASTM standard geometry (E-8) were machined. The gage section was 6.3 millimeters in diameter and 32 millimeters in length, and the total length was 84 millimeters. The threaded grip sections were 12.7 millimeters in diameter. Following heat treatment and thorough cleaning, a sample was mounted in threaded grips with teflon tape lubrication. Two transducers for AE detection were attached to the flat ends. These were a resonant transducer with the nominal center frequency of 175 kilohertz (AC 175L, Acoustic Emission Technology Corporation [AETC], Sacramento, California) and a miniature sensor with the nominal resonant frequency of 500 kilohertz (MAC-500, AETC). The former was coupled via viscous resin, while the latter was glued to the sample using cyanoacrylate ester. The transducer outputs were amplified 60 decibels using preamplifiers (160, AETC) with bandpass filter plugins of 125-250 kilohertz and 125-1000 kilohertz, respectively. The root mean square (rms) voltages of the amplified outputs were measured using true rms reading voltmeters (3400 A, Hewlett-Packard, Palo Alto, California) and an X-Y-Y recorder. Figure 1 illustrates the experimental setup.

Stressing and plastic deformation of a sample was performed using a floor-model Instron. The magnetic field on the sample was generated by a solenoid encircling the gage section of the sample. It was powered through a variac with alternating current voltages of up to 140 volts at 60 hertz. The maximum magnetic field generated was 25,500 amperes per meter rms at the center of the solenoid, the casing of which was 25 millimeters in inside diameter and 33 millimeters in length. The sample was thus magnetized longitudinally and the magnetic circuit was open-ended.

Results and Discussion

Typical results of AE output (referred to at the preamplifier input) versus the field strength are shown in figure 2. Here, applied stress, σ^A, was absent and the low-frequency transducer (AC 175L) was used. The intensity of AE at a given stress increased with the magnetic field strength. At the maximum field strength employed, the AE output tended to approach a saturation level. The maximum AE intensity was the highest for quenched and tempered wheel and quenched wheel in the decreasing order. The AE output of the quenched wheel was significantly lower than other sample conditions. In all the materials tested, the initial increase in the AE intensity was small until the field strength reached 1,500 to 2,000 amperes per meter.

An example of variation in the AE intensity field strength curves owing to stress is shown in figure 3. Results for annealed wheel steel are given for each of the two transducers at three levels of stress -- 0, ± 69 million pascals (MPa) (10 thousand pounds-force per square inch [ksi]), and ± 138 MPa (20 ksi). A significant drop in the maximum AE intensity was observed by applying external stress, which also affected the shape of the AE intensity versus field strength curve. For this material, the AE intensity decreased more rapidly with tensile stress than with compressive stress.

The AE intensity of annealed rail steel is plotted against stress in figure 4. Here, three field strength levels were selected. For each level, the AE outputs of the two transducers were shown as a function of stress. The outputs of the

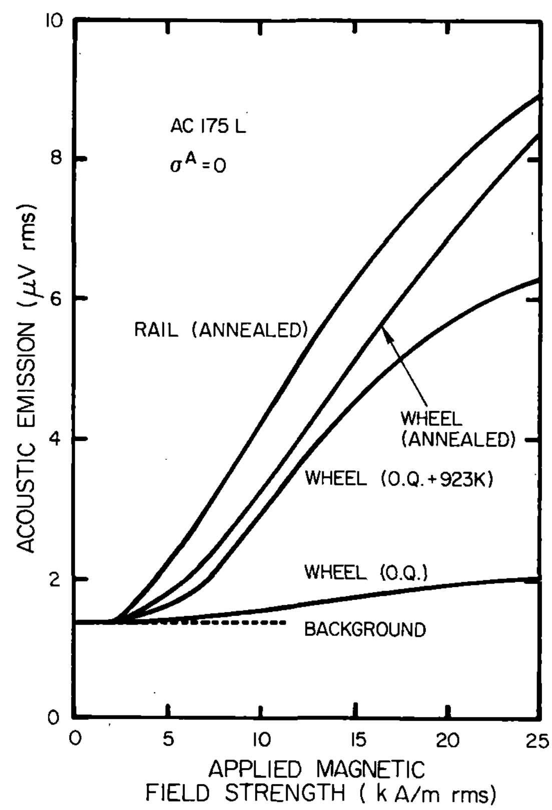

FIGURE 2. ACOUSTIC EMISSION VERSUS APPLIED MAGNETIC FIELD STRENGTH FOR RAIL AND WHEEL STEELS AT 175 KILOHERTZ WITHOUT APPLIED STRESS

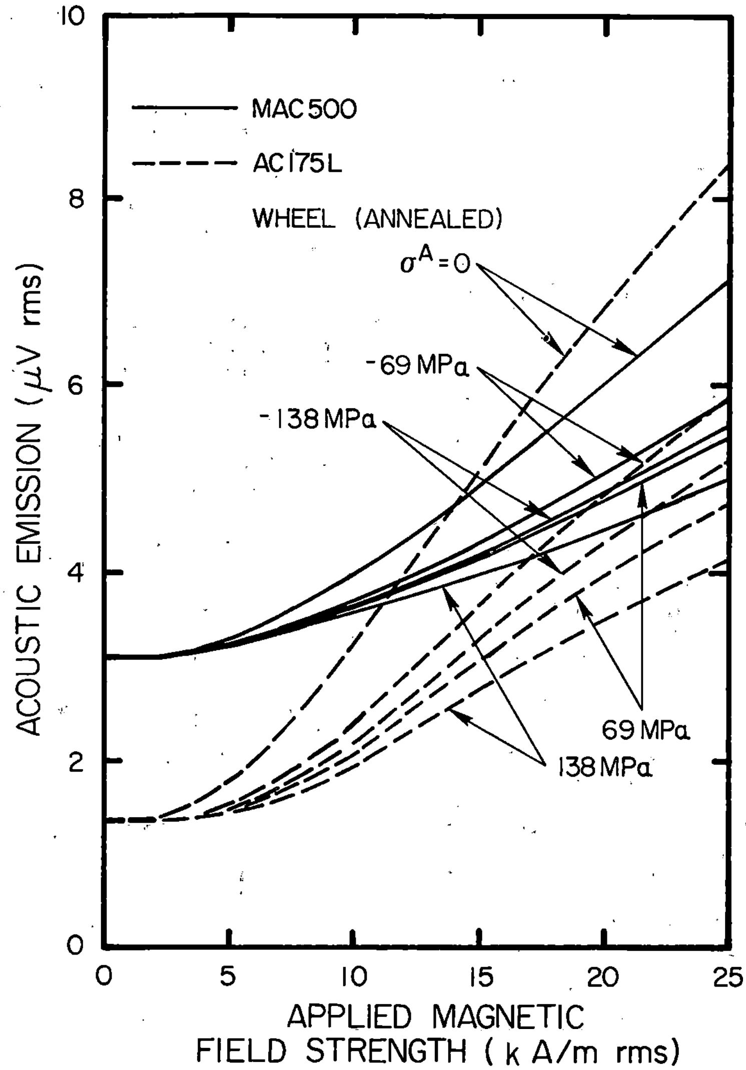

FIGURE 3. ACOUSTIC EMISSION VERSUS APPLIED MAGNETIC FIELD STRENGTH FOR ANNEALED WHEEL STEEL AT THREE STRESS LEVELS -- 0, ± 69 MPa, AND ± 138 MPa

lower frequency transducer were higher at two of the magnetization levels. Relative effects of stress were greater at lower stresses. Stress effects also depended on frequency. At the tensile stress level of 130 MPa, the AE intensity (at 22,500 amperes per meter) decreased to 62 percent at 175 kilohertz (nominal resonant frequency) and to 74 percent at 500 kilohertz (also nominal resonant frequency) in comparison to the zero stress level. Note that the AE levels were asymmetrical with respect to the direction of applied stress. Under compressive stress, the decrease in the AE output was about two-thirds that under tensile stress. When the field level was high and stress was low, notable hysteresis effects were observed. However, the difference in the AE output were less than 5 percent.

When an as-received rail sample was tested, the AE outputs at 7,500 amperes per meter and at zero stress decreased in comparison to those of annealed samples (compare figures 4 and 5). At higher field strength levels, the zero stress AE outputs were comparable between the annealed and as-received samples. However, the stress dependence of the AE output was reduced in the as-received sample; for example, the AE intensity decreased to only 73 percent instead of 62 percent (175 kilohertz, 22,500 amperes per meter, 130 MPa). This was also reflected in less steep slopes of the curves of the AE versus σ^A plots in figure 5 in comparison with those of figure 4.

In figure 6, similar plots are shown for an annealed and deformed sample of rail steel. The sample was stretched 12 percent in tension. Zero stress AE outputs were reduced 10-20 percent from the corresponding levels observed in the annealed sample (figure 4). The most notable change was the smaller stress dependence of AE output under tensile stress. The shapes of the AE versus σ^A curves on the compression side were less affected. From these results, the differences in the AE responses between the annealed and as-received

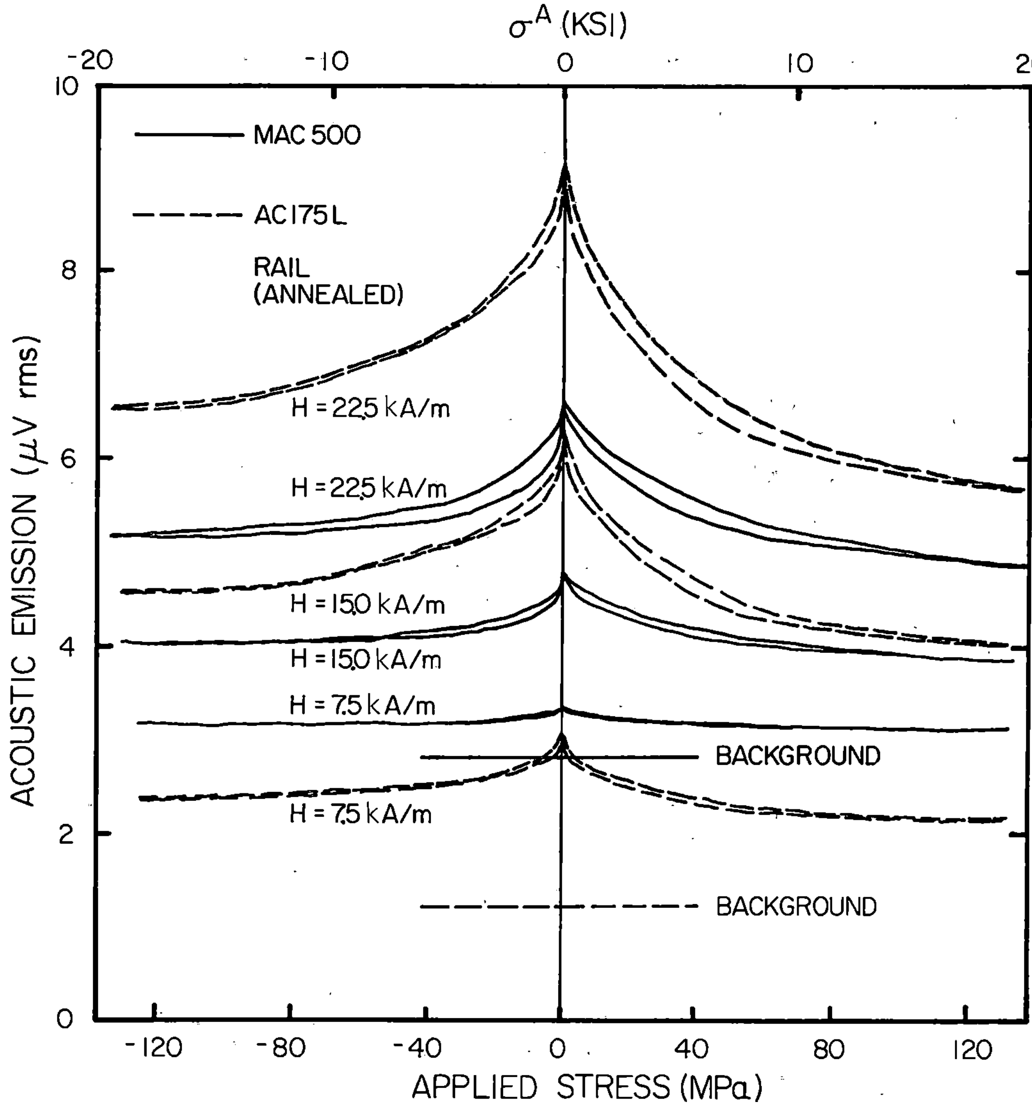

FIGURE 4. ACOUSTIC EMISSION VERSUS APPLIED STRESS FOR ANNEALED RAIL STEEL AT THREE MAGNETIZATION LEVELS

samples appear to originate from prior deformation in the latter. While various microstructural effects cannot be ruled out, the reduction in stress dependence found in the cold worked sample supports this suggestion.

When the AE outputs of the annealed and cold worked samples were compared, those of the annealed sample were always greater under compressive stress and under limited levels of tensile stress. Under high tensile stresses (for example, above 40 MPa for AC 175L transducer outputs), the relative intensities were reversed and the cold worked sample emitted higher levels of AE signals. This behavior may be a consequence of tensile deformation of the sample. Thus it is likely that compressive deformation produces an opposite effect; namely, less stress dependence under compressive stressing than under tensile stressing.

Stress dependencies of AE outputs for an annealed wheel steel sample are shown in figure 7. At 175 kilohertz, the observed AE levels were lower and stress dependencies were greater than in a rail steel sample. At 500 kilohertz, both the AE levels and stress dependencies were comparable between wheel and rail samples. Differences between the two materials are basically attributable to carbon content, which affects the fraction of ferrite. As the rail steel is expected to contain more ferrite (although not clearly observed to be under microscopic examination), the lower frequency AE signals, which were stronger in rail, may be attributed to larger ferrite content.

When wheel steel was quenched in oil, the AE output decreased greatly even under the highest applied magnetic field (see figures 8 and 9). Here, one also finds that tempering restores much

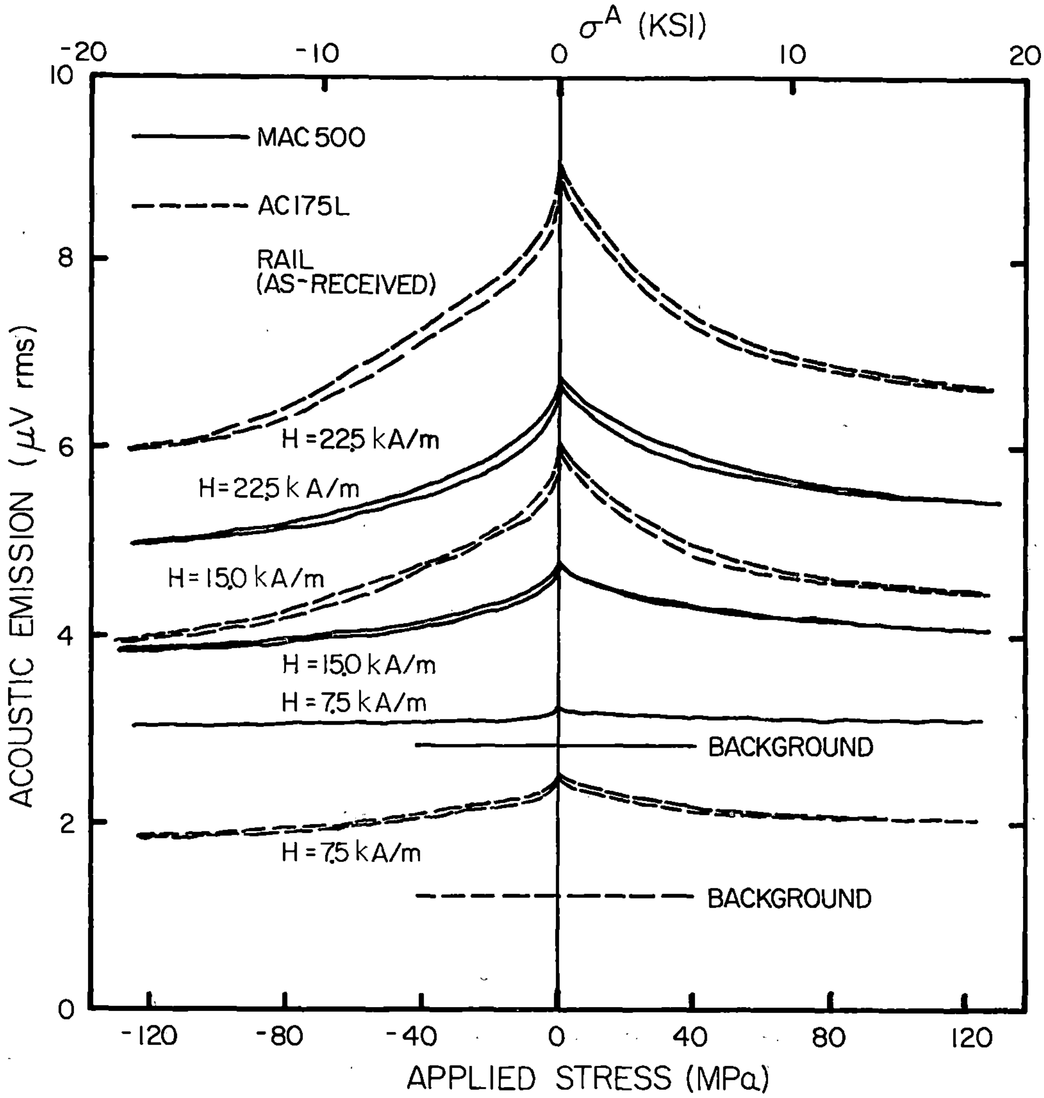

FIGURE 5. ACOUSTIC EMISSION VERSUS APPLIED STRESS FOR AS-RECEIVED RAIL STEEL AT THREE MAGNETIZATION LEVELS

of the reduction. After 773 K tempering, AE outputs at 500 kilohertz were increased to the levels for the annealed sample. In this condition, the low-frequency AE outputs were still about half those for the annealed sample. After tempering at 923 K, peak AE outputs recovered to about 90 percent of the levels in the annealed sample. The observed stress dependence under compressive stressing developed a hump at -20 MPa to -30 MPa. Similar humps were observed on the tension side in 1020 and A533B steels after 10-18 percent cold work [11].

Observed variations in AE output owing to microstructural changes can be utilized for the detection of inadvertently produced martensite regions in railroad wheels. While residual stress affects the AE level significantly, the martensite produces a very large decrease in the AE signal level so that its presence can readily be probed. The present observation also implies that residual stress measurement cannot rely on the amplitude of the AE output by itself, because of large microstructural effects.

It was reported earlier [11] that the ratio of AE output level at 175 kilohertz to that at 500 kilohertz exhibits unique stress dependence in 1020 and A533B steels. Such ratios are indicative of the frequency spectrum of AE signals and can be combined with the intensity of the AE signals to identify the residual stress, prior to cold work and microstructural changes. Using the outputs from the two transducers, we define the AE ratio, R, as

$$R = \overline{V}_r \text{ (at 175 kHz)}/\overline{V}_r \text{ (at 500 kHz)}$$

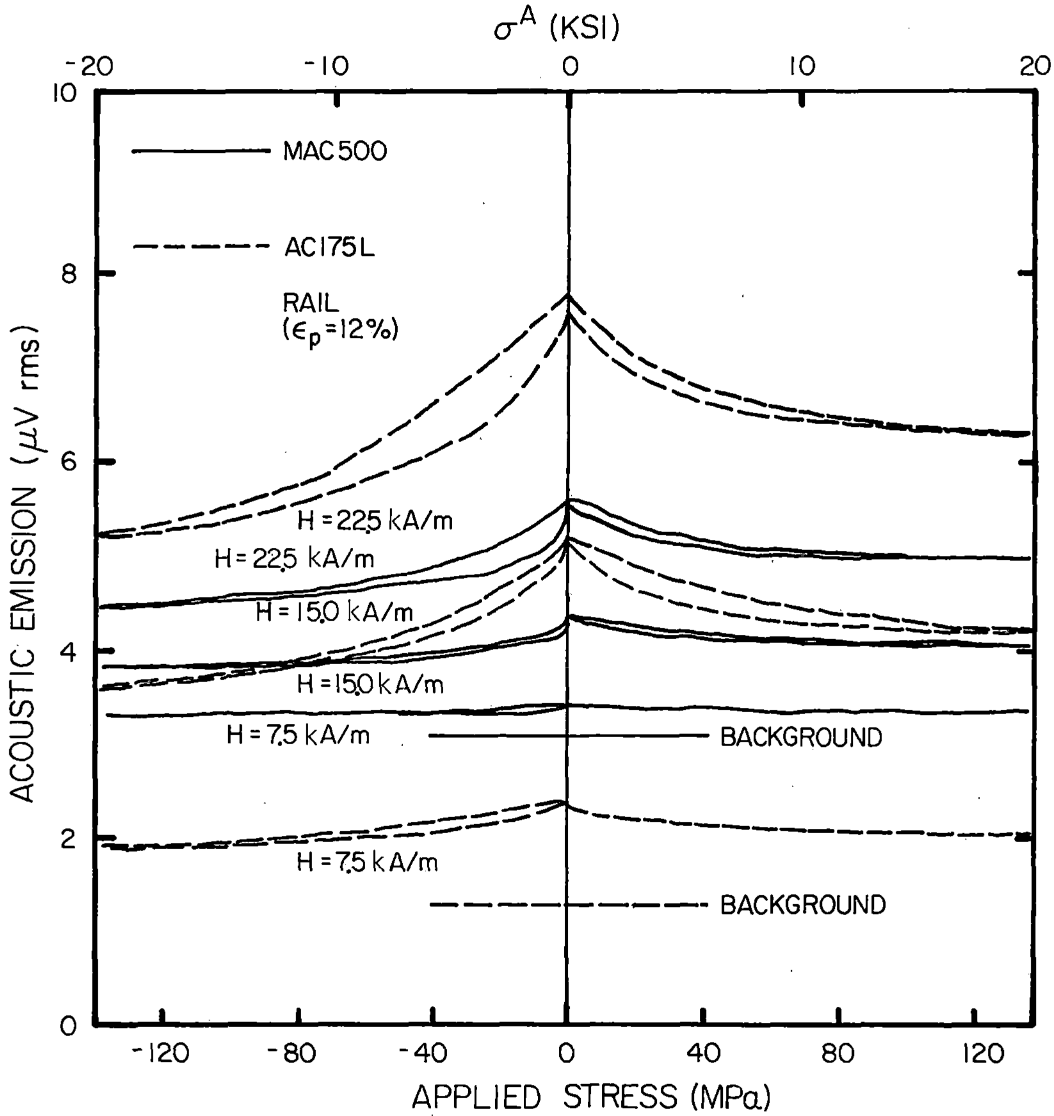

FIGURE 6. ACOUSTIC EMISSION VERSUS APPLIED STRESS FOR RAIL STEEL, ANNEALED AND PLASTICALLY DEFORMED 12 PERCENT IN TENSION

Here, the AE outputs were corrected for the different background noise levels. The background noise correction followed the usual assumption of mean-square sum; that is, the mean-square voltage output equals the sum of the mean-square voltages of signal and noise. Because the frequency range is fixed by a transducer and the independence of signal and noise can be assured, the assumption is valid. Thus, the corrected rms voltage of AE signals, $\bar{V}_r$, is given by

$$\bar{V}_r^{\,2} = (V_{r,\,obs})^2 - (V_{r,\,noise})^2$$

where $V_{r,\,obs}$ is the rms voltage observed and $V_{r,\,noise}$ is the rms voltage of background noise, respectively.

Stress dependencies of the AE ratio, R, in rail and wheel steels are shown in figure 10. In the annealed condition, both steels exhibited a broad maximum near zero stress and asymmetric stress dependence. Values of R were 1.4 to 1.5 for rail steel and 1.0 to 1.2 for wheel steel, respectively. These stress dependencies were much less than that observed in annealed 1020 steel [11]. In the latter, R decreased from 1.8 at zero stress to 1.1 at 120 MPa. In the rail steel, cold work increased R values to 1.6 to 1.7 and the maximum was more pronounced. An increase in R owing to cold work also was found in cold worked A533B steel, but the opposite behavior was noted in cold worked 1020 steel [11]. Microstructural changes brought forth complex variation in R values. Martensitic structure resulted in an essentially constant R value of 1.1.

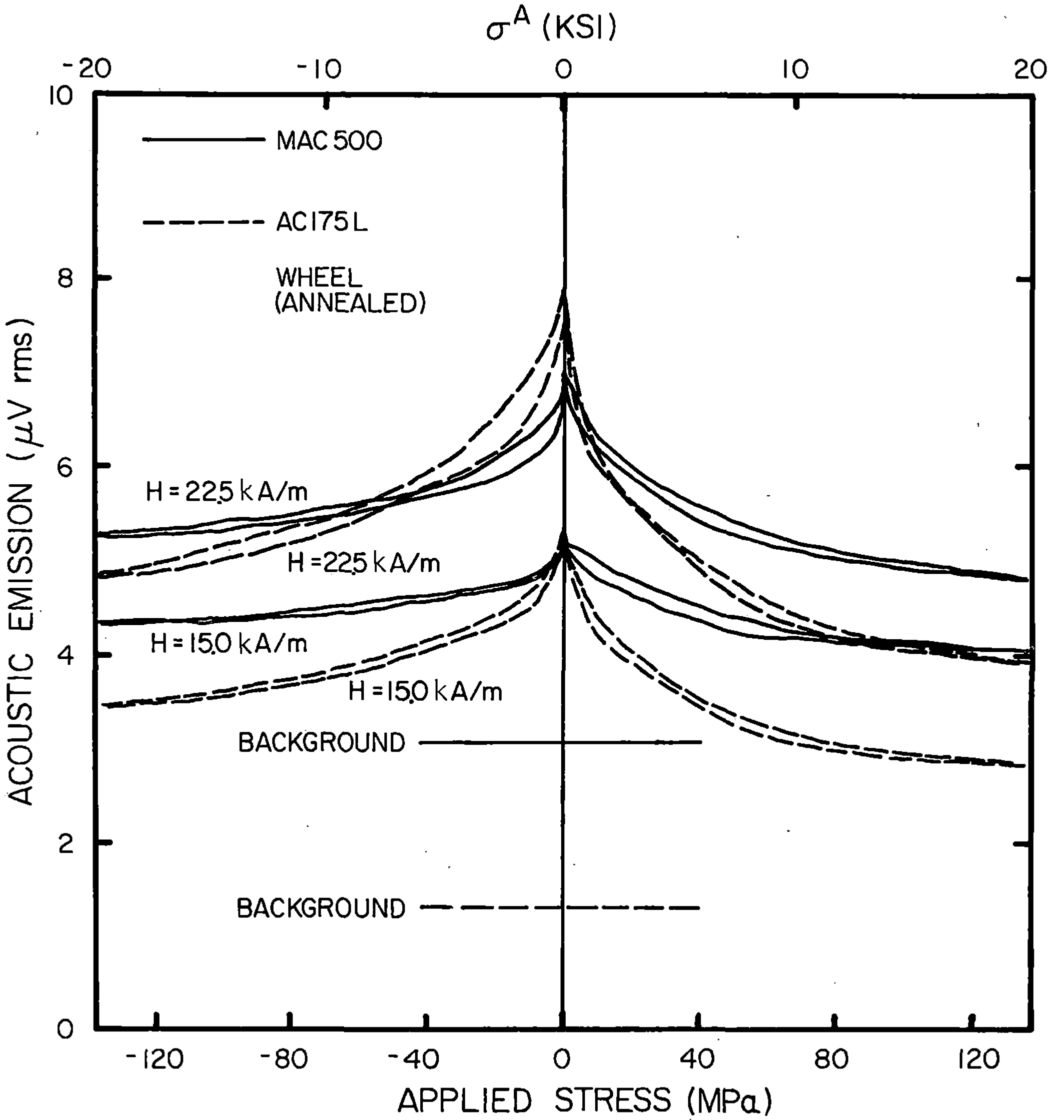

FIGURE 7. ACOUSTIC EMISSION VERSUS APPLIED STRESS FOR ANNEALED WHEEL STEEL AT TWO MAGNETIZATION LEVELS

Tempering at 773 K reduced R values to almost one-half of those for the annealed condition. That is to say, the low-frequency components in AE signals were decreased relative to the high-frequency components. Martensite tempered at 923 K tended to restore R values close to those of the annealed sample. However, a sharp maximum at zero stress was observed in the quench and temper condition and a small hump in R was also noted.

Presently, it is not understood what causes various changes in R values and their stress dependencies. However, their variation with respect to stress and microstructures can be employed in combination with the intensity of AE signals for unique determination of residual stress and heat treatment conditions. Basically, magnetomechanical AE phenomenon originates from displacement steps owing to the shift in magnetic domain structures, which elastically distort the material by way of magnetostriction. The domain structures are affected by microstructural constituents, dislocation substructures, and mechanical stresses, external as well as internal.

The mobility of domain walls also is affected by these parameters. Some of these effects have been recognized and studied [5], [7], [14], [15]. For example, the size of magnetic domains is reduced by stress [15]. This obviously is one of the reasons for the reduction of AE intensity under stress. The magnitude and sign of the magnetostriction are dependent on the material, its conditions, and applied stress [16]. As these parameters affect magnetomechanical AE signal output directly, significant influence on the AE characteristics is expected [8], [9], [11],

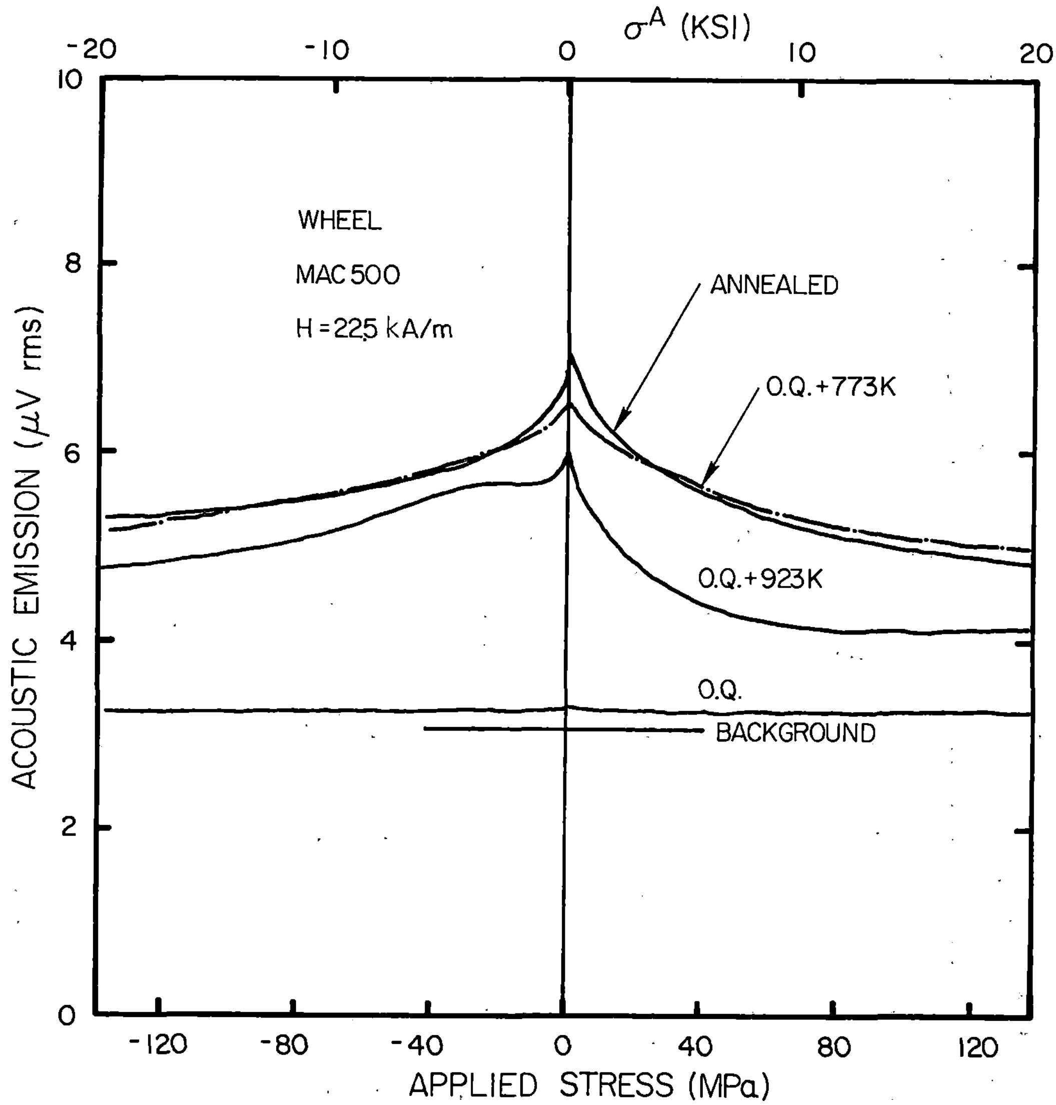

FIGURE 8. ACOUSTIC EMISSION VERSUS APPLIED STRESS FOR WHEEL STEEL OF FOUR DIFFERENT HEAT TREATMENTS AT 500 KILOHERTZ

although no quantitative study has been conducted.

Applications

From the present observations, it appears that practical devices for the inspection of rails and wheels can be developed. For rails, residual longitudinal stress can be measured by magnetizing along the length of a rail that is laid in the track and by determining AE intensities at two or more frequency ranges. The magnetization should be in the web section, because the head section of a rail is cold worked heavily after normal usages. Detection of AE signals can be at the contact surface of the rail head.

For the inspection of wheels, direct determination of residual stresses in the rim section appears to be difficult, because of severe local heating and attendant modification of microstructures that may result from successive high-speed braking stops. However, it is important to assess the degree of such microstructural modifications. Magnetomechanical AE technique should be an obvious choice for this purpose, because the output level is depressed drastically by the formation of martensite.

Thus, while much basic and developmental study remain to be done, the present findings show great promise for constructing field-usable devices to be used by railroad industry. These devices can be either based solely on magnetomechanical AE phenomenon or used in combination with other established methods. Regardless of the final configurations, it is certain that the reliability of railroad tracks and wheels will be enhanced by the use of these devices.

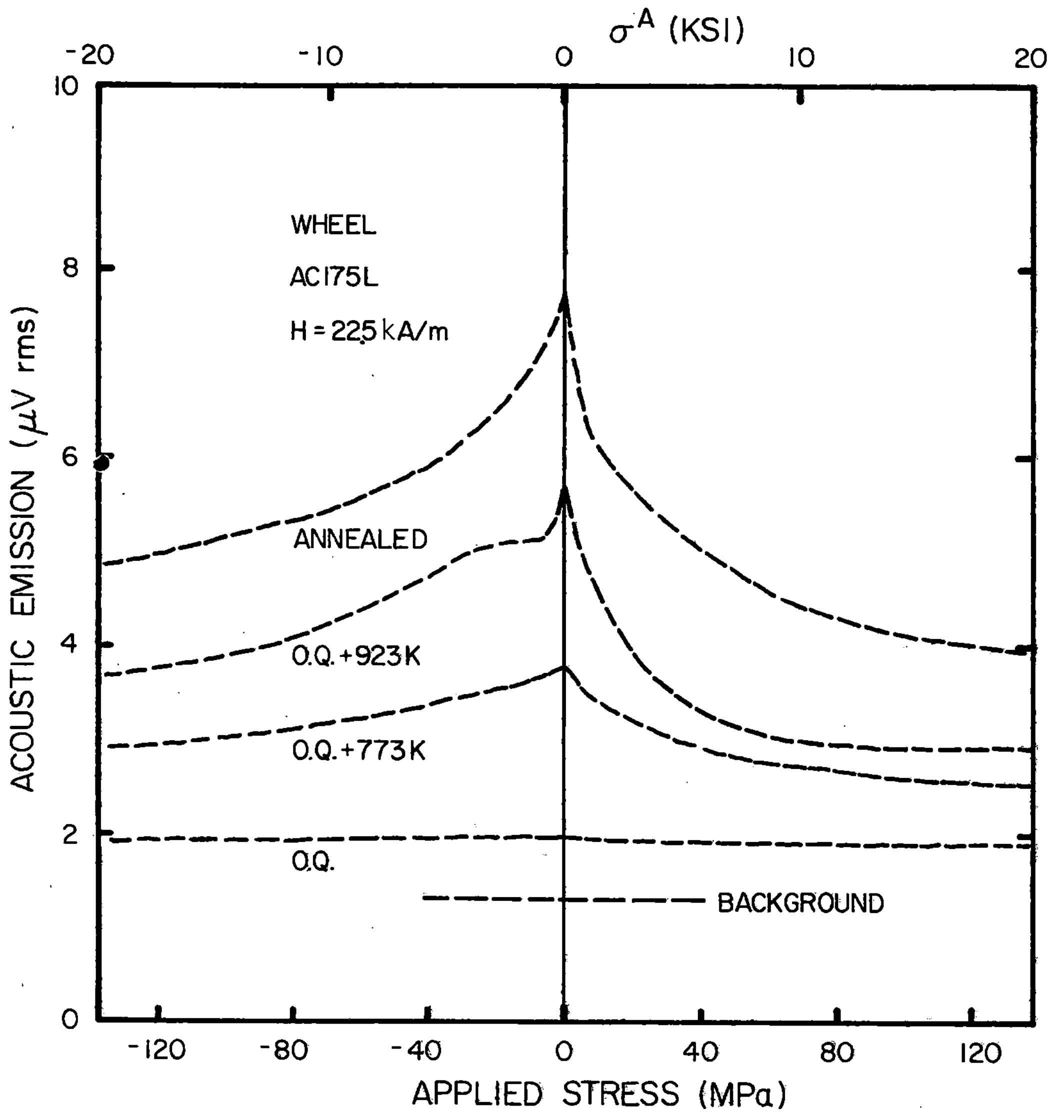

FIGURE 9. ACOUSTIC EMISSION VERSUS APPLIED STRESS FOR WHEEL STEEL OF FOUR DIFFERENT HEAT TREATMENTS AT 175 KILOHERTZ

Acknowledgments

This work has been supported by the Association of American Railroads' Technical Center (Chicago, Illinois) through a contract to NET Systems, Inc., Woodland Hills, California.

References

[1] Kerr, A. D. "Lateral Buckling of Railroad Tracks Due to Constrained Thermal Expansion -- A Critical Survey." In Railroad Track Mechanics and Technology, ed. A. D. Kerr. Proceedings of symposium held at Princeton University, April 21-23, 1975. Elmsford, New York: Pergamon Press, 1978.

[2] Carpenter, G. F. "The Cause of Thermal Fatigue Cracking in Metroliner Wheels," Federal Railroad Administration, report no. FRA/ORD-77/17 (March 1977).

[3] Cullity, B. D. Elements of X-Ray Diffraction. 2nd ed., pp. 447-78. Reading, Massachusetts: Addison-Wesley, 1978.

[4] Egle, D. M., and D. E. Bray. "Nondestructive Measurement of Longitudinal Rail Stresses: Application of the Acoustoelastic Effect of Rail Stress Measurements." Federal Railroad Administration, report no. FRA/ORD-77/09.1 (1978).

[5] Gardner, C. G., G. A. Matzkanin, and D. L. Davidson. International Journal of Nondestructive Testing, vol. 3 (1971), p. 131.

[6] Barkhausen, A. H. Physik. Vol. 20 (1919), p. 401.

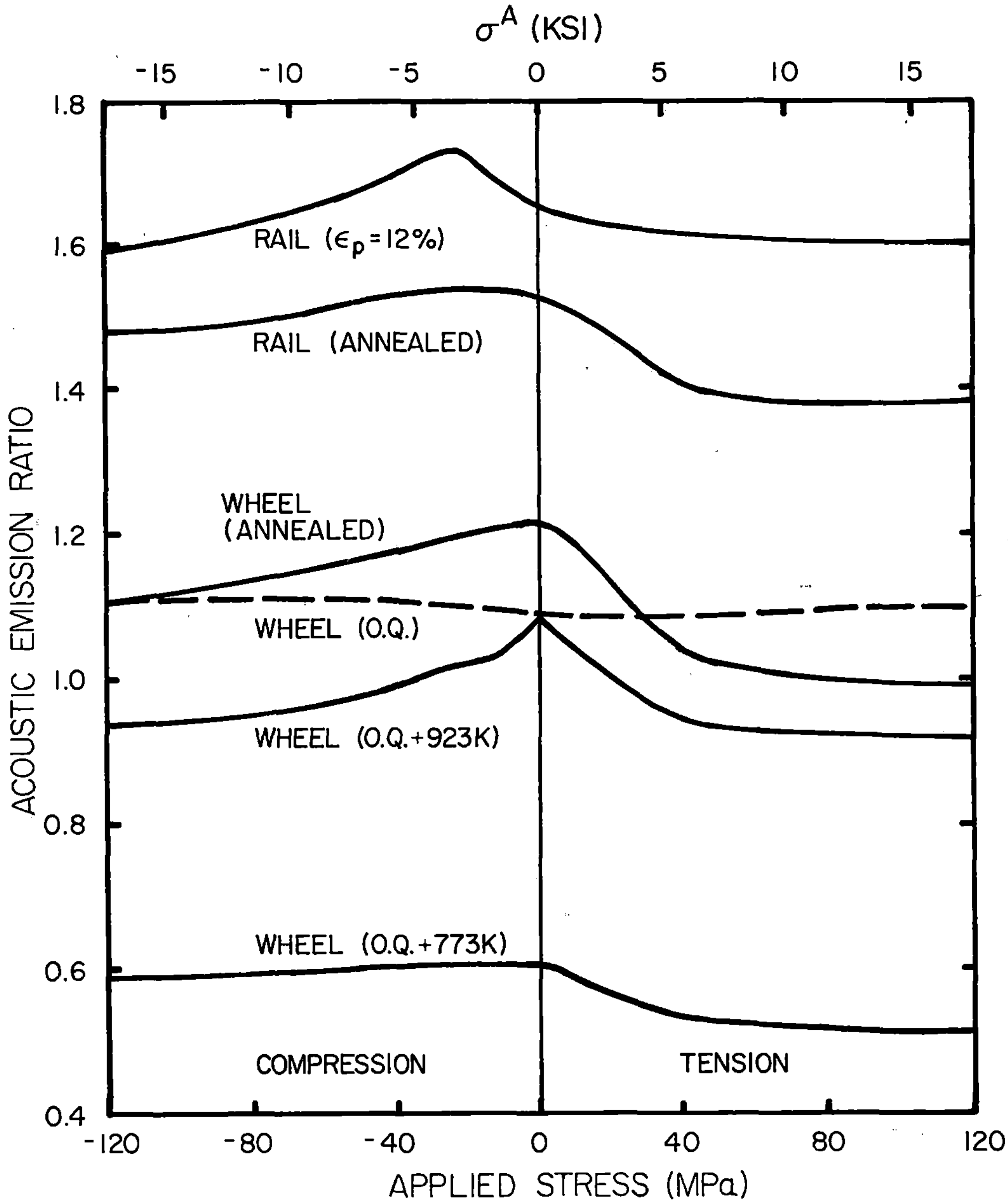

FIGURE 10. STRESS DEPENDENCE OF ACOUSTIC EMISSION RATIO OF RAIL AND WHEEL STEELS

[7] Stierstadt, K. "Der Magnetische Barkhausen-Effekt." In Springer Tracts in Modern Physics, vol. 40 (Springer-Verlag, Berlin, 1966), pp. 2-106.

[8] Lord, A. E., Jr. Physical Acoustics, vol. 11, eds. W. P. Mason and R. N. Thurston, p. 290. New York: Academic Press, 1975.

[9] Kusanagi, H., H. Kimura, and H. Sasaki. Proceedings of the First General AE Symposium (held in Tokyo, Japan, December 1977), p. 145. Tokyo: Japan Nondest. Insp., 1977.

[10] Higgins, F. P., and S. H. Carpenter. Acta Met., vol. 26 (1978), p. 133.

[11] Ono, K., and M. Shibata. "Magnetomechanical Acoustic Emission of Iron and Steel." Office of Naval Research, technical report 79-01 (Jan. 1979).

[12] Lund, R. "Effects of Prior Austenite Grain Size and Pearlite Interlamellar Spacing on the Fatigue and Fracture Properties of Rail Steels." M. S. thesis, University of California, Los Angeles, March 1979.

[13] Fowler, G. J. "Fatigue Crack Initiation and Propagation in Pearlitic Rail Steels," Ph.D. thesis, University of California, Los Angeles, December 1976,

[14] Chikazumi, S. Physics of Magnetism. New York: Wiley and Sons, 1964.

[15] Matzkanin, G. A., and C. G. Gardner. "Proceedings of the ARPA/AFML Review of Quantitative NDC," pp. 791-812. Air Force Materials Laboratory, report no. AFML-TR-75-212 (1976).

[16] Cullity, B. D. Introduction to Magnetic Materials, pp. 248-86. Reading, Massachusetts: Addison-Wesley, 1972.

"Nuclear Hyperfine and Positron Annihilation Methods for Measurements of Internal Stress"**

L. H. Bennett
L. J. Swartzendruber
R. C. Reno

Center for Materials Science
National Bureau of Standards

Introduction

Three techniques that have been considered of possible use for the nondestructive valuation (NDE) of residual stress are the Mössbauer effect, nuclear magnetic resonance, and perturbed angular correlation. These techniques, which can be classed as methods for measuring nuclear hyperfine interactions, were reviewed at a 1976 conference held in San Antonio, Texas [1], [2], [3], [4]. A fourth technique, positron annihilation, is not a nuclear hyperfine technique but will be discussed briefly here because it uses the same instrumentation as perturbed angular correlation.

The terminology "hyperfine" comes from the early days of quantum mechanics and optical spectroscopy. It was found that, upon using higher resolution, the optical spectra due to transitions between principal quantum numbers broke up into a "fine" structure attributable to quantization of the electronic moments. Then, with even higher resolution, these fine structure lines themselves broke up into "hyperfine" structure lines, which were attributed to interactions involving nuclear magnetic dipole and nuclear electric quadrupole moments.

The three nuclear hyperfine techniques mentioned above are methods sensitive to the interaction of nuclear properties with electric and magnetic fields produced either externally (such as by an electromagnet) or internally by the electronic distribution. The internal fields, in turn, are sensitive to the chemical environment, stresses, defects, and so on. In the positron annihilation technique, one detects the annihilation radiation that ensues when a positron is injected into the material under study. The electronic and defect structure of the material affects this radiation in a measurable way.

Mössbauer Effect

The Mössbauer effect is a technique for observing nuclear γ-ray fluorescence by using the "recoil-free" transitions of a nucleus embedded in a solid lattice. The methods for its observation have been extensively reviewed [5]. A typical arrangement and observed spectra are illustrated in figures 1 and 2.

Although the Mössbauer effect has been observed for more than 40 elements, the requirements for practical NDE measurements -- that is, room temperature measurements by the scattering technique within a reasonable time frame -- limit the usable elements to only a few. Chief among these are ^{57}Fe and ^{119}Sn, with ^{181}Ta being a possibility. To use these isotopes without making the sample radioactive, the samples under test must contain a significant (that is, greater than about 10 percent) fraction of iron, tin, or tantalum. If they do not, such a sample must be doped with a small amount of radioactive precursor (270 day ^{57}Co, 245 day ^{119*}Sn, 121 day ^{181}W). For this case, although the amounts of radioactivity are small, personnel hazards must be considered.

Three hyperfine interactions are observed by the Mössbauer effect. They are the magnetic hyperfine field, the electric field gradient, and the isomer shift. All three parameters are sensitive to changes in stress. For ^{57}Fe, the change in isomer shift upon application of a compressive stress of 50 thousand pounds-force per square inch (ksi) is about 0.003 millimeter per second. This is only about 1 percent of the linewidth and is readily masked by other effects -- as, for example, a change in temperature of 4° C or a change in composition of an iron-nickel alloy by 1 percent, given equivalent effects.

These effects, along with the length of time required to precisely measure changes on this order and the need to reduce vibration to a low level, are basically why the efforts using ^{57}Fe have not yet produced practical instruments for field use.

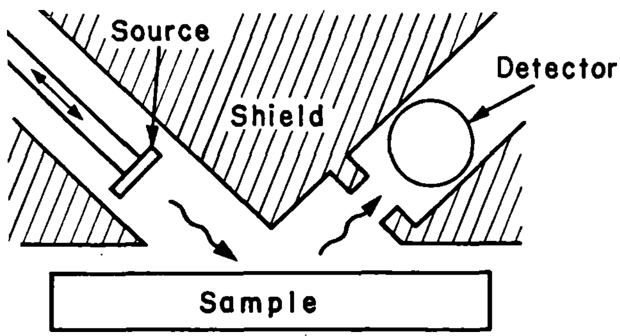

FIGURE 1. OBSERVATION OF THE MÖSSBAUER EFFECT BY COUNTING OF SCATTERED RADIATION (A radioactive source is given a velocity on the order of 1 millimeter per second with respect to the sample; the fluorescent radiation, which can be γ rays, X-rays, or internally converted electrons, is counted as a function of source velocity)

**Presentation at conference delivered by L. H. Bennett

Further development of instrumentation techniques is required before ^{57}Gr or ^{119}Sn can become practical using reasonable source strengths, and the best path of development is not clear. Even with improved instrumentation, the need to carefully control sample composition could still limit the usefulness of the Mössbauer effect to the calibration of reference materials in the laboratory. For this purpose, ^{181}Ta appears interesting as it has isomer shifts that tend to be very large compared with the natural linewidth [6]. However, it could be too sensitive; that is, the spectra may become unobservable at too low a value of stress to be of practical value. Therefore, a first step would be to investigate the range of stress over which useful observations could be made.

Even with the limited range of isotopes considered above, the possibility of rapid field measurements, such as would be required for rail surveys, appears remote with present-day instrumentation. Indeed, the considerable effort by specialized commercial instrument companies to develop Mössbauer instruments for this purpose has fallen far short of this goal. With further development, the Mössbauer technique is likely to be useful for calibration of standards. It has been used, for example, to provide benchmark measurements of ferrite contact in stainless steel welds and castings [7].

Perturbed Angular Correlation

Perturbed angular correlation measures nuclear magnetic hyperfine fields and electric field gradients by observing their effect on the coincidence of gamma rays emitted from three nuclear energy levels. For this technique, radioactive elements must be introduced into the sample under test. The amounts required are quite small, on the order of several microcuries. Compared to the Mössbauer effect, the number of isotopes that can be used is large and the possibilities include ^{111}Cd, ^{181}Hf, ^{44}Ti, ^{100}Pd, and ^{99}Rh. The gamma rays from these isotopes generally have much greater energy than those used in the Mössbauer effect, and depths up to several centimeters could be probed using suitable isotopes.

In addition, unlike th Mössbauer effect, perturbed angular correlation is insensitive to vibration or motion of the sample. As in the Mössbauer effect, the changes in the parameters being measured are generally small and can be masked by temperature and alloying effects. This leads to a problem in obtaining meaningful measurements within a reasonable time frame. Under ideal conditions the measurement time could be on the order of 1 hour, but from 1 to 2 days are more often encountered. This time cannot be reduced by simply increasing the source strength (as it can for the Mössbauer effect). Instrumentation development utilizing multicounter techniques or counters with spatial resolution have the possibility of reducing the required time by an order of magnitude. Long-range goals for the development of perturbed angular correlation should thus include instrumentation development and investigations of which isotopes would be suitable for specialized NDE applications.

Nuclear Magnetic Resonance

Nuclear magnetic resonance (NMR) uses the interaction of a nuclear magnetic moment with a radiofrequency field to probe the magnetic hyperfine field at an atomic nucleus. In NMR, radioactive sources are not required. Figure 3 schematically compares NMR with the Mössbauer effect and perturbed angular correlation techniques. Nuclear quadrupole resonance (NQR) utilizes a nuclear quadrupole moment interacting with a radiofrequency field to probe the electric field gradient. Acoustic nuclear resonance (ANR) replaces the radiofrequency field with an acoustic wave. All three methods and their potential for NDE have been previously reviewed [1], [3], [4], [5].

In metals, the depth of penetration of the radiofrequency field depends on the conductivity and permeability of the sample and is on the order of 100 micrometers. Optimum observation of NMR and NQR requires specially shaped samples, such as powders, wires, or foils with one dimension less than this penetration depth. If this criterion is not met, lineshape distortion and sensitivity become major problems and new developments in instrumentation and signal processing are needed to overcome these problems.

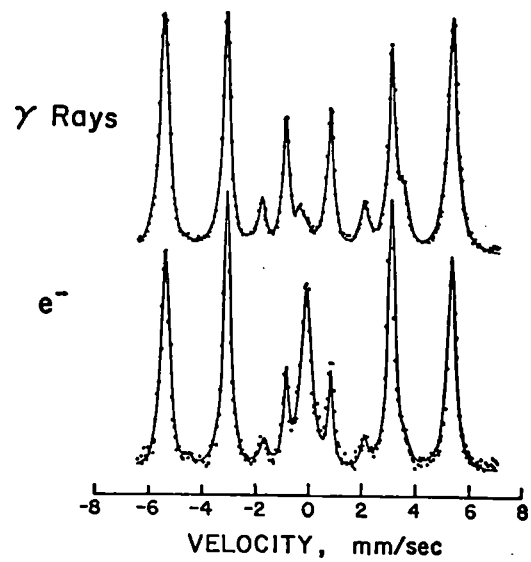

FIGURE 2. SCATTERING SPECTRA FROM A SAMPLE OF SPHERODIZED IRON CARBIDE IN IRON (NBS STANDARD REFERENCE MATERIAL NUMBER 493)

(The source was several millicuries of ^{57}Co [the precursor for ^{57}Fe] in a Pd matrix. The number of counts is plotted as a function of source velocity. In the upper spectrum the detector was set to count 14 kiloelectronvolts γ rays. In the lower spectrum, internal conversion electrons were counted. The difference in the two spectra reflects the difference in depth below the sample surface being probed by these two types of radiation.)

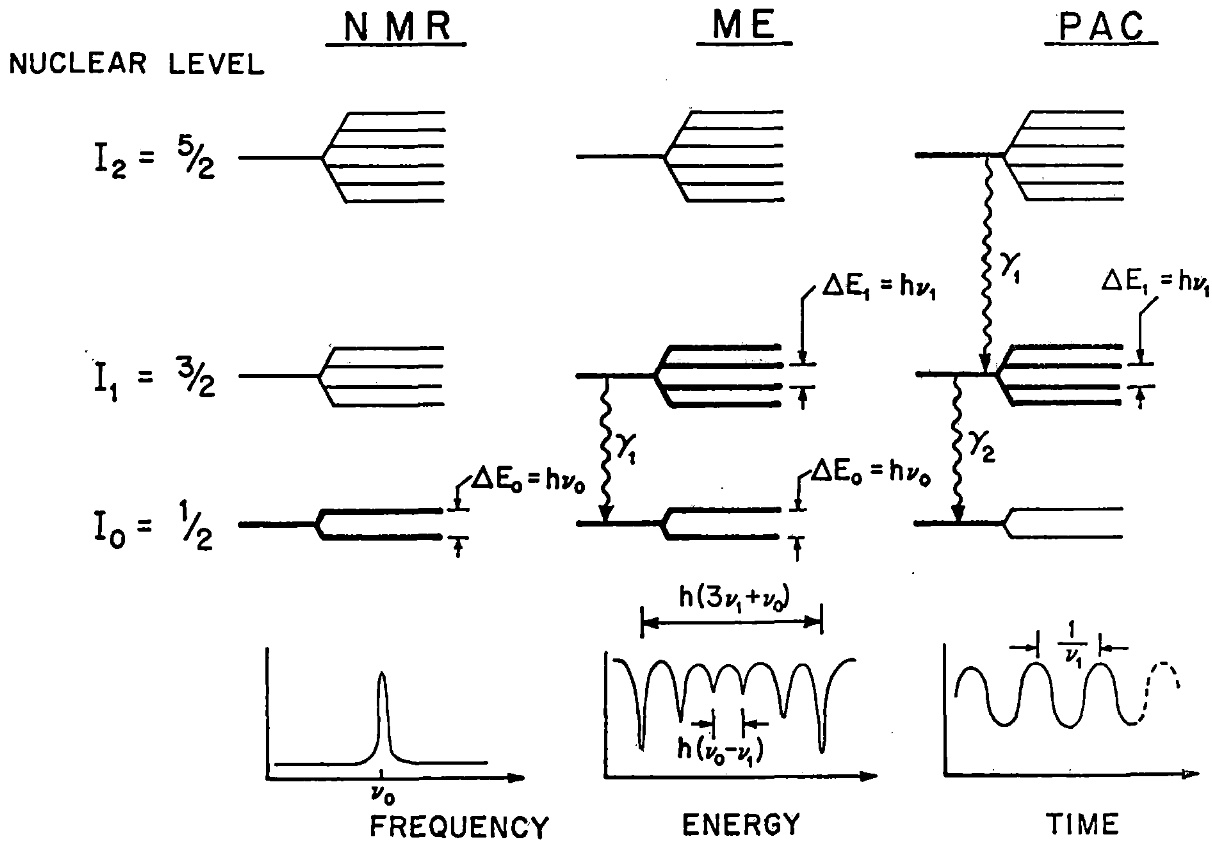

FIGURE 3. SCHEMATIC COMPARISON OF HYPERFINE LEVELS PROBED BY NUCLEAR MAGNETIC RESONANCE (NMR), MÖSSBAUER EFFECT (ME), AND PERTURBED ANGULAR CORRELATION (PAC)

For ANR, penetration depth is not a problem. However, sensitivity is a problem in ANR and observations to date have been made only under ideal conditions. New ideas in instrumentation are needed here for methods of improving the sensitivity.

Interesting developments in NMR for evaluation of nonmetals, especially biological samples, have recently been made [8], [9], [10]. A new term, "Zeugmatography," has been coined [8] to describe the computer reconstruction scanning techniques being used. These techniques are worth exploring for their possible use in NDE of such nonmetals as polymers. However, their applicability to metals, especially commercial ferromagnetic steels, appears limited.

Positron Annihilation

Positrons are the antiparticles of electrons. When injected into a metal, they interact strongly and are finally annihilated by contact with electrons. In 1964, Mackenzie et al. [11] noted that the characteristics of the ensuing annihilation radiation were sensitive to the defect structure within the metal. This observation has been followed by a large number of studies using positrons to probe atomic and microscopic scale inperfections in solids and their relationship to deformation, fatigue damage, and creep. Recently, considerable attention has been directed to the use of positron annihilation as an NDE technique. This effort has been reviewed by Coleman [12].

Basically, three types of measurements on the positron annihilation radiation are made -- angular correlation (A), lifetime (L), and Doppler broadening (D). Instrumentation for observing Doppler broadening is illustrated in figure 4. The positrons can be readily obtained from the decay of certain radioactive elements. The characteristics of several of those with reasonable half-lives are outlined in table 1. The depth to which the positrons penetrate depends upon the energy with which they are emitted from the source, and it can range from 20 micrometers for ^{65}Zn to 230 micrometers for ^{68}Ge, making positron annihilation basically a near-surface technique. Defect profiles over this range of depth could be obtained by using several sources.

It is well established that positron annihilation is selective to open volume defects, such as single vacancies and vacancy clusters [13], [14], [15]. Detection of residual stress by positron annihilation is indirect and would rely on the relationship between residual stress and internal defect structure. This area needs further exploration

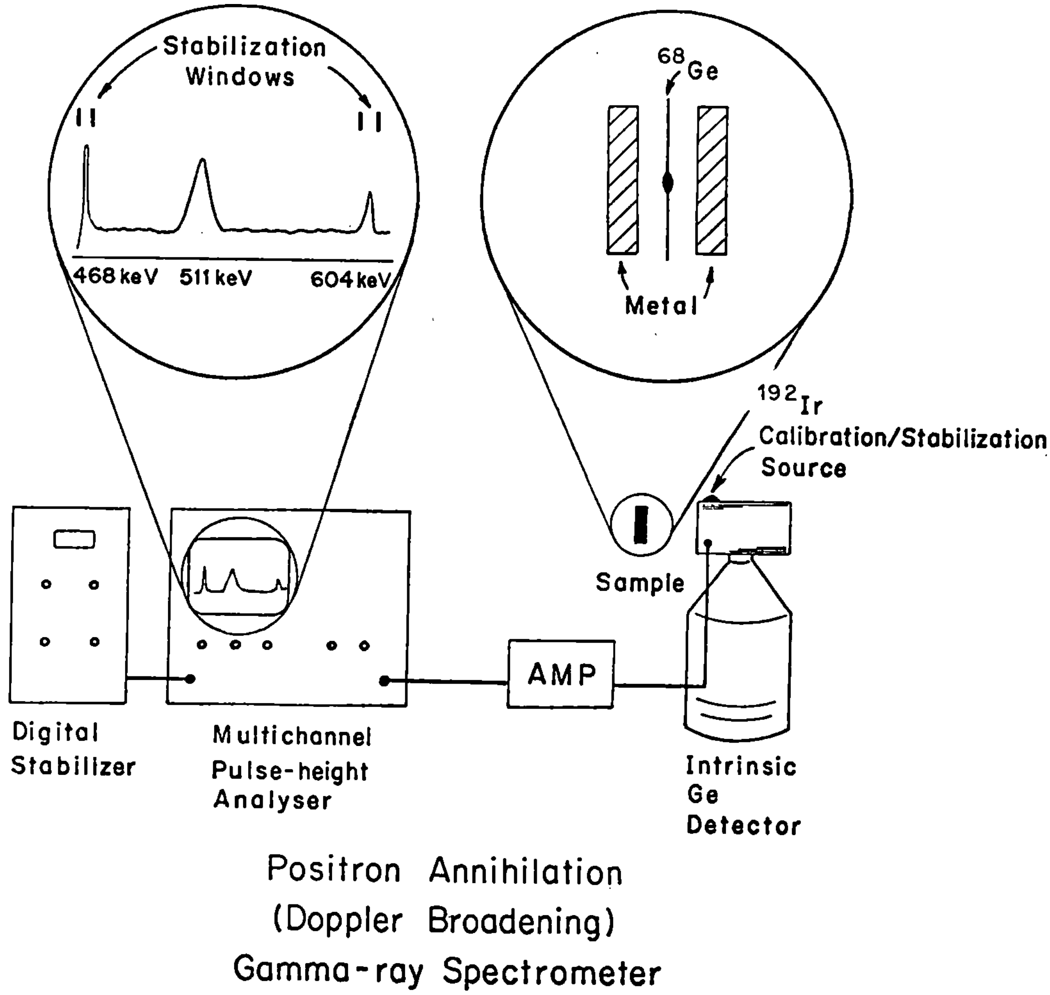

FIGURE 4. INSTRUMENTATION FOR OBSERVING DOPPLER BROADENING OF POSITRON ANNIHILATION RADIATION (Positrons from a radioactive source are injected into a metal sample; the resulting radiation is analyzed with electronics stabilized by radiation from a reference source)

TABLE 1

SUMMARY OF CHARACTERISTICS OF POSITRON SOURCES

Isotope	Half-Life	$E^{\beta+}_{max}$ (MeV)	Mean Penetration Depth (μm)	Possible β+ Experiments	Approximate $/mCi
^{22}Na	2.6 yr	0.54	50	L, A, D	300
^{44}Ti	48 yr	1.50	200	L, D	100,000
^{64}Cu	13 hr	0.65	70	A, D	5
^{68}Ge	275 d	1.90	230	A, D	300
^{58}Co	71 d	0.47	45	L, A, D	12
^{65}Zn	245 d	0.33	20	D	5

to determine under what circumstance and in which materials the potential of positron annihilation can be realized.

The methods with greatest potential for NDE applications appear to be lifetime and Doppler broadening measurements. Using current instrumentation, the time to make a measurement with reasonable precision under ideal conditions is on the order of 1 hour. To make the technique useful for field use, this time needs to be reduced. This requires the development of faster counting techniques, perhaps utilizing improved coincidence methods and multiple detectors to reduce background noise. Source strengths of the positron emitters are much less than 1 millicurie and are not currently a problem.

In the Doppler broadening method, results are generally presented in terms of a lineshape parameter, which is a sensitive measure of the effect of defects on the pulse height peak shape from the annihilation radiation. The value of this parameter is also sensitive to source strength, system geometry, and electronic instrumentation, which must be carefully controlled. In this regard, standard samples that give known variations in the lineshape parameter may be useful in the development and implementation of the technique.

Summary

A brief overview of three methods for observing nuclear hyperfine interactions of methods for utilizing positron annihilation has been presented. All these techniques yield results that are sensitive in some degree to residual stress. However, at their present stage of development, none of these techniques appears suitable for adaptation as a field technique for the rapid survey of residual stresses in rails. The Mössbauer effect and positron annihilation have potential for development as methods to aid in the standardization of reference materials.

References

[1] Bennett, L. H., L. J. Swartzendruber, and R. C. Reno. Proceedings of a Workshop on NDE of a Residual Stress. NTIAC-76-2 (1976), p. 247.

[2] Yagnik, C. M., and R. L. Collins. Ibid., p. 263.

[3] Matzkanin, G. A. Ibid., p. 275.

[4] Leisure, Robert G. Ibid., p. 283.

[5] See, for example: Weisman, I. D., L. J. Swartzendruber, and L. H. Bennett. Techniques in Metals Research, vol. 6, p. 165, ed. R. F. Bunshah, p. 169. New York: J. Wiley and Sons, Inc., 1973.

[6] Kaindl, G., and D. Salomon. In Perspectives in Mössbauer Spectroscopy, eds. S. G. Cohen and M. Pasternak, p. 195. New York: Plenum Press, 1973.

[7] Swartzendruber, L. J., L. H. Bennett, E. A. Schoeffer, W. T. Delong, and H. C. Campbell. Welding Journal, vol 53 (1974), p. 1-s.

[8] Lautebur, P. C. Nature, vol. 243, (1973), p. 190.

[9] Mansfield, P., and P. K. Grannel. J. Phys. C: Solid State Physics, vol. 6 (1973), p. 4422.

[10] Hinshaw, W. S. Phys. Letters, vol. 48A (1974), p. 94.

[11] MacKenzie, I. K., G. F. O. Langstroth, B. T. A. McKee, and C. G. White. Canadian Journal of Physics, vol. 42 (1964), p. 1837.

[12] Colman, C. F. NDT International, vol. 10 (October 1977), p. 227.

[13] West, R. N. Advanced Physics, vol. 22 (1973), p. 263.

[14] Matl, S., and W. Triftshauser. Phys. Rev., vol. B17 (1978), p. 1645.

[15] Wampler, W. R., and W. B. Ganster. J. Phys. F: Metal Phys., vol. 8 (1978), p. L1.

PANEL DISCUSSION

The participants in the panel discussion included authors J. R. Barton, L. L. Yeager, K. R. Maser, and N. Senapati; conference panel members D. P. McConnell (chairman) (Transportation Systems Center, U.S. Department of Transportation), H. Berger (National Bureau of Standards, U.S. Department of Commerce), and D. H. Stone (Association of American Railroads); and supplmental session panel members A. D. Kerr (University of Delaware) and J. Simmons (National Bureau of Standards, U.S. Department of Commerce).

J. SIMMONS: In listening to the discussion during the course of the day, it seems to me that what one is trying to do is to measure the actual longitudinal force that occurs in rails that are in service in situ. This means that what one really is looking at is an average of the normal component of stress over a transverse cross section of the rail -- that is, the force perpendicular to the longitudinal or running direction of the rail. So one of the problems that immediately comes to mind is that any method which does local residual stress measurement is really not addressing the problem.

What one is really attempting to do is to ask for this average. So, in my opinion, the question here has to be, how do the techniques we are discussing compare with the British Rail method. This is the closest method to an actual attempt I have heard discussed here, but it looks only at one part of it as an actual direct attempt at measuring the actual loading force rather than the residual stresses that are in the rail.

Of course, there are a lot of disadvantages to the British Rail method. Nobody likes drilling holes, particularly if you are going to do them 20 meters apart; in fact, that can easily become ludicrous, but it certainly comes closer to a standard of reference, against which, it seems to me, one can compare alternative techniques.

Dr. Barton, you mentioned the magneto-optic approach for making magnetic domains visible. Could you be more specific about this technique?

Also, the Barkhausen effect (magnetic domain flipping) has been detected by acoustic emission methods as well as by magnetic methods, and I believe that Don Jolly, also of Southwest Research, has had some interaction with you on this. Which is the more sensitive and what are the relative advantages and disadvantages of the two techniques? I know that Al Beatty at Sandia used it to study hydride formation. That is a phase change problem, but there have been other applications where it has been directly used on magnetic domains.

In addition, you mentioned that you use an envelope-detection type of approach, which struck me as rather strange because this approach clearly is going to be sensitive to material microstructure. If you have got a material sample with a large number of magnetic domains which are, for example, heavily pinned, then, when those domains flip, you are going to get tremendous currents in very large peaks, whereas, if the magnetic domains are not pinned so much, they will move more smoothly. Consequently, although you may have similar amounts of energy radiated, you will certainly have completely different characteristics for the type of radiation. So I am a little surprised that you used peak envelope methods rather than some other type of measurement.

Finally, what is the influence of the residual stress wavelength versus the magnetic domain size? In some cases, you may encounter very fine, very localized, highly fluctuating residual stress fields, as opposed to very long-range ones. Have you done any studies of the interrelationship between these two?

J. R. BARTON: The magneto-optic approach is a method in which you use a polarized light beam. In our case, we used a laser beam. The polarization is changed by the magnetic interaction with the domain, and you use an analyzer the same as you would with ordinary polarized light techniques. The orientation of the magnetic domain in the surface rotates the plane of polarization of the light slightly. We used a laser because the attenuation factor through this whole system was about a factor of a million and we do have some very interesting movies of the dynamic action of domains. Of course, you can get a static readout, but we used a laser for the dynamic readout.

Regarding the second question, about the comparative sensitivity of the uses, we have recently conducted some experiments on the ultrasonic method of sensing domain motions. With increasing compression stress, a nearly linear decrease in the ultrasonic signal amplitude results.

J. SIMMONS: Are we talking to the same method -- you are using the word "ultrasonic." I asked you acoustic emission. That is quite different.

J. R. BARTON: That is right, but as you move a domain wall, you can generate an elastic wave. That is the same as ultrasonically.

We had hoped that, as we moved into the tension range, we would get a straight-line continuation, which did not prove to be true. Dr. Beissner, who has been doing most of this work, believes that he has a way of separating out the influence of tension and compression. There is, of course, the possibility that the acoustic Barkhausen is at least sensitive to the stresses in the interior of the metal. With the inductive approach, we are limited perhaps to about 0.010 inch in depth. I do not think at this point that our experiments have moved far enough that we could give you a quantitative appraisal of the advantages and disadvantages and sensitivities.

The acoustic Barkhausen does have very good sensitivity. Probably, at least in the experiments we have run, you would be able to resolve about 1,000 pounds-force per square inch (psi) and that is near the order of what we can resolve on a calibration specimen with the inductive Barkhausen.

Now, in terms of the envelope detection, we have found that the characteristic shapes of the envelopes do have features that in some instances we think relate to the texture of the material, and other regions of that envelope are more sensitive to stress. At this point in time, we do not understand why this is true. Although we have some ideas of why it is true, we do not understand it exactly.

I will use an illustration (see figure A on page 132) to show you what I am talking about. The characteristics of the curve that we have are usually something like is shown, but we have found that the general region above often will get a very prominent spike -- and it varies with materials -- and this region is often the most stress-sensitive region.

On the horizontal axis we are talking about the magnetic field change; the vertical axis is the Barkhausen signal.

And often this peak has a high amplitude; in other cases -- with different materials -- it may be fairly low, as shown.

For example, if we take a ballbearing race as a specimen -- and normally we know that a ballbearing race is heat-treated to where you end up with a very high residual compression stress in the surface -- then we get a curve about like that in the illustration.

With extended endurance testing and with fairly high service loads (these were done in the laboratory but also in bearings that have been in actual gas turbine engine service), we have seen in many instances a peak that emerges as shown.

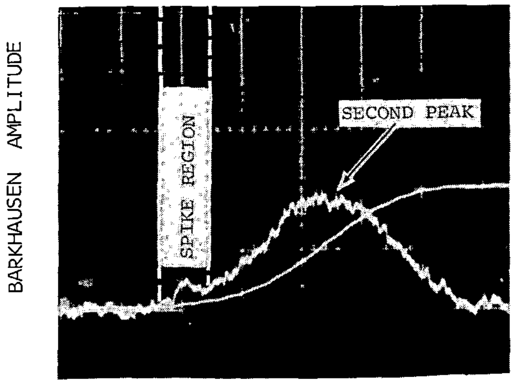

MAGNETIC FIELD CHANGE
COMPRESSIVE STRESS

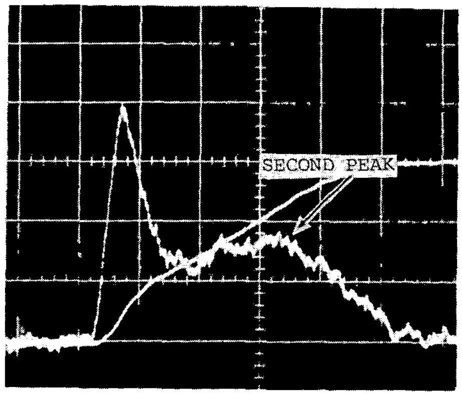

MAGNETIC FIELD CHANGE
TENSION STRESS

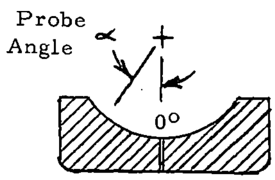

Section - Inner Race

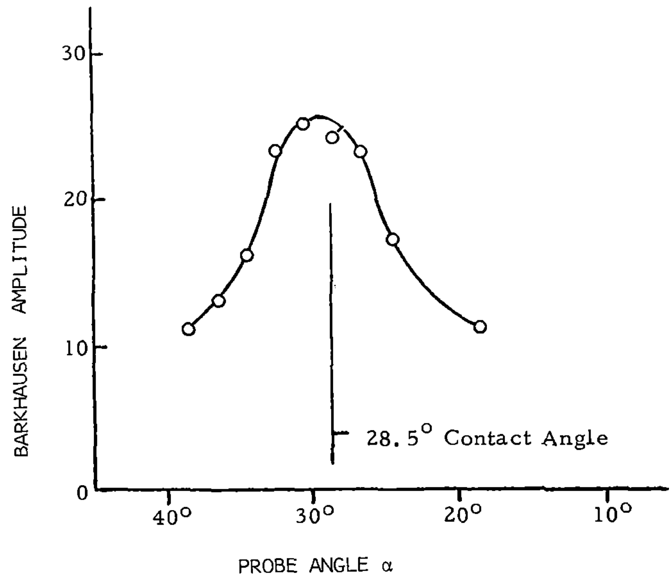

FIGURE A. ILLUSTRATION USED BY J. R. BARTON IN PANEL DISCUSSION

This one still stays the same. We believe this is load-related. We are almost certain that it is because, if you have a cross section of the race, if this is the load region, and if you plot the amplitude of this peak versus location, then you find that it peaks up near what is called the gaging contact angle (28.5°).

J. SIMMONS: What is the magnitude of the magnetic field you apply? Do you always apply it the same way? How is it applied?

J. R. BARTON: The magnitude can vary, but for any one application we would experimentally determine what the limits would be and usually the magnetic field -- I should say the current applied to the magnet that is creating the magnetic field is usually linear increasing in one direction; then, of course, when you swing it back, you go back in the other direction. The kinds of things that we vary are these end-points -- maybe it carries on up to here -- and this slope.

In general, if you go to a higher slope, you get more Barkhausen activity. However, we have also found experimentally that you get a different behavior of at least some steels, depending upon that slope.

J. SIMMONS: Sure, you are doing internal electrical friction experiments.

J. R. BARTON: Well, that could be. But for example, you take identically the same specimen and put it in tension or compression and versus slope of this field. If you increase this slope and we plot Barkhausen activity or this peak amplitude on this axis, then we find with the tension stress that you get a curve coming up here like this and peaking out and then starting back down; and identically on the same specimen, if you put it in an equal condition of compression and do the same thing, then you find a continuously increasing curve.

If you take the load off and essentially have little or no stress [you magnetize with the same kind of arrangement], with no stress it comes up here and levels out so we think that may be providing an additional parameter for trying to assess the actual value of the stress. We have done this work only recently.

But back to this experiment. This is a condition for before and after on one of these races, but we have also taken one of these specimens and cut an opening in it in which we can push or pull on this thing to generate a tangential stress. We have found that this region here is the one that produces the response in the Barkhausen. This second peak stays about the same. There is a basis for thinking that this peak is structure-related and this spike region is more stress-related.

D. P. McCONNELL: Just to follow up on that very briefly: In going back to your plots where you are looking at the behavior with compressive stress, the calibration curve has a tendency to flatten out at a point right in the stress range in which one begins to get interested in the buckling phenomena. Therefore, the sensitivity we are talking about is shown predominantly in the tension and the early part of the compressive behavior, at least for the materials on which calibration was performed.

J. R. BARTON: That calibration curve was on a specimen of 4340 steel heat-treated to a yield strength of about 200,000 psi and the region of flattening was approximately half-yield. In other words, it would be my opinion now that, if you had a compression stress in a rail that is approximately half-yield and it were then increased beyond that point, you probably would not be able to tell it from the Barkhausen signal.

However, I am talking about the yield stress in the material. I am not talking about the stress that may cause the rail to buckle. So I think it is important that the range of stresses of interest be established for buckling.

I do not know what that value is, but I have seen numbers like 10,000 or 12,000 psi. I do not know the yield in the rail material. I believe it is around 30 ksi, and sensitivity would thus extend to ±15 ksi.

J. SIMMONS: I think it can go higher than that, up to around 60 ksi.

J. R. BARTON: You probably would not get very good sensitivity if the buckling stress is 60 ksi; if 60 ksi is yield stress, range would thus extend to ±30 ksi.

A. D. KERR: At buckling of the track, the axial force in each rail may reach about 100 tons; i.e., a stress of about 17,000 psi. There is a basic question as to the wavelength and the depth of penetration to be used. It appears that, to measure the net axial force, the method that penetrates the whole section will work best, although I would not ignore any other method. With respect to the Barkhausen method, how deep do you penetrate the rail in the experimental data that you presented? If you work on the web, do you penetrate the entire web?

J. R. BARTON: No. We probably are limited to a range from the surface in of about 10,000th to 15,000th of an inch. We do not know that number exactly.

A. D. KERR: So you are picking up all the surface effects?

J. R. BARTON: We pick up all the surface effects. In terms of trying to make an appraisal of the force, you would make measurements at a number of locations on the section and at this time I do not believe that we would recommend that you would be able to go out and make a measurement on an unknown rail and have much assessment of the conditions.

If you are going to be successful in this area, you are going to have to take a little bit at a time. This is why I recommend that the first step is to go from an area that you understand to one just slightly beyond; that would be to make measurements in the field at precisely determined locations. You would make a mark to determine that location, perhaps by putting two small indents so that you can reposition your gage each time you want to make measurements, and you would make those over a period of time in which the temperature varies considerably. In other words, this would be a differential kind of a measurement.

That would be the first step to take. As for deciding whether or not a rail is under a very high tension or very severe compression, I think that can be done on an unknown rail because the Barkhausen values do vary by a large value from roughly half of the compression yield to half of the tension yield.

Although we have not made these measurements on unknown specimens of rail, I believe you would be able to go out in the field, and if you found a rail specimen that had a very, very low reading, you would say that this one is in compression. If you found one that has a very high reading, you would say that this one is in tension. To some extent, the measurements on the railhead itself confirm this. We have made measurements on a few samples of rail -- new rail and rail that had been used. While we did not get a very high reading from the new rail, it was much higher than on the used rail that had been, of course, work-hardened and put into residual compression from the traction loads.

A. D. KERR: You mentioned the acoustic Barkhausen as compared to the magnetic, and you claimed that the acoustic will penetrate deeper. Could you elaborate on this subject?

J. R. BARTON: You sense the Barkhausen phenomenon by means of the ultrasonic or acoustic waves that are caused as the domain changes volume. It is a very early technique right now, but it may have a lot of promise.

J. SIMMONS: When he spoke of going slowly, Larry Bennett reminded me this morning that the Metallurgy Division of the National Bureau of Standards was founded in 1912 in part for dealing with the problem of breaking railway wheels and it has just now been organized out of existence. Now it is called "metal science," so maybe they decided the problem has been solved.

A. D. KERR: I have a question for Mr. Yeager in connection with the damping method: What is the physical reason for the increase in damping? Is it the formation of internal cracking?

L. L. YEAGER: It would be related back to the phenomenon of dislocation density.

A. D. KERR: Will this increase essentially the attenuation of energy?

L. L. YEAGER: Yes, increasing the energy prior to a crack formation or prior to a physical change of a specimen.

A. D. KERR: What will be the mechanism that will indicate the intensity of the axial force, and how can it be measured?

L. L. YEAGER: Axial force on the member could cause this dislocation density to increase. As this dislocation density increases, the specific damping capacity number would increase likewise.

A. D. KERR: Do you have test data to justify this assumption?

L. L. YEAGER: I showed in my paper the bar specimens with the external force applied and the increase in specific damping capacity as that external force was applied or increased. There were a number of load cycles applied. This was in-house work that we performed, and we have not gone any farther than that with the generation of data.

A. D. KERR: A few years ago, when Dr. Zarembski was a postdoctoral research associate at Princeton University, he and I conducted a test on a rail (about 1.5 meters long) that was mounted in a compression testing machine. We used a lateral impact force on the rail head and then recorded the response. An impact force was used instead of a continuous vibration excitation, because for very short times the end conditions of the rail had no effect on the rail response, in that the generated waves had no time to reach the rail ends.

When the mounted rail was impacted laterally, a different sound was heard for 0 pounds and 50,000 pounds of axial compression (for the same type of impact). Then the rail was attached longitudinally to a wood tie. The sound output got less sensitive to these axial forces. One reason for this was that, because the base of the rail was fixed to the tie, many vibration modes were eliminated. Since the eight modes you showed are free modes of a rail, some of them will be eliminated once you attach the rail to the ties.

K. R. MASER: With regard to the use of an impulse, one of the reasons that we took the approach we did was because most of our work was really oriented toward trying to understand the structural dynamics of the rail. We felt that we could get more information by being able to sweep the frequency -- holding such frequency to make the mode-shaped measurements. At some time, perhaps, if the method proves fruitful, an impulse-type application would be desirable, but it would not be able to produce the information that we produced thus far.

As to the question of whether these eight modes would show up, we made all of our measurements above 1,000 hertz and actual displacements at those frequencies were on the order of 10 to 10^{-6}. Past work in looking at propagation of noise in rails has shown that the mass of the tie plates and fasteners does not couple with the vibration of the rail at those frequencies because of the very small displacement, and so we would expect, perhaps, to see some damping. We still expect that we would see those cross-section affirmations.

What you were talking about -- when you hit a rail and listen -- is a ringing which has to do with damping. We are holding a frequency and we are not looking at ringing, so we believe that those modes will still show up but that they may not propagate as far or with the same amplitude from the exciting point.

D. P. McCONNELL: One followup question to Dr. Kerr's comments: One of the things which occurs to one in listening to your material is that the end conditions were suggested as one of the explanations for the change in the resonance phenomena. Among the mode-mapping which was done, we never attempted to map the modes of behavior at the ends which would give some indication of the change in condition at that point, so I think that that piece of information might help to explain some of the behavior which has taken place. I think one thing that might want to be considered in the future is that type of measurement.

J. SIMMONS: Yes, I would like to address a very similar issue. Your method certainly looks like it could be promising. I did not understand why you never applied longitudinal loading because then you are actually loading in a direction where the longitudinal force would intuitively be thought to have the most influence.

In fact, like Bob Green said, when looking at changes in the elastic modulus which are due to elastic loading, and these are nonlinear changes, one would have expected that to most affect the Young's modulus which is directly connected to the degree of normal loading, but Bob Green would know better than I and probably should be asked.

At any rate, random variations in the Young's modulus which were mentioned earlier today should affect attenuation particularly at certain critical frequencies which are associated with, you might say, the range of variation of the Young's modulus.

For lower frequencies or higher frequencies, especially the lower frequencies, you would not expect a significant problem with variations in Young's modulus. However, you could expect that the elastic constants are going to change relative to one another under load. If you decomposed different types of loads into normal modes, which is what you are really trying to do, and if you took just a straight cylinder and loaded it normally, you could then ask how that would affect the different elastic constants and which normal modes would be most sensitive to this.

And then, one could attempt to try and apply those particular kinds of normal modes to see a maximum sensitivity associated with the longitudinal loading.

K. R. MASER: When you say "longitudinal loading," are you talking about exciting it longitudinally?

J. SIMMONS: No, I am talking about just a static long-range force and its effect on traveling normal modes in an infinite pipe -- if you want to phrase it that way. That seems closer to the real measurement problem that is facing the railway people.

A lot of the phenomena you were looking at were clearly resonant frequencies associated to the finite structure; you made that point and you are absolutely right.

K. R. MASER: What I was showing earlier in my presentation was how we used the information that we developed in our test rigs to compute what the traveling wave velocity would be on an infinite rail. We are generating traveling waves when we are exciting the waves at a point. What we did was to locate resonances which were wave speeds and wavelengths that reinforced themselves, so that we were able to identify the wave velocity.

We did measure wavelengths and frequencies and computed velocities. These velocities should be velocities that we would measure in an in situ track, but we have never gone to an in situ track and actually made these measurements or wave velocity measurements, but our measures are relevant because we are measuring wave velocities.

J. SIMMONS: My point is that perhaps you should attempt to ascertain which higher-order elastic constants were being affected by your experiments and which ones would be most sensitive to the actual longitudinal force, which is what the railway people want to know.

K. R. MASER: We are not measuring elastic constants.

J. SIMMONS: Had you changed the elastic con stants, the effects on different normal modes traveling in the bar would have been affected.

Certain normal modes will be affected very little in their speed. Other ones will be affected very greatly; by singling out the certain normal modes which are most sensitive to changes in elastic constants, you might be able to develop a most sensitive way, using your method for finding the influence of longitudinal force.

R. E. GREEN (The Johns Hopkins University): The topic is a big problem. I don't know the numbers right now, but I have them computed. In any case, there was one that is a fairly isotropic material, a variation of what I would call the effective Young's modulus because, in my opinion, the Young's modulus refers only to homogeneity of isotropic material and it should not be used for rail materials. I would question the effectiveness on quasi-modulus or something.

We have done it about two or three times on our own. So, if you are going to do something like residual stress, it probably does not change the Young's modulus even one order of magnitude so that means the antisotrophy of the different wavestream.

Essentially what we are talking about is the fact that you apply a horizontal force to the rail. It is no longer isotropic because that direction is stretched compared with the other two, and then you want to do your calculations based on that new type material.

D. H. STONE: I have a question of Bob Barton. You have done a good bit of work on problems with residual stresses in wheels, which are essentially the same steels as rail steels. Would you like to comment on what lessons you learned there or what pitfalls we might have in front of us with respect to that?

J. R. BARTON: I think Don Bray put it about as well as anybody is going to put it at this point, and that is that we have been carrying the experiments in the laboratory only so far and those that appear to have some promise then need a rather extensive field appraisal. In terms of experiments that may have potential for yielding absolute measurements, I do not know of very many of those.

I think the first step to be made is to look for differential measurements at precisely the same location from time to time. First of all, remove the scatter of the material as the first experiment. If you cannot do that one, you have to quit. But we may find in a large population that some of these skeletons that are in the closet when you do an experiment on two or three specimens might not be quite as bad as we think. As an example, we might find certain rails or wheels -- let's put in that framework -- on which you cannot make measurements. If this is a small percentage of the population, then you do not worry about it. You make it on the ones on which you can make measurements.

I think that the biggest thing that needs to be done is to get measurements on enough specimens in the field to get some idea of what the real population looks like.

If we are talking about wheels, for example, we have got, say, a hundred of those that fail a year. And if we start looking for those few wheels that fail out of, say, 32 million, it takes a pretty good sample if we hope to have in our hands one that may be near failure.

The real world is where we often find that we come to a screeching halt because it takes so much money to get those real world figures. It takes a commitment of resources, and you do not always have all the laboratory data you would like to have before you go to the people. So you have to take some risk in these things, select a few methods that show promise, get out in the field, and make extensive measurements -- not just a cursory measurement.

For example, one of the things that we know about Barkhausen now that we did not know about 3 years ago is that any time that we have got a large piece of steel extended, we are going to pick up many of the local radio stations. So it will be necessary to have a filter to eliminate at least that component, which can be done. But there are things like that that you learn. I still believe some of these methods ought to be put to the field trial, but it is going to take a pretty good budget to do that.

H. BERGER: I am coming more and more to the conclusion that no single method is going to be able to do this job, because there are so many variables involved in it. It seems as though there has to be a mixture of methods to help eliminate some of the variables that are involved Mr. Barton, you mentioned that you apparently can interpret what Barkhausen signals mean in terms of stress versus other metallurgical characteristics, such as texture. What other variations would cause problems in the Barkhausen signal? I would pose a similar question to any of the other speakers who may wish to comment.

We should recognize that, as we approach the end of this conference, we should concentrate on those two or three methods that show the most promise. These choices will probably be made on the basis that interfering signals from other variables may be minimized.

J. R. BARTON: I think hardness will make a difference. I do not know that we understand the Barkhausen phenomenon well enough to know in a range of materials how one might determine some independent measurement that would let one correct the raw Barkhausen signals.

H. BERGER: As an example, when I raised the question of the variation in the Young's modulus, Dan Stone indicated that one would expect changes in chemistry. How would that affect the Barkhausen measurement?

J. R. BARTON: I think variations in chemistry will be a rather minor influence. I am certain it will vary the Barkhausen response somewhat, but I think it is a small response.

I believe hardness might affect it rather significantly. We do know that grain size can influence Barkhausen noise, but, again, there may be regions of this response versus magnetic field in which you can tend to minimize some of this. I believe it is in Czechoslovakia or another European country that Barkhausen is used for determining grain size, so it must have a rather significant influence.

Most of the work is empirical at this time. We do not have a good model to work with. I think that is one of the things that limits magnetic methods in terms of our progress. It is difficult to get a model that means anything.

N. SENAPATI: I would like to make a comment on the statistical spread of the data due to changes in what are called "state variables." These state variables, which affect the measurements to estimate the axial stress, include the stress tensor and the local elastic, magnetic, and metallurgical properties and density. The total effect of all these local variations leads to a wide statistical spread of the measurements. The statistical spread is wider than the effect of stress alone.

What I see here as a basic problem is how to isolate the effect of stress on one property if one does not know how the other things are behaving in the system. That is why I thought of this as a different technique. If one takes two measurements of a physical property with two different state variables -- for example, stress and magnetic field -- then the difference between the two independent phenomena would then be independent of all other state variables that were identical during the two measurements, and therefore would cancel out.

H. BERGER: In the limited number of measurements you have made so far, have you gotten any feel for other variables that would impact the combination of techniques which you suggested, and specifically some of the variations which we have already discussed today in terms of material or stress variation?

N. SENAPATI: Yes. One of the typical variables is the grain size of the material. The grain size or the residual stress in the material is going to change the effects of the stress and the effects of the magnetic field. All of the state variables that are affecting the two measurements are going to be identified at the same point. So all you need to really know is the effect of the magnetic field on that kind of material under known stress.

Some spread in the data was actually seen. But we did not do any signal averaging on that, and these are oscilloscope measurements. At this point, there is only one thing I can think of that is changing -- noise in the system. Nothing else is changing, so by averaging 10 or 15 data, I am sure we can reduce the variations. That is true for all variations.

Then you are really looking for a differential effect of two phenomena, each of which is affecting the attenuation. I wanted to emphasize that we really do not have to do these measurements at ultrasonic frequency. You could to it at a lower frequency where you could average over the rail cross section.

QUESTION-AND-ANSWER PERIOD

MR. VINCENT: Earlier the statement was made that, in a continuous rail, there is no strain. Is there no longitudinal strain? Also, is there not a lateral strain. And is the lateral strain not some function of the longitudinal force? In addition, I am puzzled by the longitudinal force concept that it is talked about as if it is a single number.

My second question is, why do the British have to measure this every 60 feet or 20 meters if there is no longitudinal strain and the longitudinal force is a single number that, if I measure it in Chicago, is still the same as it is in New York?

J. SIMMONS: The question that you can ask is, okay, here is one number which represents the total integrated stress which you can call the longitudinal force over the track. But that can be a function of length along the track -- and it will be. The question is, what kind of wavelengths are there involved? If they are very short -- and apparently the British are concerned they are or may be -- then you have got to take measurements relatively close together. If they are very long, then, maybe you do not have to put these transducers so close together. Therefore, there is not just one number for longitudinal force; it is a function of the variations in track conditions from New York to Chicago. It is undoubtedly not constant. You are looking at a very complex, loaded structure which is tied down to the ground at very short intervals.

MR. VINCENT: I would have thought, though, that if the force is not constant, you would have what we call a force gradient or stress, and, if there is a stress, why is there not a strain?

D. P. McCONNELL: I think perhaps one of the sources of confusion in this discussion is whether it is a variation in stress across the rail cross section at any track location or the variation in axial or longitudinal stress along the length of the rail that is of interest. The topic of longitudinal force that is being considered here constantly gets confused with the term "residual stress."

There is a stress in the rail due to the presence of an axial load in the rail. This stress is a function of the state of constrained thermal expansion or the constrained axial "creep" of the rail. It arises from the anchoring of the rail to the ties constraining axial displacements.

This stress will vary down the length of the track. It will vary due to the fact that trains brake at one place or they are always accelerating up the hill. These actions have a tendency to "bunch" the rail at various points.

Axial rail force, taken as an average stress times the rail area, will also vary with temperature and the efficiency of the fastenings holding the rail down. Therefore, compression can begin to build up in some regions and release in other regions. But if I were to look solely at the stresses due to that axial force in the rail at any one section, they would in essence distribute themselves fairly uniformly across that section.

This behavior is in sharp contrast to the stress distributions which arise due to the local yielding of the rail material -- the "residual stresses" which we have talked about. These stresses generally have much higher values in any given cross section and vary greatly both along the length of the rail, and more importantly, across the rail cross section. Residual stresses are in equilibrium across that cross section.

Consequently, there are two different, competing phenomena present in rails. Most of the discussion -- especially the questions Dan Stone has asked -- has been focused on two facts. First, that any technique which looks solely at changes in one material characteristic with the presence of stress is not capable of distinguishing between the two types of stresses which have been superimposed. Second, whereas residual stresses are accompanied by strains, stresses due to constrained thermal expansion do not result in strains except by Poisson's effect.

Allan Zarembski, is there anything you want to add? You had some data from the Bessemer and Lake Erie which I think was the source of some confusion.

A. M. ZAREMBSKI (Association of American Railroads): The basic question is whether there is strain or whether there is not strain.

First of all, there is no longitudinal strain arising from constrained thermal expansion. The data that I showed was longitudinal strain and if you take the simple analogy of a strip of metal constrained at the ends and heated, the strip of metal has no place to displace axially. It does not strain longitudinally.

However, you most certainly have a stress buildup in that strip of metal; if you heat it high enough, it is going to buckle up because of the instability phenomenon.

As to why you cannot look at strain as occurring in a transverse plane, say, perpendicular to the axis of the rail, it is because of the complex shape of the rail section. Once you get into the cross section, there is a fairly significant distortion of the stresses due to uneven heating and due to the fact that you do not have a really symmetric or homogeneous shape. To my knowledge, there has been no successful correlation of the strain out of longitudinal plane with force in the longitudinal direction.

J. SIMMONS: I just want to make a quick comment to Mr. Yeager, who showed those attenuation curves and said he was applying a fast fourier transform (FFT). I believe that the correct method to apply on decaying curves of that type is the Prony method. I am surprised you used an FFT. It looks irrelevant for that kind of curve. It is naturally done by Prony method.

D. P. McCONNELL: One of the questions addressed to British Rail concerns the density of their gage placement. Would you comment on that, Dr. Lane?

G. S. LANE (British Railways): Gages have been placed at 20-meter intervals, but I would like to comment on this question of whether there is or whether there is not longitudinal strain.

If a rail is correctly stressed and uniformly stressed and there is no influence of braking acceleration or mining subsidence or anything else, there will be no longitudinal strain so we have nothing to worry about. But the fact of the matter is, there is a longitudinal strain when the stress conditions change for reasons as outlined by Allan Zarembski. This longitudinal strain can occur and it is in these circumstances that you had better start worrying and trying to measure it.

As to this question of how often we measure the rail forces, I said that we measure them possibly every 20 meters. Well, this is a function of the wavelength of the effect you are expecting to measure. That example of 20 meters is rather closer spacing than one would normally measure for purely production purposes. We were combining this exercise with research purposes as well. I think a more normal spacing on that particular site I described would be about five times that much, such that we are looking at wavelengths of the order of 100 meters or so on that particular site. We are expecting variations in force-free temperatures in that sort of wavelength, so we have obviously had to put rail force transducers fairly close together.

D. P. McCONNELL: I think that, if one is interested in some feeling for the distribution of longitudinal forces in fact, there was some work done in the period from about 1930 until some time in the early part of the mid-1940's by the AREA [American Railway Engineering Association], which is published in its proceedings, volumes 29 through 39. These reports specifically deal with measurements of rail creepage or motion under trains and also Berry-type mechanical strain gage measurements. In addition, there was a paper written in 1937 by Africano in the ASCE journal in which a theory of axial force development in rails was laid out which discusses some of these effects.

R. H. PRAUSE (Battelle Columbus Laboratories): When the track buckles, does it go suddenly or does it go in a gradual, slow process? In other words, is there a way of looking down and seeing when it has started to buckle?

A. D. KERR: The tracks presently in use generally buckle laterally. A straight track buckles instantaneously with a loud bang (energy release). Tracks which show lateral geometrical imperfections buckle with a smaller bang. The larger the imperfection, the slower is the buckling process and the less loud the bang. Often, track buckling may occur in front of or closely behind a moving train or between the inner wheels of a long freight car.

Additional material on this subject may be found in my paper, "Thermal Buckling of Straight Tracks; Fundamentals, Analyses, and Preventive Measures" [in Proceedings of the AREA, vol. 80 (1978), pp. 16-47].

I would like to ask Dr. Lane a question. In one of the publications, it was reported that British Rail attempted other methods prior to deciding on the development of the force measuring device that you discussed earlier [session I] in this conference. Would you like to comment on what other attempts you made and why you felt they did not work?

G. S. LANE: As far as I know, not a tremendous number of other techniques have been tried. I am aware that one other section in our department did use the ultrasonic techniques similar to Don Bray's, but a very limited amount of effort was put on the work and, generally speaking, it was abandoned when we started working on the vibrating wire gage. Apart from that, we have tried mechanical-type strain gages, and D-mec gages which are similar to the Berry gage; we generally found extremely large amounts of scatter from the results.

From those we went on to vibrating wire strain gages of a different type, which are about 5.5 inches long and simply clamped to the rail foot. Obviously, one has to clamp them on the other side to take account of lateral bending and so forth, but we generally found they fell off under traffic. It was decided that the only way of getting a reasonably long-term device was to actually physically mount it in the rail where it would (a) measure the actual physical force that we wanted to measure, and (b) be more protected from the wide variety of severe influences that generally occur in railway traffic.

Incidentially, I should say that, because of the calibration technique, I would suggest that the existing rail force transducer does in fact measure precisely the total force averaged across the rail section because the calibration technique applies a force using a hydraulic tensor at a reasonable distance from the actual transducer itself. By the nature of that technique, by the time that you get to the transducer, the force will be averaged over the whole section and you are referring the measurements to that calibration technique.

A. D. KERR: Essentially what you are doing is sensitizing the web to vibrations by introducing the wire instead of the missing disk that you drill out. Did you try the same approach to the web itself?

G. S. LANE: No. It was suggested by a member of our management, but we thought it impractical. We thought the technique with the vibrating wire gages was likely to prove more successful.

J. R. BARTON: On the fundamental interaction of the British Rail gage, is that not just the change in the resonant frequency of the wire that the tension changes because you change the endpoint location by means of the distortion that takes place in the rail? So the strain gage would work just as well.

A. D. KERR: Another method to determine the axial force could consist of drilling a hole in the unstressed web, without installing anything, and then measuring the deformed hole when the rail is subjected to a temperature change.

G. S. LANE: Well, we tried that at British Rail. However, it is not a very practical method for your average permanent way man to go down the track and use. It is a very small change.

D. P. McCONNELL: I would like to add some comments to the previous discussion, in that I am convinced we have had a certain amount of confusion over terminology.

As Dr. Benson indicated, there are residual stresses produced in the rail which are of the kind most normally associated with manufacturing processes. They are the consequences of the rolling of the rails, the welding of rails in continuously welded strings and, most strongly, the plastic deformation of the rail head under wheel loads. The deformation of the head of the rail is a function of the fact that the wheel runs directly on the rail head and, for any wheel load in excess of approximately 19,000 pounds, progressive microplastic strain occurs with each passage of a wheel. This action produces a severe cold working of the head of the rail and residual stresses due to that yielding. Those stresses exist within the rail and throughout the cross section of the rail. There is some indication that you can have substantial stresses occurring in the web of the rail due to this phenomenon, residual stresses locked into the material.

The issue with which we are dealing is that, given the fact that cold work of the rail occurs, the stress which we are interested in measuring is that stress due predominantly to constrained thermal expansion of the rails, not that due to cold working. In terms of magnitudes, axial stresses generally are of substantially lower magnitude than either the residual stresses locked in by progressive plasticity under passing wheel loads or those due to manufacturing processes. It is the variation of the stresses due solely to the axial load on the rail which is of interest in the most likely applications, such as detecting incipient buckling problems with the track.

Much of the discussion of this conference has been addressing itself to the issue of whether one can detect changes in stress in the rail rather than can one detect those changes in stress in the rail which are due to axial forces. Stress is an indirect indicator of phenomena taking place in the rail; that is, constrained thermal expansion of rail creep.

So I think it is useful for the purposes of our future discussions to clearly differentiate between residual stresses due to mechanical workings or thermal working of a rail and those which are induced by constrained thermal expansion. If this distinction is not kept in mind, we will have a mixture of terminologies -- apples and oranges.

TECHNICAL PAPERS

"Precision of the X-ray Stress Measurement Technique"

M. R. James
Rockwell International Science Center

My main purpose is to provide a review or introduction to the X-ray diffraction technique of measuring residual stresses. I want to cover the main definitions and terms that are used in the techniques and then describe some of the areas where there are minor problems with it. This will provide some idea of exactly what the X-ray technique is measuring, which is obviously a little bit different from any of the other internal probes of the material, and will serve as a preface to the following papers that deal with specific aspects of the X-ray diffraction technique.

A polycrystalline material is shown in figure 1 having a fully random orientation of the grain structure. In each of these grains, I have drawn a specific hkl plane -- for the ferrite crystals in steels we normally use the (211) plane. Note that these (211) planes are oriented differently with respect to the surface in each grain.

Some of these grains will be aligned so that, when an incident X-ray beam falls on them, the Laué conditions for diffraction will be fulfilled and a diffracted X-ray beam will be produced.

This is a diffracted X-ray beam. It is described by Bragg's Law, which relates the angle of diffraction, given in figure 1 as 2θ (the angle between the incident radiation and the diffracted radiation), and the interplanar spacing "d" (the lattice spacing between the crystallographic planes). Bragg's Law is simply: $\lambda = 2d \sin\theta$.

It is evident that not only is there diffraction from the grain shown but, in the three-dimensional case, there are many grains oriented to fill diffraction conditions and in real space a cone of radiation is produced. It is important to note that some grains do not contribute at all to the diffracted radiation.

Figure 2 depicts the same phenomena. Because the material is polycrystalline, the sample may be rotated to bring the same hkl planes -- the same (211) planes in different grains -- to fulfill the diffraction condition and obtain a diffracted X-ray beam.

If the surface of the material is under stress, as shown in figure 2, there will be a resolved component of that stress acting on the lattice planes. When one tilts the sample and looks at the same hkl planes in different grains, the resolved component of the stress on those hkl planes is going to be different than before. We measure the angle of diffraction, 2θ, related to the interplanar spacing, and thus we measure a change in the interplanar spacing between these two conditions.

It is very simple. We have not had to look at a stress-free sample. We have not had to contact the surface of the sample at all. We simply rotate the sample with respect to the incident X-ray beam and we can measure a strain in the material.

One of the important things to recognize immediately is that the X-rays penetrate the surface of the material only to a very shallow depth. For steels, that is normally on the order of about 1/1,000th inch -- 25 microns or so. We are obtaining a weighted average of the interplanar spacings over that 1,000th of an inch.

How do we obtain the needed information, 2θ? In this case, we set one orientation of the sample with respect to the X-ray beam, scan the detector along the 2θ axis, and obtain a diffraction peak, as shown in figure 3. Using curvefitting procedures and correction procedures, one may define some kind of position on that diffraction peak -- that is, the 2θ peak.

We then rotate the sample again, sweep across 2θ, and measure the diffraction peak again; because of the change in interplanar spacing, we have a peak shift, $\Delta 2\theta$, which is related to the strain.

The strain, of course, is related to the stress, and stress is a tensor property having a direction. The direction that we are measuring the stress in is defined as the intersection of the circle of rotation and the surface of the sample, as illustrated in figure 4. The angle

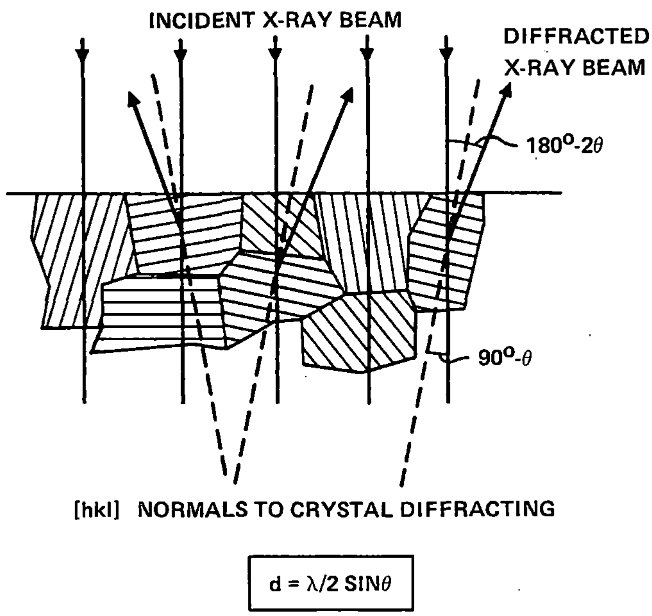

FIGURE 1. PRINCIPLES OF X-RAY DIFFRACTION

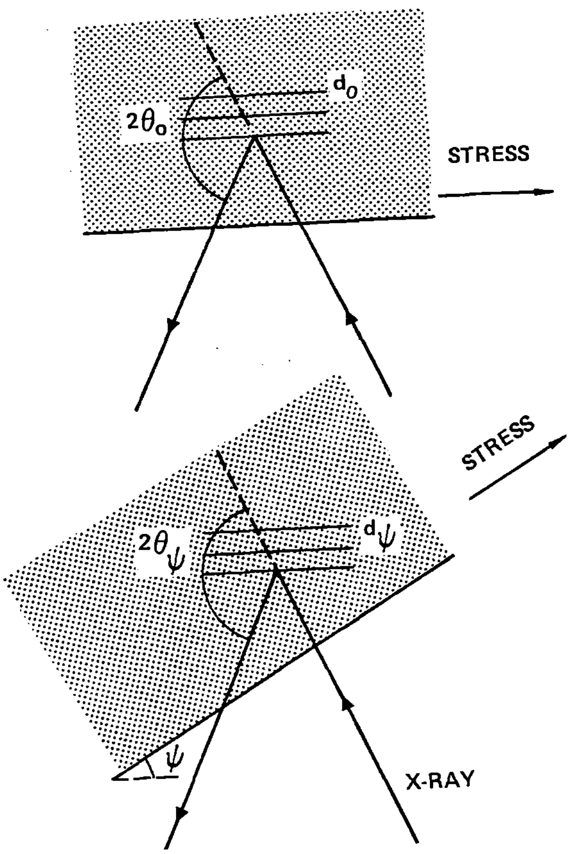

FIGURE 2. PRINCIPLES OF X-RAY STRESS MEASUREMENT

ψ (psi) constitutes a measurement of the angle of inclination of the sample as it is tilted. It is actually the angle between the normal to the specimen surface and the normal to the hkl planes that are diffracting, but may simply be thought of as the angle of sample tilt.

We also define an arbitrary direction, ϕ, which is shown in figure 4 as the direction of the measured stress with respect to some arbitrary axis. This axis could be a principal stress axis, the longitudinal axis, or whatever else one wishes to select. Of course, one can measure the stress in any direction on the surface of the material.

To illustrate the type of typical instrumentation that is normally used in a laboratory, figure 5 is a schematic of a powder diffractometer A diverging primary beam of radiation is made to illuminate an area on the sample surface of between 1 square millimeter and, say, 10 square millimeters, so we are averaging the stress over, say, an area 10 millimeters square and about 1/1,000 inch deep. The diffracted radiation comes back in a converging beam almost to a point because of the focusing geometry of the powder diffractometer, and it passes through a receiving slit.

That receiving slit is used to define that angle, 2θ, which is also dependent upon the position of the sample. It is important to be careful of the position of the sample so as not to introduce an experimental error. In terms of stress measurements on steels, that sample should be positioned to the order of, say, 1/5,000 inch or so to get errors on the order of 1-2 thousand pounds-force per square inch (ksi).

The instrumental error, then, is in determining the angle 2θ. In defining the peak of the diffraction profile, in positioning the sample and so forth, the instrumental errors usually run on the order of 1.5-3 ksi in stress. This is really the precision of the measurement. One can do better than that, but I am quoting a conservative value; it depends on a lot of things -- counting statistics, breadth of the diffraction profile, etc.

In the laboratory how long does the measurement actually take on instrumentation like this? Doing it by hand and assuming a fairly sharp diffraction profile, I would estimate that it could be done in 20 minutes or so; for broad diffraction profiles, though, the time would be about an hour or so.

With automated diffractometers and using counting statistics to optimize the time of data collection, one can get that time down to around between 15 and 30 minutes, depending on the breadth of the diffraction profile. Of course, one cannot put too big of a sample on the diffractometer, but I think Paul Prevey shows in his paper that it is possible to mount some fairly large samples.

(Two of the following papers are concerned with further instrumentation for in-field use, which does away with the powder diffractometer. They cover recent developments in portable X-ray stress equipment.)

I do not want to go into any detailed mathematics of how to derive the relationship between the measured stress and strain. However, I will mention a few assumptions. First, a biaxial stress state is assumed on the surface of the sample; this is not too bad because we are looking only at a very shallow depth. Second, it is assumed that isotropic elasticity theory is applicable. This creates a few problems here and there but, on the whole, for most materials it is not a bad assumption. Of course, where isotropic elasticity is not valid, the relationship between strain in the lattice planes and surface stress can be derived using anisotropic elasticity. The formula relating stress and strain is given in figure 6 for the $\sin^2\psi$ method. $\frac{S_2}{2}$ is a proportionality constant between the change in the interplanar spacing, the strain, and the stress. The stress is then related to the strain by a linear function of the angle of tilt, ψ.

The proportionality constant, $\frac{S_2}{2}$, is a function of the bulk elastic constants $(\frac{S_2}{2} = \frac{1 + \nu}{E})$. The relationship is not always applicable, however,

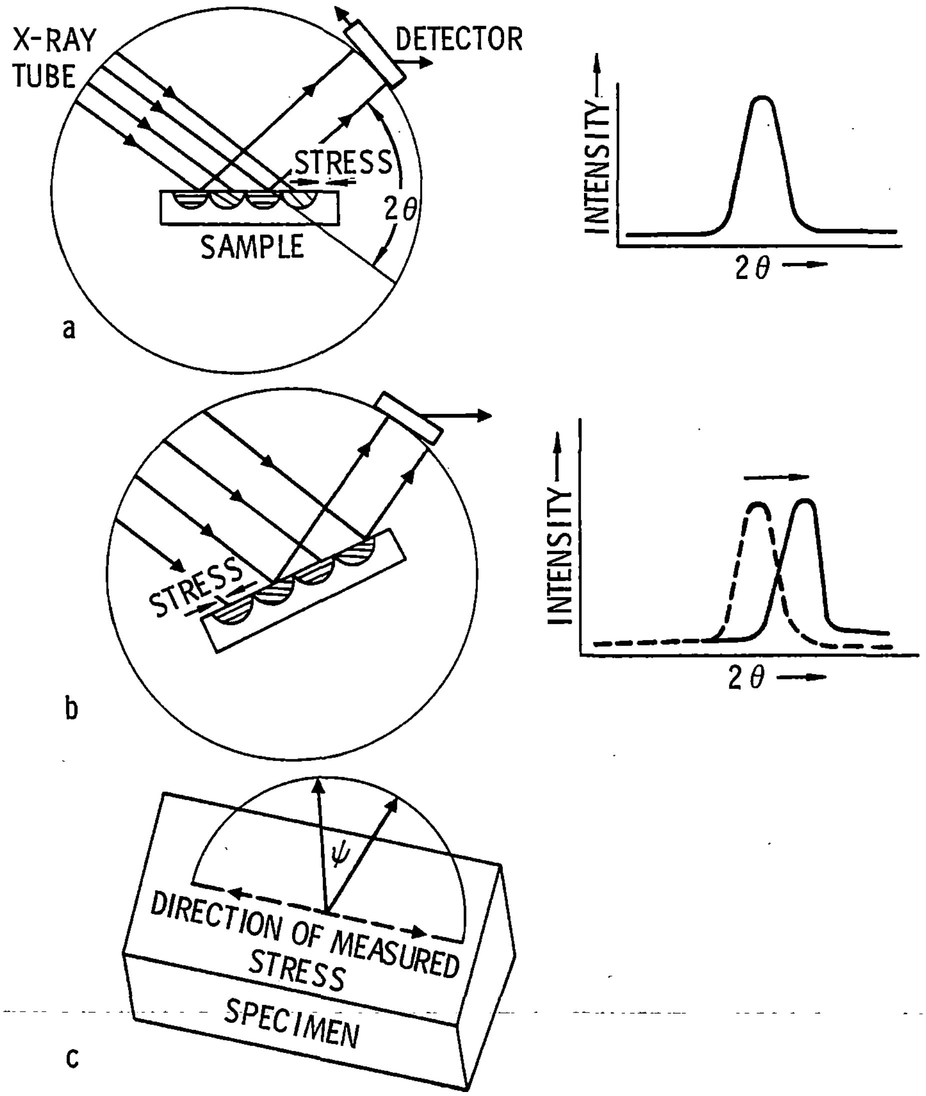

FIGURE 3. OBTAINING THE DIFFRACTION ANGLE, 2θ

because of elastic anisotropy and the selective nature of the X-ray technique, so normally we term $\frac{S_2}{2}$ and S_1 (figure 6) the X-ray elastic constants that are experimentally measured in the laboratory. If one looks at all the experimental values in the literature for medium carbon, low-alloy steels, the railroad steel type, one finds that they are pretty consistent to within 10 percent of one another. Proper values can thus be obtained from the literature.

The interesting thing to note about the $\sin^2\psi$ equation is that the change in interplanar spacing versus $\sin^2\psi$ is a linear relationship. So if we plot these two, we will find that the stress is proportional to the slope divided by the X-ray elastic constant.

All we have to do is determine the slope by measuring the lattice spacing at a number of tilts. Although this is a linear relationship, many people use four or six measurements of the interplanar spacing at various cycles. This is termed the "$\sin^2\psi$ technique."

Quite often the "two-tilt method" is used because of the linear proportionality. The lattice spacing is measured only at two ψ values. By using Bragg's Law, one can derive another equation, given in figure 7, which says that the stress is directly related to the change in a peak position through a term, K, the X-ray stress constant. Again, K is measured experimentally, and many values are tabulated in the literature.

In figure 8, part A, the lattice spacing is plotted versus $\sin^2\psi$, and a good straight line

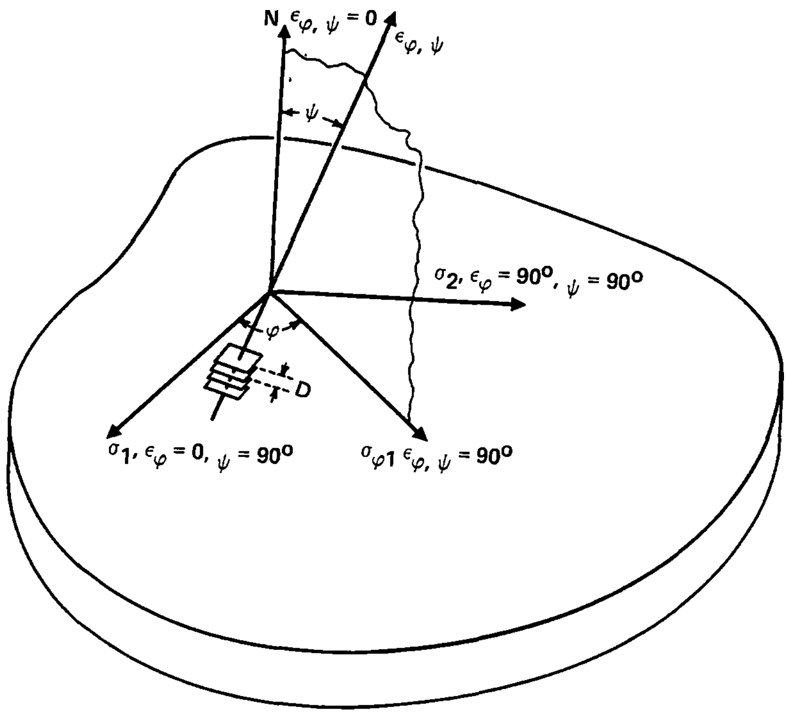

FIGURE 4. DEFINITION OF TERMS IN X-RAY STRESS ANALYSIS

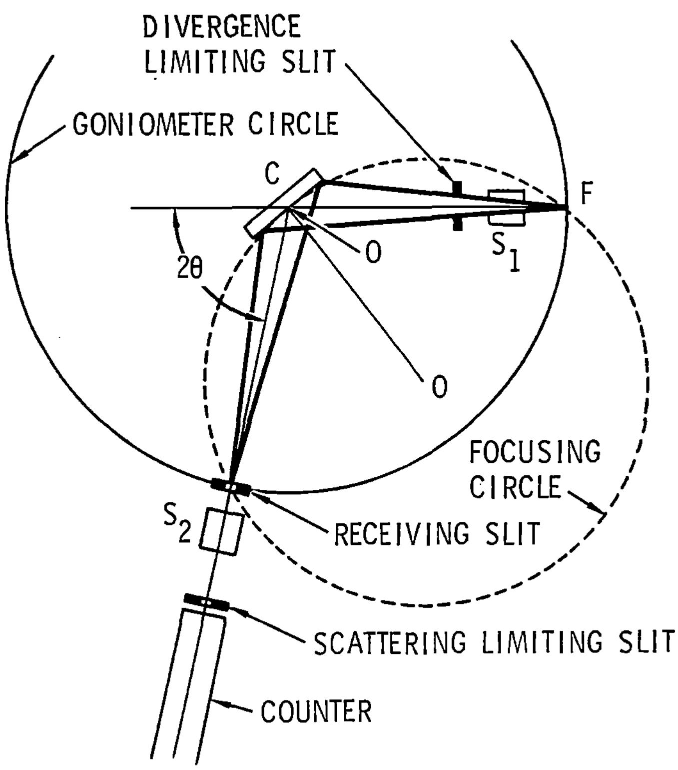

FIGURE 5. SCHEMATIC OF Ω DIFFRACTOMETER

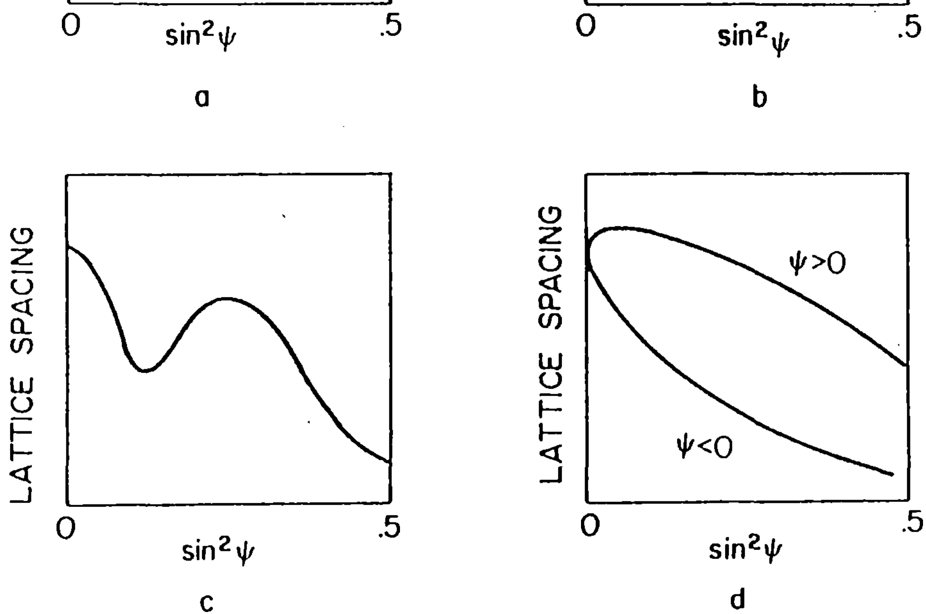

FIGURE 8. POSSIBLE DEPENDENCIES BETWEEN d VERSUS SIN$^2\psi$

$SIN^2 \psi$ METHOD

1) $\epsilon_{\phi,\psi} = \dfrac{d_{\phi,\psi} - d_{\phi}}{d_{\phi}} = \dfrac{S_2}{2} \sigma_{\phi} SIN^2 \psi + S_1 (\sigma_1 + \sigma_2)$

2) $\dfrac{S_2}{2} = \dfrac{1+\nu}{E} \qquad S_1 = \dfrac{-\nu}{E}$

3) $m^* = \dfrac{\partial \epsilon_{\phi,\psi}}{\partial SIN^2 \psi} = \dfrac{1}{d\phi} \dfrac{\partial d_{\phi,\psi}}{\partial SIN^2 \psi}$

4) $\sigma_{\phi} = m^* / \dfrac{S_2}{2}$

FIGURE 6. FORMULAE FOR $SIN^2\psi$ METHOD

TWO TILT METHOD

$\sigma_{\varphi} = \dfrac{E}{1+\nu} \dfrac{1}{\sin^2\psi} \dfrac{\cot\theta}{2} (2\theta_o - 2\theta_{\psi})$

$= K \, \Delta 2\theta$

where $K = \dfrac{E}{1+\nu} \dfrac{1}{\sin^2\psi} \dfrac{\cot\theta}{2}$

FIGURE 7. FORMULAE FOR TWO-TILT METHOD

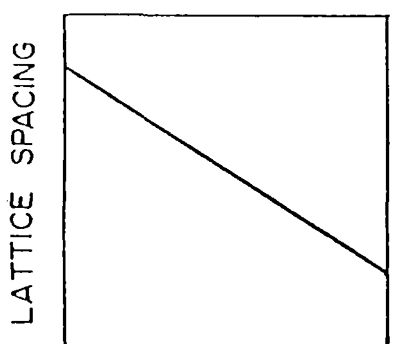

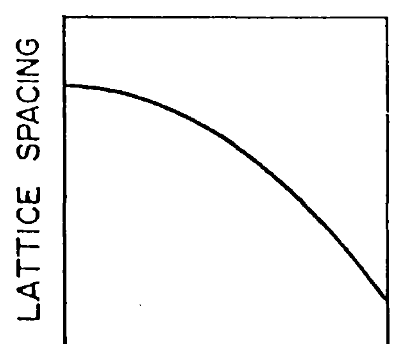

is established. In the majority of cases, one finds this kind of relationship. In his paper, Paul Prevey discusses the application of this technique on railway steels and verifies that this linear relationship is valid for the type of deformation the rail steel undergoes.

In the literature, however, some other cases are reported. In one or two Japanese papers, a curvature as shown in figure 8, part B, has been reported. This is due to a very, very strong stress gradient in the surface of the material.

In figure 8, part D, splitting of d versus $\sin^2\psi$ is shown when the sample is inclined in the negative and the positive ψ direction. This is due to a nonbiaxial nature of the surface stresses tensor. My view is that the principal axes are not coplanar with the surface. This has been seen once or twice in the general literature, and work is continuing on its cause, but it is very rarely seen and not important in general engineering practice.

What are seen more often are oscillations in d versus $\sin^2\psi$ (figure 8, part C). There is a fair amount of interesting controversy as to what they are attributable -- whether it is elastic anisotropy, plastic anisotropy, or the development of textural microstresses during the deformation process. There are various ways to treat this problem. What is most important, I think, is that we know fairly well when such oscillations are expected to occur. They are not expected to show up in a medium carbon steel.

Because the X-ray technique is so widely used, control of instrumental factors and well-defined experimental procedures have been repeatedly published, so that one may quickly become familiar with the technique. There are certain well-known fundamental limitations, such as excessively large grain size (in aluminum alloys or weldments, for example) and the effects of plastic deformation, that detract from universal acceptance of the technique, but investigations are continuing into proper interpretation of the results in these circumstances. In a majority of manufacturing processes (grinding, machining, shot peening, welding, heat treating, case carburizing), the X-ray technique is accurate.

One quite common complaint of the X-ray diffraction technique is that it is only surface sensitive, sampling a layer of less than 20 micrometers. The validity of accepting the residual stresses in this thin layer as representative of the bulk may be suspect from a design engineer's viewpoint; however, this unique advantage of the X-ray method is often used to determine the distribution of stress with depth by systematically removing thin surface layers electrochemically and then remeasuring the stress. Correction procedures for relaxation during layer removal and effective beam penetration have been developed. The fact that the X-ray technique is non contacting makes this procedure very easy. (In fact, not having physical contact with the specimen allows for remote measurements, such as at high temperatures or in specific, even aggressive environments.) Since surface initiated failures are of primary importance in dynamically loaded components, surface stresses and their distribution with depth is often very important.

The selective nature of the X-ray technique makes possible the investigation of stresses in individual phases that may be compensating each other. The ability to precisely select the area of illumination by collimating the X-ray beam provides the ability to map the stress distribution on a fine scale. This technique has been used to show that large variations in surface stress may occur in abusively ground 4340 steel and abusively end-milled nickel base samples. Restricting the areas of sampling on a surface is also useful in determining stresses on curved surfaces with radii down to about 1 millimeter.

It should be remembered that the results of X-ray investigations have often been used in the interpretation of the role of residual stresses in the deformation and fatigue resistance of engineering material. It is, in fact, the only technique used to study the stability of residual stresses during dynamic loading. The recent advances in instrumentation should help instigate a movement of the X-ray diffraction stress measurement technique from the laboratory to a general-purpose testing tool. As noted in the final two papers, the development of new instrumentation and specific packaging arrangements will allow the X-ray technique to be used in many areas where equipment limitations have prohibited its application in the past.

"The Feasibility of Employing X-ray Diffraction Techniques for Measuring Longitudinal Rail Stresses"

Paul S. Prevey
Lambda Research, Inc.

First of all, I am an experimentalist, and I am going to take the discussion from where Mike James left it, and show an actual application to railroad rails.

I would like to make a few comments at the beginning, though, about all of the methods that we have discussed so far for nondestructive stress measurement. All of these are fundamentally dependent upon measuring changes in physical properties of the material. The magnetic, ultrasonic, and X-ray diffraction methods, therefore, are all going to be affected by both residual and applied stresses. Accordingly, all of the nondestructive methods are going to require measurement both before and after the application of the stress to be measured due to thermal expansion in the rails. I think that is true, just by definition, of all material property sensitive methods.

The X-ray diffraction techniques that I am going to discuss are quite well established. They have been around since the 1930's. There is a publication by the Society of Automotive Engineers, SAEJ 784-A, which describes the standard method. All X-ray diffraction techniques measure strain in the crystal lattice and are nondestructive when applied to a surface.

X-ray diffraction techniques have not been used in many applications, for two reasons. First, the apparatus itself is not readily portable, although that situation has now changed, as noted in the following papers. There are a number of position-sensitive detector devices that are available and will make portable equipment practical. There is work going on in Japan and Germany, as well as in the United States, which will lead to portable equipment. There will probably shortly be a variety of different types of apparatus available. Second, X-ray methods apparently have not been applied because there is a fear of the effect that prior plastic deformation of the specimen will have on the accuracy of the stress measurements. There has been enough work done in this field, as Mike James has pointed out, to demonstrate that certain types of plastic deformation difficulties can arise.

What I set out to do for this conference was to examine the effects of prior plastic deformation on the accuracy of stress measurements in rails, which is one major source of possible error, particularly on the rail head. Second, I investigated the effect of any subsurface stress gradients present that can cause errors in simple surface measurements. To examine the impact of actual field conditions on stress measurements on the rail, I investigated the effect of the protective tar-like coating upon measurement accuracy. Does the coating have to be removed or can measurements be made right through it? One advantage of the X-ray technique is that the radiation penetrates through thin surface films. Finally, I tried to establish the repeatability of measurements on an actual rail sample.

After having investigated the accuracy of the technique, I went on to demonstrate the method by determining the longitudinal stress distribution across a flash buttweld, which I thought would be of interest to the participants in this conference.

Introduction

The increase in the use of continuously welded railroad rail has been accompanied by an increase in the frequency of rail failures due to thermal stresses caused by ambient temperature changes in the field. The failures have led to increasing interest in nondestructive longitudinal stress measurement techniques that could be applied to rail in the field. To date, considerable effort has been devoted to the development of the relatively new technologies of ultrasonic [1, 2, 3] and magnetic [4, 5] methods of stress measurement, while little effort has been made to apply the established techniques of X-ray diffraction stress measurement to the problem. Because experimental difficulties arising from preferred orientation, transducer couplings, and stress standards have limited the usefulness of the ultrasonic and magnetic methods to date, attention has been focused on the application of X-ray diffraction methods of stress measurement.

X-ray diffraction methods of stress measurement have not been previously applied because of the nonportability of conventional stress measurement apparatus, and because the effect of prior plastic deformation of the rail steel upon the accuracy of X-ray diffraction stress measurements has not been established [6]. The recent development of various position-sensitive detectors has made feasible the portability of X-ray diffraction apparatus [7, 8, 9, 10] that could be designed for rail stress measurement in the field.

In light of the above, it was the purpose of this investigation, employing conventional X-ray diffraction techniques in the laboratory, to establish the feasibility of performing X-ray diffraction stress measurements on both new and plastically deformed used rail. Nondestructive X-ray diffraction surface stress measurements made in the field could be potentially subject to significant experimental error due to two effects:

a. The presence of a nonrandom distribution of microstresses on a severely deformed surface resulting in a nonlinear dependence of a lattice spacing, d, upon $\sin^2\psi$ (where ψ is the angle of tilt employed during measurement [11, 12, 13, 14, 15, 16].

b. A large subsurface stress gradient resulting in erroneous surface measurements due to the exponential weighting of the data obtained at the surface and in the layers beneath [17].

If neither of the above proved to be a source of serious experimental error, the effect of the tar-like protective surface coating (used in the field to minimize corrosion of the rail) upon X-ray diffraction residual stress measurements made without removing the coating, and the repeatability of such measurement, were to be investigated. As an example of the use of X-ray diffraction stress measurement, the technique was then to be applied to a specific case study to determine the longitudinal residual stress distribution across a flash buttweld in hardened rail.

Sample Preparation

Two rail samples were supplied by the Southern Railway for use in this investigation. The first sample was a nominally 6-inch-long section of used rail, identified as sample D-44, which is reportedly of the shallow induction head-hardened variety manufactured in 1974. This sample, which was assumed to be typical of used rail found in the field, was brought to the laboratory for the purpose of this investigation with the protective coating intact.

A cross section of the used rail sample showing the four longitudinal stress measurement locations investigated is shown in figure 1. Location 1, considered the most likely for useful in-field longitudinal stress measurement, was at the center of the web. Location 2 was on the field side of the rail head beneath the layer plastically deformed by contact with the wheel. Location 3 was on the top of the rail head in the region of severe plastic deformation. Location 4, on the edge of the flange

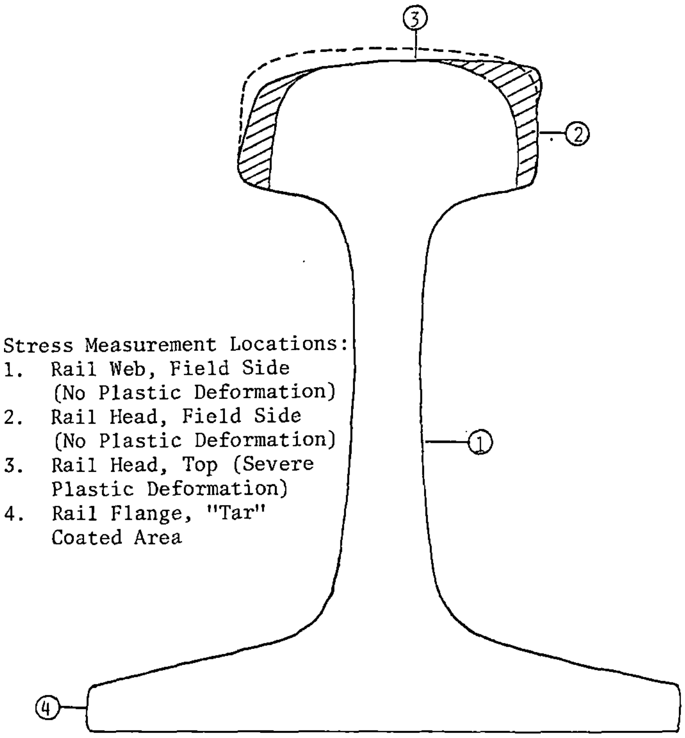

USED RAIL CROSS SECTION
SHOWING ORIGINAL RAIL OUTLINE AND HARDENED ZONE
FIGURE 1

at the base of the rail, was a location covered with the tar-like anticorrosion coating. Location 4 was employed for comparing the repeatability of measurements made through the coating with those made after removal of the coating. The original outline of the rail head, prior to wear and plastic deformation in the field, is shown in figure 1 with a dashed outline. The induction hardened zone surrounding the head of the rail, as revealed by a Nital etch, is indicated by shading.

The second sample consisted of a nominally 18-inch-long section of new, deeper induction hardened rail, which was flash buttwelded at the center. The buttwelded sample was employed to determine the longitudinal residual stress distribution along the axis of the weldment as a function of distance from the weld centerline.

The rail samples employed by this investigation were reportedly "Curve Master" rail manufactured by U.S. Steel Corporation and having a nominal chemical composition of 0.75 carbon, 0.83 manganese, 0.013 phosphorus, 0.028 sulfur, and 0.09 silicon, and a 0.2 percent offset yield strength of approximately 118 thousand pounds-force per square inch (ksi) [18]. The samples were reportedly hot-rolled followed by a controlled cool from 1600°F to 700°F, bent to offset rail head hardening deformation, and induction hardened.

Experimental Procedure

Because all measurements made in this investigation were performed in a laboratory environment, rather than on continuous rail sections in the field, the results reveal, by definition, the residual stresses present in the rail. Had these samples been constrained in track in the field, the total stress present in the rail would be simply the superposition of residual and applied stresses due to the constraint imposed by the ties.

All X-ray diffraction residual stress measurements were made employing a modified horizontal General Electric diffractometer fixtured for residual stress measurement with apparatus designed by the author. Measurements were made employing the diffraction of chromium K_α radiation from the (211) planes of the body-centered tetragonal or body-centered cubic structures of the martensite and ferrite phases, respectively. A solid state detector was employed as a monochromator in a parafocusing technique to detect the diffracted X-ray beam. The diffraction peak angular positions were determined employing a five-point parabolic regression procedure after correction for the Lorentz polarization and absorption effects and for a linearly sloping background intensity. Details of the diffractometer fixturing employed in this investigation are shown in table 1.

The single crystal elastic constant $\frac{E}{(1+\nu)_{(211)}}$, in the crystallographic direction normal to the (211) planes was determined previously for 4340 steel, 50 R_C, by loading a simple rectangular beam manufactured from 4340 steel on the diffractometer in four-point bending and determining the change in lattice spacing of the (211) planes as a function of applied stress [19]. No attempt was made in this investigation to determine the single crystal elastic constants for the alloy employed in the manufacture of the rail, because the single crystal elastic constants reported for a variety of steels in the (211) direction do not differ significantly from those obtained by the author for 4340 steel [20].

Investigation of Presence of Nonrandom Microstress Distributions. In the application of X-ray diffraction techniques for the determination of both residual and applied stresses, a condition of plane stress is assumed to exist at the surface of the sample being investigated. The principal stresses are assumed to lie in the plane at the surface. The stress, σ_ϕ, being measured at some arbitrary and unknown angle, ϕ, to the principal stresses σ_1 and σ_2 at the surface, give rise to a dependence of the lattice spacing, $d(\psi)$, measured at any given angle of tilt, ψ, to the surface of,

$$d(\psi) = \left(\frac{1+\nu}{E}\right)_{(hkl)} \sigma_\phi \, d_o \sin^2\psi - \left(\frac{\nu}{E}\right)_{(hkl)} d_o (\sigma_1 + \sigma_2) + d_o, \qquad (1)$$

where the elastic constants, ν and E, shown are single crystal constants in the direction normal to the lattice planes employed for measurement, and d is the unstressed lattice spacing of those planes.

The lattice spacing, $d(\psi)$ is then a linear function of $\sin^2\psi$ with a constant intercept for any fixed location and direction, ϕ, on the surface. Equation (1) can be solved for the stress, σ_ϕ, if the lattice spacing, $d(\psi)$, is determined for at least two angles, ψ, $\frac{1+\nu}{E_{(hkl)}}$ is known, and the assumption is made that $d_o \approx d(0)$. (The values d_o and $d(0)$ typically differ by less than 0.1 percent.)

The simplest method of solution, the two-angle technique, used extensively in the United States in a manner recommended by the Society of Automotive Engineers (21) usually employs the measurement of the lattice spacing at $\psi = 0°$ and $\psi = 45°$.

Alternatively, the value of the lattice spacing, $d(\psi)$, can be determined for several values of ψ, and equation (1) can be solved by simple linear regression. The resulting $\sin^2\psi$ method, in general use in Japan, makes any non-linearity in the dependence of $d(\psi)$ upon $\sin^2\psi$ immediately apparent. A six-angle $\sin^2\psi$ technique was employed in this investigation.

Work by Marion and Cohen [22] on the phenomenon of a nonlinear dependence of $d(\psi)$ upon $\sin^2\psi$, which has been shown to result in some cases from extensive uniaxial or biaxial plastic deformation, led to the development of their model for the dependence of lattice spacing upon ψ in the presence of a deformation texture represented by the deformation texture function, $f(\psi)$ (a normalized distribution of the pole density for the lattice planes employed for measurement). According to the Marion-Cohen model, the dependence of $d(\psi)$ upon $\sin^2\psi$ in the presence of a nonrandom microstress distribution produced by uniaxial or biaxial plastic deformation is

$$d(\psi) = f(\psi)\ (d_{max} - d_B) + \left(\frac{1+\nu}{E}\right)_{(hkl)} d_o\, \sigma_\phi \sin^2\psi - d_B, \qquad (2)$$

where the quantities d_{max} and d_B are the maximum and minimum lattice spacing resulting from the deformation process.

Equation (2) is solved by multiple linear regression after measuring $d(\psi)$ and $f(\psi)$ for several values of ψ. The presence of a coupling between $d(\psi)$ and $f(\psi)$ caused by a nonrandom deformation produced microstress distribution will lead to significant differences in the values of σ_ϕ obtained from the solution of equation (1) and equation (2). Only nonrandom plastic deformation will result in significant differences [23].

Measurements were made of the lattice spacing $d(\psi)$ and $f(\psi)$ as a function of six known angles, ψ, at the surface and at subsurface depths of 0.001 and 0.002 inch (beyond the maximum depth of penetration of the X-ray beam into the subsurface of the sample during surface measurements) at locations 1, 2, and 3 on the used rail sample. In all cases, measurements were made in the longitudinal direction. These data were then reduced by the two-angle, $\sin^2\psi$, and Marion-Cohen methods to determine:

a. The deviation from linearity of the dependence of the lattice spacing, $d(\psi)$, upon $\sin^2\psi$.

b. The magnitude of any contribution of a nonrandom microstress distribution due to coupling of the lattice spacing, $d(\psi)$, with the texture function, $f(\psi)$, after the model of Marion-Cohen.

c. The magnitude of the preferred orientation present in the samples as a potential complication of residual stress measurements in rails.

Material was removed for subsurface measurement by electropolishing in a sulphuric-phosphoric-chromic acid solution to minimize the influence of layer removal upon the subsurface stress distribution present in the samples.

TABLE 1

DIFFRACTOMETER FIXTURING

Incident Beam Horizontal Divergence	3.0° (1.0°)*
Receiving Slit	0.5°
Detector	Si(Li) set for 90% acceptance of the chromium K_α energy
Counts per Point	100,000
ψ Rotation	0.0, 18.4, 26.6, 33.2, 39.2, 45.0**
$\frac{E}{(1+\nu)_{(211)}}$	$2.45 \pm 0.04 \times 10^7$ psi
Irradiated Area	0.30 x 0.40 in. (0.10 x 0.30 in.)*

*( ) = technique for buttweld sample

**ψ angles of 0.0° and 45.0° used for two-angle measurements

Effect of Subsurface Stress Gradient. The radiation employed for residual stress measurement is attenuated exponentially as it penetrates into the surface of the sample. As a result of this effect, a "surface" measurement is actually an exponentially weighted average of the stress at the surface of the sample and in layers immediately beneath. Although, in the case of employing chromium K_α radiation to make stress measurements in steel samples, 50 percent of the radiation originates from depths of less than approximately 0.002 inch, stress gradients on machined surfaces are frequently observed that can result in errors in simple surface measurement as large as 20 ksi.

The effect of the surface stress gradient can be corrected knowing the linear absorption coefficient, μ, for the material and radiation employed, and the measured $d(\psi)$ distributions as functions of depth. Expressed in terms of the diffraction angle, 2θ, independently for each of the ψ angles chosen for measurement, the true diffraction angle in the presence of a stress gradient is given by

$$2\theta_T(Z) = 2\theta_M(Z) - \frac{1}{A}\frac{d(2\theta_M)}{dZ} \qquad (3)$$

where A is a function of μ, θ, and ψ; Z is the depth; and $2\theta_M$ is the measured diffraction angle [24].

To investigate the magnitude of the near-surface stress gradient at possible measurement sites on used rail, the residual stress was determined by the two-angle method as a function of depth at the surface and at nominal depths of 0.001, 0.002, 0.005, 0.008, 0.012, 0.016, and 0.020 inch beneath the original surface of the sample at locations 1, 2, and 3. The results, both with and without gradient correction, were compared to establish the magnitude of potential error in uncorrected surface measurements.

Effect of In-Field Surface Conditions. To determine the influence upon X-ray diffraction stress measurements of the protective coating present on the surface of the used rail, repeat measurements were made both before and after removing a nomially 0.002-inch layer of the coating material from the surface of the rail at location 4. The mean stress and standard deviation for measurements made through the coating and after removal of the coating with solvents were compared to establish the influence of the coating upon measurements made without cleaning the rail in the field.

Application to a Flash Buttwelded Rail. Two-angle residual stress measurements were made on the new rail sample in the longitudinal direction in a traverse across the surface of the rail head centered on the buttweld. The sample had been ground to remove the flash produced during welding, and Brinell hardness indentations were present along the top surface of the rail. The measurement traverse was located off center of the head of the rail to avoid local stresses produced by the hardness indentations. Prior to performing the measurements, approximately 0.008 inch of steel was electropolished from the surface of the rail head to eliminate the surface stresses produced by grinding.

Results and Discussion

The results presented here are in units of ksi (10^3 psi). Compressive stresses are reported as negative values. All results are in the direction parallel to the longitudinal axis of the rail segments.

Investigation of Presence of Nonrandom Microstress Distributions. The data obtained for six angles, ψ, at the surface and at nominal depths of 0.001 and 0.002 inch beneath the surface at locations 1, 2, and 3, reduced by the $\sin^2\psi$ method, Marion-Cohen method, and two-angle method, are presented in table 2. For the $\sin^2\psi$ method, the error shown is ± one standard deviation based upon the uncertainty resulting from a least squares fit to the data and the random error in the empirically determined crystal elastic constants. For the two-angle method, the error is ± one standard deviation due to random error in the elastic constants and an estimate of the uncertainty in the diffraction peak positions based upon the three-point parabolic technique recommended by the Society of Automotive Engineers [25].

These data are presented graphically in figures 2 through 10 for each of the measurement sites. In each figure, the lattice spacing, d, of the (211) planes and the texture distribution function, $f(\psi)$ the normalized (211) pole density, are shown as functions of $\sin^2\psi$.

As is apparent from the magnitude of the error shown for the six-angle method of data reduction and from the figures, even on the most severely plastically deformed head of the rail (location 3), the lattice spacing is a quite linear function of $\sin^2\psi$, assuming a random error in the measurement of $d(\psi)$ of approximately ± 0.00004 angstrom. As shown in table 2, there is a difference of less than 2 ksi between the stress determined by the $\sin^2\psi$ and Marion-Cohen results at any of the stress measurement sites examined, indicating an insignificant effect of nonrandom microstresses upon the stress measurements. Furthermore, when the data are reduced by the two-angle method, the results are found to agree within experimental error in all cases with the $\sin^2\psi$ results.

Effect of Subsurface Stress Gradient. The residual stress measured by the two-angle method as a function of depth at locations 1, 2, and 3 is presented to a depth of 0.002 inch in table 3, both with and without correction for the penetration of the radiation employed for measurement into the subsurface stress gradient along with the magnitude of the correction. The complete data sets obtained at the three locations are shown graphically in figures 11, 12, and 13. The maximum error observed that would result from failure to correct a nondestructive surface stress measurement for the penetration of the radiation into the subsurface stress gradient was - 3.7 ksi, observed at the surface of the severely plastically deformed head of the rail, location 3. An error of - 1.8 ksi, on the order of the random experimental error, was observed at the surface of the field side of the rail head, location 2. The most likely site for in-field

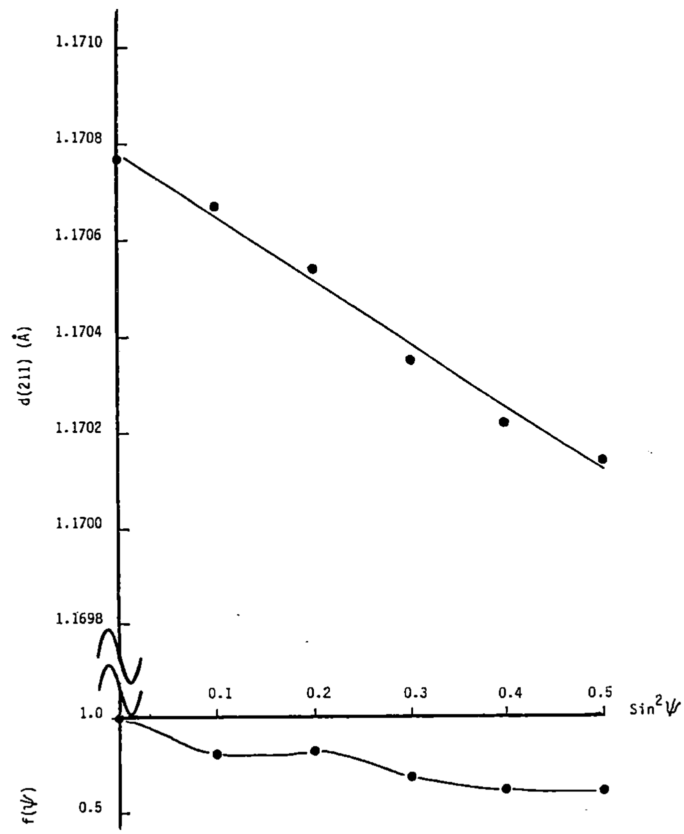

FIGURE 2. MICROSTRESS DISTRIBUTION -- d(211) and $f(\psi)$ VERSUS $SIN^2\psi$ (INDUCTION HARDENED RAIL, LONGITUDINAL DIRECTION): WEB CENTER (LOCATION 1) SURFACE

Two-Angle	-26.0 ± 0.7 ksi
$Sin^2\psi$	-27.6 ± 0.8
Marion-Cohen	-25.9

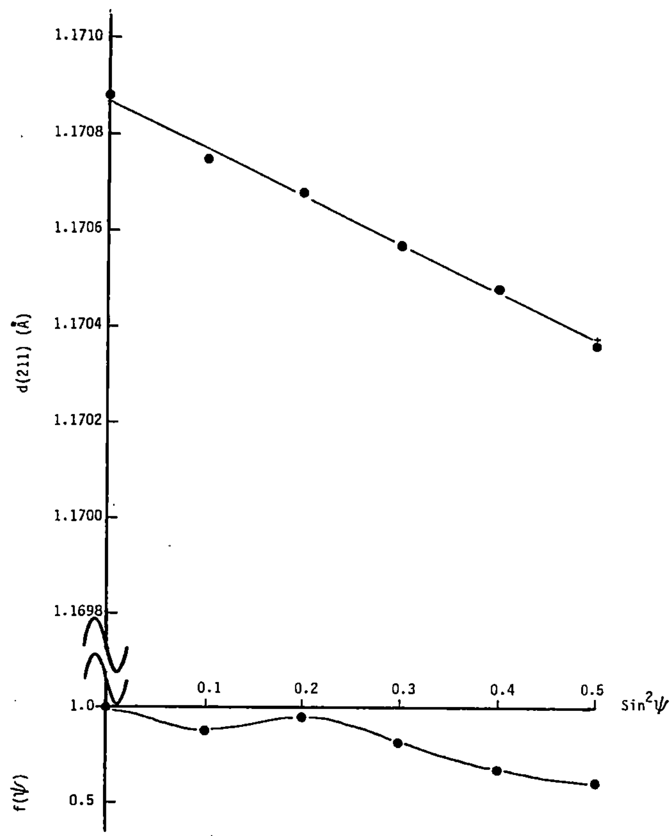

FIGURE 3. MICROSTRESS DISTRIBUTION -- d(211) AND $f(\psi)$ VERSUS $SIN^2\psi$ (INDUCTION HARDENED RAIL, LONGITUDINAL DIRECTION): WEB CENTER (LOCATION 1), 0.001 INCH DEPTH

Two-Angle	-21.6 ± 0.7 ksi
$Sin^2\psi$	-21.0 ± 0.2
Marion-Cohen	-18.7

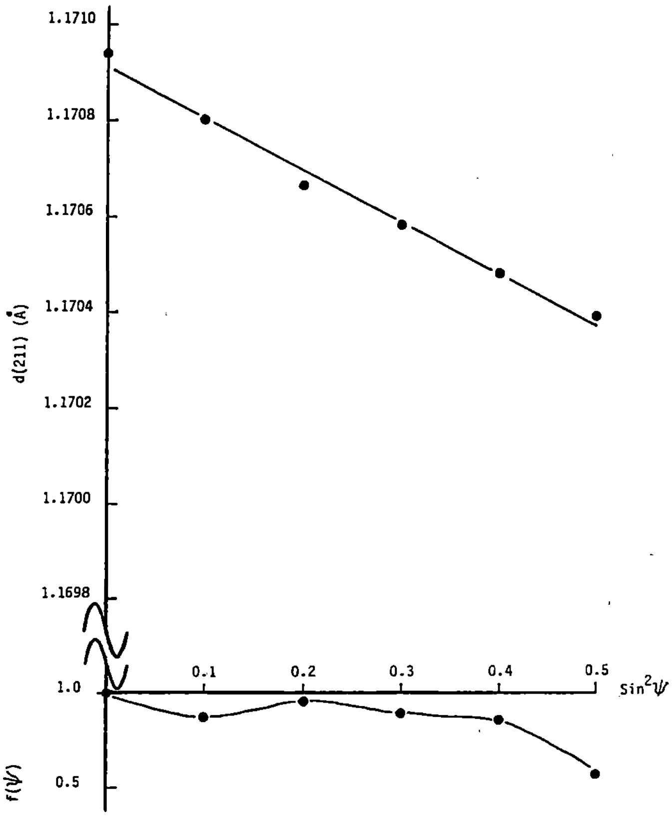

FIGURE 4. MICROSTRESS DISTRIBUTION -- d(211) and f(ψ) VERSUS SIN$^2\psi$ (INDUCTION HARDENED RAIL, LONGITUDINAL DIRECTION): WEB CENTER (LOCATION 1), 0.002 INCH DEPTH

Two-Angle	-22.8 ± 0.7 ksi
Sin$^2\psi$	-22.6 ± 0.7
Marion-Cohen	-24.6

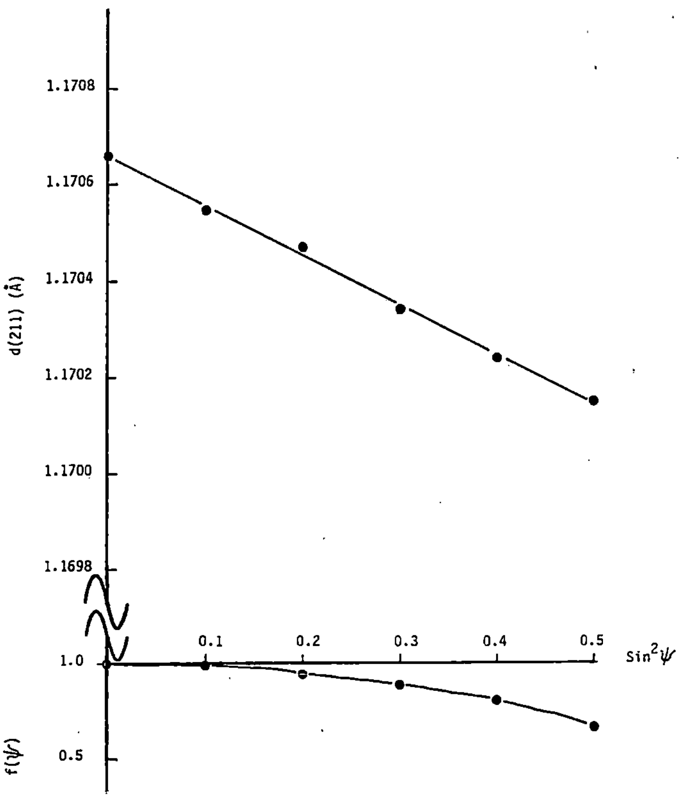

FIGURE 5. MICROSTRESS DISTRIBUTION -- d(211) AND f(ψ) VERSUS SIN$^2\psi$ (INDUCTION HARDENED RAIL, LONGITUDINAL DIRECTION): FIELD SIDE OF HEAD (LOCATION 2), SURFACE

Two-Angle	-21.6 ± 0.7 ksi
Sin$^2\psi$	-21.8 ± 0.2
Marion-Cohen	-22.2

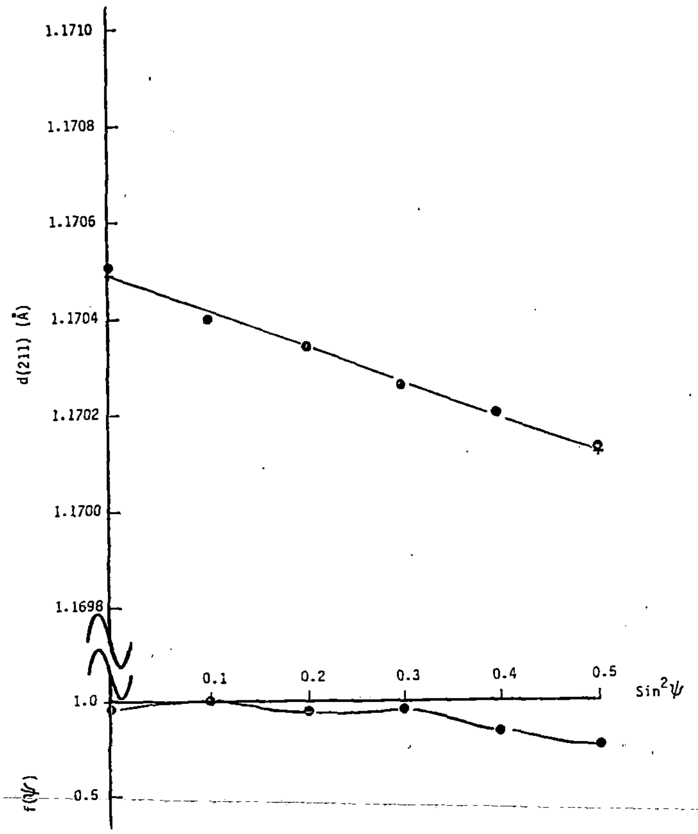

FIGURE 6. MICROSTRESS DISTRIBUTION -- d(211) and $f(\psi)$ VERSUS $SIN^2\psi$ (INDUCTION HARDENED RAIL, LONGITUDINAL DIRECTION): FIELD SIDE OF HEAD (LOCATION 2), 0.001 INCH DEPTH

Two-Angle	-15.7 ± 0.8 ksi
$Sin^2\psi$	-15.3 ± 0.3
Marion-Cohen	-17.1

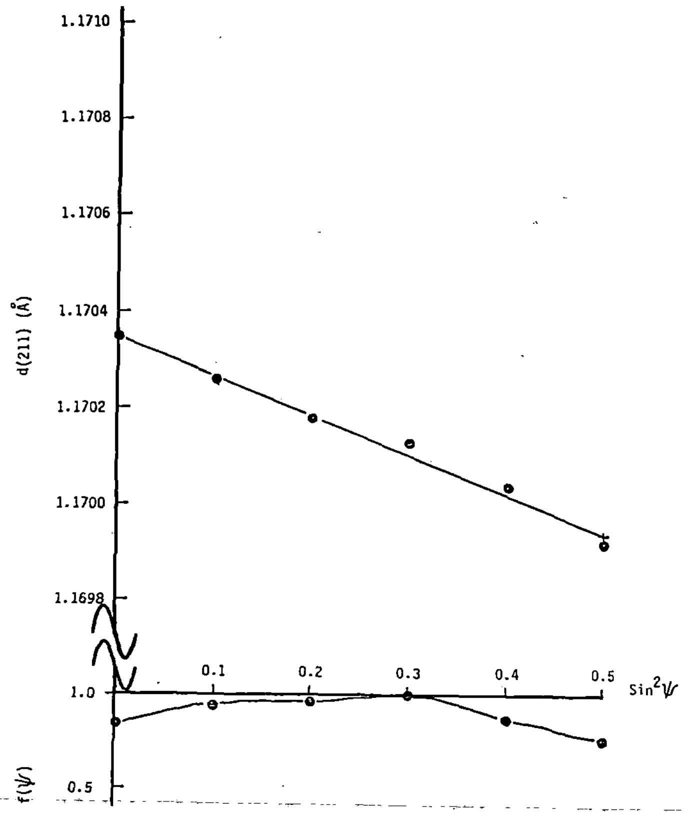

FIGURE 7. MICROSTRESS DISTRIBUTION -- d(211) and $f(\psi)$ VERSUS $SIN^2\psi$ (INDUCTION HARDENED RAIL, LONGITUDINAL DIRECTION): FIELD SIDE OF HEAD (LOCATION 2), 0.002 INCH DEPTH

Two-Angle	-17.9 ± 0.7 ksi
$Sin^2\psi$	-17.1 ± 0.5
Marion-Cohen	-16.6

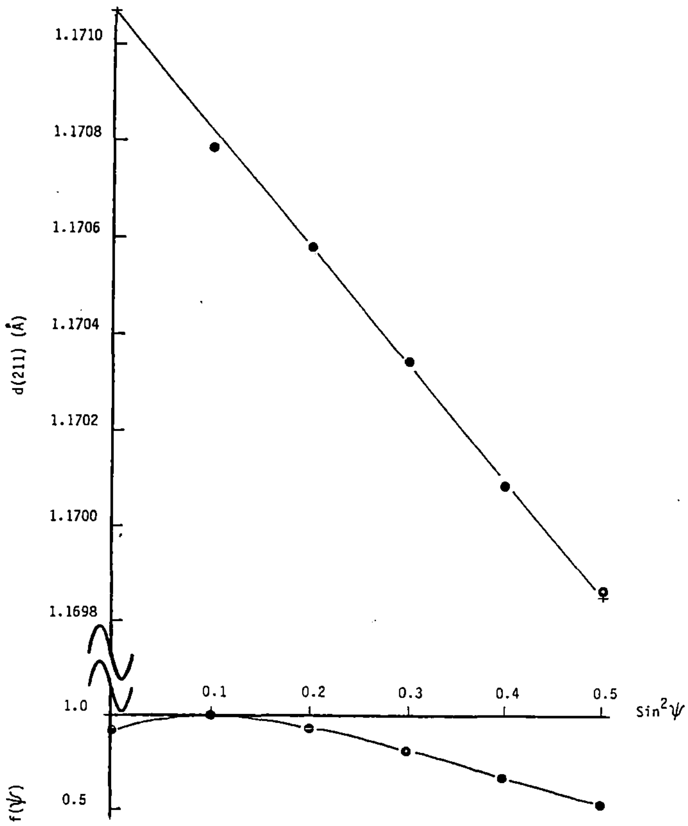

FIGURE 8. MICROSTRESS DISTRIBUTION -- d(211) and $f(\psi)$ VERSUS $SIN^2\psi$ (INDUCTION HARDENED RAIL, LONGITUDINAL DIRECTION): DEFORMED HEAD (LOCATION 3), SURFACE

Two-Angle	-52.0 ± 1.5 ksi
$Sin^2\psi$	-51.3 ± 0.3
Marion-Cohen	-56.2

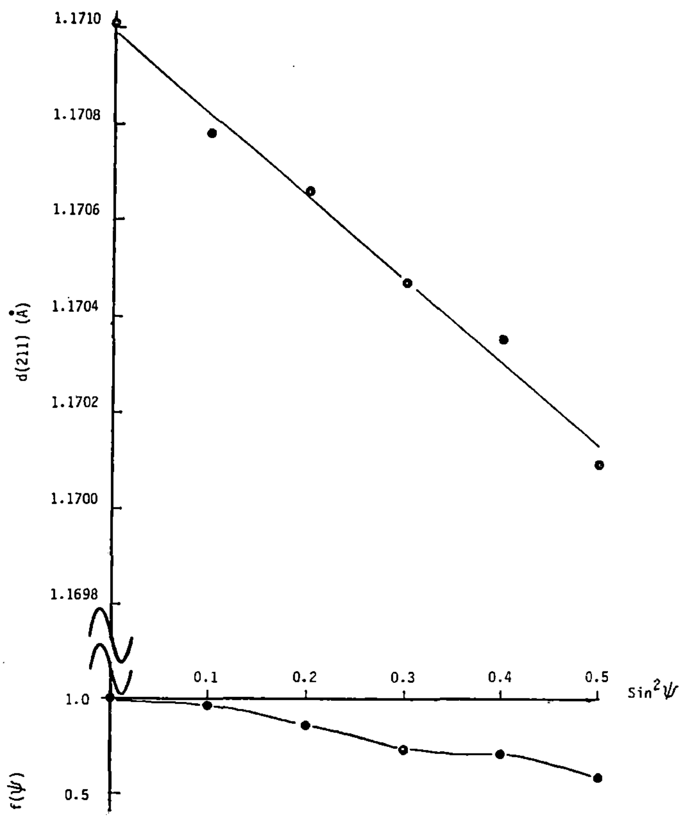

FIGURE 9. MICROSTRESS DISTRIBUTION -- d(211) and $f(\psi)$ VERSUS $SIN^2\psi$ (INDUCTION HARDENED RAIL, LONGITUDINAL DIRECTION): DEFORMED HEAD (LOCATION 3), 0.001 INCH DEPTH

Two-Angle	-38.3 ± 1.2 ksi
$Sin^2\psi$	-36.0 ± 1.1
Marion-Cohen	-36.6

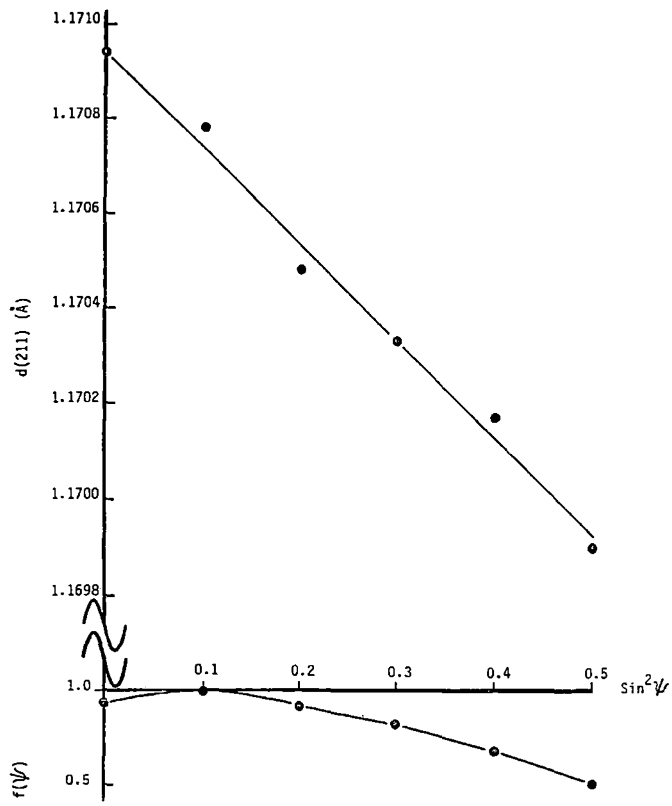

FIGURE 10. MICROSTRESS DISTRIBUTION -- d(211) AND f(ψ) VERSUS $SIN^2\psi$ (INDUCTION HARDENED RAIL, LONGITUDINAL DIRECTION): DEFORMED HEAD (LOCATION 3), 0.002 INCH DEPTH

Two-Angle	-43.5 ± 1.1 ksi
$Sin^2\psi$	-42.8 ± 1.1
Marion-Cohen	-42.1

TABLE 2

COMPARISON OF RESIDUAL STRESS MEASUREMENTS IN NEAR-SURFACE LAYERS OF USED RAIL

Location	Depth (inches)	Residual Stress (ksi)		
		Six-Angle Method	Marion-Cohen Method	Two-Angle Method
1	Surface	- 27.6 ± 0.8	- 25.9	- 26.0 ± 0.7
1	0.001	- 21.0 ± 0.2	- 18.7	- 21.6 ± 0.7
1	0.002	- 22.6 ± 0.7	- 24.6	- 22.8 ± 0.7
2	Surface	- 21.8 ± 0.2	- 22.2	- 21.6 ± 0.7
2	0.001	- 15.3 ± 0.3	- 17.1	- 15.7 ± 0.8
2	0.002	- 17.1 ± 0.5	- 16.6	- 17.9 ± 0.7
3	Surface	- 51.3 ± 0.3	- 56.2	- 52.0 ± 1.5
3	0.001	- 36.0 ± 1.1	- 36.6	- 38.3 ± 1.2
3	0.002	- 42.8 ± 1.1	- 42.1	- 43.5 ± 1.1

TABLE 3

NEAR-SURFACE STRESS GRADIENT CORRECTION

Location	Depth (inches)	Two-Angle Residual Stress (ksi)		
		Measured	Corrected	Δ
1	Surface	- 26.0	- 26.7	- 0.7
1	0.001	- 21.6	- 21.6	0.0
1	0.002	- 22.8	- 22.7	+ 0.1
2	Surface	- 21.6	- 23.4	- 1.8
2	0.001	- 15.7	- 16.4	- 0.7
2	0.002	- 17.9	- 17.9	0.0
3	Surface	- 52.0	- 55.7	- 3.7
3	0.001	- 38.3	- 39.1	- 0.8
3	0.002	- 43.5	- 43.2	+ 0.3

TABLE 4

REPRODUCIBILITY OF TWO-ANGLE
X-RAY DIFFRACTION STRESS MEASUREMENTS
ON COATED AND CLEAN RAIL (LOCATION 4)

	Longitudinal Residual Stress (ksi)		
Run Number	Coated*	Clean*	Clean**
1	- 7.0	-10.0	- 7.6
2	- 5.5	- 3.8	- 6.7
3	- 3.4	- 8.6	- 7.4
4	-14.6	- 8.7	- 7.6
5	- 7.8	- 8.0	- 8.2
Mean	- 7.6	- 7.8	- 7.50
Standard Deviation	4.2	2.4	0.54

*Sample repositioned between measurements

**Sample stationary

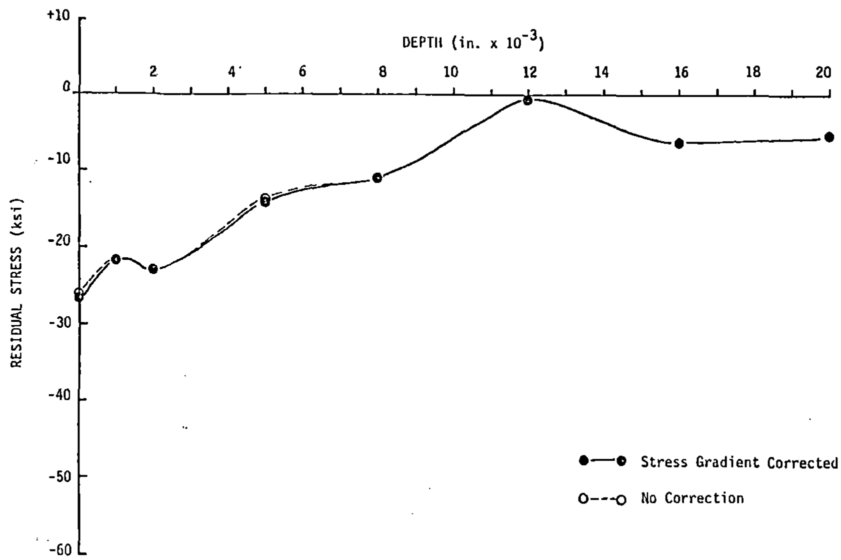

FIGURE 11. LONGITUDINAL RESIDUAL STRESS VERSUS DEPTH:
USED RAIL, WEB, CENTER (LOCATION 1)

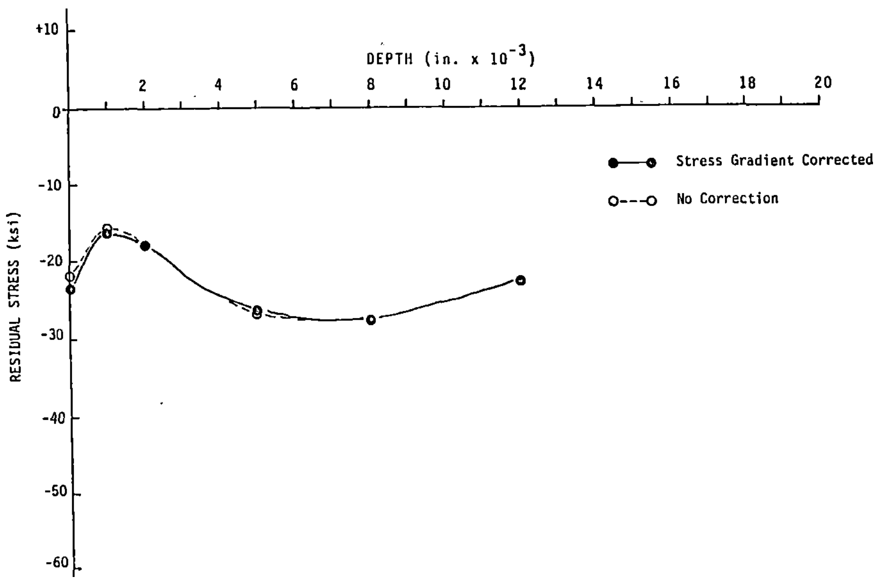

FIGURE 12. LONGITUDINAL RESIDUAL STRESS VERSUS DEPTH:
USED RAIL, RAIL HEAD, FIELD SIDE (LOCATION 2)

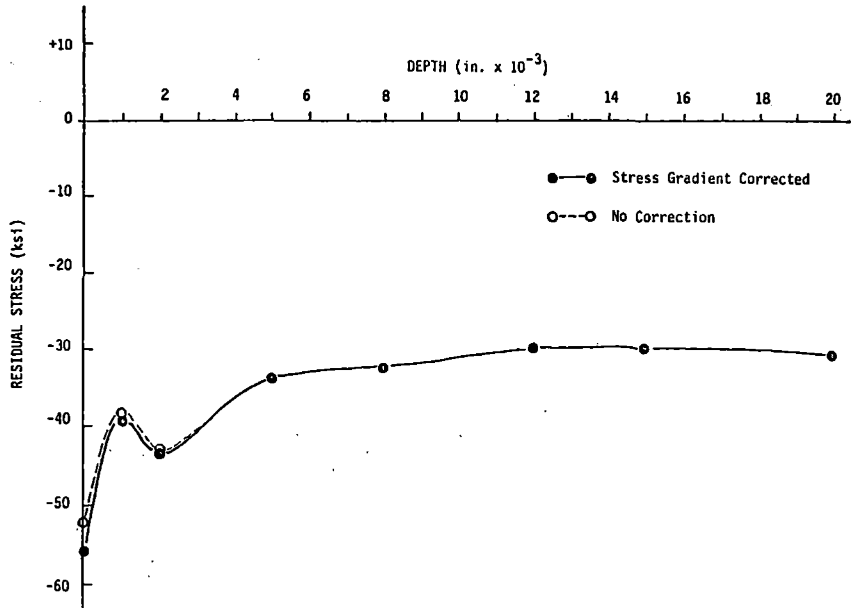

FIGURE 13. LONGITUDINAL RESIDUAL STRESS VERSUS DEPTH:
USED RAIL, RAIL HEAD, TOP (LOCATION 3)

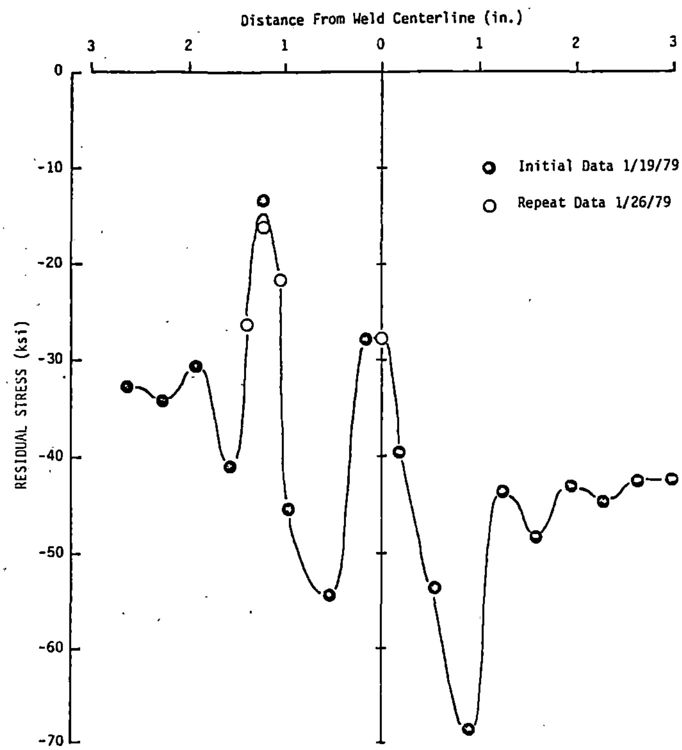

FIGURE 14. LONGITUDINAL RESIDUAL STRESS ACROSS
FLASH BUTTWELD: NEW INDUCTION HARDENED RAIL,
RAIL HEAD, TOP SURFACE

longitudinal stress measurement, location 1, in the web, was observed to have an error of only - 0.7 ksi at the surface. As seen in the plotted data, the magnitude of the error due to the presence of the subsurface stress gradient is greatest near the surface of the samples.

Effect of In-Field Surface Conditions. The repeat surface stress measurements made before and after removal of the tar-like surface protective coating at location 4 are presented in table 4. Surface stress measurements made through the nominally 0.002-inch protective coating while repositioning the samples to the measurement site manually between measurements yielded a mean value of - 7.6 ksi with a standard deviation of ± 4.2 ksi.

Measurements made at the same site, with manual repositioning of the rail between measurements and removal of the protective coating, yielded a mean value of -7.8 ksi and a standard deviation of ± 2.4 ksi. The random error shown for the coated and cleaned rail surface stress measurements includes the error due to uncertainty in repositioning the sample to the precise measurement location in the presence of an undetermined surface stress gradient, and random experimental error due to displacement of the sample from the center of the diffractometer between measurements. In order to establish the random instrumental error without the influence of repositioning the sample, repeat measurements were performed at location 4 on the cleaned surface without repositioning the sample between measurements. These data yielded a mean stress of - 7.50 ksi and a standard deviation of 0.54 ksi, the result of instrumental error and counting statistics alone.

Application to Flash Buttwelded Rail. The results of longitudinal two-angle residual stress measurements made as a function of distance across the surface of the head of the new buttwelded induction hardened rail sample are presented in figure 14. The data are shown as a function of distance from the weld centerline. It should be noted that these results were obtained on a rail head that had not been plastically deformed by rolling stock. Initial measurements, shown as solid circles in figure 14, were made at intervals of 0.35 inch across the surface of the weldment. The complexity of the stress pattern observed in the initial data warranted repeat measurements made several days later; these are shown as open circles. The repeat measurements were made to verify the rapidly oscillating pattern of residual stress that had not been anticipated. The stress distribution appears to stabilize at a distance of approximately 2.5 inches on either side of the weld centerline at a compressive value characteristic of the induction hardened rail head. The compressive values of approximately - 33 and - 42 ksi observed at extended distances from the weld centerline in each of the two rail sections correspond favorably with the subsurface compressive stresses observed in the used induction hardened rail head beneath the severely deformed surface layer shown in figure 13. The difference in compression observed in the two rail segments beyond 2.5 inches from the weld centerline may be indicative of variations in the head hardening heat treatment.

Although no tensile stresses were observed at the surface of the rail head, the relatively low compression zone at a distance of approximately 1.27 inches from the weld centerline, at which approximately - 14 ksi was measured, could rise into tension with the superposition of applied stresses due to thermal contraction of the rail and/or while bearing load in service. It is further possible that local peak stresses of the type shown in figure 14 could extend into tension in some instances depending upon the details of the welding procedure.

Conclusions

Only limited data have been obtained on specific types of rail. However, if these samples can be considered typical of the rail now in service, the following conclusions appear to be warranted as a result of this investigation.

Investigation of Presence of Nonrandom Microstress Distributions. The data obtained at all measurement locations, even on the severely deformed rail head, appear to be free from any significant effect of a nonrandom microstress distribution. The lattice spacing d(211) is found to be a linear function of $\sin^2\psi$. When the data are reduced assuming either the linear model or the model of Marion and Cohen, the results agree within a reasonable estimate of the total random experimental error.

The texture or preferred orientation observed for the (211) poles was not severe, and should not adversely effect the application of x-ray diffraction techniques to stress measurement.

Effect of Subsurface Stress Gradient. The subsurface residual stress gradient established by the two-angle measurements indicates that errors on the order of 4 ksi could result from this phenomenon on the rail head, 2 ksi on the field side of the head, and less than 1 ksi at the web of the rail, a site that is also observed to be free from questionable microstress distributions. Simple surface measurements made on the web of the rail in the longitudinal direction, therefore, should be free from errors in excess of 1 ksi due to the effect of the subsurface stress gradient.

Effect of In-Field Surface Conditions. Repeat measurements made through a nominally 0.002-inch layer of the tar-like protective coating at location 4 indicate that a random error of approximately 4 ksi may result from measurements made through the coating. These results were obtained, however, with a Si(Li) solid state detector with higher efficiency and greater immunity to background fluorescence than would be possible with the gas-filled proportional position-sensitive detectors currently available. Results made after removal of the rail indicate repeatability on the order of ± 2 ksi when the sample was repositioned between measurements and ± 0.5 ksi that were due to instrumental errors and counting statistics alone. The absolute accuracy of the measurements will be further limited by random error in $\frac{E}{(1+\nu)_{(hkl)}}$, which was ± 1.6 percent for the 4340 steel value used in the investigation. In field applications, the largest random error will be the result of errors in positioning the instrument with respect to the measurement location.

Application to a Flash Buttwelded Rail. The data obtained on a flash buttwelded sample of new induction hardened rail indicates an oscillating pattern of residual stress across the weld, exhibiting two tensile-going peaks that were not anticipated. Welds of this type may be expected to have a single tensile-going peak at the location of the weld centerline. Although no tensile stresses were observed at the site of measurement, it may be the case that local tensile stresses could result in some cases depending upon the welding procedure, or that the superposition of applied tensile stresses in the field could result in local areas in the vicinity of the weldment rising into tension and becoming subject to fatigue failure.

Acknowledgments

The author wishes to acknowledge the assistance of Mr. J. J. Yavelak of the Southern Railway, both in providing the test samples themselves and for providing literature and significant technical support concerning rail properties and rail manufacturing and installation practices in the railroad industry.

References

[1] Egle, D. M., and D. E. Bray. "Nondestructive Measurement of Longitudinal Rail Stresses: Application of the Acoustoelastic Effect of Rail Stress Measurements." Federal Railroad Administration, report no. FRA/ORD-77/09.1 (1978).

[2] Egle, D. M., and D. E. Bray. "Ultrasonic Pulse Propagation in the Cold-Worked Layer of Railroad Rail." Federal Railroad Administration, report no. FRA/ORD-77/09.2 (1978).

[3] Clotfelter, W. N., and E. R. Risch. "Ultrasonic Measurement of Stress in Railroad Wheels and in Long Lengths of Welded Rail." National Aeronautical and Space Administration, report no. NASA TMX-64863 (1974).

[4] King, R. R., J. R. Barton, and W. D. Perry. "Stress Measurement in Railroad Wheels Via the Barkhausen Effect." Federal Railroad Administration, final report, December 1974.

[5] Barton, J. R., and F. N. Kusenberger. "Residual Stresses in Gas Turbine Engine Components from Barkhausen Noise Analysis." Journal of Engineering for Power, October 1974, pp. 349-57.

[6] Egle and Bray, FRA/ORD-77/09.1 (1978), pp. 9-10.

[7] James, M. R., and J. B. Cohen, "The Application of a Position-Sensitive X-ray Detector to the Measurement of Residual Stresses." Advances in X-ray Analysis, vol. 19 (Kendall/Hunt) (1976), pp. 695-708.

[8] Ruud, C. O., et al. "Feasibility of Determining Stress in BWR Pipes with the DRI X-ray Stress Analyser." Electric Power Research Institute, paper no. EPRI NP-914 (1978).

[9] Yoshioka, Y. "Study on X-ray Stress Analysis Using a New Position-Sensitive Proportional Counter." Advances in X-ray Analysis, vol. 2] (1979).

[10] H. Gobel, Siemen AG, private communications with author.

[11] Marion, R. H., and J. B. Cohen. "Anomolies in the Measurement of Residual Stress by X-ray Diffraction." Advances in X-ray Analysis, vol. 18 (1975), pp. 466-501.

[12] Cullity, B. D. "Sources of Errors in X-ray Measurements of Residual Stress." Journal of Applied Physics, vol. 35 (1964), pp. 1915-17.

[13] Rickliffs, R. E., and W. P. Evans. "Anomolous Residual Stresses." Advances in X-ray Analysis, vol. 10 (1967), pp. 273-83.

[14] Shiraiwo, T., and Y. Sakamoto. "X-ray Stress Measurement of Deformed Steels." In Proceedings of the Seminar on X-ray Study of Strength and Deformation of Metals, pp. 15-22. Tokyo: The Society of Materials Science, Japan, 1971.

[15] S. Taira. "X-ray Approach for the Study on Mechanical Behavior of Metals." In Mechanical Behavior of Metals, pp. 111-28. Tokyo: The Society of Materials Science, Japan, 1972.

[16] Cullity, B. D. "Residual Stress after Plastic Elongation and Magnetic Losses in Silicon Steel." In Transactions of the Materials Society of AIME, vol. 227 (1963), pp. 356-58.

[17] Hilley, M. E., et al. Residual Stress Measurement by X-ray Diffraction, pp. 61-62. SAE J784a. New York: Society of Automotive Engineers, Inc., 1971.

[18] Stone, D. H. "The Fracture Toughness of Carbon-Steel, Alloy-Steel, and Heat Treated Railway Rails." AAR report no. R-163 (1974).

[19] Prevey, P. S. "A Method of Determining the Elastic Properties of Alloys in Selected Crystallographic Directions for X-ray Diffraction Residual Stress Measurement." Advances in X-ray Analysis, vol. 20, pp. 345-54, Plenum Press, 1977.

[20] Cullity, B. D. Elements of X-ray Diffraction. 2nd ed., p. 460. Addison-Wesley, 1978.

[21] Hilley et al. SAE J784a.

[22] Marion, R. H. "X-ray Stress Analysis of Plastically Deformed Metals." Doctoral Dissertation, Northwestern University, 1973.

[23] Prevey, P. S. "A Comparison of X-ray Diffraction Residual Stress Measurement Methods on Machined Surfaces." Advances in X-ray Analysis, vol. 19 (Kendall/Hunt) (1976), pp. 709-24.

[24] Hilley et al. SAE J784a, pp. 61-62.

[25] Hilley et al. SAE J784a, pp. 53-56.

"X-Ray Diffraction Analysis for Railroad Rail"

Clayton O. Ruud
Denver Research Institute
University of Denver

X-Ray Diffraction Principle

The principle of the X-ray diffraction (XRD) technique lies in the fact that the angle at which an X-ray beam is reflected from atomic planes of a crystalline material is indicative of the distance between these planes. According to the Bragg equation,

$$n\lambda = 2d \sin\theta \quad (1)$$

where n = integer usually equal to 1,

λ = wavelength of X-radiation,

d = interatomic spacing, and

θ = Bragg angle.

When a single crystal of metal is placed in a well-collimated X-ray beam, some of the energy from that beam can be diffracted with no change in frequency at an angle of 2θ with respect to the incident beam, providing that the crystal is oriented suitably. Knowing the wavelength of the radiation, λ, and measuring the angle between the incident and diffracted X-ray beam, 2θ, the interplanar spacing of the atomic planes reflecting the X-ray beam can be measured. If by some means the interplanar spacing is altered, for example by mechanical expansion or contraction of the single crystal within its elastic range, a new d results and the angle θ of diffraction is thereby altered. This is the principal of X-ray stress analysis, which is really strain analysis; that is, if an external stress is placed on a metal part, the distance between the atomic planes in the metal changes.

When a polycrystalline metal with a randomly oriented fine grain is placed normal to a monochromatic X-ray beam, the beam is diffracted back from the surface as cones of X-ray beams, as shown in figure 1. The number and angle of the cones depend upon the metal and its stress condition. If a sheet of X-ray film were placed normal to the incident X-ray beam, the diffracted cones would be seen as concentric circles with the incident beam at the center. Each of these circles represents the sum of thousands of metal grains, each reflecting a small portion of the incident X-ray beam and each in a slightly different orientation. As the grain size of a metal increases, the Debye rings can be seen to form rings of spots instead of appearing as continuous rings. If the incident X-ray beam were tilted to the specimen surface, the ring pattern would not change significantly unless there was a unidirectional stress in the surface of the metal specimen. If the stress were tensile and in the plane of the surface, and the X-ray beam were tilted in the stress direction, the Debye ring would tend to become slightly elliptical, with its major diameter in the direction of stress. Moreover, the larger the stress the greater would be the difference between the major and minor diameter of the ellipse.

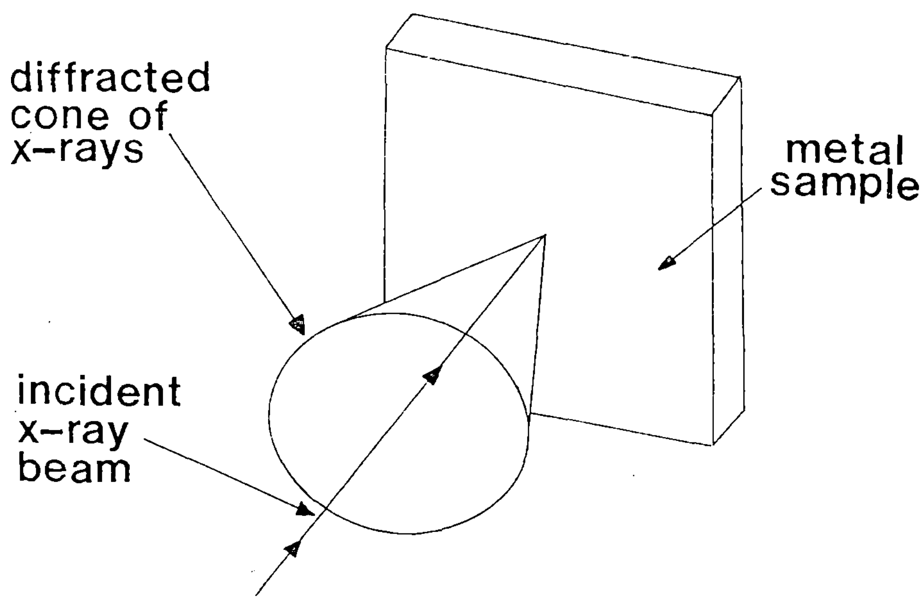

FIGURE 1. DIFFRACTED CONE OF X-RAYS FROM A POLYCRYSTALLINE METAL.

There are a number of techniques for X-ray stress analysis, including the single exposure, double exposure, and $\sin^2\theta$ methods [1]. The relation between the uniaxial macro stress, σ, in the plane of the surface of a metal specimen to X-ray parameters for the single exposure technique (SET) is

$$\sigma = \frac{(\sin 2\theta_2 - \sin 2\theta_1}{4 \sin^2\theta_0 \sin 2\beta} \frac{E}{1+\nu} \qquad (2)$$

where θ_1, θ_2 = Bragg angle for diffraction from sets of planes at two different orientations with the surface,

θ_0 = Bragg angle for unstressed powder,

β = angle between incident X-ray beam and specimen surface normal, and

E, ν = elastic constants.

$\sin\theta_2 - \sin\theta_1$ can be viewed as the deviation of the Debye ring from a perfect ellipse when the incident beam is tilted at an angle β from the normal in a plane containing the surface normal and the stress axis.

The effect of grain size on the ring of diffracted X-rays has already been mentioned; however, if the metal is cold work, micro strains that result will broaden the line forming the Debye ring. Extremely fine grain size also will cause broadening. Preferred orientation, or texture, caused by thermomechanical treatments will tend to segment the ring to the extent that there would be few if any grains reflecting X-rays at certain orientations.

Limitation of X-Ray Diffraction

As shown in the previous section, information about macrostress, cold work, grain size, and texture in a metal specimen is available from the diffracted X-ray Debye ring. However, there are limitations as to the accuracy and application of the XRD techniques to obtain that information. These limitations are discussed below in terms of how they apply to the characterization of stresses in rails.

Stress Sensitivity. Equation (2) may be rewritten as

$$\sigma = \frac{E}{1+\nu} \frac{S_2 - S_1}{4R_0 \sin^2\theta \sin 2\beta}, \qquad (3)$$

where $S_2 - S_1$ are the positions of the diffracted X-ray beam with reference to the incident X-ray beam; R_0 is the distance from the X-ray sensing surfaces to the specimen or rail; and β is the angle between the incident X-ray beam and the specimen surface normal.

The accuracy and precision of the parameter $S_2 - S_1$ are mainly a function of the X-ray instrument and will be discussed later. The angle β can be maintained at a predetermined setting without much difficulty in the application to long, reasonably straight specimens. However, the parameter R_0 must be determined or held to an accuracy of ± 0.5 millimeter to assure good precision and accuracy. For stationary readings, it would be suitable to use coincident light beams, lens focusing, or a standard crystalline powder applied to the specimen surface. The light beams also may be useful for R_0 determinations in in-motion X-ray application.

Mill Scale and Corrosion. By their nature, X-ray diffraction techniques require the application of monochromatic X-rays of rather low energy that do not penetrate deep into steel or most other metal alloys of practical importance. The X-ray methods are used to measure surface stresses, as the X-ray penetration is usually no more than 1 mil (.025 millimeter) into the steel. Thus, if measurements are to be made anywhere other than in the running surface of the rail head, the oxide and/or corrosion product must be removed. This removal cannot be done solely by machining or grinding, because that is likely to induce surface stresses. The most applicable cleaning technique has been found to be electropolishing; Bolstad and Quist [2] have described one practical electropolishing apparatus for field application. The limitation is that it requires several seconds to clean an area of a few square centimeters. This would not be a problem for stationary readings, but would present a severe problem for in-motion application of XRD techniques. It should be noted that stationary stress measurements have been made on wrought steel railway wheels, and this technique has been found to be particularly appropriate for recording variations in residual stress patterns with service and wear. Furthermore, as the result of sustained braking, the residual stresses have been known to exceed 20 MPa (29 ksi), leading to fracture from thermal cracks initiating in the tread [3].

Texture, Cold Work, and Pseudo Macro Stress. Marion and Cohen [4] and Cullity [5] have discussed the effect of texture and cold work on the precision and accuracy of X-ray stress measurements. These effects would be of little or no problem for the rail web and butt; however, for the wheel contact surface of the rail head, they would be of major consideration. Moreover, the clean upper surface of the rail head would present no cleaning problems and from that standpoint offers the promise of in-motion X-ray stress analysis. Many researchers have applied XRD to measure the amount of cold work induced in metals by various treatments [6], [7]. The technique of deconvolution of the cold work and grain size effect on X-ray peak broadening have been recognized by many workers (Hall [8] and Klug and Alexander [9]) and described in the classic paper of Warren and Averbach [10]. If the effect of cold work on the macro stress could be separated from the true macro stress, perhaps the propensity of a given rail section to buckle could be determined. It should be emphasized that the macro stress thus measured would be an absolute stress -- that is, the sum of initial residual stress and the subsequent

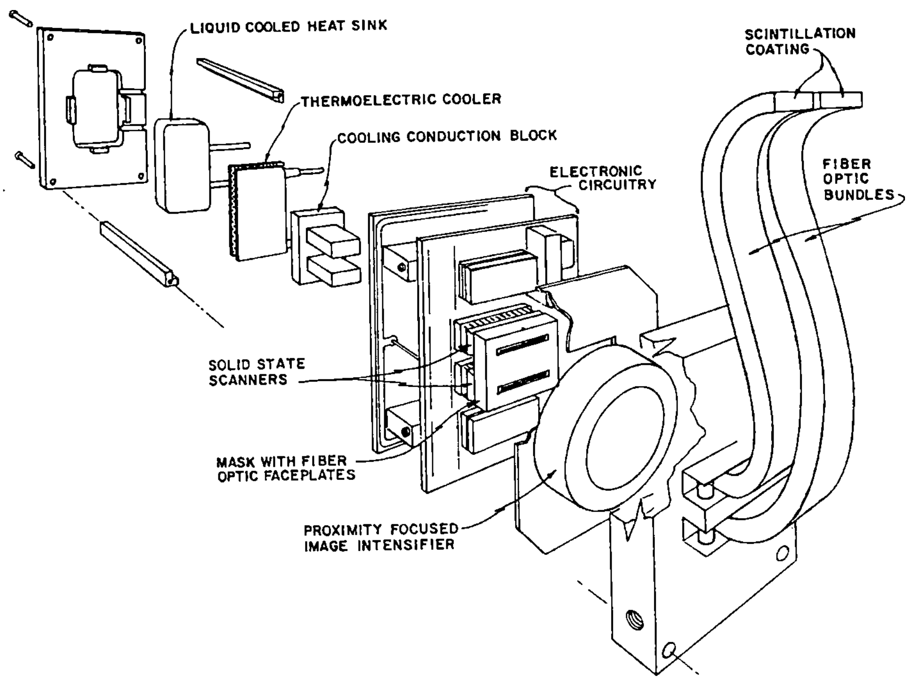

FIGURE 2. EXPLODED VIEW OF POSITION-SENSITIVE SCINTILLATION X-RAY DETECTOR

added stress from temperature changes and service induced stress -- and thus would be the total stress that could be correlated with buckling.

Taira et al. [11] described such a technique in 1973 and its applications to plastically deformed carbon steels. The problem addressed in that paper (and in many earlier ones) was one of pseudo macro stress, an error source in magnetic stress measuring techniques as well as XRD [12]. The texturing of the rail head due to cold work can be a source of error in such X-ray work; however, Marion and Cohen [4] have proposed a method that is based upon the $\sin^2\theta$ technique to overcome texture induced errors and that also has a bearing upon the pseudo macro stress problem.

Even if XRD stress analysis proved unsuitable for railroad rail application for some reason, the ability to measure cold work at the surface of the rail head could be useful to judge spalling susceptibility or wear. With another type of X-ray measurement, it would be possible to characterize the texture at the surface of the rail head, which could improve the veracity of other stress measurement techniques [13].

Instrumentation. An important limitation of the XRD technique has been the nature of the instrumentation applied to measure the angle at which the X-rays are diffracted from the specimen. The most widely used technique is based on a scanning goniometer. This consists of an electronic X-ray detector mounted on a mechanical device capable of scanning it through several degrees of 2θ angle. This produces a readout of diffracted X-ray intensity over several degrees of arc from which the position of the peak intensity can be measured by graphic or mathematical means. Unfortunately, these devices are bulky, slow, delicate and prone to misalignment if moved from the laboratory. Because the scanning goniometer and X-ray film devices have historically been the mainstay of XRD instrumentation, severe limitations have been placed upon practical field application of XRD analysis, especially with respect to stress measurement.

Advances in X-Ray Diffraction Instrumentation

This section describes the application and advantages of a new concept in XRD application through the use of position sensitive X-ray detectors.

The limitation of scanning goniometers in the application of XRD methods has been pointed out in a number of papers. The main problems are in providing speed and portability without sacrificing accuracy. The development of position-sensitive X-ray detectors has offered the possibility of circumventing the necessity of having any moving parts in XRD equipment. "Position sensitive" means that not only is the detector capable of quantifying the number of X-ray photons striking its sensing surface but it is able to ascertain the position on the sensing surface that a photon struck. James and Cohen [14] have described the application of a position-sensitive proportional detector (PSPD) to stress analysis work, and Steffen and Ruud [15] have described a position-sensitive

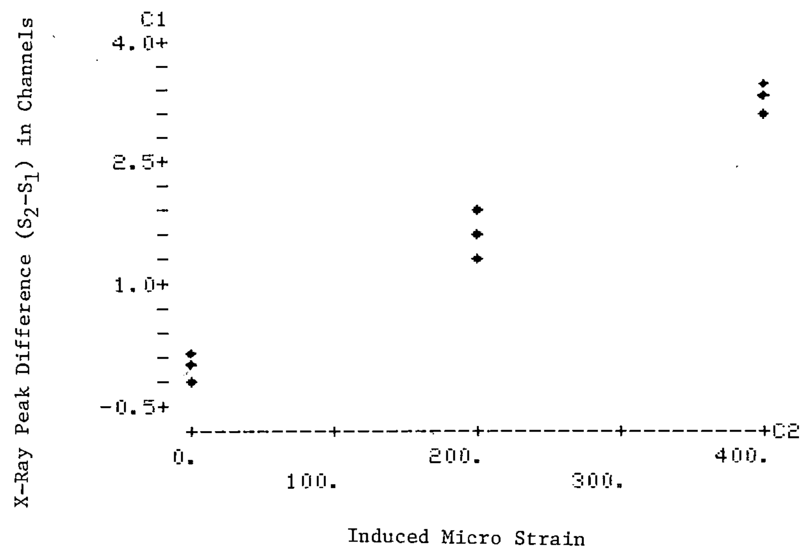

FIGURE 3. CALIBRATION CURVE FOR COLD ROLLED MILD STEEL SHOWING X-RAY PEAK SHIFT VERSUS MICRO STRAIN INDUCED BY FOUR POINT JIG

scintillation detector (PSSD), which is shown in figure 2. The PSSD, which was originally built under U.S. Army, MERDCOM, sponsorship, seems to present more possibilities for field applications because of the versatility its design allows in X-ray geometry design [16], [17].

To illustrate the applicability of the PSSD to several practical X-ray diffraction measurements, some programs presently in progress at the University of Denver Research Institute (DRI) will be described. Two projects to build stress measuring instruments are underway in the Electronics Division. One is to build a portable X-ray stress analyzer for field applications to measure residual and applied stresses in aluminum and steel components for the U.S. Army, MERDCOM. The second is to build an instrument to measure stresses inside of 4-inch Schedule 80 stainless steel pipe for the Electric Power Research Institute. This program requires that a high-power miniature X-ray diffraction tube be built as the X-ray source, and that the X-ray sensitive surfaces be located a few feet from the rest of the position-sensitive detector. DRI's Materials Analysis Laboratory has noted that austenitic stainless steel is one of the most difficult metallurgical materials in which to measure residual stress and requires careful optimization of the R_0 and β parameters shown in equation (3). This is a difficult task inside a 4-inch diameter pipe and is impossible for any X-ray stress measurement device except for one using the above-mentioned PSSD.

DRI's Materials Analysis Laboratory has demonstrated that stresses can be measured nondestructively inside 10-inch Schedule 80 pipe [18]. Presently two programs are under way in the laboratory to measure stresses as a part of a welding study for the General Electric Company and a failure analysis program for the Electric Power Research Institute on a boiling water reactor installation. These programs are being conducted on our laboratory stress analyzer which is based upon the PSSD. For all of the austenitic stainless steel studies, chromium K-beta radiation is being used for stress measurement [19]. The very-low-intensity diffraction peak that is obtained requires data collection times of 75 seconds, but the precision of stress determinations from a four-point bend specimen [20] has been shown to be better than 1.5 [18]. This is better precision than any X-ray stress data published on stainless steel to date.

With our X-ray stress device, we have also performed preliminary stress measurements on ferritic and martensitic steels. Here data comparable to those for austenitic stainless steel can be collected in less than 15 seconds. Figure 3 shows a calibration curve we obtained from a 4-point bend specimen of cold rolled mild steel.

The Materials Analysis Laboratory also is applying the DRI position-sensitive detector to other X-ray diffraction applications. The development, design, and building of a powder diffractometer for the analysis of airborne particulates collected on filters is presently under way and is a more sophisticated application than stress analysis. This concept could well result in an XRD instrument with no moving parts and capable of measuring the concentration of various crystalline species in one hundredth the time of state-of-the-art instruments and with perhaps ten times better sensitivity. This laboratory also is investigating several advanced electro-optical devices that could well expand the application of the present DRI position-sensitive detector in areas of more rapid data collection and large grain size metals stress application.

Possible Application to Railroad Rails

There are several types of information about the stressed and work-hardened condition of rails that can be obtained by X-ray diffraction with the DRI position-sensitive detector. Figure 4 shows X-ray peak information collected from the (211) planes of a cold-rolled mild steel sheet using chromimum K-alpha X-radiation. This is a photograph of the cathode-ray tube (crt) display from data collected in fifteen seconds from DRI's laboratory stress instrument. Figure 5 was recorded from a highly cold worked stainless steel and shows the results of severe cold working. Note the broadening of the X-ray peak in figure 5 that is due to the micro strains induced by the cold work. The information shown in the figures is stored in a dedicated minicomputer upon collection of the data by the PSSD. The data are then easily available for subsequent refinement, such as cold work determination, through use of a calculation method such as Hall's [8].

Information regarding the amount of cold work absorbed by a rail is available from almost any of the high Bragg angle (greater than 60 degrees) back-reflected X-ray peaks that may be used to measure stress. However, to measure texture, X-ray reflections from more than one Bragg angle are necessary, and this is not the usual practice in X-ray stress analysis. With the DRI PSSD, however, it is possible to place a third sensing surface to intercept another Debye ring, thus permitting comparisons of the intensities of the reflections from two or more crystallographic families of planes that would permit conclusions to be drawn regarding texture.

To facilitate either of these types of measurements, cold work or texture, it would first be necessary to perform studies characterizing the effect of cold work and/or texture on the metallographic and X-ray diffraction properties of rail steel. At this writing, X-ray diffraction information on texture in used rail head is sparse and any conjecture as to its nature is best left until more study is done. The quantification of the degree of cold work and of the nature and degree of texture, even without stress measurements, could be of value to the development of ultrasonic stress measurements and could provide nondestructive testing (NDT) information bearing on rail head problems caused by heavy loading, age, or spalling. There is a distinct possibility that these measurements could be made in motion by coupling high-intensity X-ray sources with recently developed electro-optical components.

Stress Analysis, Static. At this writing, an attractive approach to the X-ray stress measurement of railroad rail for use when the measurement instrument may remain static for a few minutes is to measure stresses in the web. To do this, the oxide or corrosion scale must be removed by an electrochemical technique prior to X-ray measurement, and this operation would require most of the analysis time. Furthermore, the effect of rail fabrication on the X-ray peak position (for example, pseudo macro stress) would have to be characterized. With standard X-ray sources and no improvement on the sensitivity of the present DRI detector system, less than 15 seconds would be required for actual data collection. The measurement of the β and R_0 parameters in equation (3) should present no problem and the precision and accuracy of the technique should allow stress determination to less than ± 3 ksi.

Stress Analysis, In-Motion. By far the most challenging application of X-ray stress analysis is the development of instrumentation and techniques for in-motion stress analysis. At this writing, the most direct approach to this would be to make measurements on the rail head. Cold work will cause complications in the application of the X-ray stress technique because of the presence of peak broadening, pseudo macro stresses, and preferred orientation. However, it is highly likely

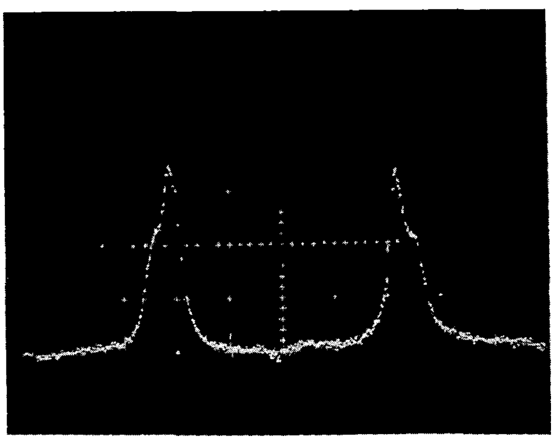

FIGURE 4. CATHODE-RAY TUBE PHOTOGRAPH OF $CrK\alpha_{1,2}$ PEAKS DIFFRACTED FROM (211) PLANES OF COLD ROLLED MILD STEEL SHEET SAMPLE

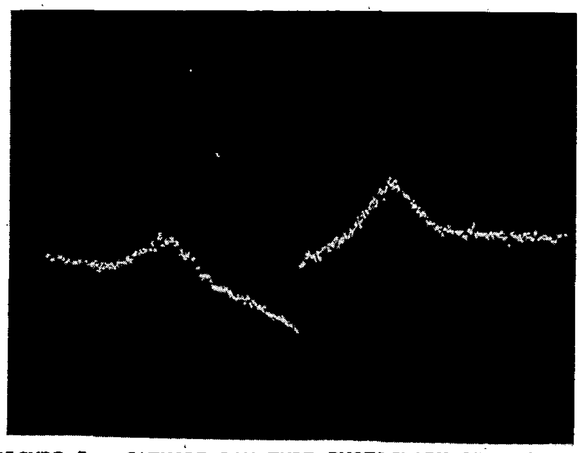

FIGURE 5. CATHODE-RAY TUBE PHOTOGRAPH OF $CrK\beta$ PEAK DIFFRACTED FROM (311) PLANES OF A HIGHLY COLD WORKED AUSTENITIC STAINLESS STEEL PIPE

that both texture and cold work will be found to be interrelated and, through application of techniques such as those cited by Taira [11] and Marion and Cohen [4], the error caused by rail usage on the X-ray stress readings could be characterized and thereby quantified. The fact that railroad rolling stock can accommodate bulky high-intensity X-ray sources is favorable to high-speed operation. The versatility and ruggedness of DRI's X-ray stress instrumentation is also favorable. In short, it seems possible to collect X-ray information in seconds or fractions of a second while in motion along a track. The texture and cold work information may be useful not only in stress analysis by X-rays but also in analysis by other methods. The value of information on surface stresses in the rail head would be obvious if it could be related to the tendency for a rail to buckle.

Conclusion

The inherent characteristics of the noncontact X-ray diffraction techniques for stress, texture, and cold work measurements coupled with new developments in X-ray methods and electro-optics technology could well lead to practical NDE methods of railroad rail.

Acknowledgements

The author thanks Drs. Charles S. Barrett and Paul K. Predecki for their constructive criticisms and helpful suggestions and James F. Smith for his effort on the graphics.

Addendum

Prepared prior to the conference, this paper was written with the assumption that X-ray stress readings could not be made on the rail web without first removing tar and/or corrosion products. However, Paul Prevey's paper showed that it is highly likely that X-ray measurements may be made through the tar protective coating on used rail. He indicated that he had made some cursory measurements on used rail in his laboratory and that readings had been taken on the web with no surface preparation. This approach is generally applicable to in-service rail, it would be superior to measurements on the rail head as proposed in this paper. That is to say, X-ray measurements on the web would not be troubled with the perturbations imposed on the rail head by the cold work induced by rail-wheel contact.

The fact that X-ray diffraction readings can be performed on used rail web in the laboratory with no surface preparation points to a high probability that X-ray techniques can be applied to the in-motion measurement of longitudinal force in railroad rails.

In his technical introduction to the conference, Dr. A. M. Zarembski of the American Association of Railroads noted that a useful longitudinal rail force measurement method should be rugged, easy to handle, nondestructive, require no disturbance of the track structure, require minimum or no calibration, require minimum or no surface preparation, provide for direct measurement of net longitudinal force (absolute), not be permanently affixed to the rail or track structure, and permit continuous or very frequent measurement of rail force from a moving vehicle. It is the author's conclusion that the X-ray technique is the only method available that has a high probability of meeting all of these requirements. In all likelihood, this could be accomplished through development and design of an instrument using available components (X-ray tubes, computers, position-sensitive detectors, etc.).

References

[1] Hilley, M. E., et al. "Residual Stress Measurement by X-Ray Diffraction." SAE J784a. New York: Society of Automotive Engineers, Inc., 1971.

[2] Bolstad, D. A., and W. E. Quist. "The Use of a Portable X-Ray Unit for Measuring Residual Stress in Aluminum, Titanium and Steel Alloys." Advances in X-Ray Analysis, vol. 8 (1965).

[3] McDonald, R. J., and R. I. Mair. "Wrought Steel Railway Wheels--A Basic Development," BHP Technical Bulletin, vol. 20, no. 2 (November 1976), pp. 7-14.

[4] Marion, R. H., and J. B. Cohen. "Anomalies in Measurement of Residual Stress by X-Ray Diffraction." Advances in X-Ray Analysis, vol. 18 (1975).

[5] Cullity, B. D. "Sources of Errors in X-Ray Measurements of Residual Stress." Journal of Applied Physics, vol. 35, no. 6 (January 1964), pp. 1915-17.

[6] Wagner, C. N. J., and W. Aqua. "Pattern Peaks from Cold-Worked Face-Centered and Body-Centered Cubic Metals." Advances in X-Ray Analysis, vol. 7 (1964).

[7] Barrett, C. S., and T. B. Massalski. Structure of Metals. 3rd ed., pp. 453-56. New York, St. Louis, and San Francisco: McGraw-Hill Book Co., 1966.

[8] Hall, W. H. "X-Ray Peak Breadth Measurements." Proceedings of the Physics Society, vol. A-62, (1949), p. 741.

[9] Klug, H. P., and L. E. Alexander. "X-Ray Diffraction Procedures." 2nd ed. New York: John Wiley and Sons, 1974.

[10] Warren, B. E., and B. L. Averbach. "The Effect of Cold-Work Distortion on X-Ray Patterns." Journal of Applied Physics, vol. 21 (June 1950), pp. 1595-1600.

[11] Taira, S., K. Hayashi, and S. Ozawa. "X-Ray Measurement of Residual Stress Induced in Carbon Steels by Plastic Deformation." In Proceedings of the 1973 Symposium on Mechanical Behavior of Materials, pp. 287-95, Tokyo: The Society of Materials Science, Japan, 1974.

[12] Cullity, B. D. "Some Problems in X-Ray Stress Measurements," Advances in X-Ray Analysis, vol. 20 (1977), pp. 259-71.

[13] Egle, D. M., and D. E. Bray. "Ultrasonic Pulse Propagation in the Cold-Worked Layer of Railroad Rail." Federal Railroad Administration, report no. FRA/ORD-77/09.2 (1978).

[14] James, M. R., and J. B. Cohen. "The Application of a Position-Sensitive X-Ray Detector to the Measurement of Residual Stresses." Advances in X-Ray Analysis, vol. 19 (1976), pp. 695-708.

[15] Steffen, D. A., and C. O. Ruud. "A Versatile Position Sensitive X-Ray Detector." Advances in X-Ray Analysis, vol. 21 (1977), pp. 309-15.

[16] Ruud, C. O. "X-Ray Detection for Stress Analysis." In Proceedings of the Air Force Material Laboratory Workshop on Nondestructive Evaluation of Residual Stress," San Antonio, Texas, August 1975.

[17] Ruud, C. O. "An Advanced State of the Art X-Ray Stress Analyzer." In Proceedings of the Bolton Landing Conference, August 1978, sponsored by AWS/ASM, Lake George, New York.

[18] Denver Research Institute. "Feasibility of Determining Stress in BWR Pipes With the DRI X-Ray Stress Analyzer." Electric Power Research Institute, report no. EPRI NP-914. Interim report, October 1978.

[19] Ruud, C. O., and C. S. Barrett, "Use of Cr K-Beta X-Rays and Position Sensitive Detector for Residual Stress Measurements on Stainless Steel Pipe." Advances in X-Ray Analysis, vol. 22 (1979).

[20] Prevey, P. S. "A Method of Determining the Elastic Properties of Alloys in Selected Crystallographic Direction for X-Ray Diffraction Residual Stress Measurement." Advances in X-Ray Analysis, vol. 20 (1977), pp.345-54.

"The Rapid Field Measurement of Residual Stresses with X-Rays"*

J. B. Cohen
The Technological Institute
Northwestern University

and

M. R. James
Rockwell International Science Center

The normal X-ray method for stress measurement is based on recording a diffraction peak by moving a detector around the specimen to record the peak shape, tilting it one or more ψ angles, and repeating the process. This is usually done in a conventional diffractometer and requires expensive, heavy gearing. The usual diffractometer also requires bulky transformers and is hardly portable, although instruments mounted on a dolly for transporting in a plant are available. The shortest time of measurement is in the order of minutes. The stress is obtained from the shift in peak position with tilt, as has been explained in previous papers.

Is it really necessary to move the counter to the various points over a peak? A new X-ray detector called a position-sensitive detector (PSD) has recently been developed [1]. It is capable of yielding information on both the quantity and relative position of incoming X-ray photons. The unit we used, manufactured by Tennelec, Inc. (Oak Ridge, Tennessee), employs an argon-3-percent carbon dioxide mixture flowing around a high-resistance graphite-coated wire. When an X-ray photon ionizes the gas in the detector, a pulse runs along the wire. By comparing the pulse shape at both ends of the wire, the ionization event can be located to a precision of about 180 micrometers. With suitable electronics, the entire peak can then be "observed" over several degrees by means of a multichannel analyzer (MCA). (The time differences at both

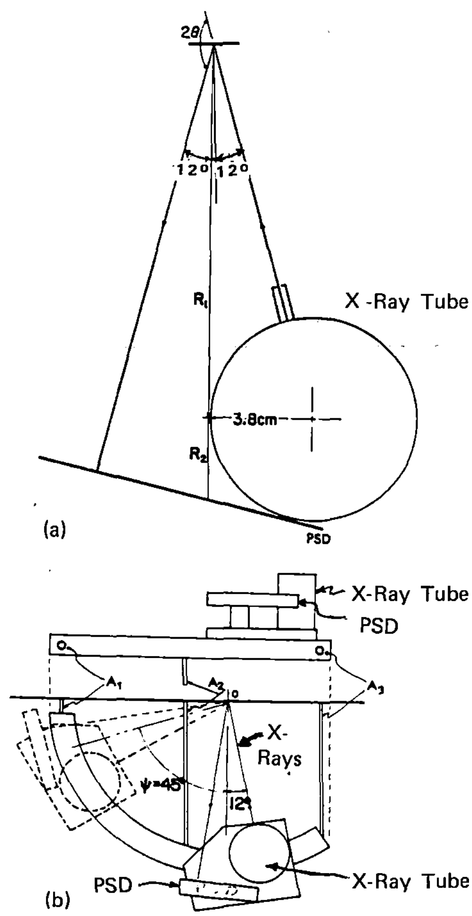

FIGURE 1. BASIC CONFIGURATION (a) AND BASIC DESIGN (b) OF PARS

*Presentation at conference delivered by J. B. Cohen.

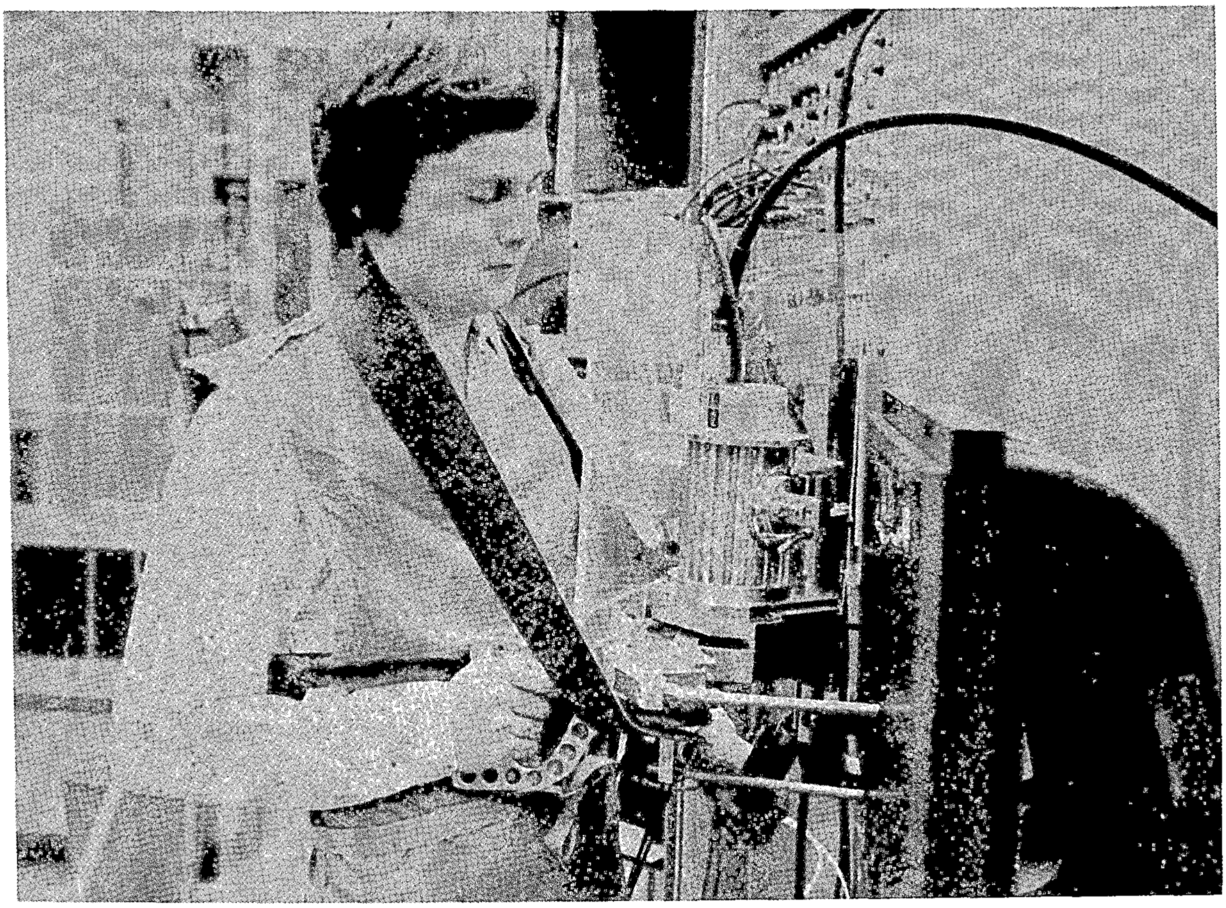

FIGURE 2. PARS INSTRUMENT

ends are used to locate a pulse in a channel.) Also, the pulses at either end can be summed to allow for energy discrimination. (If the energy is not within prescribed values, storage in the MCA does not occur.) This reduces background. The horizontal axis on the MCA is converted to degrees 2θ by calibration with known peaks. While the detector is flat and not curved to fit a circle around the specimen (as is a diffractometer), the resulting errors is small [2]. For example, for a peak shift of 2 degrees indicating a stress of 1,400 MPa (200 ksi) in steel, the error is only 5 MPa. No motion of the counter is needed with such a device, thereby eliminating the heavy and expensive gearing of a conventional diffractometer. The detector employed occupied a volume of 0.2 x 0.13 x 0.045 meter, with an active length of 0.1 meter. Because the entire peak is collected simultaneously, the time to measure a stress is reduced by large factors, 8 to 100 [3], the larger value being for sharper peaks. A least-squares parabolic fit can be made on a microprocessor or miniprocessor to all the data points in the top 15 percent of the peak (generally 15 to 200 points in that region, the number depending on the peak breadth). All these points are obtained simultaneously in the multichannel analyzer. Peaks can be located with a PSD from ± 0.01 to ± 0.02 degrees 2θ by fitting a parabola.

The gas-flow-type PSD used in this study can be pressurized for a day so that it is not necessary to consider gas supply as part of the design. Sealed units are also available commercially. Another important technological advance, the miniature X-ray tube, was adopted to make the instrument truly portable. We chose one manufactured by Watkins-Johnson Company (Scotts Valley, California). The tube is only about 0.06 meter long and, with its shielding, weighs 2.3 kilograms. It is air-cooled by means of fins. The chromium X-ray target obtained for this study was designed for fluorescence but proved to be adequate. Partly because of this design and partly because of the special grid system employed in the tube's construction, it was found that, for the same beam size, at the tube's maximum rating (50 kilovolts, 2 milliamperes), the intensity was 20 percent greater than that from a standard water-cooled X-ray tube operated at 50 kilovolts and 11 milliamperes. Furthermore, these miniature tubes are available at ratings up to 5 milliamperes. (In general the data reported here were taken at 40 kilovolts, 1.7 milliamperes. The beam size at the specimen was usually about 0.003 x 0.004 meter.)

The basic configuration of the portable analyzer for residual stresses (PARS) [4] is shown in figure 1(a). For the diffraction angle for

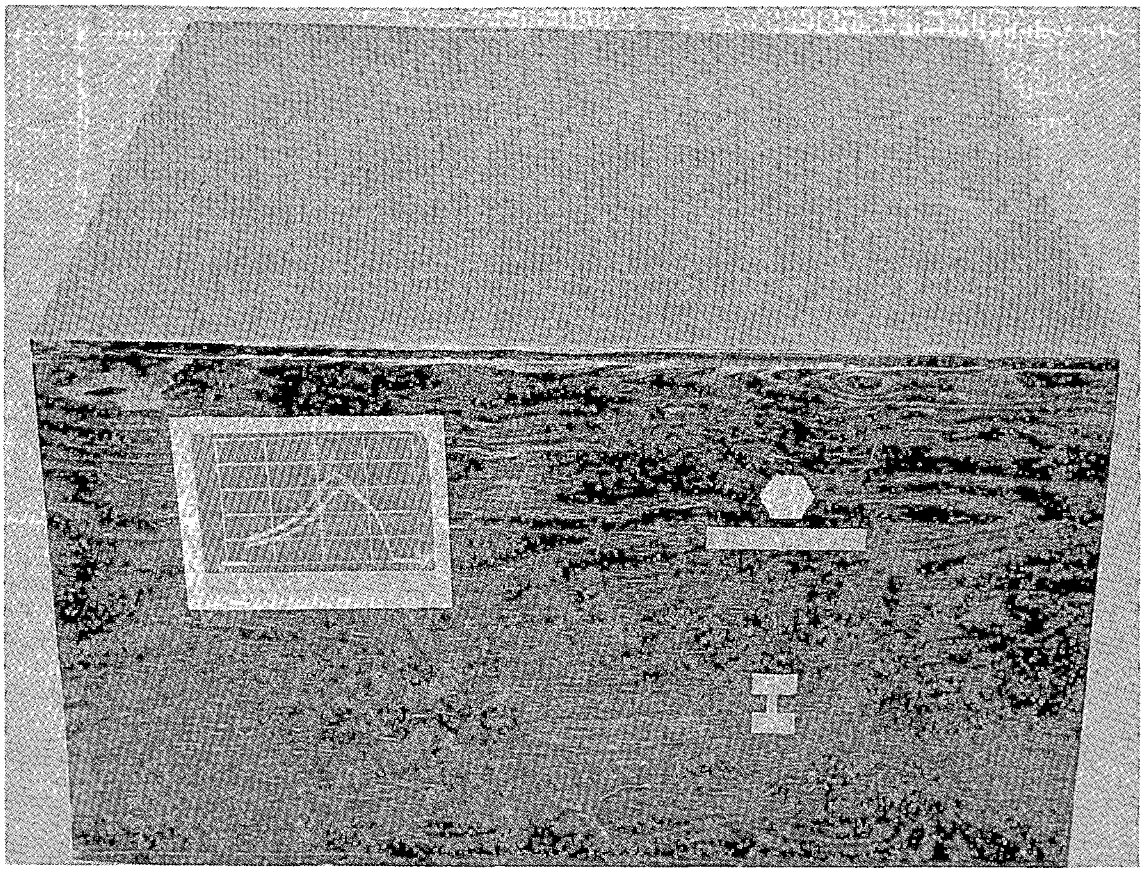

FIGURE 3. THE TWO PEAKS EMPLOYED IN A STRESS MEASUREMENT OBTAINED WITH PARS, SHOWN ON A BOX THAT SIMULATES THE POSSIBLE TOTAL ELECTRONICS PACKAGE

steel, about 156 degrees 2θ, the PSD had to be located behind the tube. The basic design of the instrument is sketched in figure 1(a). The detector and tube move on a dovetail track to a stop for a ψ tilt of 45 degrees. For these developmental studies, flat specimens were used and three positioning rods (A_1, A_2, A_3) that were not co-planar were employed to locate the tube-to-specimen distance properly. Other positioning devices are possible for other sample geometries, and the instrument could be readily designed to allow a simple interchange between these. Furthermore, electromagnets or suction pads could be used to hold the position more easily. Only a single calibration experiment is necessary to transform positional data from the PSD into scattering angles.

The prototype instrument is shown in figure 2. A stand with wheels could also be used to move the instrument from place to place within a plant. There are two grips for PARS that can be seen in the figure -- a handle and a rubber-covered rod for tilting. For safety, a trigger could be incorporated in the handle to start the X-ray tube only if all positioning devices were placed on a specimen. Also, note the plastic back-scatter safety shield.

Figure 3 shows the peaks on the oscilloscope at the two tilts from a steel specimen. One of the interesting additional features of the device is the fact that the entire peak shape is recorded and therefore the breadth is obtained, which is often useful in view of the known empirical relationships between this quantity and hardness. Because of the wide angular range covered by the detector (about 20 degrees 2θ), peaks from two or more phases could be examined. With different stops along the track for the detector and X-ray tube, either stresses in different materials can be measured or the quantity of retained austenite can be determined from the ratio of two peaks, one from the austenite, one from martensite, both recorded simultaneously. Also, by moving a specimen rapidly past the beam, the oscillation in intensity can be employed to measure grain size [5].

Not shown in these figures are the associated electronics, which were not packaged for this prototype. The entire X-ray generator is only 0.5 x 0.5 x 0.15 meter in volume (about the size of a large digital voltmeter) and weigh 23 kilograms. The entire electronics for the PSD, the MCA, and a hard-wired microcomputer could be designed into a box 0.5 x 0.5 x 0.2 meter, as

TABLE 1. REPLICATE MEASUREMENTS WITH PARS ON STEEL SPECIMENS: ψ TILT: 45 DEGREES; CrK_α RADIATION, 211 REFLECTION

Steel Sample	Stress with Normal Diffractometer	Average Stress, 5 Tests with PARS	PARS, Time	Observed Error, 5 Tests - PARS	Calculated Statistical Counting Error
	MPa	MPa	sec	MPa	MPa
1	+32	-12	10*	± 25	± 20
2	-699	-703	20	± 28	± 29
3	-397	-396	20	± 43	± 37

*Measurements to ± 34 MPa counting error in 4 seconds

seen in figure 3. The only controls needed daily are two switches -- on-off and high voltage. The peak stress (and perhaps hardness) would appear on the oscilloscope screen. Cabling to the portable head as long as 7 meters is possible.

Table 1 compares data on a variety of specimens with results from our (automated) conventional diffractometer. Note that with PARS, measurements at both tilts can be performed in a total time of 4 to 20 seconds -- and we did not employ the full power of the tube. The observed variation in five tests on each material is nearly the same as the error resulting from counting statistics, indicating that this error is the only principal one with PARS. (For the sample with the lowest stress, there appears to be a difference in both sign and magnitude of the stress measured by the portable unit and the conventional diffractometer. But the stress is so small that the sum of the errors with both methods brackets this difference.)

The prototype of the portable head weighs about 11 kilograms, but the tracks are much bulkier than actually needed and the slide for the tube and detector is not necessary. A second model would weigh only 7 kilograms.

This device has been demonstrated extensively to industry and a copy is being delivered to the U.S. Navy this month (February 1979). Commercial development has also been initiated, and a U.S. patent no. 819,985, has been granted. Our current Office of Naval Research activities in this area include the behavior of residual stresses during fatigue [6].

A few final comments are worth adding. Portable X-ray tubes with still greater power are available, and xenon-filled detectors are about twice as efficient as the one we employed. Thus it is quite feasible to make measurements in about 1 second. The beam is strong enough to penetrate thin layers of paint or oxide, so that there are minimal problems with use in the field.

These X-ray methods also can be employed to profile the stress through a part. While this involves the removal of material and is therefore destructive, it can be of considerable aid in developmental studies.

We would especially like to thank Dr. Bruce McDonald of the Office of Naval Research for his support and continued confidence in our goals.

References

[1] Borkowski, C. J., and M. K. Kopp. Rev. Sci. Instr. vol. 39 (1968), p. 1515.

[2] James, M. R., and J. B. Cohen. Office of Naval Research technical report no. 18 (June 15, 1977). Contract no. N00014-75-C-0580, NR 031-73-3.

[3] James, M. R., and J. B. Cohen. Denver Conference on Advances in X-ray Analysis, vol. 19 (1976), p. 697.

[4] James, M. R., and J. B. Cohen. Journal of Testing and Evaluation vol. 6 (1978), p. 91.

[5] Paulson, W., J. B. Cohen, and J. E. Hilliard. 15th Sagamore Army Materials Research Conference, p. 73. Syracuse, New York: Syracuse University Press, 1970.

[6] Quesnel, D., M. Meshii, and J. B. Cohen. "Materials Science and Engineering." In press.

PANEL DISCUSSION

The participants in the panel discussion included authors M. R. James, P. S. Prevey, C. O. Ruud, and J. B. Cohen; conference panel members D. P. McConnell (chairman) (Transportation Systems Center, U.S. Department of Transportation), A. Opinsky (Association of American Railroads) [substituting for H. Berger (National Bureau of Standards), who was not able to attend this session of the conference], B. R. Forcier (Bessemer and Lake Erie Railroad Company), and D. H. Stone (Association of American Railroads); and supplemental session panel member J. J. Yavelak (Southern Railway). G. D. Farmer, Jr. (U.S. Army, MERDCOM) was scheduled to participate as a supplemental session panel member, but was unable to attend the conference.

D. H. STONE: I would like to address a general question to the authors. If we are measuring strain with an X-ray technique, will this technique give us the proper stress or load that we are looking for?

P. S. PREVEY: I think that the phenomena that we are talking about here is fundamentally strain-oriented. Stresses are derived quantities. One measure strains directly. Forces are derived from stresses, but any method of "stress" measurement involves a measurement of strain.

D. P. McCONNELL: Let me recast Dan Stone's question in the somewhat different terms of a structural mechanician. Allen Zarembski displayed data taken on the Bessemer and Lake Erie Railroad some time ago which showed that there were no macro strains determinable in the rail section due to constrained thermal expansion. This is due to the nature of the phenomena of constrained expansion. It is clear that the variation in interplanar lattice spacing with mechancial stresses can be detected by X-ray techniques. The question which has arisen is this: In an instance where there is no detectable macro strain, is the strain due to constrained thermal expansion on the interatomic level detectable?

J. B. COHEN: There may not be any longitudinal strain, but there is obviously going to be a strain in other directions. The material has to express its elasticity in one way or another. I am not all that familiar with everybody's measurement, but I am sure that everybody's measurement, X-rays or any other, is going to be sensitive in the other directions to what the load was in the longitudinal direction. I would suspect that the X-ray method as well as the other methods will measure this difference and I do not see that there is any particular problem about this.

It should not be more than an afternoon's work to find out. You pick a day when it is 20°F and come back when it is 60°F outside and find out if you have got a change. It should not be any great problem to prove this.

C. O. RUUD: As long as you constrain the rail along its length and it wants to expand, it is going to, as Professor Cohen says, express that by expanding in another direction.

P. S. PREVEY: All the other data were in the longitudinal direction only, right?

A. M. ZAREMBSKI: Yes, when strain gages have been applied, though, to check vertical orientation, generally there has been very poor correlation. The sensitivity was not there.

J. B. COHEN: Well, sensitivity is not a problem. With X-ray techniques, you can certainly be quite confident with stresses of 8,000 or maybe 10,000 pounds per square inch.

A. M. ZAREMBSKI: To answer the question of elasticity, if you go back to your basic equation for strain and for stress, the stress is proportional to the mechanical strain plus the alpha-T term.

Going back to the simple analogy of a straight bar and the strain on it, if you wanted to assume it would be a single dimensional bar, nothing exists in the other two dimensions; there would be absolutely no strain. However, once you assume that it has finite thickness and depth, which you have to in that everything does, then you do have a strain. The problem is measuring it; until now, no strain measuring system has ever been sensitive enough to measure them and relate them to force.

R. B. THOMPSON (Rockwell International Science Center): Are you questioning whether one can get true data under these conditions, or are you suggesting that the data one obtains does not correlate with force?

A. M. ZAREMBSKI: Strains in the opposite direction?

R. B. THOMPSON: Yes.

A. M. ZAREMBSKI: I have not seen anything that correlates. I have not seen any significant data at all.

J. R. BARTON (Southwest Research Institute): Has everybody been so concerned about looking in the longitudinal direction that they have not bothered to make those measurements in the transverse? Can you not find them because nobody has tried?

A. M. ZAREMBSKI: I have never personally gone out and tried. However, there are cases with which I am familiar; they tried but have not been able to get any sort of real relationship with force.

R. B. THOMPSON: What techniques were employed?

A. M. ZAREMBSKI: Strain gages.

C. O. RUUD: If you take a beam and constrain it an you look at various angles with respect to the constraint axis, you can measure the distance between the atoms at these various distances and they will change according to the incident angle of your X-ray and reflected angle of your X-ray, and this difference in the lattice parameter or the distance between angles is a symptom of constraint and it can be quantified. Is that reasonable?

A. M. ZAREMBSKI: Yes. The question then is, is it directly relatable? In thinking about it right now, you would tend to guess that if it is sensitive enough you should be able to relate it.

J. B. COHEN: Well, one of the things you do is to take it in a laboratory. It does not have to be done out in Pueblo, Colorado [Transportation Test Center]. You could set up basic material on the diffractometer, on a portable device, and measure it, heat it up, and confine it, and see how much stress you measure and see what correlations you have. I think that is a laboratory task that would be easily resolvable in a few weeks' work.

J. R. BARTON: What you are talking about is exactly the kind of test we did with Barkhausen -- constrain the end of the rail where it would not move and we got the indication on those curves of about 11,000 psi change in the longitudinal direction. This was under heat, with the ends constrained.

C. O. RUUD: I would bet you would most likely find a similar test in the literature -- maybe not on rail steel but probably on steels or similar materials. I would also bet that in the literature you can find a test similar to what we have been talking about regarding X-rays.

J. B. COHEN: You also should keep in mind that the X-ray technique is the oldest one and certainly is the most established one. You do not want to use cutting or grinding or hole drilling or things like this because they can lead to additional problems, even in the measurements, not only in how the part behaves in service.

It certainly would be helpful if people using other techniques would occasionally let us see comparative data. I am a little surprised that this does not happen much. With all the other techniques, we have not seen any comparative data, so we are a little bit uncertain as to what is going on.

D. E. BRAY (Texas A&M University): Let me comment right here because, on one of the slides we had in Session I on the Pueblo data, we actually saw the data from the strain gages that were installed there. The data showed about a 500-microstrain difference in the longitudinal direction for the diurnal period.

A. M. ZAREMBSKI: Longitudinal?

D. E. BRAY: Yes and we also had transverse and vertical strain gages installed.

A. M. ZAREMBSKI: Well, you have got to be careful about getting a buildup.

D. E. BRAY: If you have an unequal stress distribution up and down the rail, as it heats and cools it will try to redistribute itself.

J. B. COHEN: We had all better start comparing different techniques, because it is pretty hard to understand what is going on or what the limitations of the technique are when everybody is trying to sell his own particular tool. There is no way for comparison and this is a real problem in this business. It is time to state that you should not present any data on a new technique unless you have such comparisons, because otherwise it is just confusing everybody.

J. J. YAVELAK: First of all, I would like to make a comment that I enjoyed the talks very much and I would like to thank you [the authors] all for coming because I think this represents some of the best knowledge that we have in this field. I will now address questions to each of you.

Dr. James, you said, regarding your limitation on your samples, that your excitation area is anywhere from 1 millimeter to 10 millimeters. Do you have any feel how that would reflect in what mimimum grain size or maximum grain size?

M. R. JAMES: Grain size sometimes presents a problem in alloys such as aluminum, where the grains can be as large as 1 millimeter and no subgrain development has taken place. Along a similar line, preferred orientation, such as in a weldment, also creates difficulties. In both cases, the diffracted X-ray beam is produced from only a few crystals and is not representative of a random structure. It is possible to overcome a grain size problem by oscillating the sample or X-ray measuring head a few degrees. The latter technique has been built into some commercial X-ray stress analyzers.

J. B. COHEN: Can I add a comment to that? It is not the grain size alone that is the problem. It is the degree of deformation to which the material has been subjected. You can take a piece of aluminum with 1-inch grains and, if it has been heavily deformed, the stress measurement is still okay because the X-ray measurement in that case is averaging over the subgrains that have developed in the material and they are quite small. So it is really a complicated business and it occurs mostly as Mike James said, in aluminum alloys and also in the turbine industry and Nimonic alloys which are cast and have grains you can see with the naked eye. I have never come across this with a steel.

J. J. YAVELAK: You have never come to a measurement on a sample and found that you could not get your diffraction cone?

J. B. COHEN: Not in a steel. In fact, we measured some engine blocks a few years ago and they were cast and we didn't have any problems with those either. I am sure there are cases, but in the steel business it is unusual because the second phase does two things for you. It minimizes these oscillations that some people have been talking about today, and it also reduces the grain size. So it is really a problem in essentially single-phase materials, especially Nimonics and aluminum alloys.

P. S. PREVEY: I have examined a large number of steel alloy samples, and I have never seen a problem with grain size. In cast materials, like Dr. Cohen has commented, there are grain size problems that may arise.

J. B. COHEN: I would like to add another point. People have mentioned some sources of stresses in rails, but there are two other sources that I am sure everybody in the rail business knows about. One is that the rails are straightened in the shop, so that is going to introduce a huge residual stress. The other is that they creep under use and so, when you take them off, they have a permanent shape and that introduces stresses. These things should not be forgotten when you are talking about stress patterns in rails.

J. J. YAVELAK: Which brings me to my question to you. When you measure, how sensitive to the location are you if you are measuring before and after? Do you have to line it up with the laser? Say we went out to a section of track and did them anyway, marking them with a piece of chalk or something like that. We are coming back 2 days later when the temperature is 50 degrees warmer.

J. B. COHEN: No particular problem there. The technique of sample positioning has especially been worked on by the Japanese, and they have developed a technique they call "Parallel Beam Geometry" that minimizes the effect of sample displacement there. It depends on the stress you are talking about. If you are going to ask me if the stress changed by 1,500 psi, I say I can't do it. But if you are going to tell me the stress changed by 10,000 psi, given a device designed to measure stresses on rails, I think that that could be done. But not 1,500 psi.

P. S. PREVEY: There is another problem, though, because the Parallel Beam Geometry is a means of correcting for displacement away from the sample, which is a source of systematic error of the instruments. I think the biggest problem will be due to surface stress gradients. If a region has been wire-brushed or ground, then you can have very severe surface stress gradients across the surface. In the positioning, it would probably be advisable to have some sort of pin locating or other means, if you want static measurements, of getting back to the same spot within some reasonable fraction of the size of the irradiated area that you are using.

As for the sizes, a quarter-inch square area may be irradiated, and you may be able to tolerate an error of a 64th of an inch. Obviously, if you use a 10-mil area and you have a 10-mil error, you are making the second measurement in different metal. There have been studies performed on ground surfaces, for example, that would indicate that failure to properly relocate the beam would appear to produce an error, but actually you are simply working on different material than you were the first time. To that extent, positioning could be a problem.

M. R. JAMES: But you are going to have that exact same error with any technique unless you physically mount the transducer on the rail and keep it there. That would be a problem in looking at the rail with a train moving at 60 miles an hour and trying to determine a change in the longitudinal force. You have to determine a residual stress when you first lay down the track and you have to compare it later and you have to compare the same position.

J. J. YAVELAK: When we are talking about change, we simply have to have some basis for change.

J. B. COHEN: I think we are all aware of the technical problems of measurement, probably more in the X-ray field than in any other field because it is the oldest one, but I think answers to these questions can only be had by somebody going out in the field and making some measurements. For example, this is what the British Rail people are doing. Maybe people do not like drilling holes in a rail, but at least they are going to get some data. We can sit around the table for days and discuss this, but somebody has got to go out there and make some measurements and then we can begin to see what are the problems.

J. J. YAVELAK: I do not think that we are attempting to question your technical ability.

J. B. COHEN: No, I am not saying that, but you can't answer those kinds of questions without getting a feel -- rail in Cleveland and rail in Atlanta, Georgia, are different rails in terms of what they look like and how they act.

J. J. YAVELAK: We have a rare opportunity to have you people here and listening to our problems, so maybe something will come out of that.

J. B. COHEN: I would strongly recommend that some measurements in the field be made of the kind we attempted one afternoon with Allan Zarembski, but of course that will take weeks again to get enough data to be useful.

C. O. RUUD: Perhaps you could mount one of these devices on some kind of a trolley and you could make a number of measurements very rapidly and then come back when the temperature changed and make the same measurements again.

P. S. PREVEY: The data that I showed was obtained deliberately to show reproducibility. You could simply conduct more tests. My results were obtained by manually repositioning rail sections without the use of fixturing to pencil marks on the rail. You get two slabs of rail cut out in different places. These were just manually positioned. There was no jig used, just a pencil line on the rail.

A. M. ZAREMBSKI: Yes but we have done some tests. You are aware of the tests, Mr. Prevey, that we did on two samples of rail web that were cut out of the web and sent to the same outfit in Ohio that was building the apparatus. One sample was taken from a brand-new piece of rail that had never seen service and one piece was taken out of a piece of rail that had seen service. I believe the sample was positioned using positioning techniques incorporated as part of the unit and there was, over three or four measurements, I think, over 20-25 percent scatter.

A. J. OPINSKY (Association of American Railroads): The level was about 30,000 or 40,000 psi compressive.

A. M. ZAREMBSKI: Now, that was the same piece that I assume had all the positioning devices that were incorporated into the PARS unit.

J. B. COHEN: Those tests, as I recall, were made in about an hour's time without much thought, just to demonstrate the unit. I was just standing there watching. I think those kinds of experiments are experiments you would want for your own personal use and I would not quote those tests. I would like to do an experiment on rails but would not expect to do the work in an hour.

D. P. McCONNELL: There have been a number of references made to the fact that X-ray diffraction is a technique which does not require zeroing, basically because the interplanar spacing acts as the reference for all strain measurements. Recalling the distinction that we have brought up before on the differences between strains due to residual stress in the rail and strains due to axial load in track, I believe there is a problem with establishing a zero reference.

With the X-ray techniques, an absolute stress state relative to virgin material property can be determined. What one cannot do is to walk out to a random rail and determine what the axial force acting on that rail is without having previously determined what the local strain conditions at a particular point were prior to the imposition of any axial force. Realizing that this dilemma is inherent to the technique, I think one of the problems with which one is faced in this environment is the existence of thousands of miles of continuously welded rails for which the initial state of strain due to cold working is not known. This is the central problem with this technique.

P. S. PREVEY: That is by definition true of any material property measuring technique -- ultrasonic, X-ray, or whatever material property sensitive technique is employed.

D. P. McCONNELL: Exactly. I am not saying it is X-ray technique, but I think I did want to clarify the business of non-zero reference since that has come up a number of times in the panel discussions on all the other techniques.

J. J. YAVELAK: However, still you have to consider the fluctuation of stress that might occur between day and night. This is an important quantity that we are very interested in. As to going out and making a reference point or a zero measurement, you could make it any way you want and then simple subtraction will tell you what the change is -- and I think the change is the important idea here.

Dr. Ruud mentioned something about going along at 30 miles an hour (0.4 second if you are going to measure 20 feet of track). I think that that lends itself to some very good ideas. One thing that you people might want to look at along those lines is the fact that if you could make measurements on a piece of rail along a certain length and then pull that rail in front of the beam and do the same type of a measure, would you get a weighted average of what those measurements might be? If that were the case, then we might want to ride along and measure segments on the railway. Does anyone have any comment on that?

P. S. PREVEY: I published a paper to investigate the effect of averaging over different sized areas on a ground surface in the presence of severe surface stress gradients of the type I described earlier on the accuracy of X-ray stress measurements. Measurements were made with a 0.5 x 0.25-inch irradiated area at a location. Numerous measurements were then made with a 0.020 x 0.25-inch irradiated area across the same region. The stress determined with the large area was very nearly the arithmetic average of the results obtained with the small area, even though the small area results included both tensile and compressive stresses because of the surface stress gradient present.

If you were riding along the rail making measurements, you should also obtain an arithmetic average stress over the area covered during the time span of the measurement. I have used a stress measurement technique on Stellite valve seats, where the sample was placed in motion by spinning the valve about the axis of the valve stem to obtain an arithmetic average stress over the circumference of the valve seat using a 1/8-inch-square irradiated area for measurement.

J. J. YAVELAK: I think that is something that we want to look at.

J. B. COHEN: I do not think there is any problem in putting together a device that you can run down a rail and, moving slowly, measure the rail in 20-foot sections and in a couple of seconds per section, and be satisfied with the average that you get. I mean, it is not a piece of equipment that you can go out and buy tomorrow.

J. J. YAVELAK: Right, but don't you think that would lead off what everyone is alluding to here? The problem with X-ray is, you might get a local error by measuring -- from heavy residual stresses in a certain location from grinding or scratching or something. Then why would that arithmetic mean not be just exactly what we would want?

J. B. COHEN: Yes, a stamp mark or a heavily abraided area or something like that can cause problems. However, by putting this result in with many others, it is swallowed by the averaging process.

J. J. YAVELAK: One final question: What differences in errors do we expect by the two detectors that were presented here? The difference between fiber optics versus wire? Are we talking about the same type of an error, relatively?

C. O. RUUD: They are both using X-rays, and inherent disadvantages of one over the other often can be overcome by innovative application design.

J. J. YAVELAK: So it is just an electronics problem?

C. O. RUUD: I think it is. One of them is a position-sensitive scintillation technique, the other is a position-sensitive proportional detector.

The proportional detector has some advantages over the scintillation detector and vice versa. I think what you have got to do is to get down to the basics, where you are talking about the situation in which you are doing the measurement and identifying your problems with respect to coatings, backgrounds, etc. Then you can start ironing out what you are going to have to give you the most advantage.

J. B. COHEN: I agree with Clay Ruud in the sense that I don't think your errors in these kinds of measurements are going to have anything to do with which detector you chose. They are going to be properties associated with the problems of the rails and have nothing to do with the detector itself.

B. R. FORCIER (Bessemer and Lake Erie Railroad Company): There was a comment I was going to make in Session II, but I have waited for the X-ray people to come on.

How feasible would it be to correlate all the features of all the different methods by taking, say, a half a dozen samples of, say, a piece of rail 5 or 6 feet long (whatever can be agreed on as being appropriate to all methods) and in turn send the samples to either a central place or to each place in turn and subject the rail to the longitudinal tests -- both compressive and tensile, and then read also what the Barkhausen would measure or the ultrasonic methods would measure and the X-ray method would measure?

You would know what the loads would be, both tensile and compressive, and the readings, and let's even put in the British Rail gage to make sure that the tensile force is read also and can be the same. How feasible is this and why don't we start it soon?

M. R. JAMES: If you wanted to look at applied stresses, I should hope that they all would measure pretty much the same value within the precision of the technique. But if you want to measure residual stresses, then you are looking at different penetration depths in a sample, and that is where you have a problem of comparing the two. X-rays only penetrate 1,000th of an inch. Barkhausen might go 1,500th of an inch. The birefringent ultrasonic technique goes through the whole bulk, so there you are looking at different residual stresses.

With an applied stress, it is different. It should be constant and uniform throughout the sample, and the methods should all be fairly comparative.

J. J. YAVELAK: As a railroad operator, I think what you are suggesting is a good idea. What you want to do, though, is not ship pieces of rail around because of the variabilities of what can happen to it in flight, etc. What you might want to do is set up a series of maybe half a dozen different samples under load or temperature in a lab and supply all those people who make measurements with a piece of rail steel so that they can measure whatever physical properties it is that they need to calibrate their device. Then, say, they come down here and we will give them two days to measure all these samples, etc.

Then you have accomplished the test under your controlled conditions. There is no question of making a mistake because the thing was bounced on an airline flight or something like that. Everybody has to meet the standards that you set up.

I think that would be a very useful test and very interesting. You could have a piece of rail that has got no load on it and then simulate a load with temperature and confinement or put a load on it or anything you would want.

B. R. FORCIER: As a railroad operator, I would comment that, when I look at a piece of track, it may be important to know the residual stresses if they are going to cause track buckling. If they are not, I am not interested in residual stresses. However, as a railroad operator, I am interested in those stresses that are just laying there like a stick of dynamite -- ready to explode.

J. R. COHEN: To measure the stresses you are interested in, you have to make two measurements -- as laid and later, and you can have these simulated in the laboratory. You could have half a dozen stations. Someone comes in with his device and this time there is no hanky-panky. You see it in operation. Here are the numbers and that is that. And there is no chance to go back and "calibrate" it again, or anything like that. He knows whether the device works or it does not. If he needs a piece of the same material for calibration, send it to him in advance and that is the way I think you will find your answer as to which technique is fast and reliable -- or at least start to find your answer. There are all kinds of conditions, and it seems to me that you could readily set up such tests and in a month's period have people come in and go ahead and make those measurements.

UNIDENTIFIED SPEAKER: May I reply? We did some work some years ago, when I was a graduate student at Brown University making ultrasonic measurements and a given peak for the material with a transistor epoxied on the subject. It was sent around to all these good labs in the country making ultrasonic measurements and the only correlation we could get was, the further away from Providence, Rhode Island, they were, the more decibels in the prime measurements. And so I am sure you cannot kick it around. I would suggest that, if you do something like that, you should have more than one person make one type of measurement.

B. R. FORCIER: Well, in my suggestion I said either in one place or ship it around and I agree, shipping around would be a problem but the Association of American Railroads' technical center in Chicago probably is as good a location as any as far as setting up.

A. J. OPINSKY: I have several questions. First, to Paul Prevey. I think you showed that there was not much of a gradient effect because there was not much of a gradient in two of your samples. But in the third one, the head (which to me is a trivial case), there is more of a gradient effect. I would like to make a point here. I think we are going to have to take our reading on the web or maybe on the foot, but anyhow not on the head because there we have the shifting sands, shall we say? We are always going to be wondering what we have.

P. S. PREVEY: I agree completely. I looked at the rail head because it is the most severe case of plastic deformation, and I wanted to determine if even the head would cause measurement difficulties. Someone might want to determine if there were stresses induced by the rolling contact, although the head is not a likely place to measure thermal expansion stresses.

A. J. OPINSKY: The point is, the 3 or 3.7 ksi -- is that a problem? It probably is not.

P. S. PREVEY: The 3 ksi variation on the head? It could be, depending on the magnitude of stress you are trying to measure. If 12 ksi will buckle a rail, I would not settle for a 3 ksi error. But that is why you would work on the web, for the thermal stress application.

A. J. OPINSKY: Yes. Now, Clay Ruud, I have a couple of questions. First of all, on the mechanics of the conversion, the scintillation count and the fiber optics -- how much error do you expect to have?

C. O. RUUD: I am not sure I understand the question.

A. J. OPINSKY: Well, the scintillation coating is applied directly to the fiber optics. Okay?

C. O. RUUD: Okay.

A. J. OPINSKY: But you are now making these discrete, aren't you? Do you have discrete fibers?

C. O. RUUD: Yes, we do.

A. J. OPINSKY: So don't you get an error from that standpoint?

C. O. RUUD: The error in the fibers themselves is negligible. We lose spatial resolution due to the conversion. Now, perhaps that is what you are alluding to.

A. J. OPINSKY: Yes.

C. O. RUUD: So, we have a fiber optic, the fibers of which are 10 microns in diameter. It is coated with a scintillation material. We have done very little development to improve our scintillation coating. There are definite possibilities for improvement of efficiency and resolution in this coating. With our present silicon diode array, our limiting resolution is 25 microns. Presently, we are getting 60 microns for the whole system.

A. J. OPINSKY: Obviously you have not gone into trying to make this unit portable. In other words, you are stuck with a regular tube which means you have probably got a fairly large power supply and so forth, but have you thought of making this thing portable?

C. O. RUUD: By the way, I neglected to mention that the Mobility Equipment Research and Development Command at Fort Belvoir supplied money for our original development. To prove out the idea of the detector, the Denver Research Institute's electronics division presently has a contract to build a portable unit.

Let me qualify "portable." The head itself, the X-ray source, X-ray tube, and detector, will weigh perhaps 8 pounds and will be on the end of a 20- or 30-foot cable that weighs about a third of a pound per foot. That is connected to the electronics, power supply, etc., which weighs about 500 or 600 pounds.

A. J. OPINSKY: Are you thinking about trying to get that smaller?

C. O. RUUD: We actually have looked at the same X-ray tube that Jerry Cohen is presently using, and we have found that it would be quite adequate for ferritic and martensitic steels.

J. B. COHEN: In both cases -- the instrument that Mike James and I had and the one in Clay Ruud's case -- it is only a matter of dollars to miniaturize things. There is only so much that those of us in the university environment or research institute environment can do. I checked with an electronics firm as to how to take that package and condense it to something the size of that lectern, total package. It only costs about $25,000. There is no problem in having a box that is that big that you could carry with a handle, and I am sure the same thing is true of Clay Ruud. The problem is money, and since we have no reason to try to walk around with a suitcase filled with electronics, we did not spend the $25,000. But it is a one-man-year development. There are outfits to do that sort of thing, if that is what you are after.

A. J. OPINSKY: Is there any possibility the vibration could sever some of these fiber optics? In other words, supposing you finally wind up putting this on a railroad car?

C. O. RUUD: I asked that question of the people that make the fiber optics and they said that they had put these through 90-degree bends for several million cycles and had observed a negligible number of breaks.

A. J. OPINSKY: Now, at the risk of muddying the waters, to get back to the question of what we are going to determine as the temperature goes up, it is my understanding of X-rays that we have the internal calibration of the lattice space, which was supposed to change, even if we are constrained. Is this not correct?

So that if we move up 50 degrees we see no macro strain by strain gages, yet our lattice parameter zero has changed so shouldn't we see that?

P. S. PREVEY: A condition of plane stress is assumed to exist at the sample surface. Then, the interplanar spacing, $d(\psi)$, used for stress measurement varies with the angle of inclination, ψ, of the lattice planes to the sample surface normal as,

$$d(\psi) = (1 + \nu)/E\, \sigma_\phi d_0 \sin^2\psi - (\nu/E)$$
$$d_0 (\sigma_1 + \sigma_2) + d_0.$$

Thus, $d(\psi)$ is a linear function of $\sin^2\psi$ with slope,

$$M = (1 + \nu)/E\, d_0\sigma_\phi,$$

and intercept,

$$d(\psi = 0) = d_0 - (\nu/E)\, d_0 (\sigma_1 + \sigma_2),$$

where σ_ϕ = stress to be measured,

d_0 = unstressed lattice spacing of planes used for measurement,

$(1 + \nu)/E$ = material-dependent single crystal elastic constant obtained empirically,

(ν/E) = material-dependent single crystal elastic constant that need not be known, and

$(\sigma_1 + \sigma_2)$ = sum of maximum and minimum normal principal stresses at measurement locations.

The unstressed interplanar spacing d_0 is unknown, but differs from $d(\psi = 0)$ by less than 0.1 percent due to the Poisson's ratios term, $-(\nu/E)\, d_0 (\sigma_1 + \sigma_2)$. If d_0 is approximated by $d(\psi = 0)$, which is simply the interplanar spacing measured at $\psi = 0$, then

$$\sigma_\phi \cong E/(1 + \nu)\; 1/d(\psi = 0)\; M.$$

In practice, $(E/1 + \nu)$ is determined empirically by measuring the crystal lattice strain for the planes to be used for measured as a function of applied stress.

The slope is simply

$$M = \frac{d(\psi = \psi) - d(\psi = 0)}{\sin^2\psi}.$$

Then, the stress to be measured is

$$\sigma_\phi = \frac{E}{(1 + \nu)}\left(\frac{d(\psi = \psi) = d(\psi = 0)}{d(\psi = 0)}\right)\frac{1}{\sin^2\psi}.$$

Even if no longitudinal strain is present due to external constraints, as in the case of thermally loaded continuous rail, a difference will exist between $d(\psi = \psi)$ and $d(\psi = 0)$ as a result of the Poisson's ratios term, because the rail will strain laterally. The stress in the rail may still be measured using X-ray diffraction techniques.

J. B. COHEN: And that will be the correct stress, when you get the slope. It will not be some empirical correlation.

A. J. OPINSKY: So you are now saying that we will get the right stress.

J. B. COHEN: Yes.

A. J. OPINSKY: Even though we do not supposedly have strain?

J. B. COHEN: But you do, in the other direction.

P. S. PREVEY: Yes, as Dr. Cohen said, in a week you could test the technique if you are still worried about it.

A. J. OPINSKY: What we really want to know is, is it big enough for us to see?

J. B. COHEN: Yes. An that is a job you can easily do in a few days. It is not a big deal.

A. J. OPINSKY: I want the authors to give me an idea as to whether we have to clean up the surface at all or how much we should clean the surface before we make these measurements.

P. S. PREVEY: You saw the data I presented. Those measurements were made through 0.002 inch of that tar-like coating, which added to the uncertainty in the measurements. The measurements were made, by the way, with 100,000 counts using a five-point parabolic technique.

A. J. OPINSKY: How much rust did you have on it?

P. S. PREVEY: The surface was not silvery when we cleaned it. I don't know how much rust was on it. The rail was laid in 1975. The rail preservative was still on the surface, so that the rust was no problem.

A. J. OPINSKY: We have the impression, therefore, that we do not have to do any surface preparation of the rail.

J. B. COHEN: That depends on the condition of the rail on site. I would like to do some more work on the real rails before I would insist that we don't have to worry. Again, that is not a major problem, really, because there are hand-held electropolishing devices that you can take in the field if you want to, but in order to do anything like that you just have to look at a few typical situations.

In the one we tried to measure, there was going to be a change in the stress and we found a change in the stress. We did not try to get highly accurate results, but I am not sure how much scatter would come from the roughening of the surface.

You have some places where oxide has flaked off and some places where it has not; if they are both under the X-ray beam at the same time, this is like a small sample displacement.

Again, I think these are detailed questions which are easily answered if you do some work in a laboratory. It is not necessary to go out on the railroad lines to find the kinds of answers, but I do not think that we are in a position to answer that.

I measured railroad wheels, which had all kinds of colored oxides on them that were, supposedly, indications of when they were bad. We did not take off the oxides. We just went right through them and never had any problems.

Now, you have to specify, what you want. Let me ask you a question. Do you want to know the stress to 500 pounds load, 500 pounds per square inch, 1,000 pounds? The key to all of these techniques is you telling us what you want to know and I know you want to measure changes in temperature. I think all the techniques that have been described here claim that they have a precision of about ± 2.5 ksi or better. Now all of you have to do is set up a test and all these people with all their claims can come down and you can see if they are real.

C. O. RUUD: Let me say something about this offset scale, because I have not looked at steel things but I have looked at aluminum. I have looked at aluminum parts that have been laying around outside at Fort Belvoir, Va., for 8 years, and I have done so without removing the scale. I have also looked through olive drab paint. Let me also say this, when you chip away the snow around a rail and clean it, it turns out not to look very pretty.

P. S. PREVEY: I would like to add one thing to the surface oxide question. I have worked on numerous steel specimens, making stress measurements on them with and without scale for the last 8 years, and there is one phenomenon that clearly should be noted. You can make measurements through the scale if it is thin enough. It is that simple. The oxide coating is going to affect the diffraction peak intensity, not the angular position of the peaks or the stress measured. But there is one problem that may arise due to the stress associated with the oxide-steel interface. When materials corrode, there can be stresses at that interface that form because of the shrinkage or expansion of the oxide, as the case may be. It would be a good idea to work on a reproducible surface.

B. R. FORCIER: Yes, the point has been well done as far as temperature change; as far as rail is concerned it is probably the most fluctuating thing. In the track structure itself, you may be working in an area where the track is in a sag where rail accumulates, so that you know, in this particular case, a 15° to 20° rise in temperature might result in adding the critical force necessary to buckle that track; yet over a crest, you could take a 500° rise in temperature, because the rail is in such a tensile state to begin with that you may be just approaching what we call the neutral, or laying, temperature. This point should not be forgotten.

On repeatability of any of the methods that are used for testing in the 5- or 6-foot rail lengths that we use, say, in Chicago, the various locations on the rail that you pick are going to show whether the surface condition is going to have any great effect as to changing the kind of reading. So that is one of the areas that is going to help everybody in using the same samples.

A. J. OPINSKY: What area should we irradiate before we have a number that is "representative"?

J. B. COHEN: What is it representative of? Rail between Chicago and Cleveland? Representative of what? What is it that is being represented? On a curve? On a bend? On an incline? What is it that you want to know? I mean, you are not stating exactly what you want to know before we can answer that question. It has to be bigger than the grain size, definitely a lot bigger than the grain size.

P. S. PREVEY: We should make the measurement area as large as possible to measure the change in applied stress and minimize the other errors.

J. B. COHEN: I don't think we can answer those questions. Nobody has data along the length of a rail. This is the kind of thing that, if you are interested, you have to follow up on and get some research done, either in-house or someplace else.

A. J. OPINSKY: What are the radiation hazards if we had this thing, not as a moving device but as a stationary device?

J. B. COHEN: Are you talking about X-rays? I mean, I do not know what ultrasonics does, but --. Anybody that tells you no effect -- tomorrow, somebody else will find an effect. Anyway, we do know that X-rays have an effect and you just shield it. You box your device in to your particular use. It can be shielded in such a way that it will not be any problem and there is no permanent damage to the piece.

C. O. RUUD: The X-rays which are used for X-ray diffraction are very, very low-energy X-rays. We are not talking about medical X-rays. We are not talking about industrial X-rays. We are talking about X-rays that a quarter-inch of plexiglass will absorb almost completely.

P. S. PREVEY: That is all I used for shielding on that X-ray instrument.

C. O. RUUD: It is only the primary beam that will be a problem, not the scattered radiation.

P. S. PREVEY: You certainly have to worry about safety. It is a matter of shielding the device properly. Once you have specified the application and built the equipment, you shield it accordingly.

QUESTION-AND-ANSWER PERIOD

R. C. FAULKNER (Illinois Central Gulf Railroad): Dr. Cohen, is there information available for the manufacturers of that miniaturized equipment that you showed?

J. B. COHEN: Allan Zarembski has some information.

R. E. GREEN (The Johns Hopkins University): Is this new tube that you are talking about a modern version or a newer version of Jerry Cohen's or is it a rotating anode-type tube?

C. O. RUUD: As a matter of fact, it is made by the same people, but it is not a rotating anode.

J. B. COHEN: In fact, they sell one off the shelf. It goes to 10 milliamperes. It is air cooled, but a bit bulkier than the zma tube.

C. O. RUUD: But the one they are developing for us will be water-cooled.

J. R. BARTON: This question of lattice spacing or change in lattice spacing with temperature: As the rail temperature rises, the lattice spacing in a transverse direction where you are not constrained changes. On top of that change, from the temperature expansion alone, you can have the influence of the constraint and Poissons effect so you have to know intensity, do you not?

J. B. COHEN: You know the thermal expansion coefficient.

J. R. BARTON: Is the point that you need to know the temperature of the rail? Not necessarily the ambient temperature?

J. B. COHEN: No, because you make the measurement in different directions, and the thermal expansion coefficient in steel, which is essentially cubic, is independent of direction. So when you take a difference, you cancel out the thermal expansion part. You measure only the stress.

I still think the thermal expansion part -- not at the longitudinal direction but in the other directions that you are measuring, perpendicular to the rail and other angles -- is going to cancel in the difference.

R. B. THOMPSON: I would say that, if you could measure on the rail head and on the side, that would work. You would have good access to the top of the rail, but interpretation may be limited because of all the other cold working effects.

J. B. COHEN: I don't know. I have to think about that.

A. M. ZAREMBSKI: The top of the rail just can't really be a practical measurement because you have to run trains in between and you are basically changing your stress every time your train runs by.

D. P. McCONNELL: There have been tests conducted in which people have observed surface strains changing with train passage. You can see material flowing in different directions, depending on both the direction of train motion and on the relative positioning of the wheels on the rail head, so the tread surface becomes a rough place to make any kind of measurement in this context.

R. EHRENBECK (Transportation Systems Center, DOT): Dr. Ruud, you mentioned a possibility of putting this on a vehicle and traveling along at 30 miles an hour or whatever it is. But isn't your system sensitive to the point of interest on the rail from the time of transmission until the information is recorded on your counter where your actual lines fall?

C. O. RUUD: You mean, what is the distance between the counter and the rail?

R. EHRENBECK: No, I am saying that in order to obtain detectable signals, you have to sit over a fixed location to get your readings.

C. O. RUUD: You can collect the data while it is being generated. We are talking micro sets versus milli sets.

R. EHRENBECK: But you are also moving over the original position. In other words, are you thinking of pulsing an X-ray and then taking a reading and moving on?

C. O. RUUD: No, what I was thinking when I threw that out was the averaging bit. You averaged over several feet.

J. B. COHEN: Assuming that the geometry works out, the sample is going to be scattering all the time the piece is moving past the detector, so it is just like having a huge sample all at one time as it is scattering. The only time element requirement is having enough time to get enough counts to get good statistics. But that does not necessarily mean that the sample has to be stationary. It can be moving.

By the way, you can get other things out of these measurements. The oscillations in intensity will tell you the grain size. While this piece is moving past the 20 feet, you could obtain both the stress and the grain size, if that is of any assistance.

R. EHRENBECK: But you also have got an error due to the positioning of the transmitter on the rail's curved surface and the curvature of the collector.

J. B. COHEN: That is the geometry question which is not clear. It depends on how well you can maintain distances and things like that.

C. O. RUUD: That is right. It is also how you would maintain distances. I have heard some ideas, some of them wild, some of them not so wild. We have not approached that, but certainly you don't have to hold the distance constant. You just have to know what the distance is at the instant you are making the measurements. And that is a matter of how fast an electronic device will respond.

D. E. BRAY: As I mentioned in Session I, I have mellowed considerably in my enthusiasm for the 60-mile-an-hour vehicle. As a result, I have been thinking in the last 2 or 3 years about the usefulness and the applicability of a hand-held portable device. Of course, when your capabilities diminish, you try to enhance the capabilities of what you have left, but I think what this points out is this, and these comments really apply to everybody.

I think the essential thing that we could develop that would be most useful at this time is a maintenance tool, a device used when track is installed so that the track men can insure that the stresses are evenly distributed when track is installed.

Now, in an ideal case -- that is, straight track with no perturbations -- it would be simple to periodically come back and, at key points on the rail, make measurements and take the temperature. This is really all that you would need. We do have inputs, as some people have mentioned, of braking downhill and other abnormalities. Nevertheless, looking at this as a maintenance tool, the prudent person can decide where the testing shall take place. I think there is a lot of benefit for the operating railroad for a track man to possess a portable stress measuring device. It can be carried in a high rail car or a maintenance of way truck or anything like that. Just so as the man has access to a device which gives some indication of both the stress and the temperature at a point on the rail. At this time, this becomes a part of the maintenance data. I think that would be a useful tool. It is less than the first goal, but as somebody mentioned earlier, it is a heck of a lot more than nothing.

N. SENAPATI (Battelle Columbus Laboratories): There are some implications that we have to make two measurements -- when it is at low temperature and when it is at high temperature. I don't really see the necessity for always making two measurements. I believe that even the X-ray technique or the ultrasonic technique or the technique I proposed would simply monitor some average value of the stress without any reference to data when it is cold.

J. B. COHEN: I would like to make a comment on that point. You have got all kinds of things going on in that rail. As Paul Prevey was showing, stress is all the way through the bulk and those stresses are going to be a function of how the rail was manufactured, how it was laid, whether it is uphill or downhill, whether it is going to curve, whether it is going to creep and leave unequal stresses, and so forth.

Assume for example just the ideal situation that, when we are all done, the rail has uniformly 50,000 pounds per square inch of compression. The buckling load has to overcome that before the tensile part of the buckling load causes any problems. So you have to know what it was to start with and what it is later on to know whether you are going to get into trouble.

N. SENAPATI: I don't think so. If you have a residual stress distribution due to, say, cold working or the creep or due to things that have been changing from day to day, unless the net effect is an average compressive stress along a piece of fairly large length (comparable to "the wavelength"), it is not going to cause any buckling.

D. P. McCONNELL: I think the issue to consider at this point is that the track structure has evolved over a period of time. It is a remarkably well-adapted structure at this point in time. However, it is a remarkably uncontrolled structure. It varies drastically from point to point along the rail or between two rails. There are movements which take place in the rail with respect to the ties. The ties themselves can move through the ballast. Furthermore, the ties do not provide a fixed reference point for ideal restraint of the rails.

There are many reasons why rail moves. Bernie Forcier alluded to the fact before that, on virtually any piece of railroad you look at, rail does not want to be at the top of the hill, but would like to be at the bottom of the hill. That is largely because the train would like to cross the top of the hill and the rail is the only thing that is resisting the traction force required to get it over.

As a consequence, from the viewpoint of the conference we are now completing, all of those mechanical effects which produce stresses on the rails which we have gone through over and over again become, against the issue of longitudinal force on the rail, the noise background against which we are trying to make measurements. Unfortunately the noise level is very high and it is very inconstant as you move along the rail. So I think that one of the key issues here is that temperature is being used as a surrogate for the axial force behavior within those rails and I think we ought to keep that in mind as we proceed with our concluding remarks.

Let me explain the problem about which the track mechanician worries. It is a view somewhat different from that of the track engineer, because we do not come down from the ivory tower often enough to have his problems.

Fundamentally, with constrained axial loads within the track due to thermal expansion or due to accumulation of creep due to train action, there is a buildup of axial force either over time or through the daily temperature cycle.

Like any structural element under compressive load, there is some buckling load at which there is a problem. With the rail, current theories basically indicate that the problem exhibits the type of behavior which is shown in the diagram. If I look at displacement of the track versus the axial load, N, the type of behavior which is exhibited is something that, roughly speaking, looks like this.

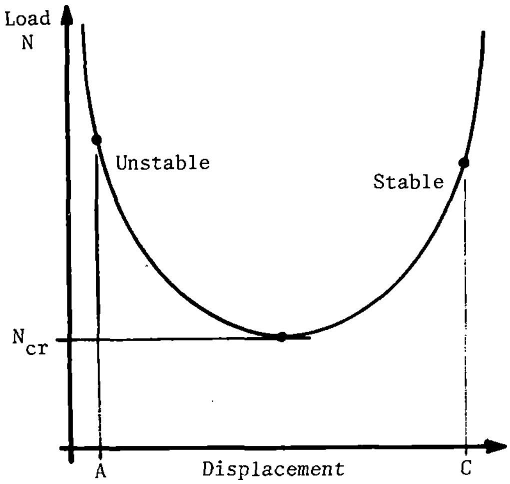

Above N_{cr}, the portion of the branch to the left of the minima point is unstable and consequently is displacement which cannot be manifested during the actual buckling phenomena. So what would happen in an ideal case is that you would load up along the vertical branch; that is, there would be an increasing load but no further deformation.

At any load below the N_{cr}, there is no adjacent state of equilibrium. There is no problem with buckling. Once the load exceeds N_{cr}, the track can achieve a state where any external input may cause the track to cross an energy threshold and buckle. It will go from point A to point C. In an actual track, that represents a displacement somewhere between 12 and 18 inches over a length of 40 to 60 feet. That represents an irregularity in the track difficult to traverse with a train. When this happens, there is a shift within that axial load within the track, as the track moves to a lower energy state.

I think that one of the issues which is of great concern here is that, for any given track structure, this allowable increment in axial force and its associated allowable change in temperature varies with the ballast restraint properties and with the structural properties of the track panel. We do not know a priori what the critical axial load for any given piece of track is. It can be calculated only once we have the local restraint characteristics at that particular location. The critical question in the context of this conference is the question of how to detect the axial force in the track, so that subsequently one can determine how close the track is to the critical axial load for that track.

Conversely, when the track goes into tension, tensile forces act in consort with the stresses induced by wheel passage to act as a promulgating mechanism for cracks. So we are interested in looking at the management of tensile forces largely because they represent a threat from rail failure. In very gross terms, that is the ballpark within which we are testing to see if there is something happening to the axial force in the rail.

The reasons that buckling is such a problem is because, due to the nature of the jump discontinuity in the response, you can be in a position where the track could have just slightly less than sufficient axial force to buckle and a small amount of energy input, for example, passage of a train, can cause it to go out. That is why it is that railroad people are so concerned about constrained thermal expansion rails and what they represent. It is an incipient problem that results in over 200 derailments per year.

R. H. PRAUSE (Battelle Columbus Laboratories): Just a general question to the railroad members of the panel or else to the audience: How do you view the relative practical difficulty of offering some type of moving inspection that either looks at the head of the rail or goes around the side and looks at the web of the rail? I know it is desirable to look at the head, but how much more difficult do you think it is to look at the web with the obstructions of joint bars and turnouts, etc.?

B. R. FORCIER: For those of you who are familiar with detecting or checking for rail failures or flaws, riding or checking the head of the rail is much easier because it is available to you at all times. The web of the rail would be available to you for checking most of the time, but you would have railroad crossings, highway crossings, switches, or turnouts, and so on that could be a problem. Naturally you could raise the equipment for that, but looking at the web, the preponderance of the checking would be easy, both inside and outside, either one.

R. H. PRAUSE: You can also get debris and lots of other obstructions between the rails, and these can be as high as the lower part of the head.

B. R. FORCIER: Geographically it could be a problem, once they get a lot of sand and so on built up.

R. H. PRAUSE: I have seen old tires lying between the rails, too.

UNIDENTIFIED SPEAKER: Yes, but if you can't solve that problem, then you are in real trouble.

D. P. McCONNELL: It is a general rule in railroading that, if equipment is not in the shadow of the axle, forget about it; it won't be there the next time you look for it.

J. H. SULLIVAN (Federal Railroad Administration): I have a comment about the difficulty of looking at things on the head of the rail or on the web of the rail or on the base. I was personally responsible for operating a track inspection car for about 12 years before working for the FRA. If you can stay on the head of the rail, you have got a pretty good chance of everything operating all day long without too much trouble. As soon as you get to the gage side of the head of the rail, you have to start being concerned about such things as switch frogs and how you get through them. When you get to the side of the rail, which is right under the head of the rail, you get into a problem that my friend J. J. Yavelak over there at Southern Railway gets into about every day, I expect, on their ARWISS car.

When you get to the base of the rail, you have got to reach down further yet and it seems to me that, for a moving vehicle, it is going to be a very difficult problem to look at the web, which may be an inch above the spikes. Once you get down that low you don't have to worry about a spike. You have got rail anchors and everything else, so it seems to me that once you get down on the web of the rail, you are approaching the rail with an impossibly difficult problem.

A. M. ZAREMBSKI: Why don't you try something with a contact, with a contact shoe?

UNIDENTIFIED SPEAKER: Why do you want a rolling vehicle? Why not have one that is made portable and that can come up here and check a piece of rail and then move on to another section. We have got to learn something about what is in a particular location. We have got 24,000 miles of railroads. We don't care about finding out about the whole thing.

G. A. DAVIDS (Federal Railroad Administration): To go a little further on this matter of rail flaws and track geometry, we want to make a fairly continuous search because, of course, there is liable to be a flaw or a geometry defect in an area that we might have skipped. But as far as trying to determine stresses and forces in the rail, I just do not see that there can be that great a change in force through a highway crossing or turnout or even through a track crossing. We would not miss very much by skipping those areas. In other words, if we made two or three stress measurement in a rail, say a 39-foot rail length, we would be doing pretty well. I don't see any problem there at all, for now.

UNIDENTIFIED SPEAKER: You might find one later on though.

D. P. McCONNELL: If there are no further questions and comments, I would like to thank all of the authors from all of the sessions for a job well done and I would especially like to thank the permanent panel members who have had to be here under rapt attention for the last day and a half. I would also like to thank the supplemental panel members for a job well done and at this point in time we end as we began with Allen Zarembski.

CLOSING REMARKS

A. M. Zarembski
Association of American Railroads

I would like to end this conference by briefly reexamining what I initially identified as the requirements for a longitudinal force measurement system and then, based on what we have seen for the last two days, try to evaluate what is practical and feasible, what may be practical and feasible, and where we are sort of whistling in the wind.

As given in my introductory remarks, the requirements for the measurement system are as follows:

1. It should be ruggedly constructed and capable of surviving in the field.

2. It should be easy to handle and require only limited interpretation of data.

3. It should be nondestructive to the rail and track structure.

4. It should not require the disturbance of the track structure either during application or during "zeroing," if the latter is at all necessary.

5. It should require minimum or no calibration. If calibration is needed, it should not require heavy equipment or significant track time.

6. It should be independent of or readily compensated for:

   a. rail size

   b. rail metallurgy

   c. heat treatment

   d. rail head wear

   e. work hardening or softening of the rail head

7. It should require minimum or no surface preparation of the rail.

8. It should provide for direct measurement of net longitudinal force (absolute).

9. It should not have to be permanently affixed to the rail or track structure.

10. It should permit "continuous" or at a minimum very frequent measurement of rail force from a moving vehicle.

The first requirement is easy. I think there is no question that we can build a rugged device as the pictures that Dr. Cohen and I have shown earlier on the snow-bound Chesapeake and Ohio trackage have proven; you can build a device that can go out in 10°F weather and conduct measurements.

The second requirement is a question of packaging and instrumentation. If you get the proper design, even if it is just a pair of red and green lights, you can come up with a design that is easy to handle and use.

The third requirement is not a problem. I think the techniques we are looking at are generally nondestructive in nature in that they do not do any permanent damage to the track or rail while measuring.

The fourth, fifth, and seventh requirements -- minimum disturbance, minimum calibration, and no surface preparation -- are such that I think we have a good chance of accomplishing all three of them. Surface preparation seems to be a fairly straight forward problem. Minimum track disturbance and calibration, while posing more significant problems, still appear to be solvable.

The sixth requirement -- to be able to use the device on all rails -- constitutes one of the more difficult problems. There are still some questions regarding the effect of material variations within the same type of what we call standard carbon rail, variations between heat-treated and non-heat-treated rail, and between alloy rails, and even questions as to differences in using rail that has seen significant amount of service (and, consequently, wear) and rail that has not. However, I think (and this is just my own opinion) that we can overcome that problem with time and money.

The eighth requirement involves measuring net force. Towards the end of this discussion people seemed to be reaching the conclusion, possibly rightly so, that you are going to need to make two measurements to measure net force, one at a stress-free state and one at a non-stress-free state (a loaded state), and then use the difference to give you your force values. That may be practical -- except for the magnitude of the problem.

The North American railroad system consists of 300,000 miles of trackage, of which about 70,000 miles is continuously welded rail (CWR). Being conservative, let us say we need to take a measurement every quarter of a mile -- and I think that may be too far apart but let's be generous and say every quarter of a mile. Furthermore, let us say we can rule out approximately half the CWR territory where we comfortably feel that we do not have a buckling problem. (I am not sure that we can do that, because I know of derailments that have occurred in cold weather. As a matter of fact, I was just looking at data on an accident where the buckle occurred at 15°F. Conventional track buckling?)

We have now cut down to the total trackage with which we are concerned to 35,000 miles -- and four measurements per mile. We are talking about 140,000 measurements, each one requiring a stress-free (zero) measurement.

Somebody alluded to the fact that you can go out when the track gang is laying the rail and take your stress-free measuremenrt during the laying procedure.

However, rail in main-line services is replaced roughly every 8 to 10 years. As for rails on branch lines, every once in awhile I stumble over some rail that has been stamped 1910 or 1920 and is still out in the field; these rails have been known to last 50 or 60 years. Therefore, for rails already in place and not scheduled for near-term replacement, you have to go out and obtain a stress-free measurement, and that represents a significant concentration of time and effort.

This is a problem, and to this problem I want to add both the ninth requirement (nonfixation) and the tenth requirement (continuous measurement). I do think that you can use a discrete measurement system for major problem areas -- that is, locations where you have a history of buckling. However, there are other things a railroad can do if they know one particular area is susceptible to buckling. As was alluded to earlier, you can maintain that particular piece of track to a better standard if you know it is a problem location. What really causes trouble is the buckling of track that you do not expect to buckle. For that you have to be able to go out and measure all of your track, and as one railroad representative noted, his railroad has 24,000 miles of track.

Thus, to perform measurements on a discrete basis becomes a problem of scale. Given enough time, money, and people, you probably can do it, but railroads are cutting back on basic maintenance, so I would like to submit that this problem is still very significant.

To conclude, I think that this conference has served a most useful purpose. The basic result of these two days has been that we have helped to lay down a consistent formulation of a problem. We have laid the groundwork for trying to attack the problem in a consistent and organized manner.

I do think we have managed to spark some interest at this conference, and feel we have had a very useful exchange of information. As a matter of fact, I was very surprised to see people come in with tests they performed on their own, not supported by either the Association of American Railroads (AAR) or the Federal Railroad Administration (FRA). I guess when there is a suitable incentive, people go out and do initiate research efforts. I would like to see that continue.

We do have programs currently under way to look into these areas; as noted, the Transportation Systems Center (TSC), the FRA, and the AAR have sponsored and are currently sponsoring research programs in this area, and this particular conference is a part of this ongoing research effort.

Central to this conference is that we have gotten many people talking about the same problem in the same place at the same time, and I certainly hope that the effort we have seen during these two days soon can come up with a successful and useful measurement technique.

APPENDIX: LIST OF CONFERENCE PARTICIPANTS

PAPER PRESENTERS

John R. Barton
Vice President
Instrumentation Research Division
Southwest Research Institute
8500 Culebra Road
San Antonio, Texas 78284

L. H. Bennett
Group Leader, Alloy Physics
National Bureau of Standards
Building 223, B150
Washington, D.C. 20234

Robert W. Benson
President
Bonitron, Inc.
2970 Sidco Drive
Nashville, Tennessee 37204

Donald E. Bray
Department of Mechanical Engineering
College of Engineering
Texas A&M University
College Station, Texas 77843

J. B. Cohen
Frank C. Engelhart Professor of Materials Science and Engineering
The Technological Institute
Materials Science & Engineering Department
Northwestern University
Evanston, Illinois 60201

Michael R. James
Member of Technical Staff
Rockwell International Science Center
1049 Camino Dos Rios
Thousand Oaks, California 91360

Geoffrey S. Lane
British Railways Board
The Railway Technical Centre, Room 103B
London Road
Derby DE2 BUP, England

Kenneth R. Maser
Manager, Materials and Structures Division
Foster-Miller Associates
135 Second Avenue
Waltham, Massachusetts 02154

Robert E. Parsons
Associate Administrator for Research and Development
Federal Railroad Administration, RRD-1
400 Seventh Street, SW.
Washington, D.C. 20590

Paul S. Prevey
Director of Research
Lambda Research Inc.
7213 Market Place
Cincinnati, Ohio 45216

Clayton O. Ruud*
Materials Research Laboratory
The Pennsylvania State University
University Park, Pennsylvania 16802

Nagabhusan Senapati
Applied Dynamics and Acoustics Section
Battelle Columbus Laboratories
505 King Avenue
Columbus, Ohio 43201

R. Bruce Thompson
Rockwell International Science Center
1046 Camino Dos Rios
Thousand Oaks, California 91360

Larry L. Yeager
Program Engineer
Daedalean Associates, Inc.
Spring Lake Research Center
15110 Frederick Road
Woodbine, Maryland 21797

Allan M. Zarembski
Manager - Track Research
AAR Technical Center
3140 South Federal Street
Chicago, Illinois 60616

CONFERENCE PANEL MEMBERS

Donald P. McConnell (chairman)
Research Engineer
Structures and Mechanical Branch
Transportation Systems Center
Kendall Square
Cambridge, Massachusetts 02142

Harold Berger
Chief, Office of Nondestructive Evaluation
National Bureau of Standards
Building 221, B-312
Washington, D.C. 20234

Bernard R. Forcier
Manager - Maintenance Planning
Bessemer and Lake Erie Railroad Company
P.O. Box 471
Greenville, Pennsylvania 16125

Arthur J. Opinsky**
AAR Technical Center
3140 South Federal Street
Chicago, Illinois 60616

Daniel H. Stone
Director of Metallurgy
AAR Technical Center
3140 South Federal Street
Chicago, Illinois 60616

*Formerly with Denver Research Institute, University of Denver, Denver, Colorado.

**Substitute for Harold Berger in Session III.

SESSION CHAIRMEN

Donald M. Forney, Jr.
Chief, Nondestructive Evaluation Branch
Metals and Ceramics Division
Air Force Materials Laboratory/LLP
Wright-Patterson Air Force Base, Ohio 45433

Charles H. McGogney
Structures & Applied Mechanics Division
Office of Research, HRS-11
Federal Highway Administration
400 Seventh Street, SW.
Washington, D.C. 20590

SUPPLEMENTAL SESSION PANEL MEMBERS

Henry H. Chaskelis
NRL Code 8431
Naval Research Laboratory
Washington, D.C. 20375

Arnold D. Kerr
Department of Civil Engineering
University of Delaware
Newark, Delaware 19711

John Simmons
Research Mathematician
Metal Science and Standards Division
National Bureau of Standards
Materials Building, B-118

Ta-Lun Yang
ENSCO, Inc.
5408A Port Royal Road
Springfield, Virginia 22151

James J. Yavelak*
1841 Carriage Lane (#101)
Alliance, Ohio 44601

OTHER ATTENDEES

C. J. Bechtobdt
National Bureau of Standards
Building 223, B-118
Washington, D.C. 20234

R. G. Brohaugh
Chief Engineer - Maintenance
Burlington Northern
176 East Fifth Street
St. Paul, Minnesota 55101

G. Richard Cataldi
Senior Engineer
Unified Industries Incorporated
5400 Cherokee Avenue
Alexandria, Virginia 22312

Lloyd R. Cayes
Office of Research, HRS-11
Federal Highway Administration
400 Seventh Street, SW.
Washington, D.C. 20590

*Formerly with Southern Railway System, Research and Test Labs, Alexandria, Virginia.

Harry P. Clapp
Parsons, Brinckerhoff CENTEC Inc.
7900 Westpark Drive
McLean, Virginia 22101

Gordon A. Davids
Office of Safety
Federal Railroad Administration
400 Seventh Street, SW.
Washington, D.C. 20590

Raymond Ehrenbeck
Transportation Systems Center, Code 731
Kendall Square
Cambridge, Massachusetts 02142

Paul Elliott
Program Manager
Unified Industries Incorporated
5400 Cherokee Avenue
Alexandria, Virginia 22312

Robert C. Faulkner
Rail Test Supervisor
Illinois Central Gulf Railroad Company
233 North Michigan Avenue
Chicago, Illinois 60601

John D. Ferguson
Federal Railroad Administration
Office of Research and Development, RRD-31
400 Seventh Street, SW.
Washington, D.C. 20590

John T. Ferguson
Manager - Rail Welding and Track Testing
Union Pacific Railroad
Room 1023
1416 Dodge Street
Omaha, Nebraska 68179

H. Ghonem
Senior Research Engineer
Canadian Pacific
Windsor Station, Room 369
Montreal, Quebec H3C 3E4

Robert Green, Jr.
Department of Mechanics and Materials Science
The Johns Hopkins University
Baltimore, Maryland 21218

H. Ingrao
Transportation Systems Center, Code 733
Kendall Square
Cambridge, Massachusetts 02142

William M. Kaufman
ENSCO, Inc.
5408A Port Royal Road
Springfield, Virginia 22151

Robert Krick
Chief, Improved Track Structures Research Division
Office of Research and Development, RRD-32
Federal Railroad Administration
400 Seventh Street, SW.
Washington, D.C. 20590

H. F. Longhelt
Amtrak
400 North Capitol Street
Washington, D.C. 20001

W. Scott Lovelace
Manager, Research and Tests
Southern Railway
Research and Test Labs
P.O. Box 233
Alexandria, Virginia 22313

Richard L. Lusignea
Project Engineer
Foster-Miller Associates
135 Second Avenue
Waltham, Massachusetts 02154

Douglas E. MacDonald
National Bureau of Standards
Materials Building, B-118
Washington, D.C. 20234

William S. C. McLaren
Chief, Current Technology
Transport Canada
Research and Development Centre
1000 Sherbrooke Street West
Montreal, Quebec H3A 2R3

K. J. Mathewson
CN Rail Research Centre
3950 Hickmore Avenue
St. Laurent, Quebec H4T 1K2

R. K. Meyers
Amtrak
400 North Capitol Street
Washington, D.C. 20001

John C. Mould
Office of Research and Development, RRD-31
Federal Railroad Administration
400 Seventh Street, SW.
Washington, D.C. 20590

William B. O'Sullivan
Office of Rail Safety Research
Office of Research and Development, RRD-32
Federal Railroad Administration
400 Seventh Street, SW.
Washington, D.C. 20590

B. F. Overbey
Engineer - Track
Amtrak
1617 J. F. Kennedy Boulevard
Philadelphia, Pennsylvania 19103

Wilson Pak
Research Department
Canadian Pacific Limited
Windsor Station
Montreal, Quebec H3C 3E4

Frederick Prahl
Senior Engineer
Foster-Miller Associates
135 Second Avenue
Waltham, Massachusetts 02154

Robert H. Prause
Section Manager
Applied Dynamics and Acoustics Section
Battelle Columbus Laboratories
505 King Avenue
Columbus, Ohio 43201

Robert R. Reeber
U.S. Department of Energy
20 Massachusetts Avenue, NW.
Washington, D.C. 20545

H. David Reed
Chief, Track Systems Branch
Transportation Systems Center, DTS-731
Kendall Square
Cambridge, Massachusetts 02142

Ronald G. Rosemeier
Department of Mechanics and Materials Science
The Johns Hopkins University
Baltimore, Maryland 21218

Rajendra Saroop
Office of Rail Safety Research
Office of Research and Development, RRD-32
Federal Railroad Administration
400 Seventh Street, SW.
Washington, D.C. 20590

Fred Schloss
DT Naval Ship Research and Development Center
Carderock, Maryland 20084

J. Frank Scott
Research Engineer
CN Rail Research Centre
3950 Hickmore Avenue
St. Laurent, Quebec H4T 1K2

James R. Smith, Jr.
Engineer - Maintenance of Way
Richmond, Fredericksburg & Potomac Railroad Co.
2134 West Laburnum Avenue
Richmond, Virginia 23227

Paul R. Spencer
Technology Development and Deployment, UTD-30
Urban Mass Transportation Administration
400 Seventh Street, SW., Room 6429
Washington, D.C. 20590

J. H. Sullivan
Project Manager
Office of Rail Safety Research
Office of Research and Development, RRD-32
Federal Railroad Administration
400 Seventh Street, SW.
Washington, D.C. 20590

W. A. Swartz
Engineer of Standards
Consolidated Rail Corporation
6 Penn Center Plaza
Philadelphia, Pennsylvania 19104

Lydon J. Swartzendruber
National Bureau of Standards
Building 223
Washington, D.C. 20234

D. E. Turney, Jr.
Assistant Chief Engineer - Maintenance
Norfolk and Western Railway Company
8 North Jefferson Street
Roanoke, Virginia 24042

Milan Velebit
Chief Designer
Illinois Central Gulf Railroad Company
233 North Michigan Avenue
Chicago, Illinois 60601

Winfred C. Wilcoxon
Wilcoxon Research
12526 Parklawn Drive
Rockville, Maryland 20852

J. W. Winger
Assistant Chief Engineer
Chessie System
P.O. Box 1800
Huntington, West Virginia 25718

James B. Winn
Chief, Improved Inspection, Detection, and
Testing Research Division
Office of Research and Development, RRD-31
Federal Railroad Administration
400 Seventh Street, SW.
Washington, D.C. 20590

J. G. Wood
Director - Track Quality & Test
Burlington Northern
176 East Fifth Street
St. Paul, Minnesota 55101

Jia-Dong Yu
Department of Mechanics and Materials Science
The Johns Hopkins University
Baltimore, Maryland 21218

* U.S.G.P.O. 723-939/1302-779

Nondestructive Techniques for Measuring the Longitudinal Force in Rails: Proceedings of a Joint Government -Industry Conference, Held in Washington, DC, February 26-27, 1979, 1980 - US DOT, FRA, Paul Elliot